TIDE INTEGRATED HYDRODYNAMIC AND SEDIMENT TRANSPORT CHARACTERISTICS IN TIDAL CHANNELS AND THE EFFECT OF DEEPENING

Tide Integrated hydrodynamic and sediment transport characteristics in tidal channels and the effect of deepening

M.SC. THESIS JAN GERT RINSEMA

23 SEPTEMBER 2016
FINAL REPORT

[1]

ARCADIS
UNIVERSITY OF TWENTE.

[1] Cover picture retrieved from: beelbank.rijkswaterstaat.nl

Submitted to acquire the degree of Master of Science

To be presented in public

On 30 September

At University Twente, Enschede, the Netherlands

Jan Gert Rinsema

s1129988

j.g.rinsema@alumnus.utwente.nl

University of Twente

Faculty of Construction Engineering Technology

Water Engineering and Management

Members of graduation committee:

Dr. ir. C. M. Dohmen-Janssen	Chairman, University of Twente
Dr. ir. M. Fernandez-Mora	Supervisor, University of Twente
Dr. ir. B. T. Grasmeijer	Supervisor, Arcadis

ABSTRACT

Estuaries are places where rivers meet the sea. Estuaries have different characteristics dependent on their location. An important factor is the shape of the estuary. Natural estuaries have a funnel or trumpet shape, which means the estuary, has a large width near the seaward boundary and is converging stream upward. Other estuaries are man-made and have a straight channel from the sea landward; these estuaries are called prismatic estuaries. The Rotterdam Waterway is an example of such a prismatic estuary.

Estuaries are often used as access channel for harbors. Due to economic development and technology development ships size increases, which makes the harbors less accessible. To reduce this problem harbors are deepened to keep them accessible. The effects of the deepening on estuary processes are another key question which is unknown for prismatic estuaries.

The sediment transport processes result in an Estuary Turbidity Maximum (ETM). The ETM is a suspended sediment front near the mixing of the saline and fresh water. The sediment is trapped at this location due to the estuarine circulation. The magnitude of the ETM is determined by several other processes determined by the boundary conditions of the study area. These processes include tidal asymmetry, internal asymmetry, tidal phase lag, turbulence damping and flocculation. The change of the ETM due to these processes in prismatic estuaries is relatively unknown.

The Rotterdam Waterway is used as case study to evaluate the sediment transport characteristics of prismatic estuaries, using the process based numerical model Delft3D. A schematized study area is created which only consists of a straight channel including the fresh water boundary and a schematized sea of 40 kilometers along the coast and 20 kilometer perpendicular to the coast. The model is setup and validated based on available sources.

A sensitivity analysis is done to evaluate the contribution of the different processes towards the hydrodynamics and the sediment transport characteristics. The wave conditions and discharge are changed in the sensitivity analysis. The fresh water discharge is changed towards the 5%, 25%, 75% and 95% discharge of the Rotterdam Waterway. The waves are changed towards the significant wave height during summer, during winter and during storm conditions at the North Sea.

The change in discharge is an important driver for the salinity, hydrodynamics and the suspended sediment concentration. The internal asymmetry does not play a role with the changing fresh water discharge. The increase in tidal asymmetry with increasing discharge increases the available sediment in the water column. A combination of the increased estuarine circulation and the turbulence damping increases the sediment concentration in the lower layers of the water column. The sediment concentration in the top layer increases with decreasing discharge because the turbulence isn't damped anymore.

The waves have only small influence on the hydrodynamics and small influence on the suspended sediment concentration for the Rotterdam Waterway in the short term. If the waves occur for a longer period, the impact ETM increases resulting in the increase of suspended sediment concentration in the ETM.

A scenario study is executed to evaluate the effect of the harbor basins and to determine the effect of deepening. The harbor basins are important for the suspended sediment concentration, in particular for the available sediment in the bottom layer. The sediment settles less in the Rotterdam Waterway, but it settles in the harbor basin instead where the velocities are lower and the turbulence is low.

The effect of deepening is evaluated for two types of deepening. The first deepening is the deepening of the first step in the Rotterdam Waterway and the second deepening is near the location where the ETM moves to and fro in the estuary. The difference between the original depth and the deepened scenario is small for the deepening of the step. The salinity intrusion increased with 3 kilometers with increasing tidal prism. The step deepening results in decreased influence of the discharge on the location of the null point and leads towards a small increase in the suspended sediment concentration under average discharge and yearly average significant wave height due to increased ebb and flood velocities. The long term effect for the 5% discharge decreases, while the effect of the 95% discharge increases.

The impact is small if the deepening is in the area where the ETM occurs. The salt intrusion length is increasing but for the same tidal prism. The salinity intrusion increased with 3 kilometers, and the near bed velocities increase in the first part of the estuary. The influence of the discharge on the salinity null point has also decreased for the ETM deepening, but the difference is smaller compared with the step deepening. The increasing velocities near the bed lead to increased suspended sediment concentration in the ETM. The long term change shows also decreasing effect for the 5% discharge and increasing effect for the 95% discharge.

PREFACE

This report is the last part of my program of Civil Engineering and Management at the University Twente. Since my first lecture during the start of the bachelor program in 2010, I've learned a lot about civil engineering, but also soft skills like organizational skills and about myself. I've had the honor for example to organize the symposium for the study association ConcepT, was able to develop myself within student association 'In Den Natte' and to do my bachelor theses at the University of Tasmania in Hobart, Tasmania.

A lot of research has been done during the past years about estuaries and the estuarine turbidity maximum. Surprisingly not a lot of research has been done about one of the most important access channels of the Netherlands, the Rotterdam Waterway. I had the honor and joy to extent the knowledge about this interesting part of the Netherlands.

I want to thank some people in particular. First I want to thank Bart Grasmeijer for giving me the opportunity to do my master thesis by Arcadis in Zwolle. He was always kind to answer my questions and giving coffee in the early morning. I'd like also to thank Jos van der Laan, Nathanael Geleynse and Jeroen Adema from Arcadis for helping me with Delft3D and all the questions about the area and their results during their project about the Rotterdam Waterway for Arcadis. I'd also like to thank my supervisors from the University Twente Marjolein Dohmen-Janssen and Angels Fernandez-Mora for their supervision and feedback during the thesis. Last but not least I want to thank all my friends and family for their support during the process. They had to hear all the good things, but also all the frustrations.

Jan Gert Rinsema

TABLE OF CONTENTS

1 INTRODUCTION

1.1 Context

The Rotterdam waterway is part of the Rhine – Meuse estuary located in the Southwest of the Netherlands in the province of South-Holland (see Figure 1). The Rotterdam Waterway is located from Hook of Holland until the bifurcation of the Rotterdam Waterway in the Old Meuse and the New Meuse.

The Rotterdam Waterway has a length of 20,5 km, with a width varying from 480 to 675 m and a depth varying from -16 to -14.5 m NAP (Verdieping Nieuwe Waterweg, 2014). The width is dependent on the occurrence of structures like for example the Maesland barrier which creates a local decrease of the channel width.

The ongoing economic development of the Rotterdam harbor in the 20th century and the increase of the ship size caused demand for an increase of the capacity and the size of the access channel of the harbor. The main entrance of the harbor in the 20th century was entering the Netherlands by Haringvliet and going through the Voorne canal towards Rotterdam. The capacity of this route was however not sufficient anymore. A committee was established to find a solution of this problem. In 1862 the parliament and the minister-president Thorbecke initialized a law which stated the construction of the Rotterdam Waterway (Van de Ven, 2008). The total costs for the construction of the Rotterdam Waterway were in total 36 million Dutch guilder by the finishing of the Rotterdam Waterway in 1895. This was six times higher than the budged derived at the start of the project in 1862.

Figure 1 The Rotterdam Waterway in red (Maps, 2016)

The further increase in economic development and ship sizes increased the depth of the Rotterdam Waterway even more during the years after construction. To decrease the salt intrusion a ladder shape was introduced in the 60s and 70s of the 20th century (van Dreumel & Struyk, 1988), see Figure 2. Man induced interferences were also done to ensure the depth of the channel for the harbor. Groins were introduced in the bend near Maassluis and gravel was introduced at several locations to decrease the erosion of sediment. In 1976 the Rotterdam Waterway became the only 'free' runoff possibility of the river Rhine with the closure of the Haringvliet. The Haringvliet is still a possibility for fresh water runoff, but only regulated by the dam.

Until 2002, few maintenance had been done to secure the shape of the ladder line. This decreased the effectiveness of the ladder line and cause salt intrusion further upstream, especially during low discharges (van der Kaaij et. all, 2010).

Over time the demand for container terminals increased. First Maasvlakte and later Maasvlakte 2 were put into operation to fulfill this demand. The total transshipment of the Rotterdam Harbor Authorities is 466 million metric tons in 2015. This includes dry bulk, wet bulk (mainly oil) and container transshipment. The amount of transshipment is expected to increase further due to the development of Maasvlakte 2 until its capacity is fully utilized.

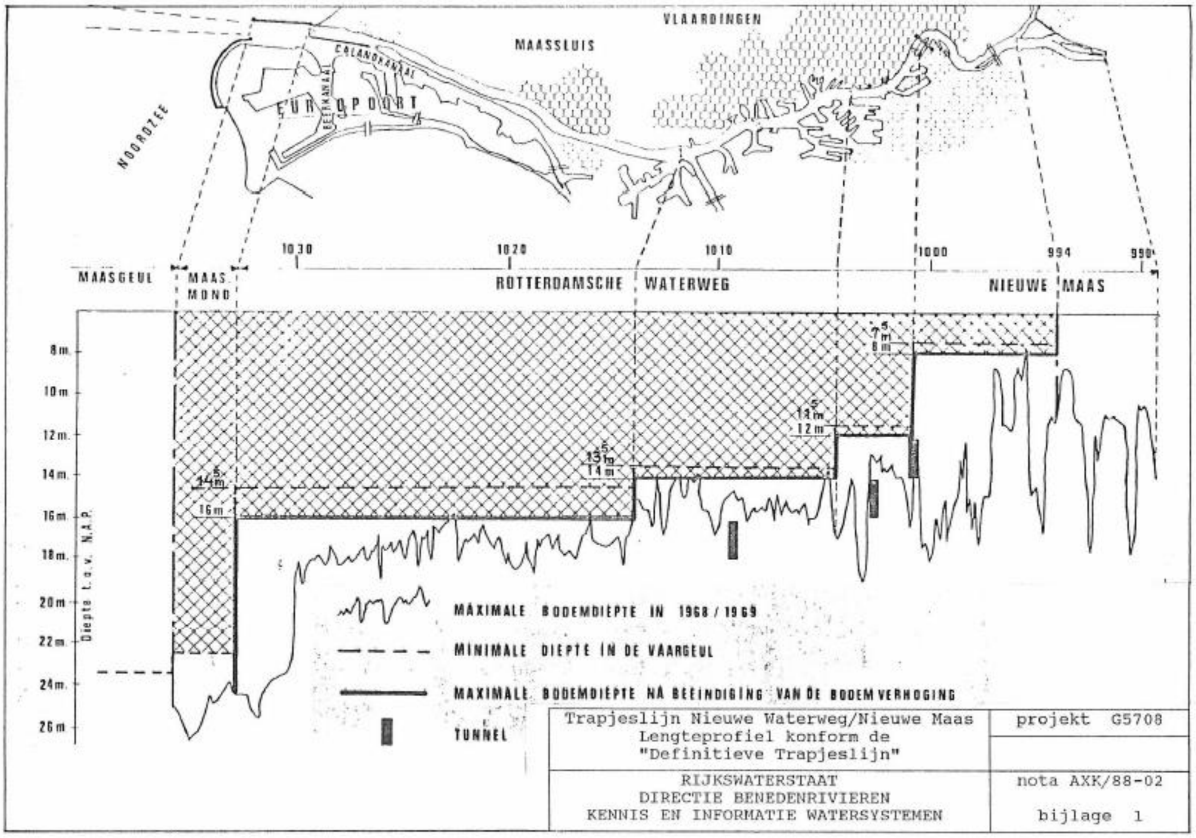

Figure 2 Ladder line in the Rotterdam Waterway (van Dreumel & Struyk, 1988)

1.2 Research background

Estuaries appear where a river meets the sea. The definition of an estuary according to Pritchard (1967) is: "an estuary is a semi enclosed coastal body of water which has a free connection with the open sea and within which sea water is measurably diluted with fresh water derived from land drainage". In the estuary fresh water from the river mixes with the saline water from the sea, causing a saline to brackish environment. Estuaries have a lower estuary where the marine system is dominant, a middle estuary where the mixing process is dominant and an upper estuary where the river discharge is dominant (Colling & Park, Waves, Tides and Shallow-water processes , 1999).

The shape of the estuaries is an important characteristic for the estuary. Two type estuaries exist: funnel shaped (or trumped shape) estuary and the prismatic estuary (Savenije, 2005). The funnel shape estuary has a wide lower system and a converging middle estuary which results in a smaller estuary for the upper estuary. The prismatic shape estuary has a constant width for the lower-, middle and upper estuary. The Rotterdam Waterway is a typical example of a prismatic estuary.

The mixing of the saline sea water with the fresh water from the river results in hydrodynamic, salinity and morphological processes which are typical for the type of estuaries. The processes of funnel shaped estuaries are described for several estuaries like for example the Ems, the Western Scheldt or the Fraser. However the research done for the dominant processes for prismatic estuaries is less.

De Nijs et al. (2009) is one of the first to describe the processes in prismatic estuaries, specific for the Rotterdam Waterway. The research focused on the processes determined based on a 13 hour measurement campaign. The important processes in the Rotterdam Waterway are described based on the salinity, the hydrodynamics and the morphology.

1.2.1 Salinity

The salinity is important for the water intake locations and for agriculture and because it determines several hydrodynamic processes (see section 1.1.2). The Rotterdam Waterway has a large discharge and a small tidal range (see section 2.3.1.). According to these phenomena a salt-wedge estuary (also called stratified estuary) develops (De Nijs *et al.*, 2011).

The strong stratification can be seen in Figure 3, with the salinity of the top layer in the upper panel and the salinity of the bottom layer in the lower panel. The top layer of the water column remains fresh (0 PSU) during the tidal cycle, while the bottom layer has a strong stratification from 22 PSU towards the seaward boundary towards 0 PSU at the fresh boundary within 14 km estuary length (de Nijs *et al.*, 2011). So the maximum stratification is 22 PSU during one tidal cycle.

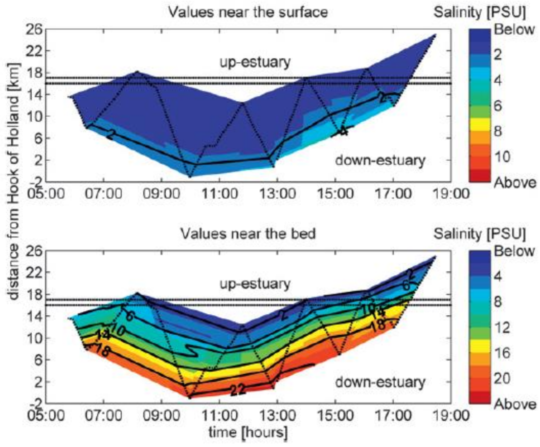

Figure 3 Along channel salinity distribution in at the surface in the upper panel and the salinity at the bottom at the lower panel (de Nijs et al., 2011)

Important for the stratification are the hydrodynamic conditions during the measuring campaign. The measurements were done two days for spring tide. The tidal amplitude is large and which is important for the length of the salinity intrusion. The stratification of the measurements is as expected based on the salt wedge classification of the estuary.

The salt wedge is not located at one position, but moves back and forth with the tide. The maximum intrusion of the salinity near the bed is called the null point of the estuary (Colling & Park, Waves, Tides and Shallow-water processes , 1999). The saline start of the salt wedge retreats 2 km upstream of Hook of Holland during ebb-tide at the surface, and 11 km stream upward of Hook of Holland near the bed in the middle of the waterway. During the second half of flood the salt wedge moves 9 km upstream near the surface, until the bifurcate of the Rotterdam Waterway with the Old Meuse and the New Meuse (De Nijs & Pietrzak, 2012). The intrusion length near bed has moved 21 km upstream near the bed. The shape of the salt wedge remained stable throughout the observation campaign and moves up and down the estuary with the tide (de Nijs *et al.*, 2011).

1.2.2 Hydrodynamic processes

The important hydrodynamic processes in estuaries are tidal asymmetry, internal asymmetry and gravitational circulation (Winterwerp, Fine sediment transport by tidal assymetry in the high-concentrated Ems River: indications for a regime shift in response to channel deepening, 2011).

1.2.2.1 Tidal asymmetry

Tidal asymmetry is the difference in length and amplitude of the ebb and flood in the estuary (Colling & Park, Waves, Tides and Shallow-water processes , 1999). The velocity profile corresponds with the asymmetry of the water level. A short flood period with high amplitude results in higher velocities compared with a long flood with a small amplitude. The left panel of Figure 4 shows the water level (in black) for the Rotterdam Waterway. The ebb duration has a long period (between 5:00 and 12:30) with a small amplitude (-0.9 m), compared with the flood duration which has a short period (between 12:30 and 19:00) with a large amplitude (1.1 m).

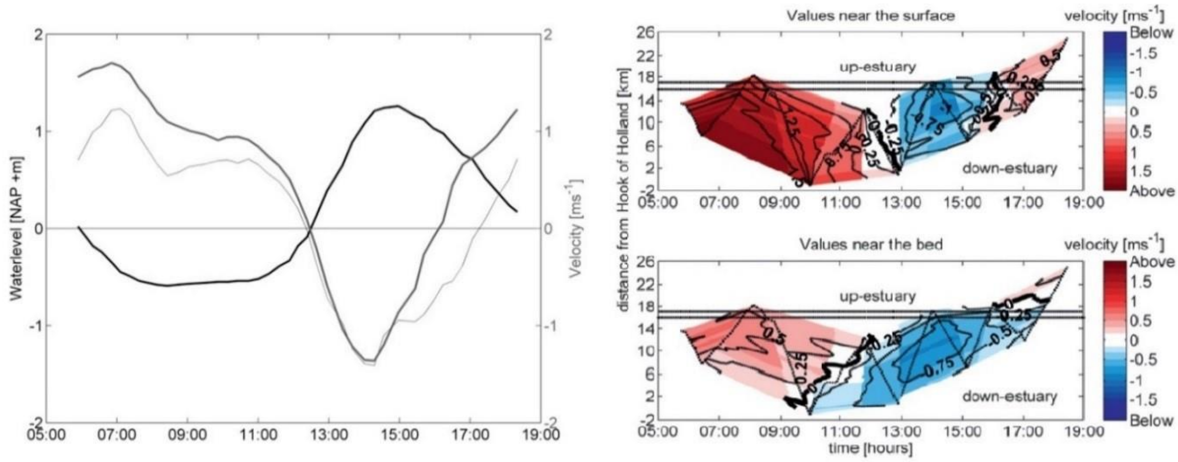

Figure 4 Left: Water level (black) velocity; velocity 2.5 m below surface (dark grey); velocity 12.5 m below surface (light grey line) 15 km upstream of Hook of Holland. Right: velocities near the surface (upper panel); velocity near the bottom. Negative velocity indicates flood velocity (lower panel) (De Nijs et al., 2011).

The water level suggests flood dominant estuary with higher flood velocities, the large discharge however increases the ebb velocity significant as can be seen in Figure 4 in the left panel for the lighter and dark grey lines. The maximum ebb velocity for the upper layer show larger ebb velocities (positive velocities) compared with the flood velocity (negative velocity) near the surface. The ebb velocity near the lower in the water column shows smaller ebb velocities, while the flood velocity is constant. In the lower part of the water column the maximum ebb and flood velocity is almost equal, 1.1 m/s for the ebb velocity and -1.5 m/s for the flood velocity. So the upper column seems to be sensitive for the discharge.

The large difference between the ebb and flood velocity is not only for the location 15 km upstream of Hook of Holland, it can be distinguished in all measured locations in the estuary as can be seen in the righter panel of Figure 4. The velocities are shown near the surface in the upper panel and velocities near the bottom in the lower panel with the flood velocities in blue and the ebb velocities in red. The ebb velocities near the surface are about 1.5 m/s while at the same time the ebb velocities near the bottom are about 0.75 m/s. The flood velocity is 0.75 m/s near the surface and near the bed.

The difference between the maximum ebb and flood velocity determines the estuarine circulation. For estuaries it often means an estuary outward directed flow near the top and an estuary inward directed flow near the bottom.

The length of the ebb and flood velocity shows a clear asymmetry in the estuary. The near bottom layer has a much longer flood period compared with the flood period in the near surface layer. The dominance of the tide determines the velocity in the estuary. Flood dominant means a longer ebb period which results in higher flood velocities. Internal asymmetry leads towards changing velocity profiles in the estuary. The difference in the near bed and near surface layer is due to the difference in the baroclinic pressure gradient.

The velocity in the water column is determined by two types of pressure gradients: the barotropic and the baroclinic pressure gradient. The barotropic pressure gradient is determined by the difference in water level and reads (De Nijs *et. al*, 2009):

$$\boldsymbol{\frac{1}{\rho}\frac{\partial P}{\partial x} = g\frac{\partial \eta}{\partial x}} \qquad \text{(eq. 1)}$$

Where $\boldsymbol{\eta}$ is the difference in water level over the x axis (estuary inward) and g is the gravitational acceleration. The barotropic pressure gradient is not dependent on the depth. The baroclinic pressure gradient is determined by the difference in density in the water column and reads (De Nijs *et. al*, 2009):

$$\boldsymbol{\frac{\partial u}{\partial t} = \frac{g}{\rho}\frac{\partial \rho}{\partial x}z} \qquad \text{(eq. 2)}$$

Where $\boldsymbol{\rho}$ is the density of the water column, which is determined by the salinity. Near the bed the baroclinic pressure gradient remains directed estuary inward because the density difference between the fresh and saline water remains intact due to the form of the salt wedge. The baroclinic pressure gradient is dependent on the stratification and therefore depth dependent.

The tidal asymmetry as described can summarized with the phase lag and relative amplitude between the M2 and M4 constituent of the tide (Friederichs & Aubrey, 1988). The M2 and M4 constituents are the most important constituent determining the ebb or flood dominance of the estuary. The equation for the phase lag reads:

$$phase\ lag = 2\theta_{M2} - \theta_{M4} \qquad \text{(eq. 3)}$$

Where a phase lag between 0 and 180 indicates a flood dominant estuary which means the tide rises faster than it falls. Asymmetry between -180 and 0 determines an ebb dominant estuary, which means the tide drops faster than it falls. The relative amplitude determines the relative strength of the M2 constituent and its first harmonic (Friederichs & Aubrey, 1988). The equation for the relative amplitude reads:

$$amplitude = a_{M2}/a_{M4} \qquad \text{(eq. 4)}$$

1.2.2.2 Internal asymmetry

The second asymmetry which is important for the hydrodynamics in the estuary is the internal asymmetry. Internal asymmetry is the deformation of the tidal wave, measured based on the M2 and M4 constituent of the tidal wave like the tidal asymmetry. The deformation is general due to the bathymetry. Shallow areas or change in estuary with deforms the tidal wave which leads to internal asymmetry.

The Rotterdam Waterway does not generate internal asymmetry based on the measurements. The tide has already been deformed due to the interaction with the geometry in coastal zone and the topography. It is assumed the tide is not deformed due to the absence of intertidal flats, the prismatic shape of the Rotterdam Waterway and the relative small tidal amplitude related to the water depth (De Nijs *et al.*, 2011). So the Rotterdam Waterway does not create internal tidal asymmetry by itself, but the asymmetry is forced externally. This is also seen in the velocity pattern of the Rotterdam Waterway in Figure 4 in the left panel. No large distortion of the velocity is visible for the tidal velocity, only due to the discharge in the upper water part of the water column. This indicates that the effect of non-linear water interactions on the generation of M4 due to the bathymetry over tides is small (De Nijs *et al.*, 2009).

1.2.2.3 Gravitational circulation

The last important hydrodynamic process discussed in estuaries is the gravitational circulation (Hansen & Rattery, 1966). Gravitational circulation is the vertical velocity which is formed due to density differences. So the density difference does not only generate horizontal velocity (due to the baroclinic pressure gradient), but also vertical velocity. This increases when the stratification of the estuary increases, because the density difference becomes creates a horizontal stratification component. The vertical velocity tends to create a net landward current near bed.

1.2.3 Sediment transport

The sediment transport is determined by the interaction of the hydrodynamics with the bathymetry and the sediment available in the waterway.

1.2.3.1 Fine sediment

The fine sediment is important for the formation of the Estuary Turbidity Maximum (ETM) in the estuary, because the fine sediment small enough to be kept in suspension in the estuary. Several processes are important for the formation of the ETM, which are tidal pumping, turbulence damping and flocculation. For the formation the available sediment is as last discussed for the formation of the ETM.

Tidal pumping
The tidal pumping is the result of tidal asymmetry or internal asymmetry (Brennon & Le Hir, 1999). In a flood dominated estuary the flood velocity is higher compared with the ebb velocity. More sediment of larger grain size is therefore eroded from the bottom and moved estuary inward. Although the ebb duration is longer, the ebb velocity is lower resulting in less eroded sediment picked up and moved back estuary outward again. The resulting direction of the sediment transport is estuary inward, leading to the net import of sediment in the estuary.

The measurements of the Rotterdam Waterway show a maximum flood velocity of 0.75 m/s near the bed and a maximum ebb velocity of 0.5 m/s, as indicated in section 1.1.2. So there is tidal pumping near the bed of the Rotterdam Waterway with a residual velocity estuary inward.

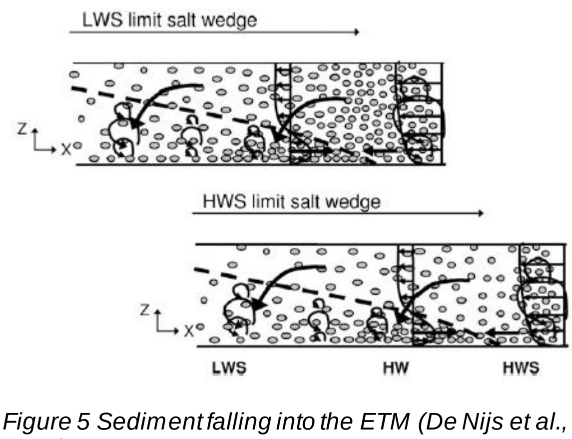

Figure 5 Sediment falling into the ETM (De Nijs et al., 2009)

Turbulence damping
The second important process for the fine sediment is the turbulence damping. Turbulence is introduced when the water flows over the bottom facing roughness. The introduced turbulence is decreasing towards with the increasing height in the water column. The interaction between the saline near the bed and the fresh water near the top is low, also due to the salt wedge with the

sharp distinction between saline and fresh layers. The turbulence is damped due to the small interaction between the saline and fresh part of the water column.

When the water column contains suspended sediment and the turbulence has damped, the sediment 'rains out' in the lower saline water column during slack tide, as can be seen in Figure 5. Due to the turbulence damping, more sediment is able to settle compared with a situation without turbulence damping.

The ETM occurs at the null-point of the halocline of salinity. The trapping process is associated with the trapping of Suspended Particle Matter (SPM) from the upper fresh part of the water column in to the more dense salt water below (Nijs *et al.,* 2011).

Flocculation
Flocculation is the last important factor for the suspension of sediment in the ETM. Flocculation is the formation of larger grain sizes of smaller flocs (Colling & Park, Waves, Tides and Shallow-water processes , 1999). When the sediment enters the saline environment, the biological activity creates the larger flocs leading to increased fall velocity.

For the Rotterdam Waterway however, there seems to be no formation of flocs in the estuary. The flocs have already been formed when the sediment enters the estuary from the fresh water discharge of the Old Meuse and the New Meuse (de Nijs *et al.*, 2011). So the settling of SPM is not increased in the Rotterdam Waterway.

Available sediment
The formation of the ETM is only possible if enough sediment is available. The suspended sediment concentration for the Rotterdam Waterway was measured until 2012 near Maassluis, of which the period from 1995 until 2010 is shown in Figure 6. The sediment concentration was measured every two weeks. The water from the top 1 meter of the water column is pumped into a small reservoir. The amount of sediment is dried and weighted to determine the sediment concentration. The average concentration is 30 mg/l between 1995 and 2010. The minimum suspended sediment concentration is 3 um or smaller, and the maximum of 230 mg/l.

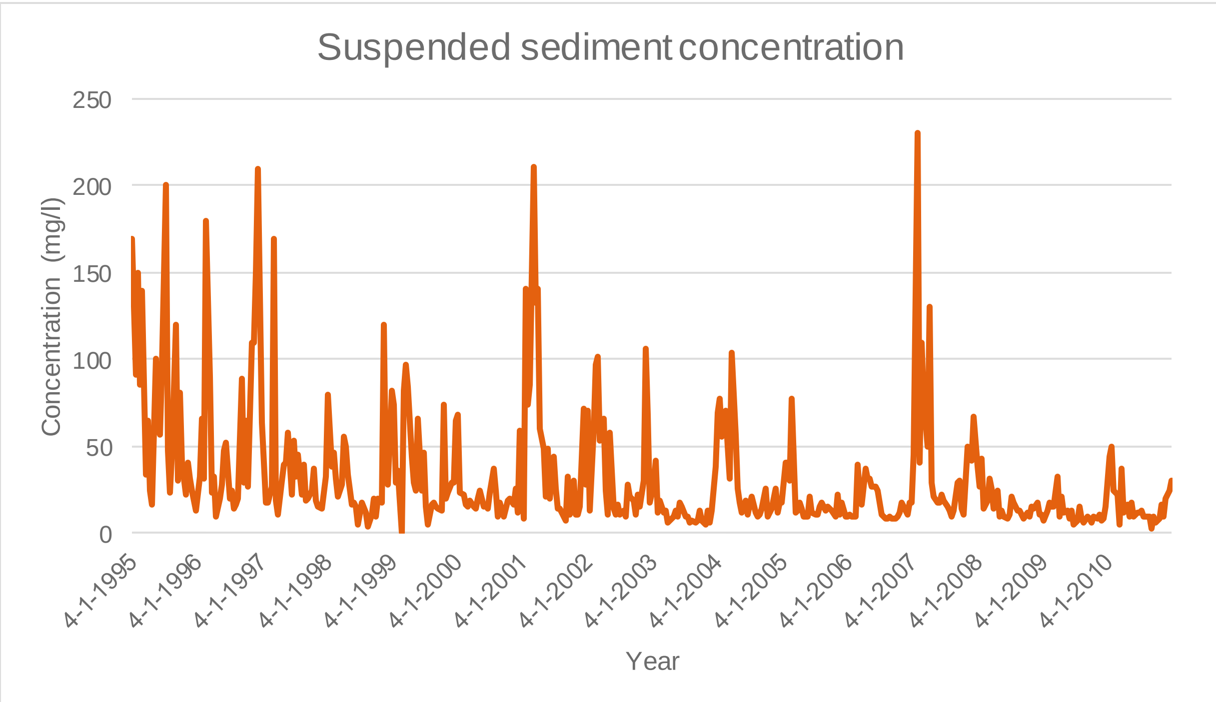

Figure 6 Suspended sediment concentration near Maassluis (Rijkswaterstaat, 2016)

The available sediment seems to be dominated by the sand based on the dredged material, because approximately 80% of the dredged volume is sand near the mouth as can be seen in Figure 7. The Sand is defined as sediment larger than 200 um (Colling & Park, 1999). The remaining 20% of the dredged material consist of silt, gravel and clay.

The dredged material is not the same everywhere in the waterway. There is variation in sediment between the bifurcation and the mouth of the estuary. The percentage of sand is decreasing and the percentage of silt is increasing estuary upward. The d50 is decreasing due to the increased percentage of silt. The percentage of gravel is varying, but not with a clear structure. Where for example the potholes exist in estuary upstream of kilometer 115, the amount of dredged gravel has increased compared with the dredged material near kilometer 115.

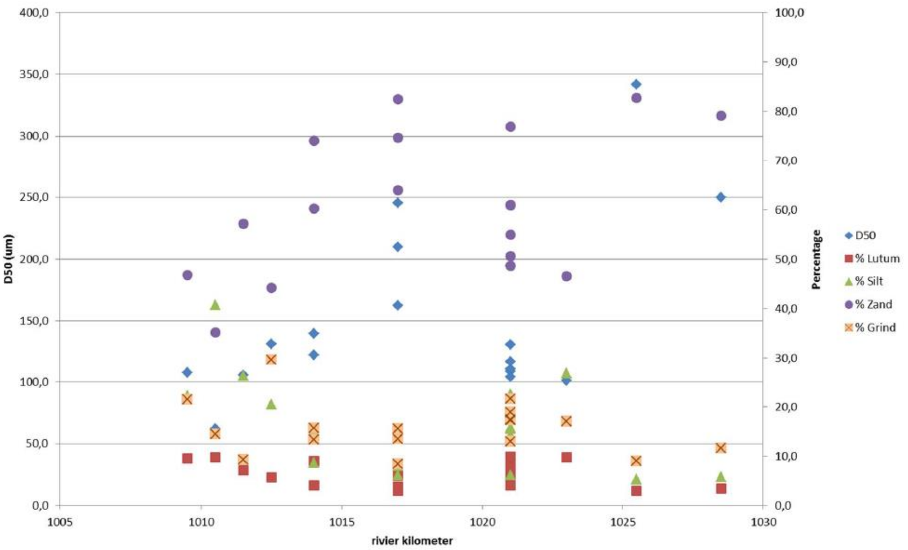

Figure 7 Sediment characteristics Nieuwe Waterweg (van Westeren et al., 2004) for clay (red square), silt (green triangle), sand (purple circle) and gravel (orange square).

The concentration of suspended sediment in the ETM is determined by the sediment import from sea, from the river and the resuspension of settled SPM from the bed. Man induced operations disturb these processes by the continuous dredging operations to keep the harbor and the channels accessible. A contribution of the dredging towards the SPM in the ETM is the upwelling of sediment from the bottom into the column.

The SPM in the Rotterdam Waterway is mainly originated from the river discharge (de Nijs *et al.*, 2010). All the available SPM is trapped in the ETM, because no sediment settles in the Rotterdam Waterway. If the sediment settles during HWS or LWS, it is immediately re-suspended if the current velocity increases again. The re-suspension indicates the transport capacity of the water column is not yet fully utilized (de Nijs *et al.*, 2010). This is subscribed by the dredging operations in the Rotterdam Waterway which mainly dredge sandy sediment particles, so no fine sediment settles near the bed.

The siltation of harbors in the lower marine area like the Europoort is due to storm events bringing in large amounts of suspended sediment into the estuary, and only about 20-25% of the dredged sediment has fluvial origin (Verlaan & Spandhoff, 2000). So in this part of the Rotterdam Waterway suspended sediment from the sea is present, but is not in the middle estuary.

Formation of ETM

The combination of the available sediment and turbulence damping results in the ETM in the Rotterdam Waterway, as can be seen in Figure 8. The location of the ETM is at the null point of the salinity, because the sediment from the top layers rains out in the saline layer and the baroclinic pressure is moving the sediment towards the null point.

A clear distinction in sediment concentration is visible between the concentration near the surface in the upper panel and the concentration near the bed in the lower panel. The suspended sediment concentration at this point is about 0.8 kg/m^3 near the bottom while the concentration near the surface at the same location at the same time about 0.03 kg/m^3 is.

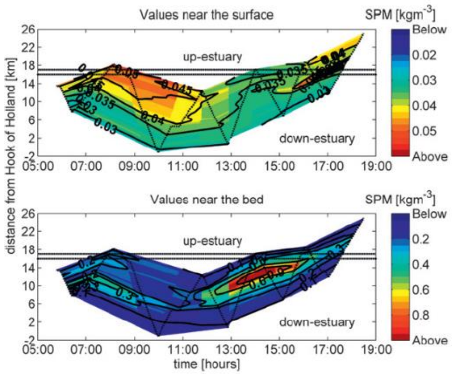

Figure 8 SPM concentration near the surface (upper panel) and near the bottom (lower panel) (De Nijs et al., 2011)

The time period for the suspended sediment exchange between the fresh top layer and the saline bottom layer is observed is longer during LWS than at HWS. This is due to the decrease of the density driven current in the x direction at the end of HW relative to LW. The barotropic pressure gradient is also larger near HWS compared with LWS.

During flood the ETM travels upward and moves into both the Old Meuse and New Meuse together with the movement of the salt wedge. The ETM has the maximum intrusion length during HWS. A part of the water and sediment travels into the Botlek Harbor. During ebb tide the ETM travels downstream and increases in density due to the combination of the two ETM's from both channels (Nijs *et al.,* 2011). So the bifurcation of the Old and New Meuse drives the ETM to split up. The concentration of suspended sediment of the ETM in both bifurcations is unknown.

Not all the sediment is continuous being trapped in the ETM. About 50% of the available sediment escapes towards the sea (De Nijs *et al.*, 2010). Other removal of sediment from the ETM is the siltation of sediment in the harbor basins (De Nijs *et al.*, 2009). The harbor basins seem to be efficient sediment traps for fine sediment. The sediment flows into the harbor basins due to advective processes during the tidal movement. So the location of the ETM is important for the siltation of the harbor.

1.2.3.2 Sand

Not only the dynamics of the fine sediment is important for the morphological development, also the coarser grain size sediment is important for the physical processes carrying larger sediment particles, mainly sand. Due to erosive patterns in the Rotterdam Waterway, the ladder line eroded see Figure 2. The erosion of the ladder line leads to natural deepening of the estuary and possibly the increase in bed roughness and thus an increase in turbulence. An increase in deepening will enhance the ETM processes as described in the previous section.

The erosion of bed material is due to events like storm surges, but also due to man-made structures like grid bottoms and groins in the river bends. The sediment balance seemed to be constant between 2000 and 2008, but this is mainly due to the dredging maintenance of 412x10^3 m^3/year in this period. The dredging volume was even 530x10^3 m^3/year between 1990 and 1999 (Snippen, et al., 2005).

Most of the bedload sediment entering the estuary is originated from the sea (1660000 tons/year) during the years 1990-2000, while only a minor amount of bedload sediment is originated from the river (440000 tons/year) (van der Kaaij *et al.*, 2010). The tidal asymmetry is important for the bed load sediment due to the differences in flow velocity (Dronkers, 1986). Higher flood velocities transport more bedload into the estuary than the ebb current will do towards the sea.

1.2.4 The effect of deepening

Because of the need for deepening for many years, the effect of channel deepening has been topic of research for many years. O'Brien (1969) derived a relationship between the tidal prism (P) during spring tide and the cross sectional area (A):

$$A = \alpha P^{\beta} \qquad \text{(eq. 5)}$$

Indicating a deepening wil lead to increased salt intrusion and thus sediment transport. An overall synthesis on channel deepening is introduced by Winterwerp (2011). According to Winterwerp (2011) three stages can be distinghuised for the deepening of estuaries:

1. The equilibrium situation will be restored due to accumulation of sediment. This is done by a decrease in river-induced flushing and the decrease of the ebb velocity due to the increase of flood velocity. Gravitational circulation increases leading to increased tidal and or internal asymmetry. The effect depends on the net effect of the increase in water level and the decrease in the generation of higher harmonics. Accumulating of sediment possibly causes a rigid bed form which decreases the bed roughness. If the accumulating fine sands do not form a rigid bed form, they are available for resuspension, and thus increases the ETM concentration.
2. A further increase in channel depth increases the suspended sediment concentration and the remobilized sediment as well. If the bed becomes muddy intertidal asymmetry becomes dominant over gravitational circulation due to the decrease of the turbulence induced by the bed. This increases the remobilization of sediment, increasing the sediment concentration and increasing the accumulation. This feedback loop is initialized in this phase. The water column is stratified during ebb. The rate of the accumulation of fine sediment is due to the import of sediment at the boundary condition.

3. During the final and third phase the import of sediment is strong. The gravitational circulation does not play a role anymore, because there is almost no turbulence due to the bed anymore, so more sediment is able to settle during slack tide. The suspended sediment is moved towards the river head by tidal asymmetry. The river becomes highly turbid over the alongshore direction, not only in the ETM. A fluid mud develops in the total length of the estuary which can carry sediment concentrations over 100 g/l (Colling & Park, 1999).

1.3 Problem definition

The interaction of fresh and salt water is one of the main drivers of hydrodynamic and sediment transport processes in estuaries, as described in the previous section. Other important drivers are the tidal range and the river discharge determining the tidal asymmetry. The internal asymmetry is determined by a combination of tidal range and the estuary geometry. With changing conditions, these processes and their influence towards the hydrodynamic and sediment transport processes also change.

For the naturally funnel shaped estuaries these processes have been studied a lot. For example the Ems by Talke *et al.* (2009) and Winterwerp *et al.* (2011); The Yangtze by Guo *et al.* (2014) and Hu *et al.* (2009) or the Western Scheldt by van der Wegen *et al.* (2012), a more extensive evaluation of the used models in estuaries is given in appendix A. For prismatic estuaries however, typical estuarine processes have hardly been studied in the past, while the shape is an important element in the hydrodynamic and sediment transport processes for the estuary.

Economic developments cause man induced changes in the system if the estuary is for example the access channel for a harbor area. These changes cause increased sediment transport for fine sediment in funnel-shaped estuaries. The increased sediment transport demands increased maintenance to keep the channel accessible for ships (van Maren *et al.*, 2004).

The Rotterdam Waterway is an important prismatic estuary for the Netherlands. To increase the accessibility of the Botlek harbor for example, the Rotterdam Harbor Authorities want to deepen the Rotterdam Waterway (Verdieping Nieuwe Waterweg, 2014) from the mouth until the Beneluxtunnel.

The deepening probably affects the hydrodynamic and sediment transport processes in the Rotterdam Waterway. De Nijs et al. (2009; 2011; 2012) did a 13 hour measurement campaign to evaluate the estuary processes in the Rotterdam Waterway near Hook of Holland and the Botlek harbor, as described in chapter 1.2. The synthesis about the processes was only based on the 13 hour measurements, not on a spring neap tidal scale. The effect of deepening on the estuary processes is also unknown. In order to understand and predict morphological changes for prismatic estuaries like the Rotterdam Waterway, the hydrodynamics and the sediment transport characteristics for prismatic estuaries need to be understood.

The effects of deepening are difficult to determine if for example the Harbor Authorities of Rotterdam wants to know the change hydrodynamics and suspended sediment concertation due to the intended deepening. The hydrodynamics are important to know for the conditions under which the ships are entering the harbor. If the flow velocity increases or decreases at certain, this should be known in advance to determine if they are acceptable for the ships who enter the harbor. The suspended sediment transport is one of the drivers of the morphological changes in the channel, and is therefore important for the dredging strategy to determine. The harbor authority can determine the difference in dredging costs and decide if the changes are acceptable.

1.4 Objective and research questions

1.4.1 Research objective

The research objective is to identify important estuary processes which determine hydrodynamic and sediment transport characteristics of prismatic estuaries and to determine the effect of changes in the estuary bathymetry, for example due to deepening, on the hydrodynamic and sediment transport characteristics, using numerical modeling. The Rotterdam Waterway is used as a case study to evaluate the processes and the effect of deepening for prismatic estuaries.

1.4.2 Research questions

1. *Which processes determine the salt intrusion in the Rotterdam Waterway?*
2. *Which processes determine the hydrodynamics in the Rotterdam Waterway?*

3. *Which processes determine the suspended sediment transport in the Rotterdam Waterway?*
4. *What is the effect of channel deepening for the described processes for the Rotterdam Waterway?*

1.5 Methodology

The general processes in estuaries and the specific estuary processes for the Rotterdam Waterway specific are examined based on literature to answer research question 1. Typical variables which indicate changes in these processes are also identified based on the literature review.

A schematized 3D model is used to determine the most important hydrodynamic and sediment transport processes. Use is made of the numerical model Delft3D. Delft3D is chosen because it makes it possible to evaluate the combination of, and the interaction between the hydrodynamics and the sediment transport. The hydrodynamics is a combination of the tide and the short waves. The model includes a FLOW module to simulate the tide and a WAVE module to simulate short waves. The online coupling makes it possible model receives new information The waves are included to include the hydrodynamic motion partly determined by the waves and to include suspended sediment coming from sea to which is brought into suspension by the waves.

The area is schematized as a simple rectangular foreshore of and a long small rectangular estuary. The schematization of the area gives several advantages. Due to its simplicity it is easier to determine what caused the change. In a detailed model the variation in width, depth and orientation give all kind of implicit changes that increases the difficulty for the analysis. Another advantage is the speed of the model time. Due to the simplicity the simulations are relatively fast which makes it possible do a sensitivity analysis for the several discharges and wave conditions.

The boundary conditions of the model are determined based on measurements of the tide, the waves and the fresh water discharge. Then the model is calibrated based on the water levels from the calibrated Harbor Authority Model (HBR) (Arcadis, 2015). The Harbor Authority Model is a calibrated model from the Harbor Authorities based on three phases of the tide which are neap, average and spring tide and based on the different discharges from the Rotterdam Waterway. The calibration based on the HBR makes the calibration easier, because the boundary conditions are known and constant. The salinity, flow velocity and suspended sediment concentrations are validated based on the measurements of De Nijs *et al.* (2009).

A sensitivity analysis is executed with the validated model. The boundary conditions are changed to determine the effect of the change in conditions for hydrodynamics and the sediment transport characteristics. The elements that are changed are the fresh water discharge and the wave conditions based on the conditions as they occur in study area. The variation of the boundary conditions is determined within the range of realistic values of the Rotterdam Waterway. The first three research questions are answered with the results of the sensitivity analysis.

A scenario study is executed to determine the effect of deepening. scenarios with the changes are executed for both the current situation, which is called the 'reference depth', and for the deepened situation. The parallel execution of the scenarios has the aim to determine the sediment transport characteristics of the Rotterdam Waterway, and determine the effect of deepening. This effect of deepening will answer research question 4.

To include the effect of special characteristics of the area of the Rotterdam Waterway, one scenario includes simplified harbor basins in the model. This tests the hypothesis of the siltation of the sediment, which has been assumed to be true but has only briefly evaluated by for example De Nijs *et al.* (2012). One harbor basin is included at the mouth of the estuary to be a possible sediment trap for the sediment from sea, and one harbor basin is included near the estuarine turbidity maximum (ETM) of the estuary to be a sediment trap for the sediment from the river and the turbidity maximum.

The results are analyzed based on the changes for several variables. These variables are:

1. Salinity
2. Tidal asymmetry
3. Turbulence
4. Gravitational circulation
5. Flocculation
6. ETM shape and size
7. Sediment availability in bottom layer

For the salinity the shape of the salt wedge (stratification) is evaluated, as well as the location of the null point. The salinity is important for the surrounding area, but also for the location of the ETM. The influence of flocculation and turbulence damping corresponds with the location of the salt wedge and the length of it. Increasing length of turbulence damping.

Tidal asymmetry determines the flood- or ebb dominance of the water level and thus the asymmetry of the depth averaged velocity and the maximum velocity near the bed. Increase in tidal asymmetry means an increase in length or amplitude difference between ebb or flood. This possibly causes larger velocities which carry sediment more upstream or downstream.

Turbulence is important for the suspended sediment to keep the fine sediment in suspension, especially when the accelerations in the water are low like during slack tide. Increased turbulence possibly increases the suspended sediment concentration. Decreased turbulence or increased turbulence damping leads to higher concentration in the upper part of the water column.

The flocculation is evaluated based on the fall velocity. The sediment transport formula used includes the effect of increasing grain size of suspended sediment in saline environment due to flocculation. An increasing grain size leads to increasing fall velocity of the sediment, which could lead to a larger amount of silt in the bed at the location where the sediment flocculates.

The ETM is evaluated based on the size, the location and the maximum concentration for both the initial response and the response after some time. The evaluation does not explain the changes in the ETM, but detects changes in the ETM which can be explained by the other factors that are evaluated. To include all the elements the evolution of the ETM is evaluated. First the initial response as a result of the imposed changes is evaluated by changing the boundary conditions after a month of run up time. Then the simulation is extended with 12 weeks to evaluate if the suspended sediment concentration is still growing, or stable in time.

The availability of sediment in the bottom layer shows the settling of sediment at the bottom. It possibly explains the increase of the ETM at the initial response of the system to changing conditions, because the available fine sediment at the bottom is eroded during the first period after the change.

1.6 Outline

The thesis is organized in 9 chapters. In the chapter 2 the study area is introduced more extensively. Chapter 3 describes the model and the setup of the model. The calibration and validation of the model explained in chapter 4 and the scenarios are explained in chapter 5. The results of the scenario study with the model are elaborated in chapter 6. The discussion of the results and the research is done in chapter 7 and the conclusion and recommendations with respect to the research questions is elaborated in chapter 8.

2 STUDY AREA

The characteristics of the Rotterdam Waterway are introduced in this chapter. First the geometry of the Rotterdam Waterway and the geometry of the North Sea are discussed. Second the tide, waves and fresh water discharge are addressed.

2.1 Geometry

2.1.1 Rotterdam Waterway

The Rotterdam Waterway is human made. In the early 19th century the Rotterdam Waterway was a natural river, but to stop the sedimentation the channel was created. In the 20th century the ladder line was created to prevent salt intrusion, as can be seen in Figure 2.

The ladder line is introduced between km 990 and 1035 of the river Rhine (van der Kaaij *et al.*, 2010). Although the counting is from the beginning of the river Rhine, the study area has different names. The Rhine is called the Rotterdam Waterway between km 1014-1035 and the Old Meuse is between km 990-1014, see Figure 2. Man-made interferences caused change of the ladder line shape, which can be seen in Figure 9. Variations are due to groins near Maassluis (called ‘Kribben Maassluis’), the decrease in channel width due to the construction of the Maeslantkering (storm surge barrier) or the bifurcation of the Rotterdam Waterway into the Old and the New Meuse (‘Splitsing Oude Maas’). Other interruptions of the ladder line are due to several parts of potholes (‘kuilen’) near for example kilometer 1015. These are probably formed due to better erodible bed material at these locations, compared with the bed material elsewhere.

The lower panel of Figure 9 shows the cross section width of the Rotterdam Waterway. The cross section is disturbed with the man-made interferences. The cross section of the last kilometers of the river Rhine (km 1005 – km 1035) is linear increasing towards the mouth, from 400 meter width near kilometer 1005 towards 600 meter width near the mouth of the estuary. The variation of the Rotterdam Waterway however is small, which is approximately 500 m wide at the bifurcation and 600 m wide at the Maesland barrier.

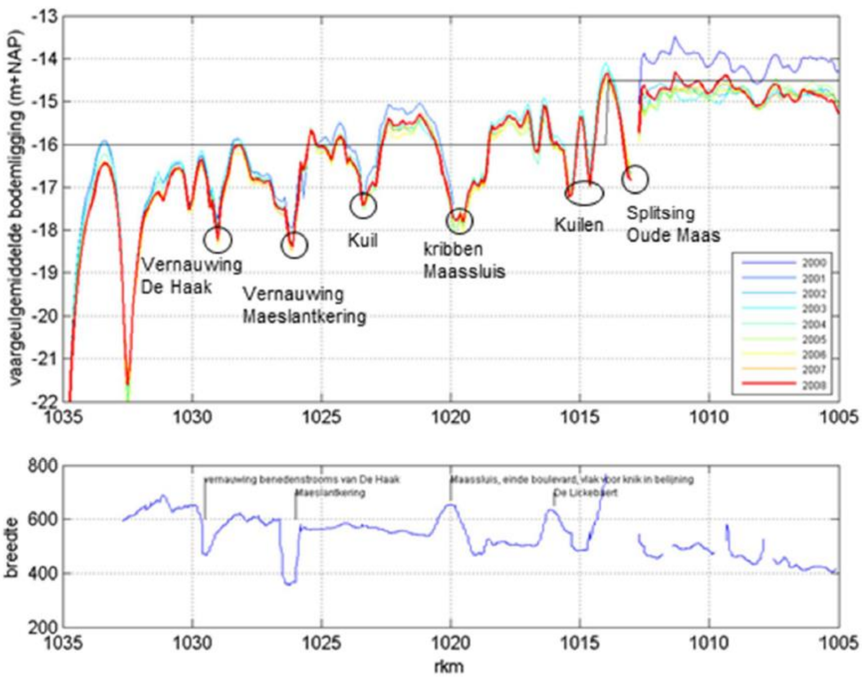

Figure 9 Bathymetry (upper panel) and the width (lower panel) of the Rotterdam Waterway (van Dreumel et al., 2010)

2.1.2 North sea

The geometry of the North Sea is also influenced by human interventions. In front of the Rotterdam Waterway the construction of the Maasvlakte and the Maasvlakte 2 change the morphodynamic system in front of the Rotterdam Waterway. At the southern boundary the construction of the Haringvliet change the hydrodynamic flow and thus the morphodynamic system.

Figure 3 shows the foreshore of the North Sea at four locations. Scheveningen and Ouddorp are situated at the boundary of the study area. Ter Heide and the Maasvlakte are in the middle between the Rotterdam Waterway (and the navigational channel) and the boundaries. The depth profiles are taken perpendicular towards the coast (Bathymetry, 2016).

Ouddorp, Ter Heide and Scheveningen show a small increase from -20 meter NAP 20 kilometer offshore towards -15 m NAP about 5-8 km offshore with some smaller irregularities (sand banks). Then the increase in bottom slope steepens towards the beach. The Maasvlakte shows a large depth of -35 m NAP between 5 – 8 km offshore.

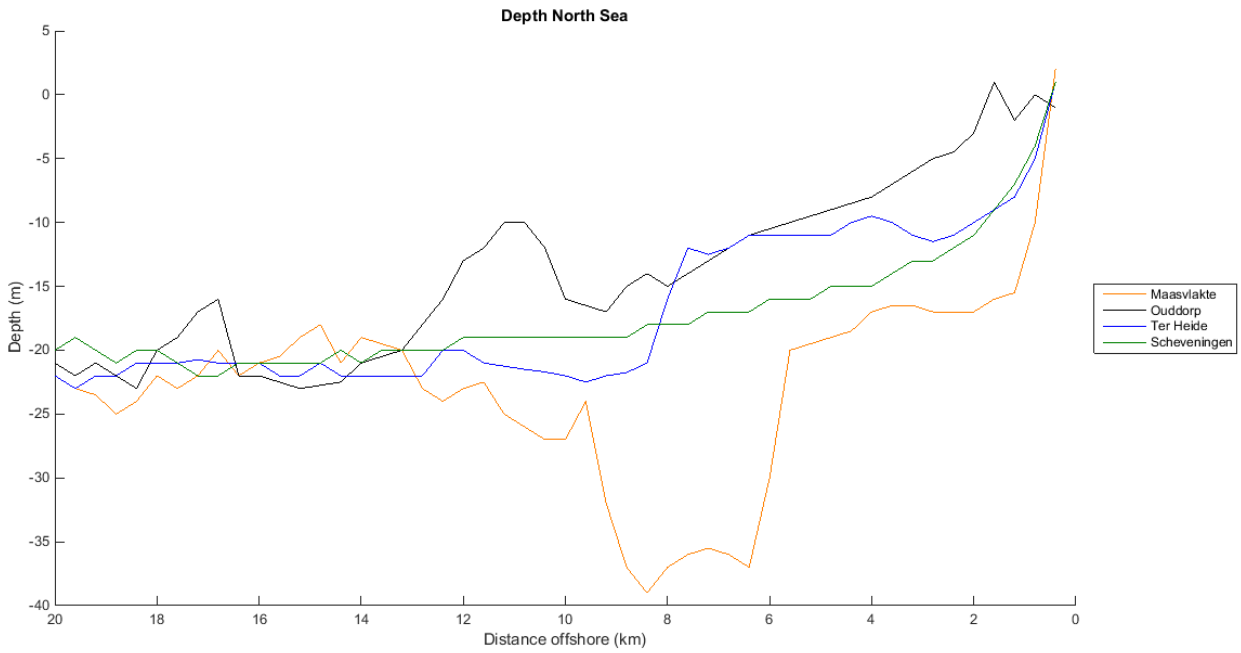

Figure 10 Bathymetry North Sea for four locations

2.2 Tide, waves and discharge

The hydrodynamic conditions for the tide and waves are described based on measurements of the Europlatform. The tidal and wave conditions in the North Sea are registered by a several measuring platforms; one of the platforms is called the Europlatform. The Europlatform is located 45 kilometers offshore of Ouddorp in the North Sea. The tidal and wave conditions for the Europlatform are representative for the North Sea in front of the Rotterdam Waterway.

2.2.1 Tide

The tide is a large wave with a period of 12 hours and 25 minutes determined by the interaction of the earth and moon, in combination with the rotation of the earth. The result is a wave moving around an amphidromic point. In the center of the amphidromic system, there is no movement of the water. For the North Sea an amphidromic point is located near Scotland. This results in a Kelvin wave moving around the center of the system from South to North.

The most important constituents for the tide are the M2 and S2 tide. The M2 is principal lunar semi-diurnal and is the basic elevation of the tide, while the S2 is the principal solar semi-diurnal tide which determines the neap spring tide elevation. The M4 tide is the first lunar overtide and determines the daily inequality of the water level.

The astronomical tide for 2015 can be seen in Figure 11, with the water level on top panel and the astronomical tide in the bottom panel. The maximum tidal amplitude for the astronomical tide is 1,98 meter, the minimum is 0,3 meter and the average tidal amplitude is 0,98 meter. The measured water level is influenced by both the tide and the short waves.

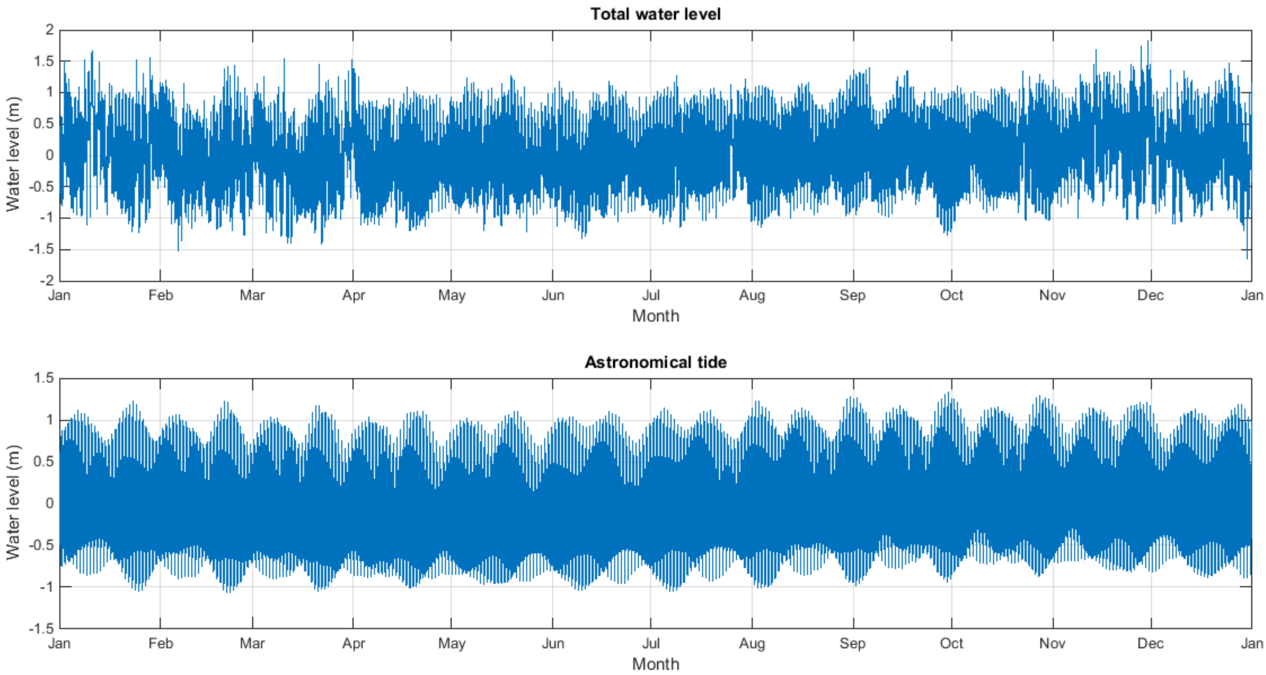

Figure 11 Tidal characteristics Europlatform in 2015 (Rijkswaterstaat, 2016)

Internal processes in the estuary deform the tidal wave as explained in section 1.1.2. This is due to the interaction with the fresh water discharge and the geometry of the channel. A first impression of the internal processes can be formed based on measurements done in the Rotterdam Waterway, as can be seen in Figure 12. The tidal wave decreases towards Maassluis with 13 cm, but increases again after the bifurcation. The flood duration increases slightly towards Maassluis with 13 minutes. From Maassluis towards Rotterdam the flood duration decreases again with approximately the same amount.

Although Figure 12 suggests that the tidal amplitude and the ebb duration are increasing linear from Maassluis towards Vlaardingen, this cannot be stated based on the data from Rijkswaterstaat. The data only includes several points, so it can only be stated that the tidal amplitude near Vlaardingen after the bifurcation is larger than near Maassluis.

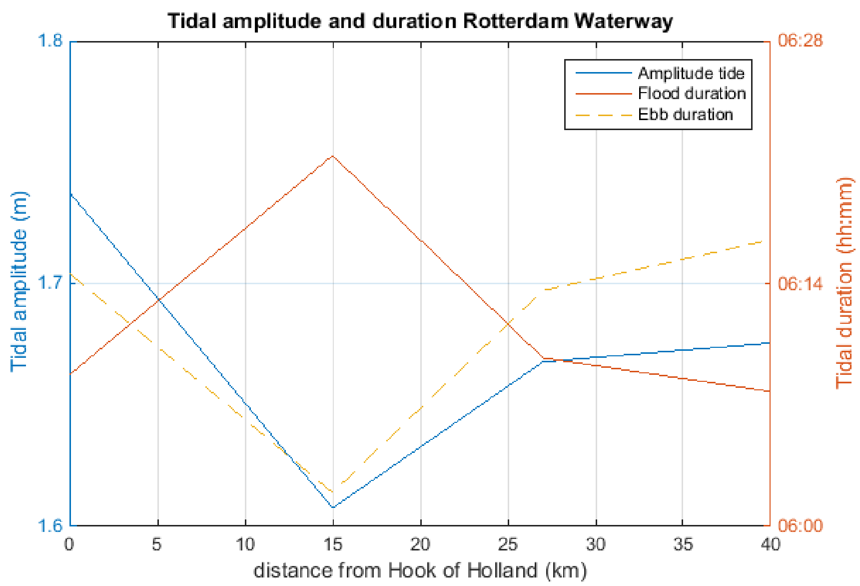

Figure 12 Tidal amplitude and duration in 2015 for Hook of Holland (km 0), Maassluis (km 15), Vlaardingen after bifurcation (km 27) and Rotterdam (km 40) (Rijkswaterstaat, 2016)

2.3 Waves

Short waves approach the shore in the shallow sea, together with the large wave caused by the tide. These waves are generated by the wind, and have a small wave period of seconds. The impact of individual short waves is less due to the large variation in length and height of the waves. The waves deform due to shoaling, refraction and breaking when they enter shallow water and approach the shore.

The short wave conditions for the North Sea are measured by the Europlatform and show a large variation in wave height, wave period and wave angle as can be seen in Figure 13. The data includes the significant wave height, the average wave period and the dominant wave angle for every hour. The average significant wave height is 1.3 meters for the year. The minimum significant wave height is 4.76 meter while the maximum significant wave height is 0.17 meter.

The seasonal variation is also visible for 2015, with increasing wave height and wave period in the winter and decreasing wave height and wave period for the summer. The wave height show some large variation for the winter and the autumn with relative large significant wave height events indicating storm events.

The wave period of the short waves corresponds with the wave height, increasing wave height leads also to increasing wave period. The wave period varies between 2.5 and 7 seconds as can be seen in the middle panel of Figure 13.

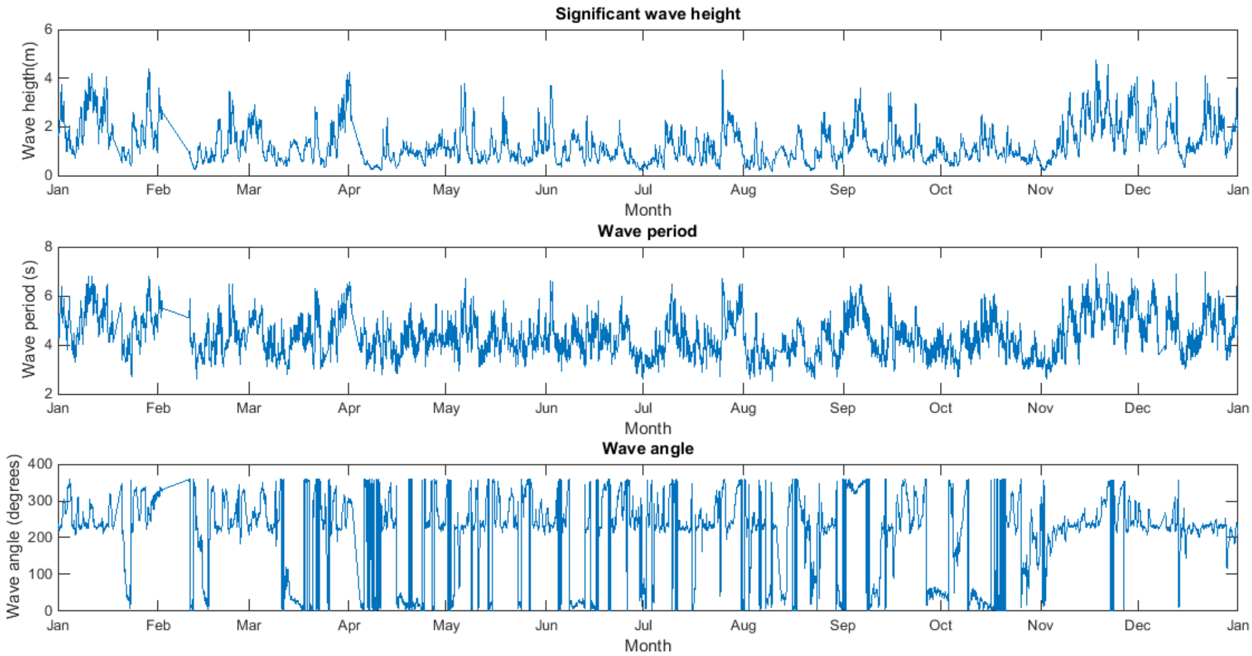

Figure 13 Wave characteristics of the waves at the Europlatform

2.4 Fresh water discharge

The Rotterdam Waterway is important for fresh water discharge in the Netherlands. Most of the fresh water enters the Netherlands by the Rhine and the Meuse. Very roughly the fresh water flows into the sea or lake at four locations in The Netherlands,: the IJssellake near Kampen, the Noordzee canal near Amsterdam, the Rotterdam Waterway and the Grevelingen.

Most of these runoff possibilities determine the fresh water discharge by constructions for example the Grevelingendam or the lock near IJmuiden. The water that discharges through the Rotterdam Waterway and the Grevelingendam is determined by the Grevelingendam. The total amount from the Meuse, Waal and Lek is running off through both the Rotterdam Waterway and the Grevelingen. If the discharge through the Grevelingendam is decreased, the discharge through the Rotterdam Waterway is increased.

A sluicing program is determined by Rijkswaterstaat for the distribution of the water based on the incoming discharge in the Netherlands. The Haringvliet is closed and all fresh water is discharged through the Rotterdam Waterway if the total water discharge from the Waal, the Meuse and the Lek drops below 1700 and 3900 m^3/s the discharge in the Rotterdam Waterway is regulated to about 1500 m^3/s (Rijkswaterstaat directie beneden rivieren, 1987).

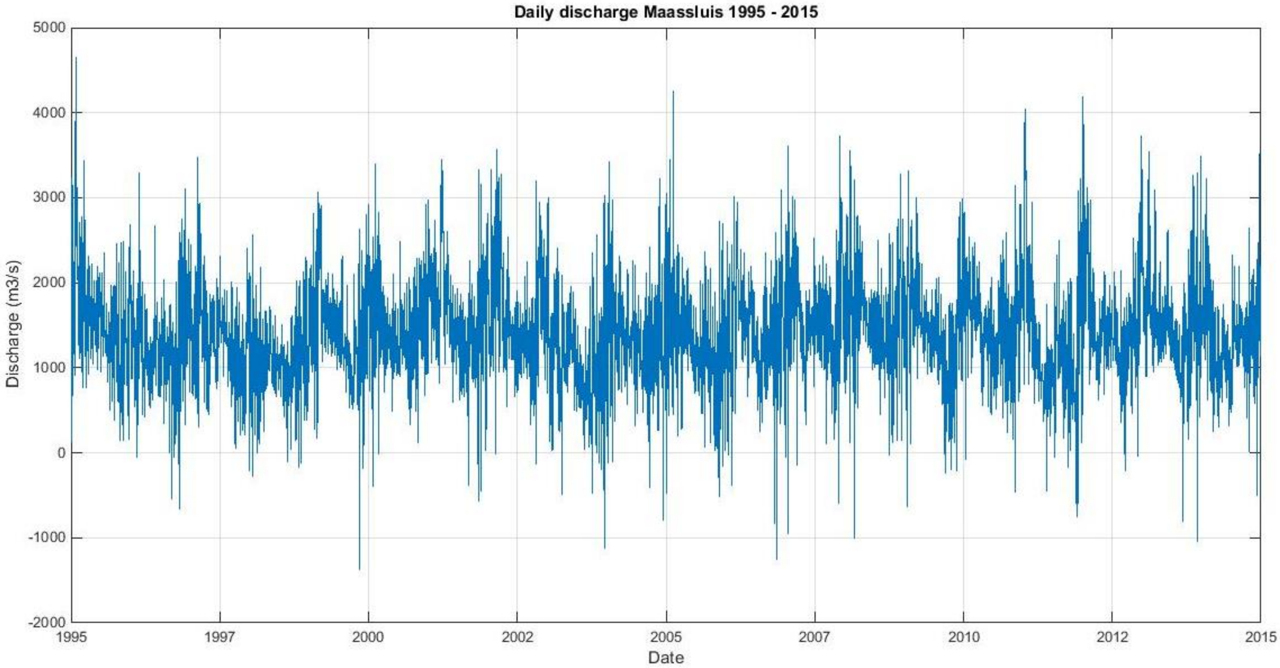

Figure 14 Daily discharge Maassluis for the period 1995 – 2015 (Rijkswaterstaat, 2016)

The discharge from 1995 until 2015 is retrieved from Rijkswaterstaat (Rijkswaterstaat, 2016). The discharge is estimated by the numerical model ZWENDL from 1995 until 2000. From 2000 onward the discharge is estimated based on results of the numerical model Sobek. The models generate a discharge every 10 minutes, these discharges are averaged over 24 hours to determine a discharge per day.

The fresh water discharge in the Rotterdam Waterway varies between -1371 m^3/s and 4649 m^3/s, as can be seen in Figure 14. Negative discharges occur when the seawater intrudes into the Rotterdam Waterway, for example when there is a combination of a small fresh water discharge in combination with flood during spring tide. The average discharge at Maassluis between 1995 and 2015 is 1350 m^3/s.

3 MODEL SETUP

The model setup for this research is based on assumptions. The most important assumptions are addressed in this section. The governing equations of the model and the complete set of parameters used can be found in Appendix B.

3.1 Process based model

3.1.1 Hydrodynamics

The process based numerical model Delft3D is used to evaluate the sediment transport characteristics and the effect of channel deepening. The model is contains three parts: the tide is simulated by the FLOW module, the waves are simulated by the WAVE module and the sediment transport is determined by a sediment transport formula.

The FLOW-model simulates several processes important for the simulation of coastal areas. The FLOW model is able to simulate for example the tide and wind-driven flows (incl. storm surges), stratified and density flows, river flow simulation, salt intrusion etc. (Deltares, Delft3D-FLOW, User manual, 2014a). During these simulations the model includes tidal forcing (as boundary condition), the Coriolis force although this effect is small on the scale of the Rotterdam Waterway, the density driven flow, advection – diffusion, time varying sources and sinks (e.g. river discharges) and robust simulation of drying and flooding of inter-tidal flats.

The WAVE-model uses the SWAN model to simulate short waves, for example generated by wind. The module includes for example shoaling and refraction of the short waves, energy dissipation due to white capping and depth induced wave breaking (Deltares, 2014b).

The coupling of the WAVE and FLOW module make it possible to simulate both the tidal current and the current related to short waves for the same period. The communication files make it possible the waves and the tide interact and create combined water level and flow velocities. The resulting flow velocities and water levels are the superposition of the results of the FLOW and WAVE module.

3.1.2 Sediment transport

The sediment is included in the model based on a sediment transport formula. The default transport formula is the van Rijn formula (1984). Other possibilities are the total load transport formula of Engelund-Hansen, for fine sediment the formula of Parentiatos-Krone, the sand transport formula of Peter-Muller-Meyer or the revised transport formula of van Rijn (2007a). The sediment transport formulas are solved for every grid cell with the result of the FLOW and WAVE modules as hydrodynamic input.

The revised sediment transport formula of van Rijn (2007a; 2007b) is used for the Rotterdam Waterway. The transport formula of van Rijn determines sediment transport generated by the orbital velocity of waves for fine sediment (<63 um) and the remaining sediment (>63 um) and sediment transport generated by tidal velocity for fine sediment and the remaining sediment. The formula also includes flocculation, hindered settling and stratification for the fine sediment based on fixed parameters.

The sediment transport formula of the model of van Rijn (2007a) is used to compute the sediment transport. The formula consists of both bed load transport and suspended sediment transport. Both the current of the tide and the waves are included. The total sediment transport is the sum of the bedload, wash load and the suspended sediment load:

$$S = S_b + S_s \qquad \text{(eq.6)}$$

Where S is the total amount of sediment transported, S_b is the sediment transported by the bed load transport, and S_s is the sediment transported by the suspended sediment transport.

3.1.2.1 Bed load sediment

The bed load is defined as the sediment transported in the 0.05 m above the bed. Bedload formula yielding:

$$S_b = 0.015\rho_s uh \left(\frac{d_{50}}{h}\right)^{1.2} {M_e}^{1.5} \qquad \text{(eq.7)}$$

In which Me is the mobility parameter defined by: $M_e = \frac{u_e - u_{cr}}{[(s-1)g\,d_{50}]^{0.5}}$

where u_e is the effective velocity defined by: $u_e = u + \gamma U_w$ with γ is 0.4 for irregular waves and 0.8 for regular waves, u the depth averaged velocity and U_w the peak orbital velocity and s the relative density of the sediment. The last unknown is the critical velocity u_{cr}. This velocity is divided in the critical velocity due to waves ($u_{cr,w}$) and the critical velocity due to the current ($u_{cr,c}$). The solution for the critical velocity of the current is based on the Shields parameter, and the critical value for waves is based on the critical value of Komar and Miller (1975).

3.1.2.2 Suspended sediment

The suspended sediment concentration is calculated based on the advection/diffusion equation (see appendix B). The sink or source term for the suspended sediment is calculated by the model of van Rijn (2007b), which automatically defines fine sediment if the sediment is smaller than 64 um. The suspended sediment is divided into an component affected by the current and a component affected by the waves. The current related sediment transport is described by:

$$q_{s,c} = 0.012\rho_s u d_{50} M_e^{2.4} (D_*)^{-0.6} \qquad \text{(eq.8)}$$

In which

D_* = dimensionless particle size determined by: $D_* = d_{50}[\frac{(s-1)g}{v^2}]^{1/3}$

The suspended sediment transport determined by the waves is controlled by:

$$q_{s,w} = \gamma V_{asym} 0.012\rho_s u d_{50} M_e^{2.4} (D_*)^{-0.6} \qquad \text{(eq.9)}$$

In which:

V_{asym} = velocity asymmetry factor based on: $V_{asym} = \frac{[(U_{on})^4 - (U_{off})^4]}{[(U_{on})^3 - (U_{off})^3]}$ with U_{on} is the onshore directed peak orbital velocity and U_{off} is the offshore-directed peak orbital velocity.

γ = 0.1 = phase factor

This model includes the effect of flocculation, hindered settling and stratification of sediment. These effects affect the fall velocity by:

$$w_s = \phi_{floc} \phi_{hs} w_{s,0} \qquad \text{(eq.10)}$$

In which:

ϕ_{floc} = the flocculation factor
ϕ_{hs} = the hindered settling factor

3.2 Model grid

A schematized 3D grid is used to for the model to represent the study area, see Figure 15. The grid includes the depth and the alongshore direction. To schematize and simplify the study area, the cross shore direction is excluded. The prismatic character of the Rotterdam Waterway makes it acceptable to do this assumption.

The grid is a simplified grid based on the characteristics of the Rotterdam Waterway. The grid is created with the function '*delft3d_io_grd.m*' of OpenEarthTools for MatLab provided by Deltares. The grid is defined in Cartesian notation.

The smallest grid size can be found in the Rotterdam Waterway and the fresh channel where the grid size is 200 x 125 m. The largest grid size is at the boundary of the sea, where the grid is approximately 500x500 m. The grid sizes decrease gradually towards the Rotterdam Waterway, which is at the center of the sea. The sea is described by a rectangle of 20 kilometer in the m direction and 40 kilometer in the n direction. The Rotterdam Waterway is described by a long channel of 500 meter in the n direction and 150 km in the n direction. The specific grid characteristics are included in Table 1.

The model is used in 3D, which means also the depth layers are included for the domain for the stratification of the salt. 11 sigma layers are included for the Rotterdam Waterway. The top layer describes 10% of the depth while the other 10 layers described 9% of the depth.

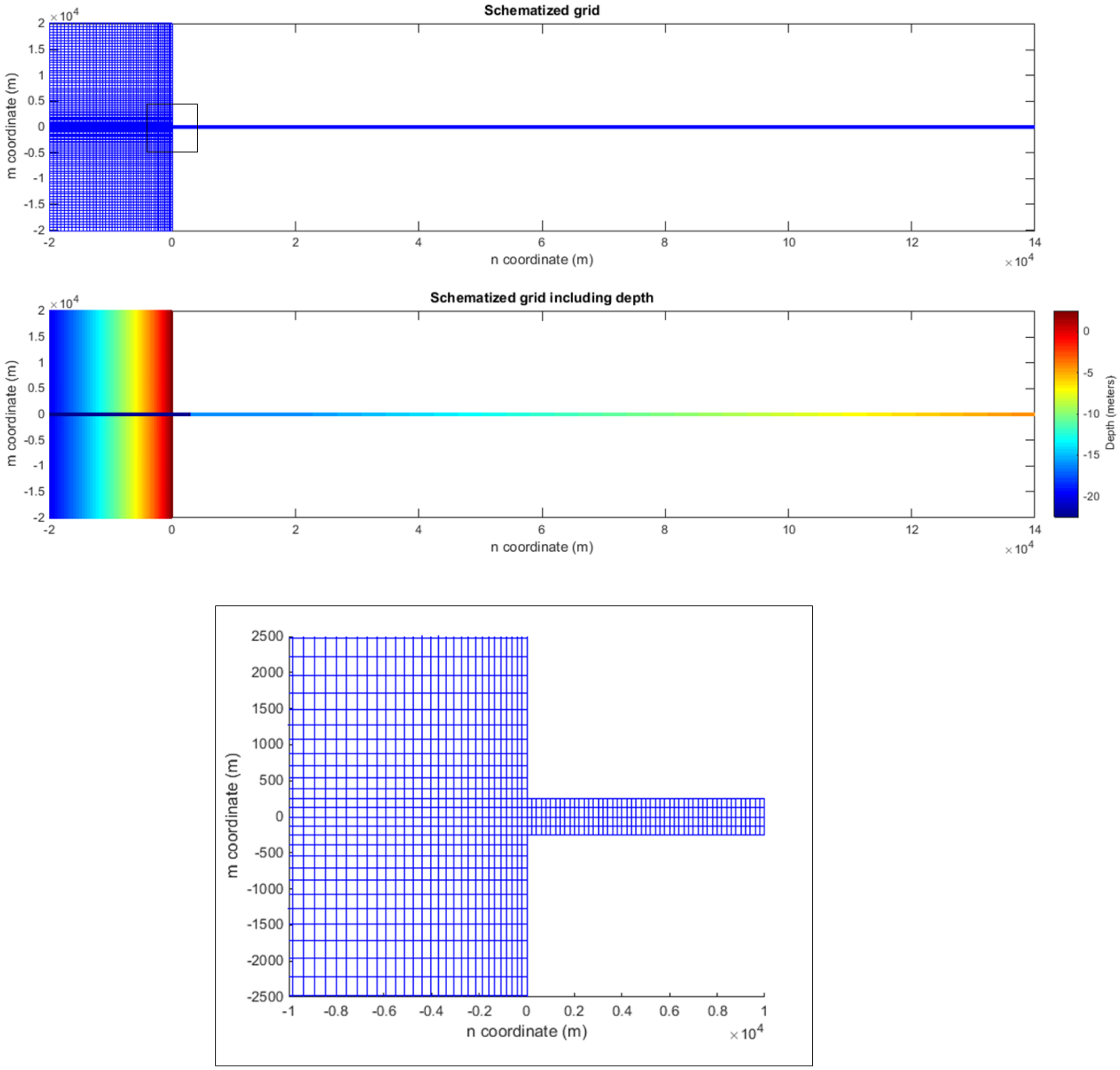

Figure 15 Schematized grid Rotterdam Waterway

Table 1 Grid properties

	Number of cells	Length
N cells	756	200 – 500
M cells	4-104	125 – 500

3.3 Numerical parameters

Several parameters need to be determined before the simulations can be done. The numerical parameters the most important for the simulations are:

- Bathymetry
- Boundary conditions
- Time frame
- Initial conditions

3.3.1 Bathymetry

The depth of the North Sea and the Rotterdam Waterway are based on the bathymetry of the North Sea and the Rotterdam Waterway and is created using the '*delft3d_io_dep.m*' function provided by Deltares in the OpenEarthTools.

For the North Sea the conditions are based on the JARKUS profile of the coast near Rotterdam. One JARKUS profile is assumed to be linear increasing from deep water (-20 m) until 3 meter at the coast, see Figure 16a. This is without the irregularities of sand banks or navigational channel in front of the coast.

The bathymetry or the Rotterdam Waterway is based on the desired depth based on the ladder line. These depths are included in Figure 16b. Although the sea has a different depth, the navigational channel has the same depth as the mouth of the Rotterdam Waterway at the coast. After the ladder line a constant bottom slope is assumed. This slope is the same as the average slope of the middle Rhine in the Netherlands, which is 0.1 m/km slope.

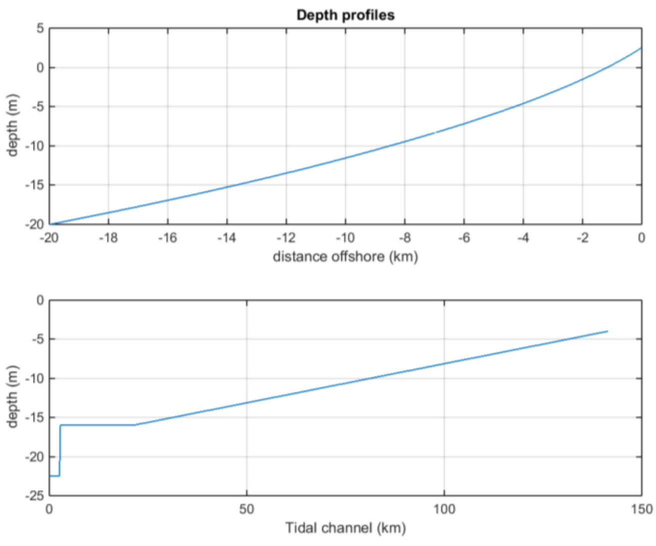

Figure 16 Bathymetry of a) the foreshore of the North Sea; b) the depth of the Rotterdam Waterway including the navigational channel

3.3.2 Sediment boundary conditions

The boundary conditions for both tide and fresh water discharge determine the incoming flow in the model domain.

The tidal boundary condition is represented by a harmonic water level of several tidal constituents, see section 4.1. The tidal boundaries are set to the Northern and Southern boundary of the North Sea. At the same boundaries also the salinity and the sediment is introduced. The boundary salinity is set to 34 PSU, and the incoming fine sediment is set to 0,04 kg/m^3. The incoming sand is set to 0 kg/m^3. These boundary conditions correspond with the boundary conditions determined by De Nijs *et. al* (2012).

The wave conditions are introduced by uniform waves at the western boundary, see section 4.2. The waves approach the shore with an incoming angle. Due to the rectangular shape of the boundary, the area where the waves would be absent influences the analysis. To decrease the influence of a leeside, smaller waves are introduced at the southern boundary. These boundary waves decrease towards the coast, to prevent them from breaking immediately.

The fresh water discharge is introduced at the end of the Rotterdam Waterway as a total discharge for the cross section. The salinity of this water is 0 PSU which is fresh water. The concentration of the fine sediment is 0,04 kg/m^3, while the concentration for the sand is 0 kg/m^3. The fine sediment from the river is defined as MUD2, while the sediment from the sea is defined as MUD. This makes it possible to evaluate the origin of the sediment.

3.3.3 Time frame

The time frame for the simulations is the startup time, the simulation period of the model and the time step.

During the first time steps of the simulation, the model has not yet reached realistic conditions. The model is still 'filling' with motion, salinity and sediment, because the first few boundary conditions have not yet reached the complete domain. To analyze realistic results, a run up time is used. The analysis of the results starts after the run up time. The hydrodynamic run-up time of the domain is 30 days. The length of the run-up time is determined based on the results of several length runs. In the first month of the run the salinity and the suspended sediment have different concentrations during the spring neap cycle. After 30 days the concentration during the spring neap cycle becomes equal, indicating that the system has reached some equilibrium.

The simulation period is 15 days excluding the run up time. The simulation period is determined based on the tidal cycle such that one spring and one neap period is included in the simulated tidal cycle. A '.map' file is used to reduce the simulation time of the scenario study. The '.map' file is the result of the startup run of 30 days, so the initiation of motion of the last day of the startup time is used as initial condition.

The time step is the time between two simulation steps. For the time step it is important to not have any numerical instabilities. These instabilities can cause unrealistic values of different parameters of the model. The numerical instabilities are caused when the grid is to large or the time step between the simulations is to large. The numerical instabilities are determined based on the Courant number. A method to test the maximum time step for the grid is the Courant-Friederiechs-Lewy number (CFL), defined by:

$$\boldsymbol{CFL} = \frac{\Delta \boldsymbol{t}\sqrt{\boldsymbol{gh}}}{\boldsymbol{min}\{\Delta \boldsymbol{x}, \Delta \boldsymbol{y}\}} \qquad \text{(eq. 11)}$$

Where Δt is the time step (in seconds), g is the gravitational acceleration (9,81 m/s^2), h is the water depth and $min\{\Delta x, \Delta y\}$ is the smalles grid size in the horizontal or vertical direction (using an xyz coordinate system). The CFL value should not exceed 10. Following this approach the following maximum time step is usable:

$$\Delta t = \frac{CFL\ \{\Delta x, \Delta y\}}{\sqrt{gh}} => \frac{10\ \times 125}{\sqrt{9{,}81 \times 22{,}5}} = \ 84{,}13\ s$$

So the maximum time step for the grid is 84,13 seconds which is equal to 1,25 minutes. However a time step of 0.5 minutes is used for the simulations, because an error occurred with a time step of 1.25 and 1 minute. One of the solutions is reducing the time step, which solved the error.

3.3.4 Initial conditions and parameters

The initial conditions are the conditions at the beginning of the simulation. Specified parameters for the initial conditions are the initial water level, initial concentration of salinity and sediments and the initial thickness of sediment at the bed.

The initial conditions for the scenario study are the results of the map file. The initial conditions for the map file are a uniform water value of 1 meter, a (suspended) sediment concentration of 0 kg/m^3 and a salinity of 0 PSU.

Three types of sediment are included in the model: mud from the sea, mud from the river and sand. The characteristics of the mud are the same, only the origin is different. The density of the mud is 2650 kg/m^3, the dry bed density of the mud is 500 kg/m^3 and the median sediment diameter (d_{50}) is 30 um, which corresponds with the 0.5 mm/s fall velocity as used by De Nijs *et al.* (2011). The density of the sand is 2650 kg/m^3, the dry bed density of the sand is 1600 kg/m^3 and the median sediment diameter (d_{50}) is 200 um.

The initial condition of the bed is mixed for the sediment fractions. Three sediment layers are determined for the bed at the initial stage. The top layer is an active layer of 0.1 meter which contains 2% fine sediment at the Rotterdam Waterway and 0.5% fine sediment at the North Sea. The second layer consists of 1 meter of sand. The mixture of this layer changes without changing the morphology. So based on the change in the layer, a change in morphology can be detected as well.

The initial conditions of the water are a density of the saline water of 1023 kg/m^3 with an temperature of 10 ºC. The gravity is 9,81 m/s^2 at the latitude of 52,5 decimal degrees.

4 HYDRODYNAMIC CONDITIONS

For the simulation of the boundary conditions are assumed to be constant for the schematized study area. First the boundary conditions are determined based on measurements subsequently the results are validated with the measurements of *De Nijs et al.* (2009).

4.1 Boundary conditions

4.1.1 Tide

One of the main typical features of the water level near Hook of Holland is the double low water. This feature is important for the tidal asymmetry in the Rotterdam Waterway, because it determines the length and magnitude of the resulting flow velocity.

The tide is determined by the astronomical constituents of the tide. The tide can either be dominated by the semidiurnal tide or the diurnal tide. To determine the relative importance of the tidal constituents, a form factor F is calculated. F is determined by:

$$\boldsymbol{F} = \frac{\zeta_{K1} + \zeta_{O1}}{\zeta_{M2} + \zeta_{S2}} \quad \text{(eq. 12)}$$

In which K1 and O1 are the diurnal tides and M2 and S2 are the semidiurnal tides. Because the Rotterdam waterway is the important study area, the form factor is calculated for Hoek of Holland (Rijkswaterstaat, 2014):

$$F = \frac{\zeta_{K1} + \zeta_{O1}}{\zeta_{M2} + \zeta_{S2}} = \frac{0.08 + 0.11}{0.79 + 0.19} = 0.20$$

This means the tide at Hook of Holland is semi-diurnal. For the tidal boundary condition the semi diurnal tides and its higher harmonics gives sufficient realistic tidal boundary conditions. The constituents of the harmonic tide for the boundary condition are listed in Table 2.

Table 2 Tidal constituents of the boundaries

Location	Constituent	Amplitude (m)	Phase (°)
North	M2	0.94	54
	M4	0.20	130
	M6	0.11	186
	M8	0.01	140
	S2	0.33	111
South	M2	0.86	64
	M4	0.15	126
	M6	0.11	190
	M8	0.03	119
	S2	0.10	121

The water level as simulated in the model compared with the calculated tide based on the measured water level (Rijkswaterstaat, live.waterbase, 2016) is shown in Figure 17 in the left panel. The propagation of the water level in the Rotterdam Waterway is shown in the right panel of Figure 17 between Hook of Holland near kilometer 1034.6 and the Botlek Harbor near kilometer 1009.6.

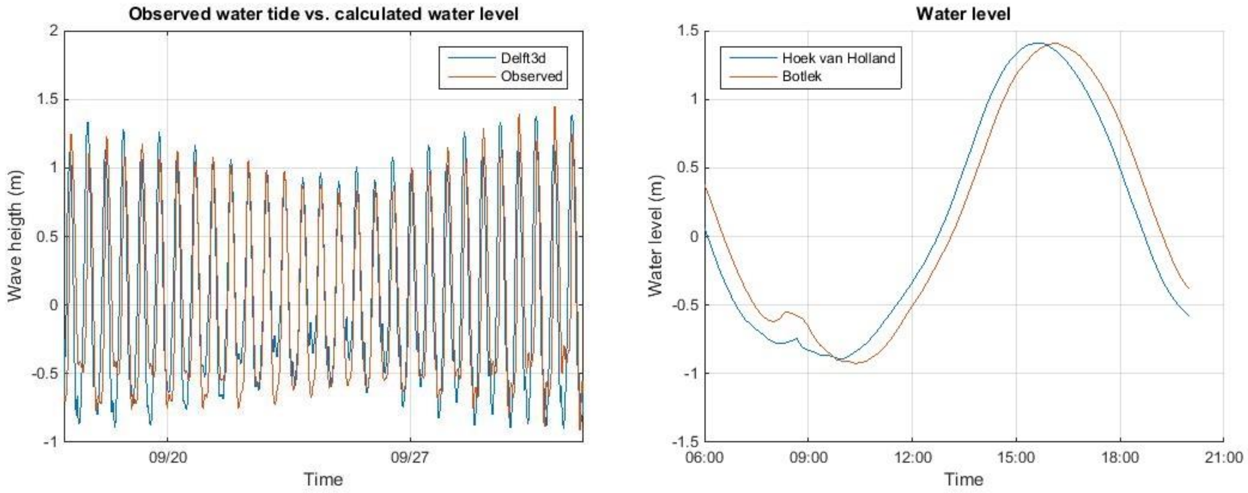

Figure 17 Left panel: Observed (orange) vs. calculated water level (blue). Right panel: water level of Hook of Holland (blue) and Botlek (orange)

The schematized model does not simulate the observed water level perfect. The conditions for the measured water level however are unknown. The daily inequality seems to be underestimated for the neap tide and overestimated for the spring tide. This is probably due to the S2 spring neap cycle. The S2 tide has already been lowered with 10 centimeter compared with the observed tide in the Getijdentabel. Because the schematization and the validation show fairly good results, the change compared with the observed water level is accepted. The propagation in the waterway seems to be ok. The water level has a time delay of about 20 minutes, which is the same compared with the measurements of De Nijs *et al*. (2009).

4.1.2 Waves

Although the variation of the short waves is large, a long period of short waves however has a significant impact on the hydrodynamic and morphological development of the area. The net movement of these waves determines the direction of the impact on these processes. The breaking of the waves generates turbulence which can generate erosion and the movement of sediment if the combination of shear strass and pressure gradient and turbulence is strong enough to initiate movement of the sediment.

The wave conditions for 2015 are shown and discussed in chapter 2.1, for the determination of the boundary conditions however the wave data for 1995 until 2015 is used.

There is no wave data available for some periods for the retrieved data. This can be due to a measurement error, or failure of equipment. The failure of equipment is not necessarily for all three variables. So it is possible there is no data wave height available, but there is data for the wave period. The data is neglected for the periods where one of the three variables has no data to equalize the data.

4.1.2.1 Significant wave height

The input for Delft3D is one significant wave height for the waves. The SWAN module creates a significant wave spectrum and repeats the spectrum for the simulation. The significant wave height over the year is used for the validation. This means the high wave heights during the storms is averaged with the low wave height during summer. The wave height is averaged for the calibration because average conditions are reproduced during the calibration. The average significant wave height over the between 1995 and 2015 is 1.30 m.

4.1.2.2 Wave period

The wave period depends on the type of wave passing by, also determining its energy. The wave period mostly determined by the sort wave. The tidal wave has an amplitude of 12 hours and 25 minutes while short waves have an wave period of seconds.

The wave period input for Delft3D is one value of the wave period corresponding with the input for the wave height. The input for the wave period is therefore averaged over the time corresponding significant wave height. The average wave period over the year is 4,48 seconds.

4.1.2.3 Wave angle

The Europlatform is located in deep water, which means the waves are not yet influenced by refraction an shoaling. This also means waves can possible have an angle between 0 and 360 degrees. For the boundary near the shore some wave angles are unrealistic, because the waves are orientated from the land. The coast of South Holland has an orientation of 30 degrees. Therefore all the waves with the orientation between 20 and 200 degrees are neglected for the analysis.

The wave angle is the orientation of the waves approaching the shore. The wave angle is important for the waves when approaching shore, because the direction of the velocity is determined by it. It can generate alongshore sediment transport determined by the angle at which the waves break on the shore. This sediment can flow into the mouth increasing the sediment from sea.

The waves approach the shore with different angles during a period. It is not possible to simulate all these different wave angles during a period. For the schematized wave are it is important to simulate the a realistic concentration of suspended sediment in the Rotterdam Waterway. Therefore a dominant wave angle is determined, which is the angle which is measured the most for the period.

For the sediment transport characteristics of the Rotterdam Waterway it is important to include the waves to include the incoming sediment from the sea, but it is less important to simulate the waves with respect for their angle. The morphological change is not important for the sea, the sediment needs to flow inside the Rotterdam Waterway. To include the effect of sediment and for the simplicity a dominant wave angle is determined for the period of simulation. The dominant wave angle is 227.

4.1.3 Fresh water discharge

Due to the schematization of the study area, the bifurcation point near the Botlek is not included. Therefore the fresh water running through the Rotterdam Waterway near Maassluis is used as boundary condition, which is explained in chapter 2.4.

A constant boundary condition of fresh water discharge is used to be able to ignore the processes caused by a varying discharge for this study. Also for the validation average constant boundary conditions is used. The average discharge based on the period of 1995 and 2015 is 1350 m^3/s.

4.2 Validation

The aim of the validation is to evaluate the skill of the model for the water level. The flow velocity, salinity and the concentration of suspended sediment are validated with the results of the measurements as presented by De Nijs *et al.*, (2009) near the surface of the water column and near the bottom of the water column.

4.2.1 Water level

The water level is validated based on the water level of the calibrated Harbor Authorities model HBR. The HBR model is a hydrodynamic model including all fresh water input from the river. The calibrated model is simulated in SIMONA. The HBR model includes 14 components, and is calibrated based on measurements from juli to august 1998 (Arcadis, 2015). Water levels for the neap tide, spring tide and average tide are available for average discharge from the HBR model.

The distribution profiles of the HBR model are available for km 1035 until km 1009 of the Rotterdam Waterway. The water level is validated for three representative locations: Hoek of Holland (km 1032), Maassluis (km 1020) and the Botlek (km 1009). These locations represent the mouth of the Rotterdam Waterway (Hook of Holland), the middle of the Rotterdam Waterway (Maassluis) and the bifurcation of the Rotterdam Waterway into the Old and the New Meuse (Botlek), see Figure 18.

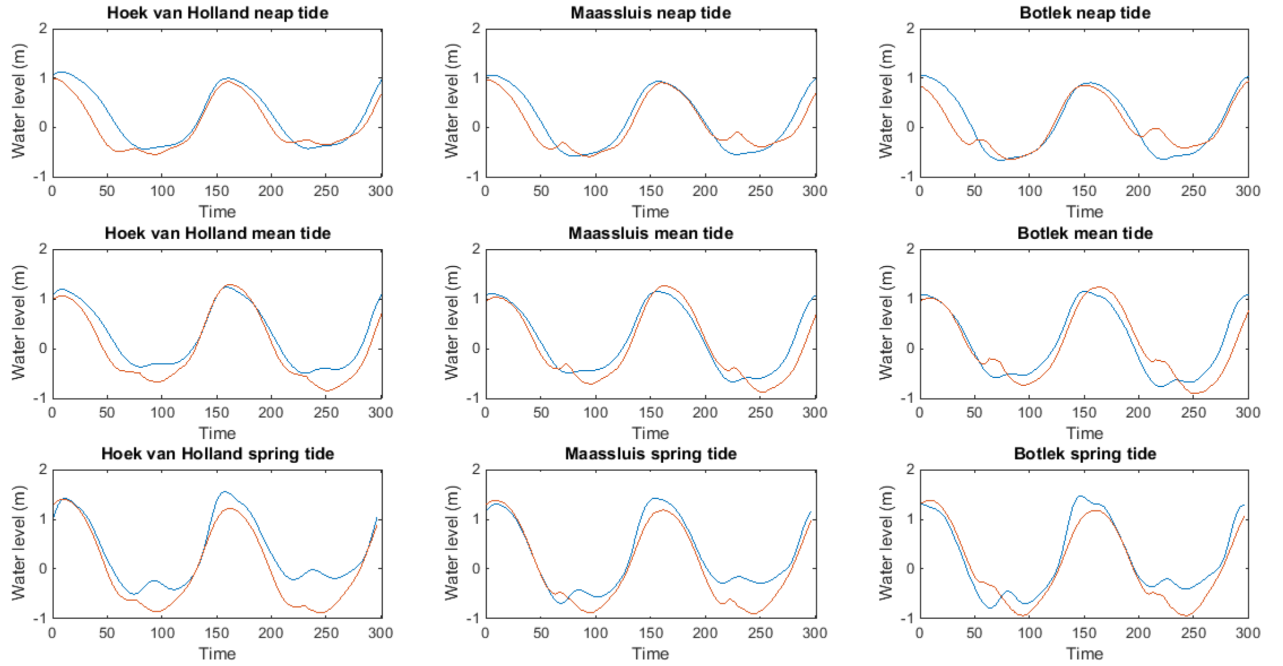

Figure 18 Water levels for Hook of Holland, Maassluis and the Botlek for three tides of the HBR model (in blue) and the calculated values (in orange).

The water level is validated based on the Nash Sutcliffe method (Nash & Sutcliffe, 1970), which reads:

$$NS = 1 - \frac{\sum(X - Y)^2}{\sum(X - \bar{X})^2} \qquad \text{(eq. 13)}$$

Where X is the comparison value, Y is the calculated value and $\bar{X}$ is the average of the comparison values. The NS values are listen in Table 3.

Table 3 NS values

	Hoek of Holland	Maassluis	Botlek
Neap tide	0,84	0,85	0,76
Average tide	0,84	0,88	0,82
Spring tide	0,55	0,8	0,64

The NS values indicate a good simulation of the water level for average tide and spring tide (near 0.8). the model results for the spring tide are not very good. The double low water is overestimated for all locations and the high water is under estimated, resulting in low NS values for these tides.

The low water for the Botlek is overestimated for all conditions and includes a phase lag, but still resulting in acceptable NS values. The HBR model near the Botlek area has already been influenced by several structures and obstacles like the Measland barrier and the junction between the Old and the New Mheuse which deform the tidal wave. The schematized study area only includes the first step in the bottom line and the linear increasing river bed.

A small checkup for the tidal asymmetry of the M2/M4 tide shows no internal asymmetry is present in the schematized study area, with almost the same tidal asymmetry compared with de Nijs *et al.* (2010) which is an asymmetry of 0.2 between Hook of Holland and the Botlek area. The checkup is summarized in appendix F. The phase lag also indicates a flood dominated system as expected (phase lag larger than 0).

The overall reproduction of the water level is acceptable. The main flood asymmetry is well reproduced for the schematized grid, although the low water period is being reproduced less well. The tidal amplitudes are implemented for the scenario study.

4.2.2 Salinity

The salinity during the measurement campaign is advecting from Hook of Holland upstream towards the end of the Rotterdam Waterway. The top layer is fresh during the measurements, as can be seen in Figure 19 in the left panel. The calculated location of the salinity moves landward during the simulation period, as can be seen in Figure 19. Hook of Holland is located at kilometer 1032 while the calculated stratification is present between kilometer 1010 and 990.

The profile of the calculated stratification corresponds with the measurements with a fresh top layer and the salinity near the bottom layer moving land inward with flood. The length of the calculated salt intrusion is about 15 kilometer form 20 PSU towards 0 PSU while the measured length is about 9 kilometers. This could be because the water level near spring tide is overestimated for the Delft3D model. The water levels of De Nijs *et al.,* (2010) however are only available for Hook of Holland. The intrusion of the salinity during flood during spring tide is 10 kilometers for both the measurements and the simulated salinity. The length of the salt wedge is also stable during the ebb and flood.

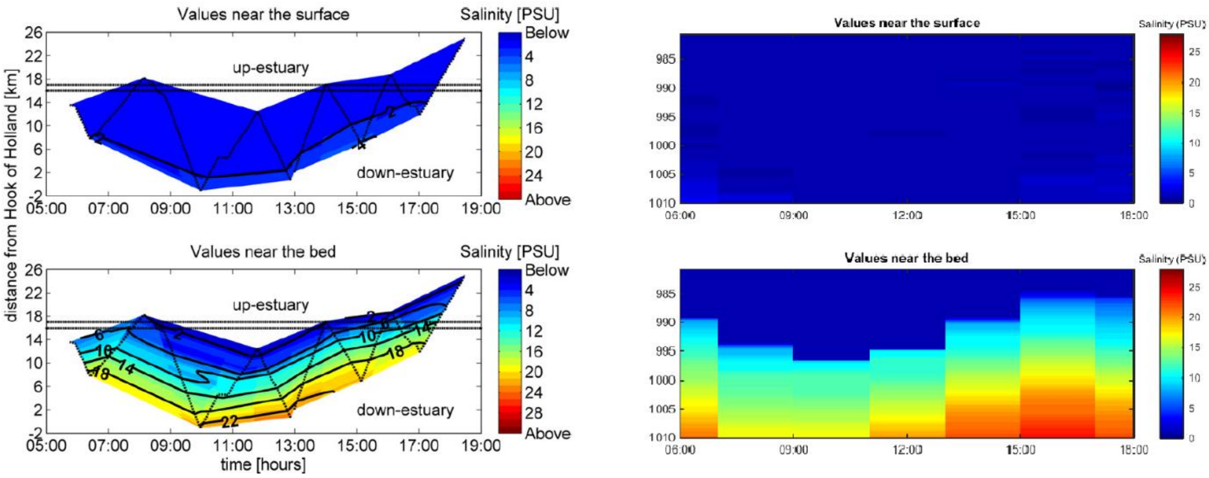

Figure 19 Left panel: Salinity measured by de Nijs et.al (2010). Right panel: calculated salinity with 4 weeks run up time

The movement of the stratification area more land inward is probably due to the schematization. There are no harbor basins included and the channel has a constant length of 500 meter without river bends. This makes it easier for the saline water to travel further upstream. For the validation of the velocity and the suspended sediment the same location is used for validation, so 20 km land inward compared with the measurements. The validation is shifted to compare the area of the salt wedge where the processes due to the null point and stratification occur.

4.2.3 Velocity

The measured velocity (left) is compared with the calculated velocity (right) in Figure 20. Important to notice is the velocities from the color bar from De Nijs *et al.* (2010) give values ranging from 0 towards -1.5, while in the contour lines in the plot indicate that the color bar is from -1.5 (red) to 1.5 (blue).

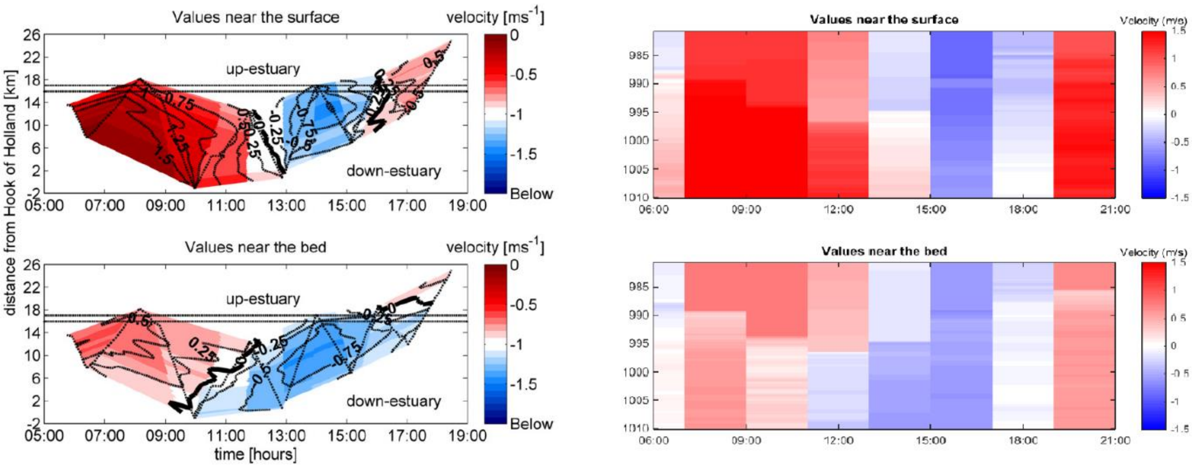

Figure 20 Left panel: Velocity measured by de Nijs et.al (2010). Right panel: calculated velocity with 4 weeks run up time

The maximum velocity measured during ebb is 1.5 m/s, while the calculated maximum velocity is 1.9 m/s, which indicates a overestimation of the velocity the model. The flood velocity is of the same order for the measured (0.75 m/s) and calculated (0.8 m/s). Also the length the increased length of the flood near the bed is well reproduced. Therefore the model reproduces the velocity well compared with the measurements of De Nijs *et al.* (2010).

4.2.4 Sediment concentration

The sediment concentration near the surface are low compared with the measured concentration near the bed, as can be seen in the right panel of Figure 21. The surface layer shows relatively high concentrations for the location where the surface and bottom layer are relatively fresh. The amount of sediment near the bed is especially high where the salt wedge near the bed becomes fresh and is in the order of 0.9 kg/m^3.

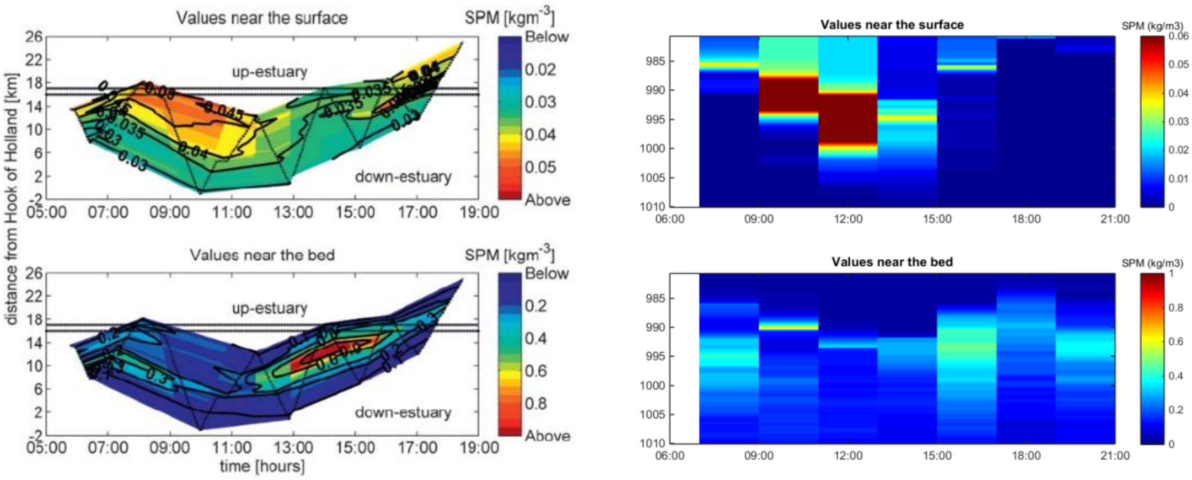

Figure 21 Left panel: SPM concentration measured by De Nijs et.al (2010). Right panel: calculated SPM with 4 weeks run up time

The highest concentrations near the surface occur during ebb where the bottom layer in front of the null point. During flood tide the concentrations increase near the bed towards 0.25 kg/m^3 for the simulation. This is much lower than measured during the campaign. But the pattern of the sediment concentration in the Rotterdam Waterway is the same, so the validation shows no perfect results however the results are good enough to evaluate the pattern of sediment concentration for the different scenarios.

4.3 Conclusion

Overall it can be concluded the model predicts the right pattern for the salinity intrusion, flow velocity and suspended sediment concentration, although it is much 20 kilometer inward. The water level however is reproduced fairly well, although there is a phase lag in the low water especially near the Botlek area. The NS values of the Delft3D water levels compared with the HBR model are all right (near 0.8), except for the spring tide near the Botlek and Hook of Holland.

Given the very schematized study area of the model compared with the measurments of De Nijs et al., (2010) and compared with the calibrated and validated HBR model, the results are good. Therefore the explained settings are used for the sensitivity and scenario analysis in the next chapters.

5 METHODOLOGY

The changes for the model for the sensitivity analysis and the scenarios to identify the important processes for the Rotterdam Waterway are addressed here. For the sensitivity analysis the discharge and wave conditions are changes. For the scenario analysis the harbor basins are included, a deepening is executed at the first step of the depth and a deepening is executed near the location of the ETM.

5.1 Sensitivity analysis

The sensitivity analysis focusses on the processes in the Rotterdam waterway which is determined by hydrodynamic processes in the channel.

5.1.1 Fresh water discharge

With the change in the fresh water discharge the salt wedge possibly deforms or moves. Also the available amount of sediment changes with the changing discharge. So the importance of the form of the salt wedge and the amount of sediment is evaluated with the fresh discharge scenarios, because more water is running into the domain carrying sediment.

The average discharge running through the Rotterdam Waterway near Maassluis is 1350 m^3/s, as explained in section 2. This is also the discharge used for the calibration. With the same method as the average discharge the other discharges are determined. The other scenarios for the fresh water discharge are:

- 5^{th} percentile discharge: 490 m^3/s
- 25^{th} percentile discharge: 1030 m^3/s
- 75^{th} percentile discharge: 1690 m^3/s
- 95^{th} percentile discharge: 2350 m^3/s

5.1.2 Wave conditions

The wave conditions are assumed to be yearly average for the calibration. For the scenario study the wave conditions are changed into wave average conditions for summer, autumn, winter and an extreme storm from the last years. The extreme storm is the storm of 2007. This is the last storm which predominant occurred and had the most impact at the coast of South Holland.

The waves determine the sediment concentration in the water column in the seaward boundary of the Rotterdam Waterway. The waves also determine part of the flow velocities due to the orbital motion of the water beneath the waves. The characteristics for the wave conditions are summarized in Table 4.

Table 4 Wave conditions for different scenarios

Scenario	Significant wave height (m)	Wave period (s)	Wave angle (degrees)
Summer	1.01	4.26	226
Winter	1.68	4.73	225
Extreme storm	2.30	5.20	225

5.2 Scenario analysis

A scenario analysis is executed to determine the effect of the harbor basins and the effect of deepening. Two types of deepening scenarios are determined. The first deepening scenario is to determine the effect from the offshore conditions, while the second deepening scenario determines the effect when the area deepened where the maximum suspended sediment concentration occurs in the schematized grid.

5.2.1 Harbor basins

For the Rotterdam waterway specifically the harbor basins are very important elements for the sediment transport characteristics. The basins act as sediment trap, because of very low flow velocities. So if the sediment enters the basin, the sediment is able to settle there. With the inclusion of the basins the sediment is able to settle at more locations.

The harbor basins are included very schematized in the area. The basins located near the Rotterdam Waterway are included. These basins are: the Maasvlakte and the Botlek Harbor. The entrance has a refined gird. The refinement is due to the local acceleration and decreasing of the flow near the entrance of the harbor. The grid properties are included in Table 5, the final for the harbor basins can be seen in figure 22. **Fout! Verwijzingsbron niet gevonden.**

Table 5 Harbor basins

Harbor basin	Grid size	Number of grids	Depth (m)	Total area (m^2)
Maasvlakte	100x125	200	-22.50 until -15	20 km^2
Botlek	100x125	15	-13 until -8	1.5 km^2

The grid surrounding the harbor basins are refined until 100 meter wide. The refinement is linear from 200 to 10 meters for the basin entrances. There are areas with larger depths to simulate the accessible channels in the harbor basin.

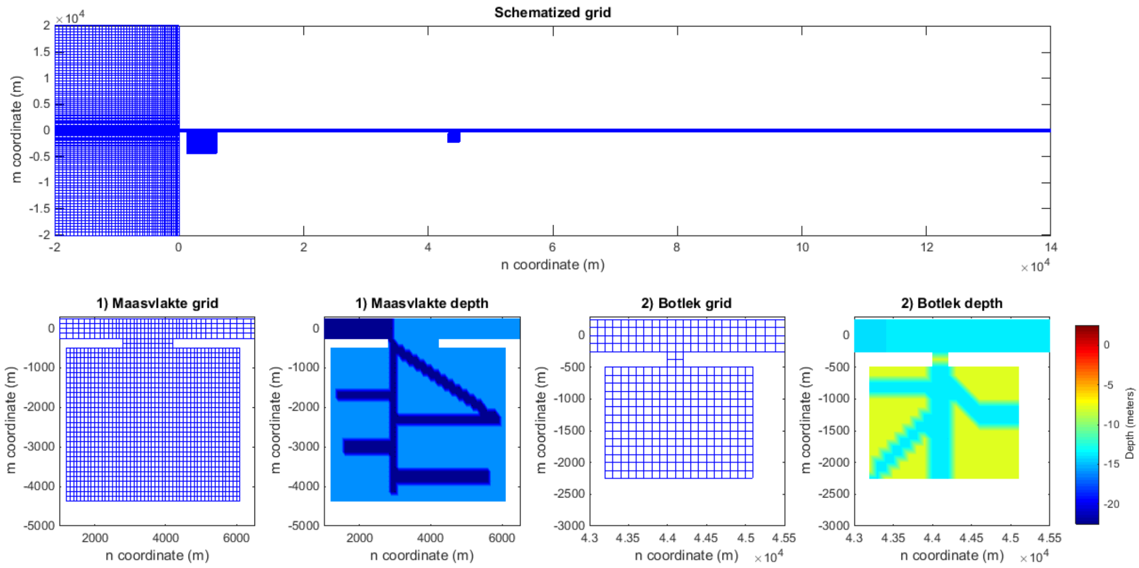

Figure 22 Grid including harbor basins

5.2.2 Step deepening

The deepening is executed near the location where the lower layer of the water column is still saline, which is at the flat bottom of the channel. The step is deepened with one meter, see Figure 23.

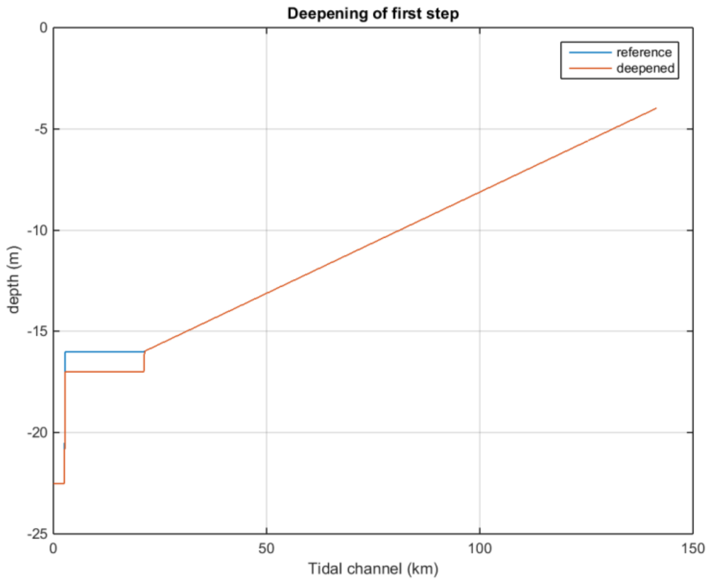

Figure 23 Deepened depth vs. original depth

5.2.3 ETM deepening

In the schematized study the ETM is located much more inland compared with reality. In reality the deepening is executed near the location where also the ETM travels with the tide, while in the schematized study area the deepening is executed far before the ETM. To evaluate the effect of the deepening near the ETM, the study area is deepened near the ETM with 1 meter from kilometer 1000 towards km 960 see Figure 24. From kilometer 960 towards kilometer 930 the bottom slop increases gradually towards the original depth. The gradual increase towards the upstream area is used to decrease the effect of an introduced step, like for the other deepening scenario.

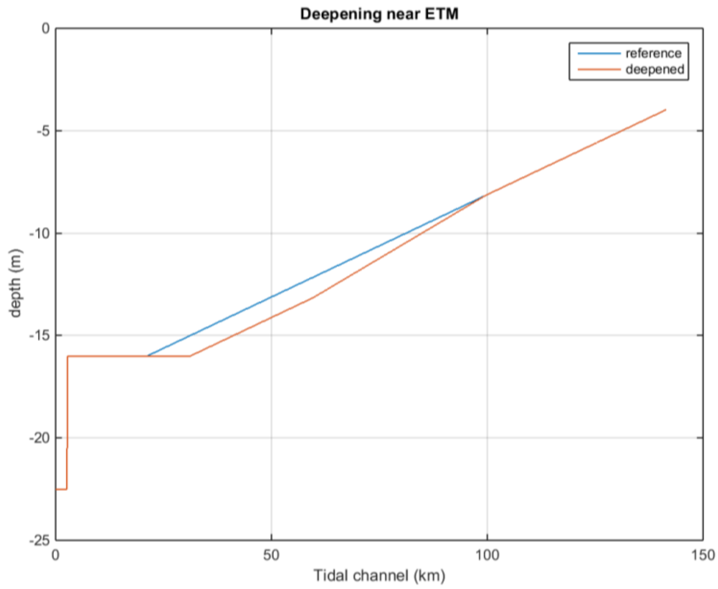

Figure 24 ETM deepening 1 meter vs. the original depth

6 RESULTS

The results are discussed in two sections. In the first section the sensitivity of the salinity, hydrodynamics and sediment transport of the reference scenario is discussed. In the second section the results of the scenario analysis for the harbor basins and the deepening are discussed for the same processes.

6.1 Sensitivity analysis

The sensitivity analysis contains multiple spring neap tidal cycli, which is called the medium term response, and changing boundary conditions. First the change of several spring neap cycli are discussed.

6.1.1 Results for average conditions

6.1.1.1 Salinity

The salt intrusion for the Rotterdam Waterway can be seen in Figure 25 where the blue color indicates a salinity between 0 and 1 PSU which is fresh water. The red color scale indicates increasing salinity with a maximum of 34 PSU for the deep red color. The arrows indicate the magnitude and direction of the flow velocity in the waterway. A large difference can be seen between the upper layer of the water column which remains relative fresh until maximum of 3 PSU and the remaining lower layers of the water column which are relative saline decreasing from 30 PSU near the harbor until 0 PSU near the null point. This indicates a strong stratification between beneath -4 meter depth and above -4 meter depth, where the top layers remain fresh and the lower layers remain saline. The strong distinction between the layers indicates a salt wedge as expected.

The step from the deep navigational channel towards -16 meter causes a large decrease (upstream) in salinity for the water surface towards -10 meter depth. For the lower layers the step has only a small impact, which is only visible near the step. This can also be seen in figure 99 in appendix D, where the values of the salinity per layer are plotted.

The Rotterdam Waterway becomes fresh near kilometer 977, where all layers have a salinity of 0 PSU. The lowest layer determines the location of the null point so the null point of the estuary is at kilometer 977.

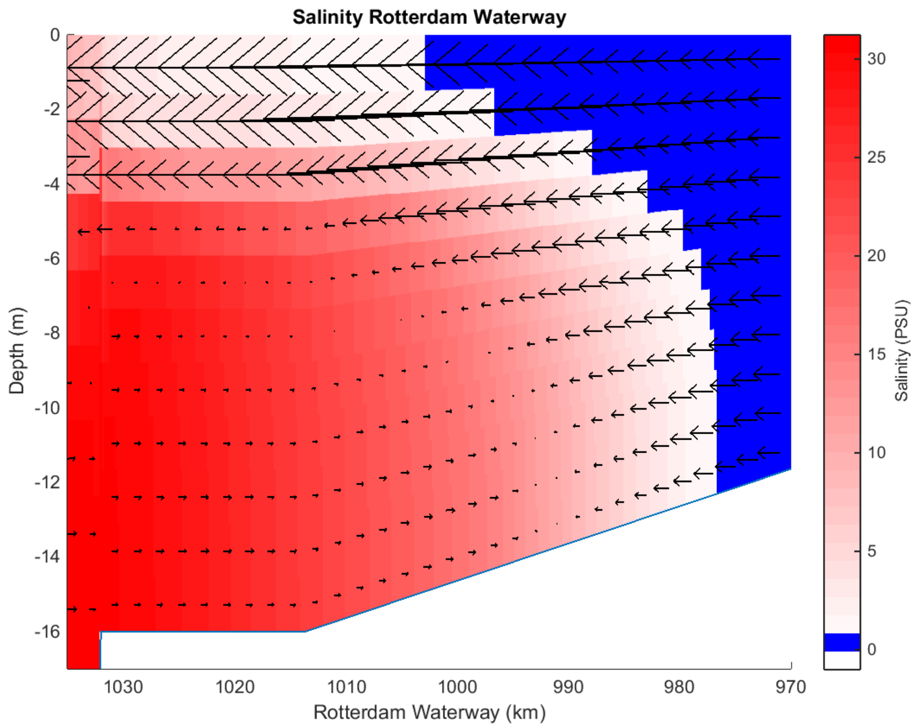

Figure 25 Salinity per layer with velocity

6.1.1.2 Hydrodynamics

The hydrodynamics in the channel can be distinguished in floating top layers over the saline lower layers. The top layers of the water column are directed estuary outward averaged over the tide as indicated by the arrows in Figure 25, while the lower layers are directed estuary inward until kilometer 990 where the velocity becomes zero near the bottom. The velocity in the inward lower layer is lower (+/- 0.06 m/s) compared with the outward directed top layers (+/- 0.8 m/s) as can be seen in Figure 26 in the righter panels.

The location of the null point according to the salinity is different compared with the location where the average velocity is zero for the bottom layer. The salinity travels with the tide which results in salinity in front of the location where the average velocity is zero, where the average velocity is still directed outward. The location where the average velocity is zero is at kilometer 994, while the null point of salinity is near kilometer 977.

The step in the depth is visible in layers with the decrease of velocity over the tidal period for the top layers, while for the saline layers there is a local decrease in velocity however it becomes of the same order again at the flat bottom, comparable with the salinity.

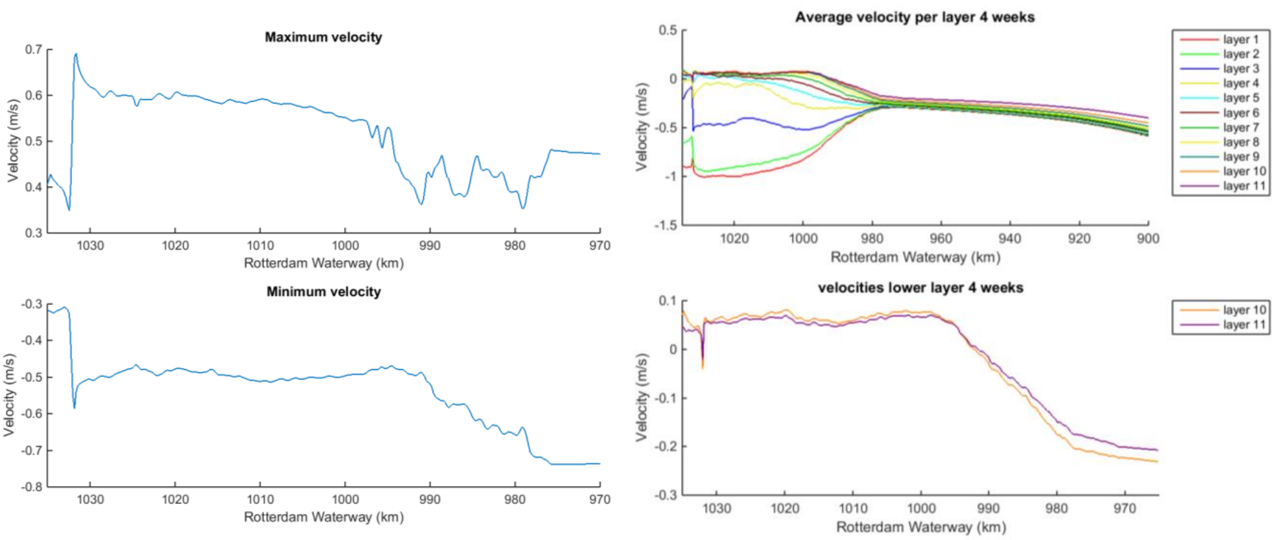

Figure 26 Velocity per layer reference scenario

The tidal asymmetry is determined by the difference in ebb and flood length and the water level during ebb and flood. The average ebb (minimum) and flood (maximum) can be seen in the left panels of figure 26. The velocity combined with the tidal period result in the average velocity for layer 11 in the lower right panel. One tidal cycle has a total duration of 745 minutes. For Maassluis under average conditions the flood velocity has an average flood duration of 151 minutes per tidal cycle, while for the bottom layer the average flood duration is 409 minutes. So the small residual flood velocity of 0.1 m/s has also a longer duration resulting on average in an estuary inward velocity.

Two locations are interesting to point out in the ebb and flood velocity. First the step in depth increases both the ebb and flood velocity both with 0.3 m/s. The second interesting observed is the location where the salinity front is moving is clearly visible with a decrease in average flood velocity between kilometer 995 and kilometer 990.

Turbulence damping is an important process for the formation of the ETM. The turbulent energy can be seen in the left panel of Figure 27, where the energy given is located between the layers. The top layer has no turbulence, because on the top of the first (top) layer there is no turbulent energy anymore. The turbulence damping is clearly visible in the turbulent energy. The turbulence decreases where the water column becomes saline from kilometer 977 outward. From the fifth turbulence layer (which is near -6 meter depth) there is turbulent energy, while the turbulence has disappeared in the upper turbulence layers from the fifth layer towards the upper part. So the turbulence is damped in the upper layers of the water column.

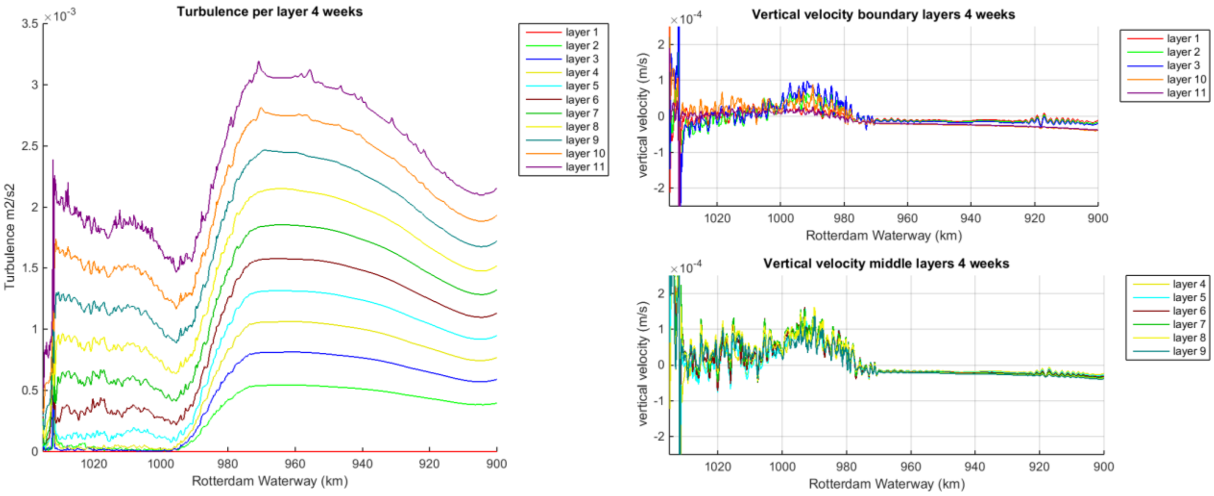

Figure 27 Left panel: turbulence per layer; Righter panel: vertical velocity of the boundary layers (upper panel) and of the middle layers (lower panel)

The vertical velocity determines the gravitational circulation, which can be seen in Figure 27 in the right panel. The positive velocity indicates that the velocity is directed towards the top between kilometer 980 and 1010. The large stratification of the salinity should force large vertical velocity.

The top two boundary layers and the lowest two boundary layers show small vertical velocities, while the middle layers show a larger vertical velocity. So there is a small velocity which is directed to the top, possibly taking sediment with it. This is however very small, and given the hydrostatic pressure assumption of the model, it can be discussed if the given values are not just numerical instabilities. Although there seems to be a pattern near the salinity front directed upward.

6.1.1.3 Sediment transport characteristics

The salinity and hydrodynamic conditions are processes cause sediment transport. The tide average sediment concentration for the top layer can be seen in Figure 28 in the upper panel and the tide average sediment concentration for the bottom layer is shown in the lower panel. An estuary turbidity maximum forms, and grows in time for both the layer near the surface and the layer near the bottom if the simulation time is extended with spring neap cycles. The top layer shows growth until 10 weeks of simulation. The lower layer is still constant after this period. The growth and location of the ETM shows also some variation for the bottom layer. The suspended sediment concentration for the ETM grows eventually towards 270 mg/l after 12 weeks of simulated time.

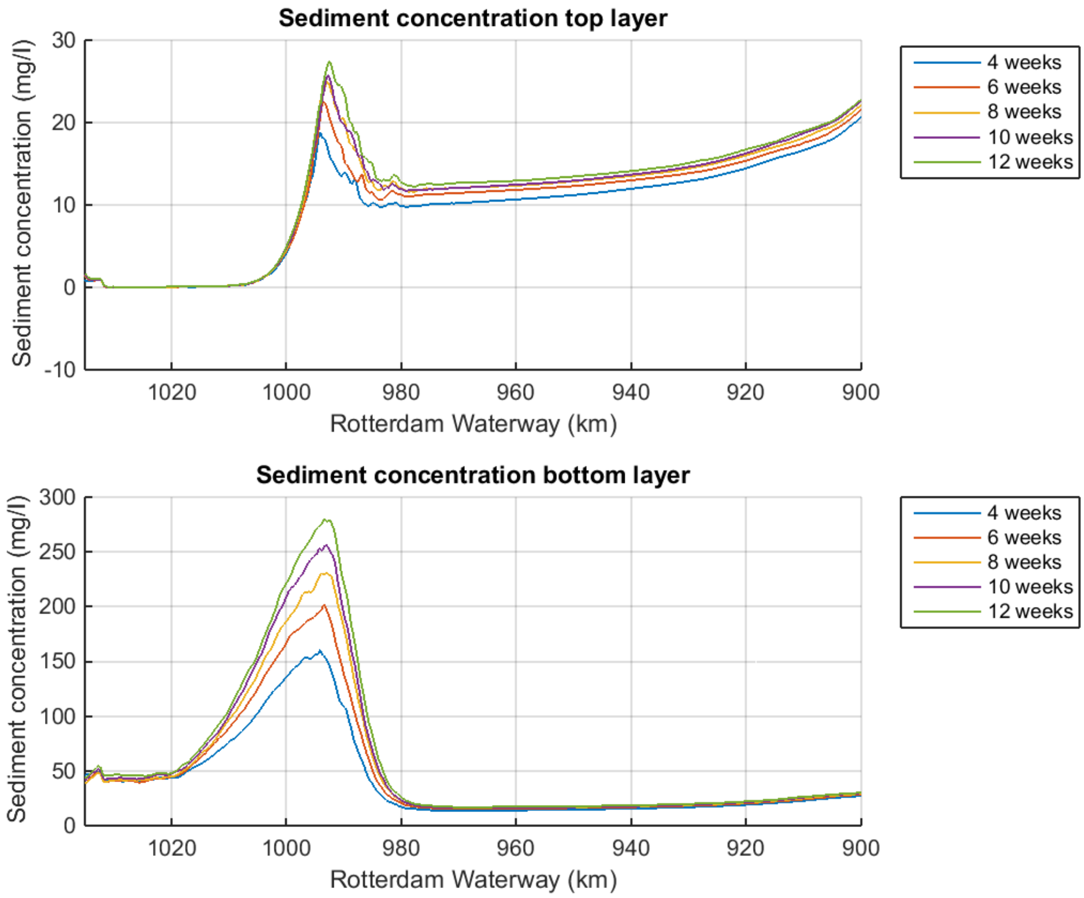

Figure 28 Tide averaged concentration SPM in time near the surface (top panel) and near the bottom (lower panel)

The length of the ETM is approximately 44 kilometer. The boundaries of the ETM are determined by the locations where the ETM is above average value and where the concentration of the ETM is constantly increasing or decreasing. So the suspended sediment concentration has increased over 44 kilometers.

The sediment is 'raining out' from the top layer due to damping of the turbulence from kilometer 990 towards the estuary mouth as be seen in Figure 28. The sediment in the top layer becomes zero near kilometer 1005, which indicates an efficient sediment trap during slack tides. This raining of the sediment appears in the upper three layers of the column, where the turbulence is zero.

Flocculation appears to be an important factor in estuaries which determine the fall velocity and thus the concentration suspended sediment in the estuary. Flocculation increases the fall velocity in saline water. With constant conditions over a spring – neap tide, the flocculation is not important, see Figure 29. The fall velocity even decreases in the saline water. This is due to the hindered settling of the sediment. Suspended sediment increases the density of the water column. The increased density makes it difficult for the sediment to settle which decreases the settling velocity, instead of increasing it due to the marine influence.

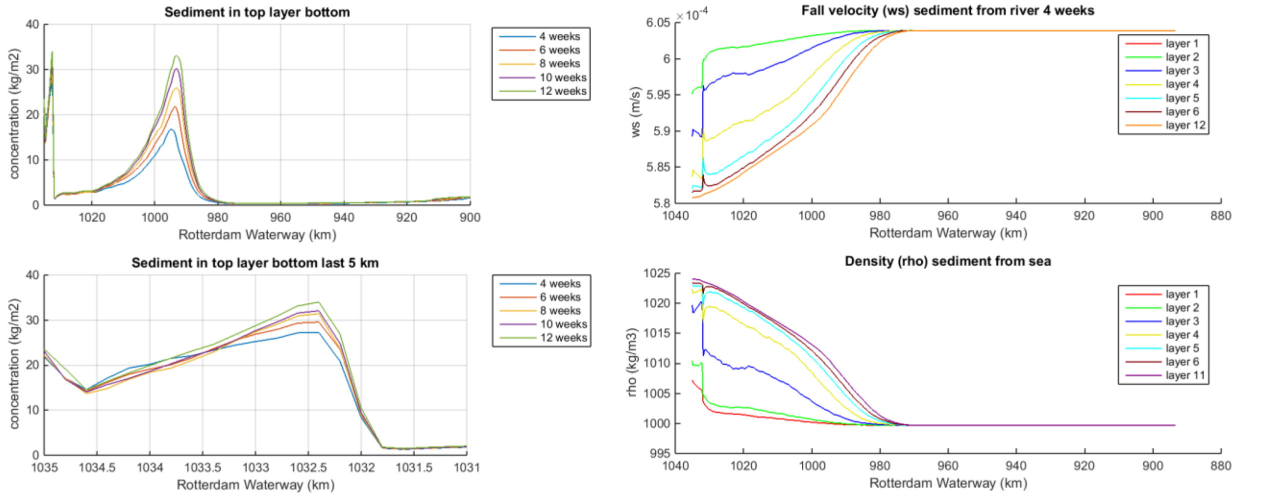

Figure 29 Left: Available fine sediment in top layer; Right upper panel: fall velocity righter lower panel density water column

The available sediment in the bottom shows the locations where the sediment is able to settle, and store the sediment. It also shows if there is enough sediment for the formation of the ETM. The available amount of fine sediment in the top layer is shown in Figure 29. A maximum for fine sediment in the top layer of the bottom also forms at kilometer 994 just estuary upstream of the turbidity maximum (km 993.2) of 32 kg/m2 after 12 weeks. The sediment is able to settle at the location just after the ETM due to the low turbulence and the low velocity for both the ebb current as the flood current. Near km 1032.2 another formation of fine sediment in the bottom layer grows. This is due to the step in bottom shape is present in the bottom line, which decreases the flow velocity at this location, but also blocks a part of the sediment.

6.1.1.4 Stability

The stability of the hydrodynamic conditions is important to evaluate, because it shows how much the sediment transport is due to changing conditions. The results do not vary much in time, which means the hydrodynamics for the estuary are stable after the run-up period of 4 weeks. The results for the different simulations in time are summarized in Figure 30 for the salinity, turbulence and the velocity and in Table 6 for the sediment transport. The first value of the salinity in table 6 indicates the location of in the top layer, the second value indicates the lowest layer.

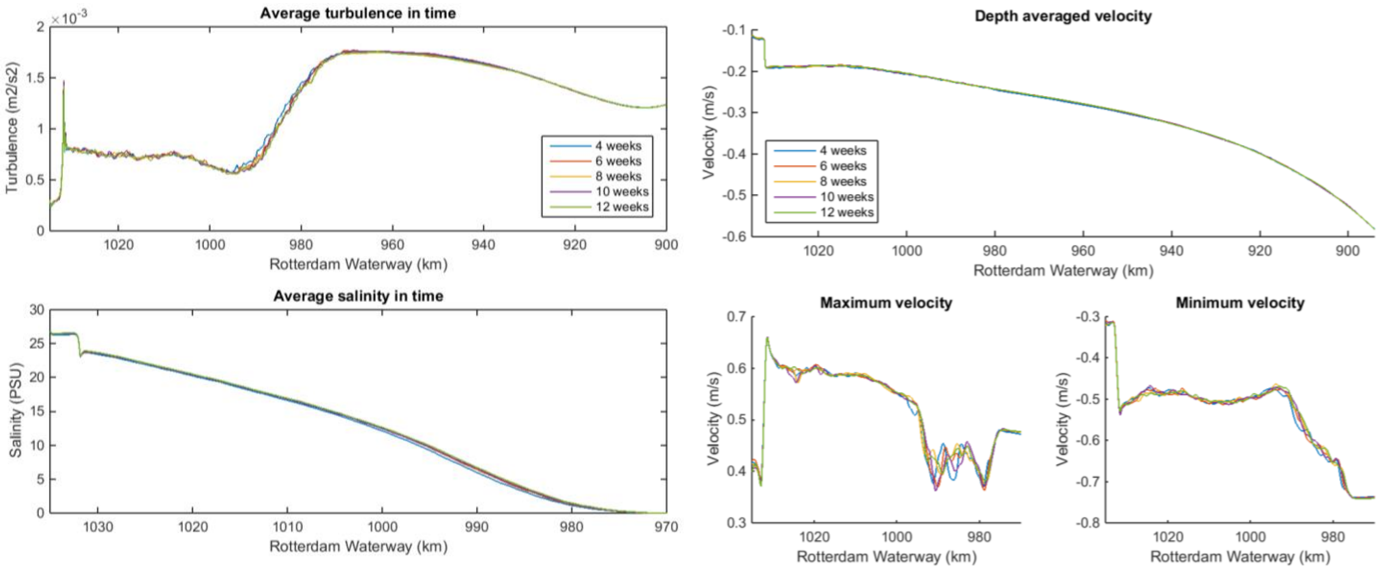

Figure 30 Righter panels: Average turbulence (top) and salinity (bottom) in time; Left panels: depth average velocity (upper panel), maximum velocity (lower left panel) and minimum velocity (lower right panel)

The change of the salinity in time is small. With the extension of the simulation time, the salinity is slowly intruding less far into the estuary near the bottom, as can be seen in Table 6 for second value of the salinity fresh. The salinity moves from kilometer 977.2 towards kilometer 766.4. The values in the table show the location where the water column becomes fresh (<0.1 PSU). The salt intrusion of the top layer shows some variation between kilometer 1022.6 and 1022.8.

Table 6 Results changing fresh water discharge conditions

	4 weeks	6 weeks	8 weeks	10 weeks	12 weeks
Loc. max. (km)	994	993.4	993.6	993	993.2
Length ETM (km)	44.8	43.8	46.4	45.6	43
ETM (kg/m^3)	0.103	0.124	0.143	0.156	0.172
Salinity salt (km)	N.a./ 1023.4	N.a./ 1022.8	N.a./ 1022.6	N.a./ 1022.8	N.a./ 1022.6
Salinity fresh (km)	1004.4/977.2	1004.8/976.8	1003.8/976.4	1004.6/976.4	1003.8/976.4

6.1.2 Changing fresh water discharge

6.1.2.1 Initial response

Salinity

An increase in discharge moves the average salt wedge and the null point estuary outward towards for example kilometer 985 for the 95% discharge. A decrease in discharge moves the null point of the salt wedge more upstream, towards kilometer for example 1019.4 for the 5% discharge. The location where the bottom layer becomes highly saline (>28 PSU) also moves 4 kilometer upstream. The upper layer stays relative fresh until outside the estuary.

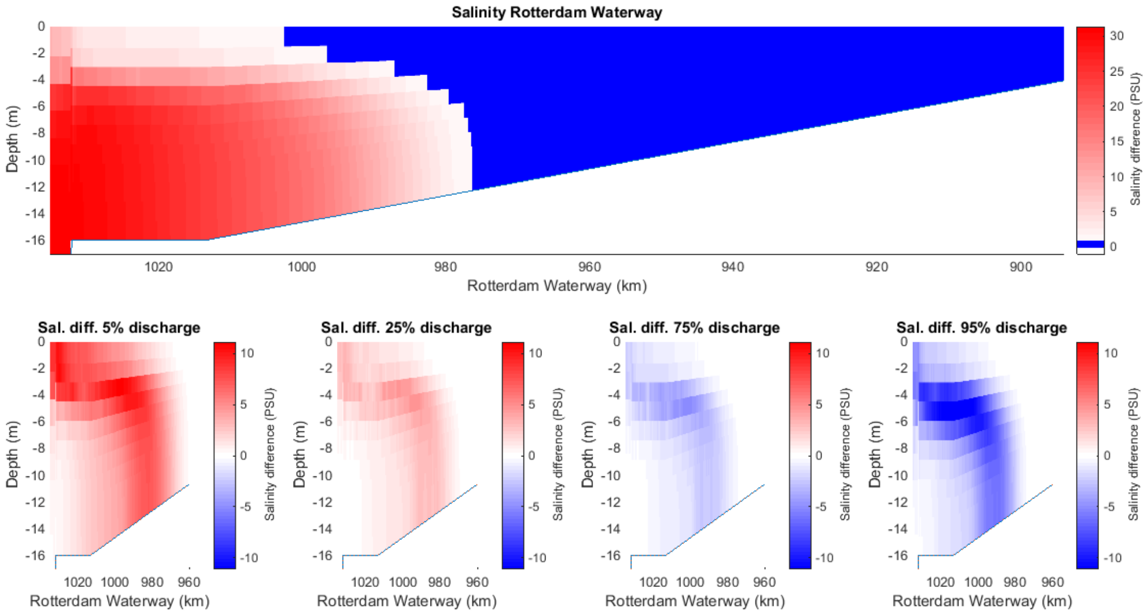

Figure 31 Salinity of the reference case (upper panel); Salinity difference for the 5% discharge (lower left panel); Salinity difference between reference case and 95% discharge (lower right panel)

The salinity pattern over the water column for increasing and decreasing discharge is similar. The layers between the fresher top layers and the saline layers below (fourth and fifth layer, depth around -4 meter) changes with the boundary which are the boundaries of the salt wedge. So if the boundary discharge increases, the salinity decreases. Also the layer between the fresh and saline section of the water column changes with the discharge. The changes for the 5% discharge seem to be more diffuse compared with the 95% discharge, because the length of the increasing salinity is larger at the front and at the top of the salt intrusion.

The location of the null point in the Rotterdam Waterway can be seen in Table 7. The movement due to the 5% discharge estuary upward (-12.6 kilometer) is larger compared with the change due to the 95% discharge estuary downward (7.8 kilometer).

Table 7 Changing location null point due to discharge (kilometer)

5% discharge	25% discharge	Average discharge	75% discharge	95% discharge
974.2	982.6	986.8	989.2	994.6

Hydrodynamics

The depth average velocity changes with changing boundary conditions as can be seen in the upper panel of Figure 33. Increasing discharge results in increasing depth average velocities in the Rotterdam Waterway. The depth average velocity increases, mainly due to the increased velocity in the upper part of the water column (appendix B). The velocity of the bottom two layers also increase with the increasing discharge, although the increase is small. The near bed velocity increases from 0.06 m/s with a discharge of 490 m^3/s towards a velocity of 0.08 m/s with an discharge of 2350 m^3/s. This is due to the tidal amplitude increase of 15 centimeter for the 95% discharge as can be seen in appendix C.1. This increases the barotropic pressure and thus the velocity. This is however hardly visible in Figure 32. What is visible is the increase in ebb velocity in the higher part of the water column, which is further increasing estuary outward.

The length over which the velocity becomes zero is also determined by the discharge, with a movement of the average zero velocity outward, as can be seen in appendix D.3. So the increased velocity is over a shorter length for the 95% discharge.

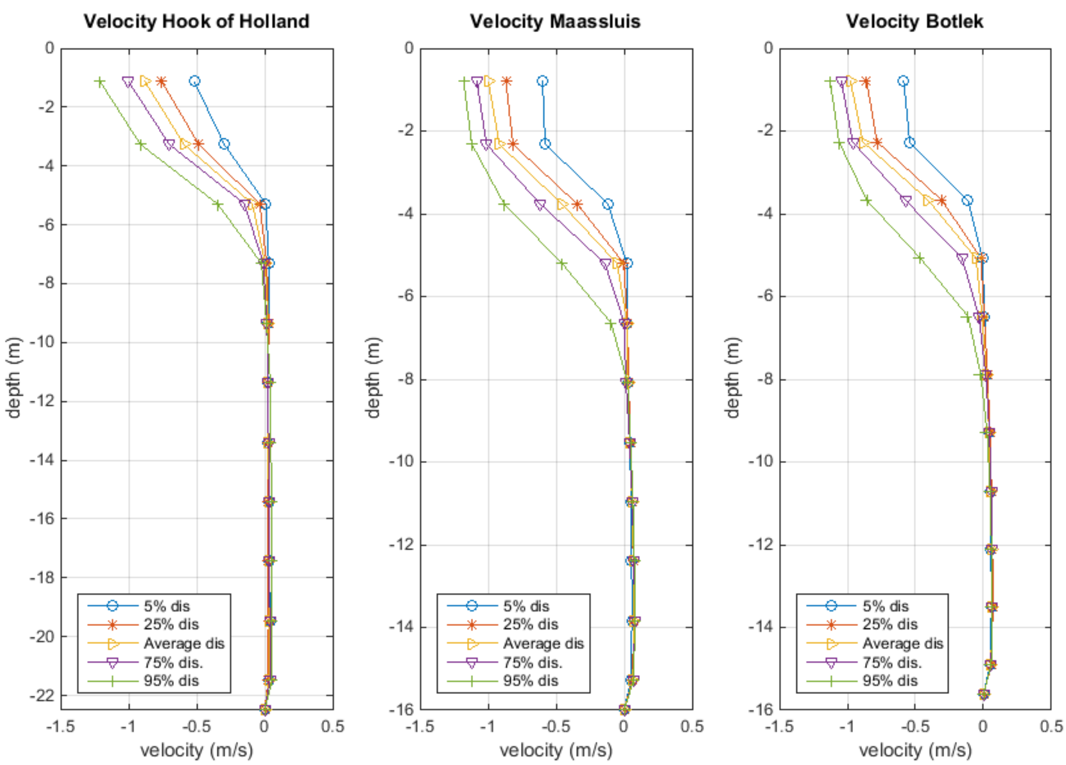

Figure 32 Average velocity for the discharge sensitivity for Hook of Holland (km 134.6), Maassluis (km 121.8) and Botlek (km 1009.6)

The asymmetry between the ebb and flood velocity decreases near the bottom with increasing discharge. The maximum velocity decreases while the minimum velocity increases with increasing discharge. The maximum velocity also decreases faster with increasing discharge, towards the location where the ETM moves. The difference in the velocity where the ETM moves is also larger for the 95% discharge and almost zero for the 5% discharge. However there is a difference between the saline part (from the ETM estuary outward) and from the ETM estuary upward. The ebb (minimum) velocity is roughly constant near the bottom from the ETM towards the sea of about 0.5 m/s.

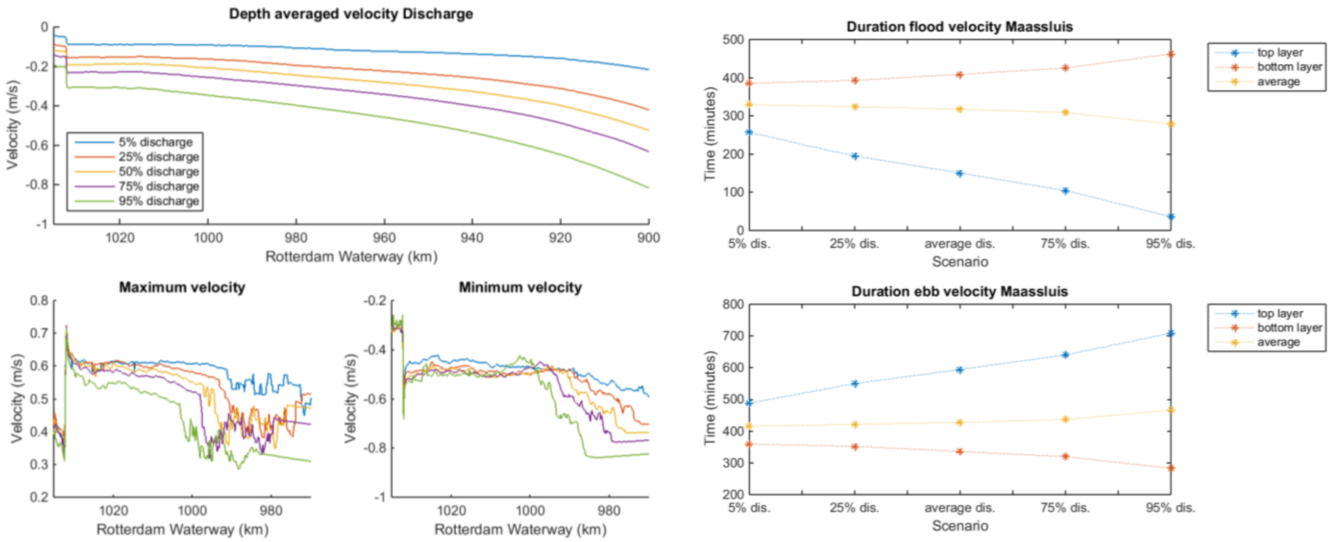

Figure 33 Left upper panel: depth average discharge; Lower left panel maximum (flood) velocity; Lower right panel minimum (ebb) velocity

Not only velocity increases or decreases, also the length of the ebb and flood velocity changes, as can be seen in Figure 33 for Maassluis. The duration of the ebb velocity increases with the increasing discharge for the top layer. Near the bottom however, the length of the flood increases with the increasing discharge between the ETM and the mouth of the estuary, resulting in a higher average velocity for layer 11.

The discharge also influences the turbulence and the damping of the turbulence as can be seen in Figure 34 with the turbulence for the 5% discharge left and the 95% discharge right. For the 5% discharge the turbulence is only 0 in layer 1 (at the top of the water column) and there is very small turbulence for the first 4 layers which is nearly 0. For the 95% discharge the turbulence is damped for until – 10 meter (layer 5 in Figure 34). The turbulence in the remaining layers is also smaller.

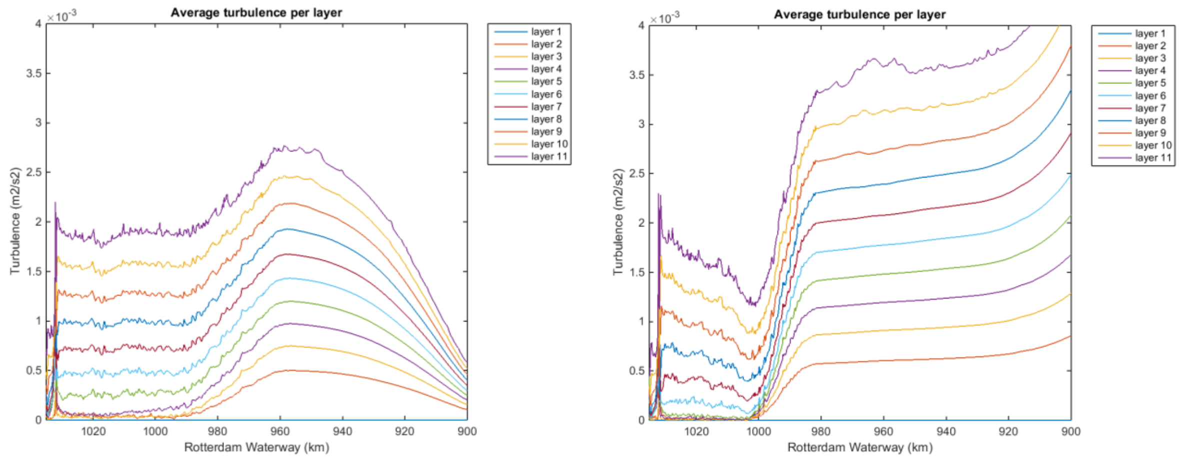

Figure 34 Turbulence for the 5% discharge (left) and the 95% discharge right

The vertical velocity clearly shows an increase with increasing discharger for the middle (saline) layers, as can be seen in Figure 35 for the 5% discharge in the left panels and 95% discharge in the right panel. The increasing vertical velocity increases also the vertical movement of sediment. The gravitational circulation increases due to the increase of the salinity gradient. For the increasing discharge, two locations of gravitational circulation seem to exist after one spring neap cycle.

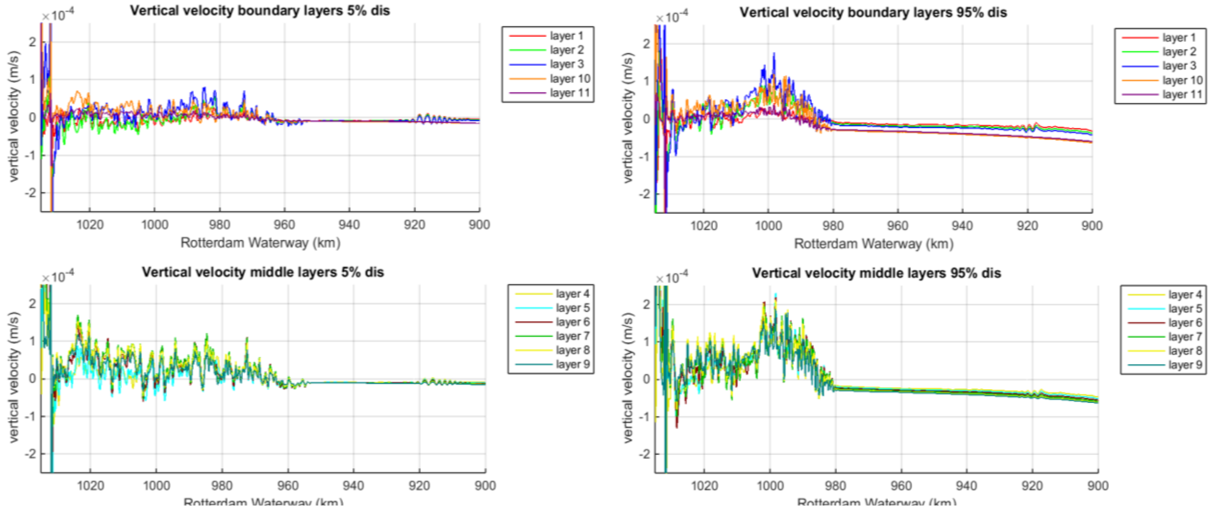

Figure 35 Gravitational circulation for 5% discharge (left) and 95% discharge

Sediment transport

Figure 36 shows the sediment concentration for the different fresh water boundary conditions. An increasing discharge leads to increasing sediment availability stream upward, because the import of sediment increases and the increased velocity which picks up more sediment from the bottom.

The concentration in the active top layer does increase for the fine sediment regarding to large discharges. The 5% discharge results in higher suspended sediment concentrations in the top layer compared with the 25% discharge. This is due to a combination of the turbulence damping and the availability of sediment. For the 25% discharge the import of sediment from the fresh water boundary decreases, however the turbulence is still damped out in these layer which makes it possible for the sediment to rain out in the lower layers. For the 5% discharge the import of sediment from the fresh water boundary decreases to zero, however the velocity difference is too low to damp the turbulence. So the sediment which is already in the water column stays in the water column due to the turbulence.

For the near bed layer however, the concentration does not increase anymore when the 75% discharge and the 95% discharge are compared. The concentration of the suspended sediment with the decrease from 50% to 25% discharge also does not lead to a decrease in suspended sediment concentration for the initial response in the near bottom layer, due to (increasing/decreasing) tidal asymmetry.

The length of the ETM is changing with changing conditions. The length of the ETM is nearly 60 kilometers for the 5% discharge and only 30 kilometer for the 95% discharge. So the discharge is decreasing the length of the ETM.

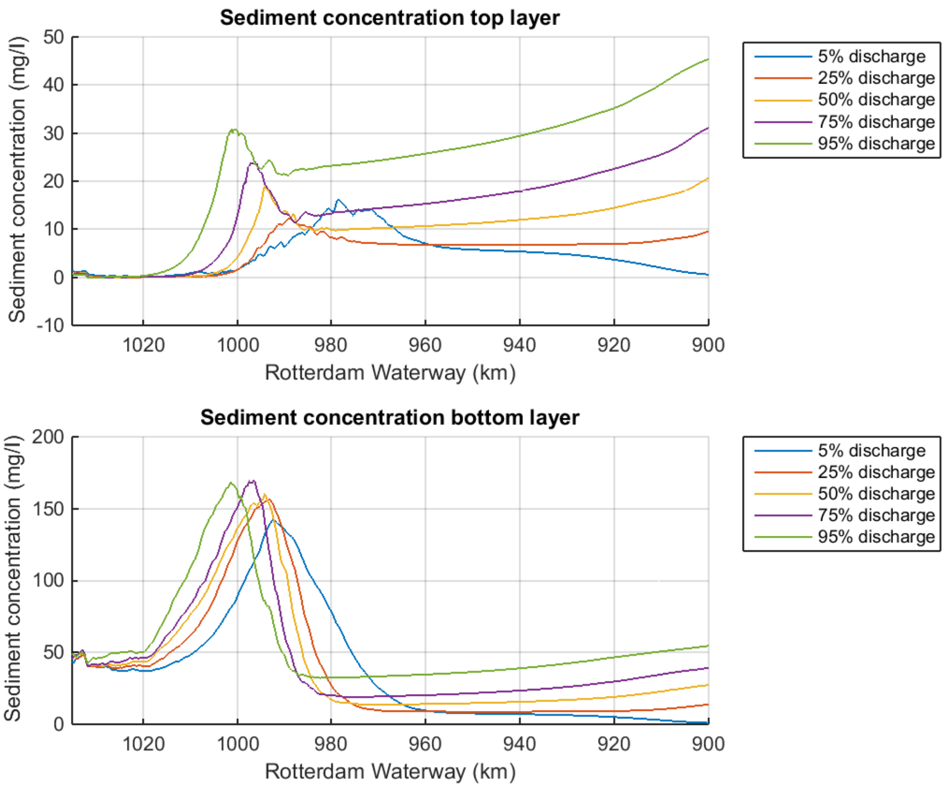

Figure 36 Tide integrated sediment concentration with varying discharge for the top layer (upper panel) and near bottom layer (lower panel)

6.1.2.2 Medium term response

For the extension in time hydrodynamics do not differ much from the initial response. The salinity moves towards an new equilibrium location with the change of the discharge. The equilibrium location has been reached after two spring neap cycles after the change in discharge. The described hydrodynamics in chapter 6.1.1. change with the salt wedge towards the new location.

The medium term response of the ETM for the 5% discharge (left) and the 95% discharge (right) is shown in Figure 37. The medium term response of the ETM for the 25% and 75% discharge can be seen in appendix F.

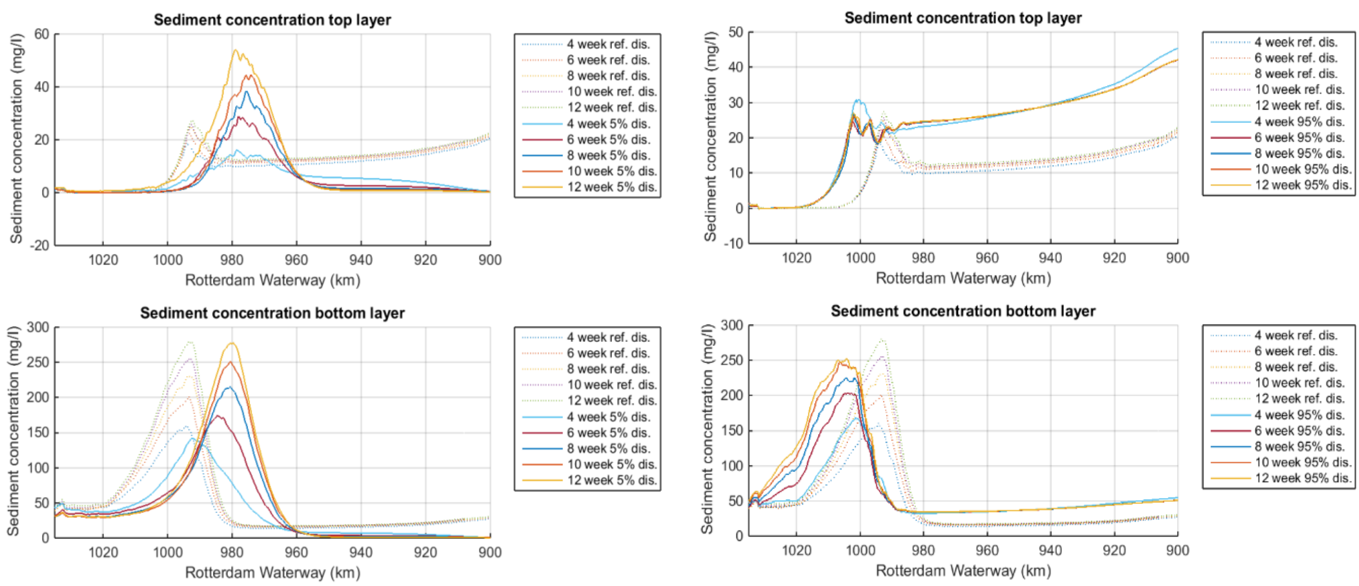

Figure 37 Long term response of the sediment in the ETM for 5% discharge in the left panel and 95% discharge for the right

The change of the discharge leads to a movement of the ETM for the 5% and 95% discharge, which are not yet reached after one spring neap cycle. The increased discharge pushes the ETM outward while the lower results in a movement estuary upward. The concentration near the bottom is 20 mg/l lower after 12 weeks. The concentration in the upper layer is about 5 mg/l higher.

The concentration of suspended sediment does not change for the lower discharge near the bottom. Roughly the same concentration has been reached after 12 weeks at another location. The concentration of suspended sediment in the top layer however almost doubled.

The long term response of the ETM with a discharge of 95% shows more variation. The ETM increases in the first time step of after the change in discharge, however after 12 weeks the ETM decreases for the bottom layer. This is due to the high flow velocity in the top layers, because not only the top four layers are floating over the saline layers, also the fifth layer is now floating over the saline layers. Furthermore asymmetry is decreasing due to increase of the ebb velocity in the lower layer. So more sediment is transported estuary outward instead of moving to the ETM.

The top layer of the bottom shows the same pattern, as can be seen in Figure 38. The peak in fine sediment shifts estuary upward and decreases in concentration for a decrease in discharge. For an increase in discharge the concentration in the top layer of the bottom increases and becomes wider, and the location is shifted estuary outward. The concentration sediment being blocked by the step is also affected by the changing discharge. For the decreasing discharge the concentration of sediment being blocked is also decreasing in time while for the increasing discharge the blocked sediment is still increasing in time. So the sediment settling in front of the step is also sediment escaping from the ETM and flowing to the sea, because the wave conditions are exactly the same.

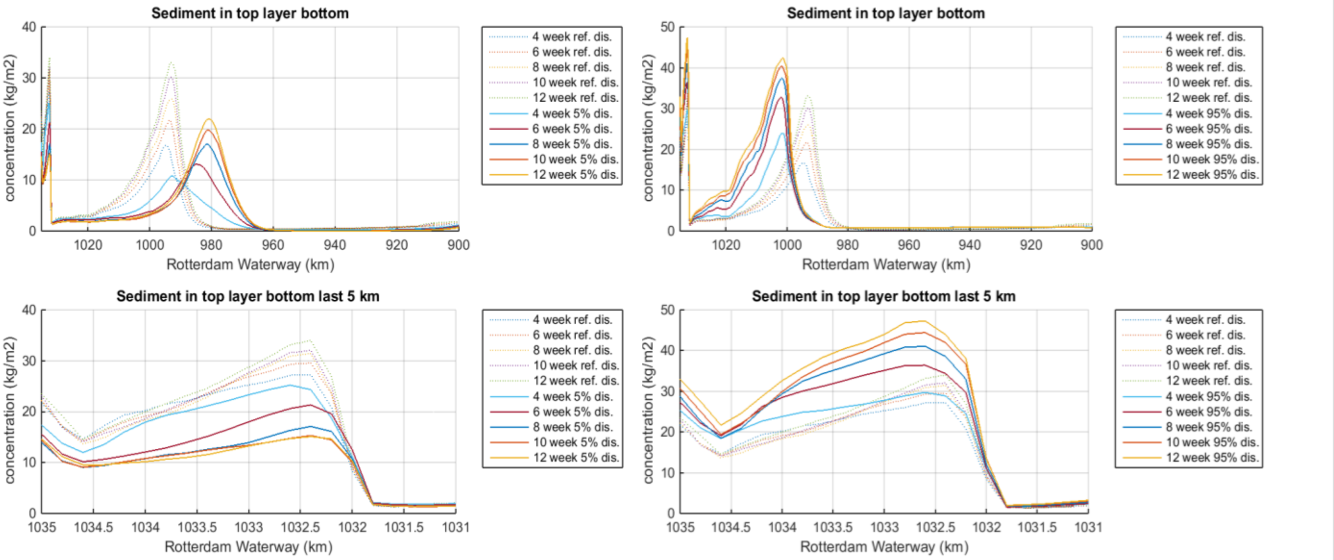

6.1.3 Changing wave conditions

6.1.3.1 Initial response

Salinity

The salinity profile does not show significant changes compared with the reference case with average wave conditions as can be seen in Figure 39. The summer waves in the lower left panel show a small decrease in the salinity compared with the reference case (in the upper panel). The increase due to storm waves is larger in the lower right panel, but still small compared with the changes due to changing discharge. The change is however maximum 2.5 PSU, which is less compared with the maximum change of 10 PSU for the changing discharge. The increase in salinity is due to a very small increase in water level of 10 centimeter during ebb, as can be seen in 91 appendix C.1., so the barotropic pressure gradient is increasing for storm waves resulting in increasing salinity.

The pattern of increase is also different from the increasing discharge. The saline area until the null point increases equal while the top layers are almost nog affected by the changing wave conditions. Only the head of the salt intrusion has some increased salinity compared with the other area.

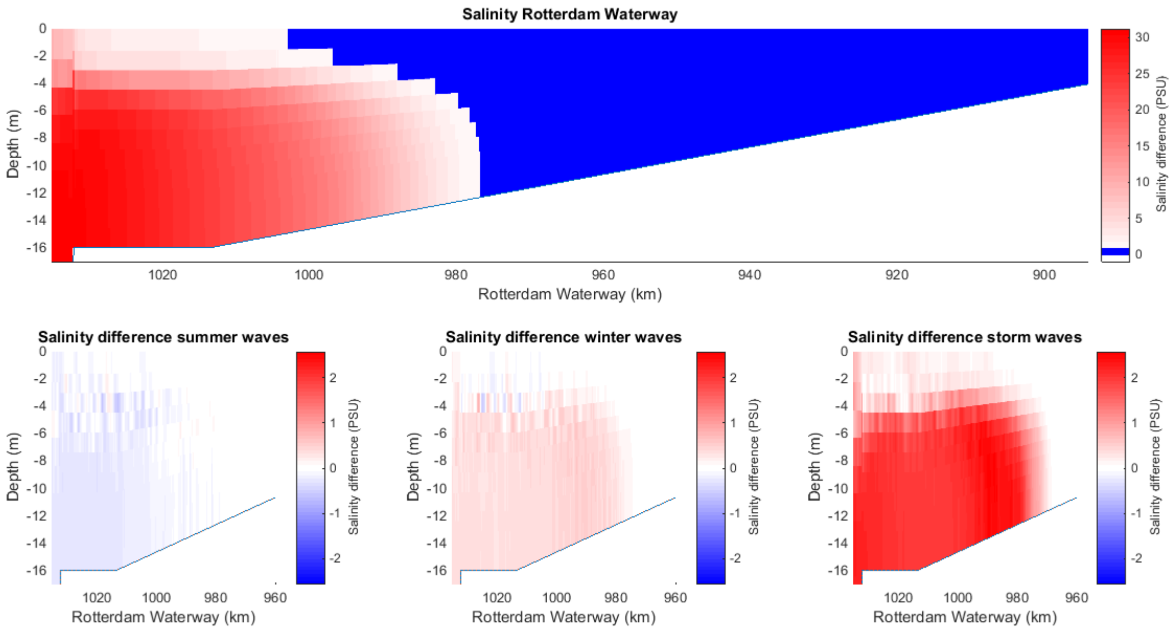

Figure 39 Salinity for the reference case (upper panel); Salinity difference between reference case and summer waves (lower left panel); Salinity difference reference case and storm waves (lower right panel)

The change due to the changing wave conditions can be seen in Table 8. Only the storm waves show an change in null point, as also indicated by Figure 39. The null point moves 4 kilometer estuary upward due to the increasing wave conditions.

Table 8 Location of null point for changing wave conditions (kilometer)

Summer waves	Average waves	Winter waves	Storm waves
986.6	986.8	986.2	982.4

Hydrodynamics

The wave conditions don't change the hydrodynamics in the waterway significantly compared with the hydrodynamic change due to changing discharge. This is confirmed by the hydrodynamic change which is small compared with the reference situation, due to the dissipation of the waves on the foreshore of the sea.

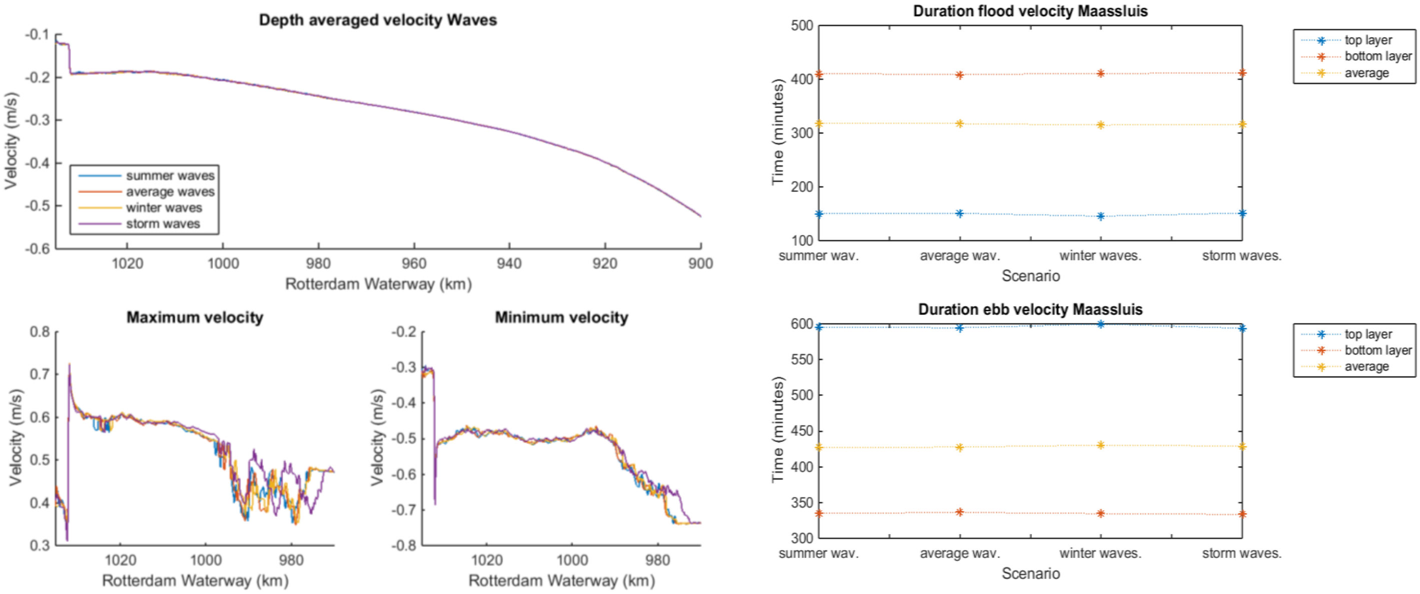

Figure 40 Top: Depth averaged velocity for the different scenarios; Lower left panel: Maximum (flood) velocity; Lower right panel minimum (ebb) velocity

The waves have been broken on the foreshore which means they do not contribute significant to the flow velocities in the Rotterdam Waterway, as can be seen in the depth averaged velocity for the different scenarios in Figure 40. The depth average velocity is constant for all four conditions.

The ebb and flood velocity however show some variation for the storm waves. The area where the ETM moves is replaced estuary inward due to the salinity intrusion for the flood velocity in the lower left panel. The velocity in this area has slightly increased compared with the other scenarios. Also the velocity in front of the ETM has slightly increased for the storm waves. The magnitude of the ebb velocity in the lower right panel has not been changed. The increased salinity moves the velocity profile slightly estuary inward.

The average velocity for Hook of Holland, Maassluis and the Botlek area show almost no change compared with the reference conditions, as can be seen in Figure 41. The flood velocity is small for the lower layers and the ebb velocity on top is flowing estuary outward.

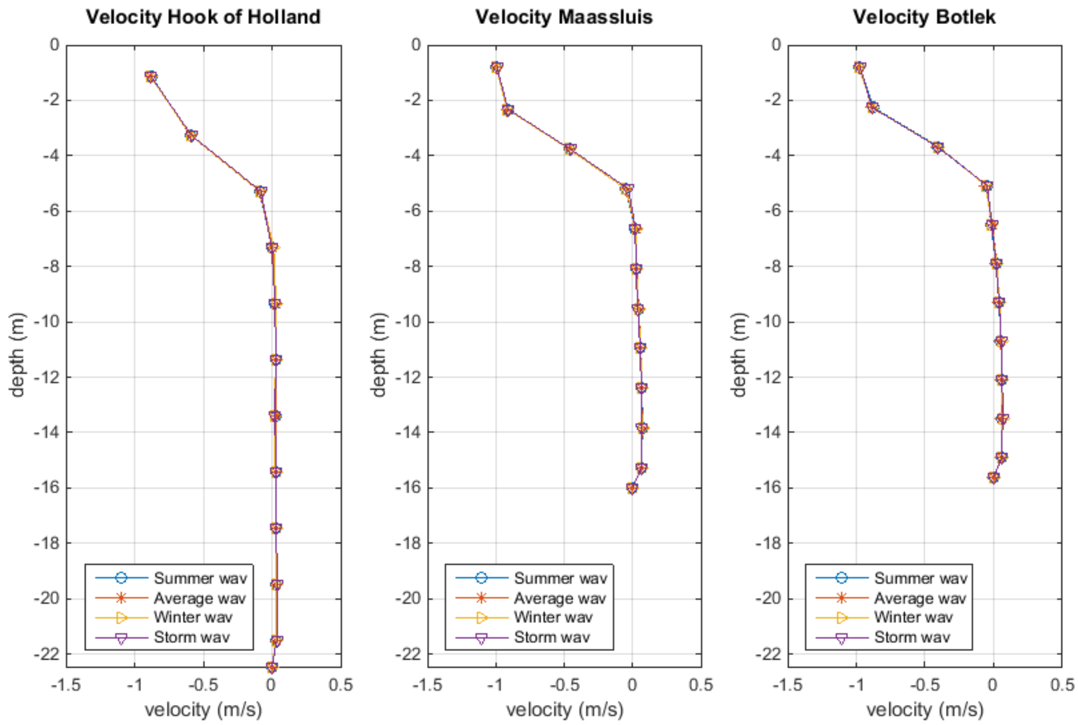

Figure 41 Velocity profiles due to changing wave conditions

The duration of the ebb and flood velocity show no change, so the tidal asymmetry is slightly increasing during storm waves, but constant for summer, winter waves compared with the average waves. The turbulence and gravitational circulation show no change as can be seen in appendix F.

Sediment transport

Figure 42 shows the suspended sediment concentration for the sensitivity due to changing wave conditions near the sea for the top layer and the layer near the bottom. The waves affect the sediment transport by increasing the available amount of sediment from the seaside corresponding to the scenario. During storm conditions the incoming sediment increases, especially in the near bottom layer. Summer waves show a small decrease in sediment availibility near the beginning of the waterway until the step in bottom depth.

Winter waves and storm waves show a decrease in the sediment availability in the top layer, while the summer waves and average waves almost the same availibilty of sediment. The decrease in suspended sediment concentration in the top layer is 4 mg/l. Compared with the suspended sediment concentration of 19 mg/l for the maximum is the increase significant. The variation is small compared with the total concentration of 160 mg/l for the suspended sediment concentration near the bottom.

The ETM has sligtlhy been moved estuary upward due to the increased salinity intrusion for the strom waves, as can be seen in the lower panel of Figure 42.

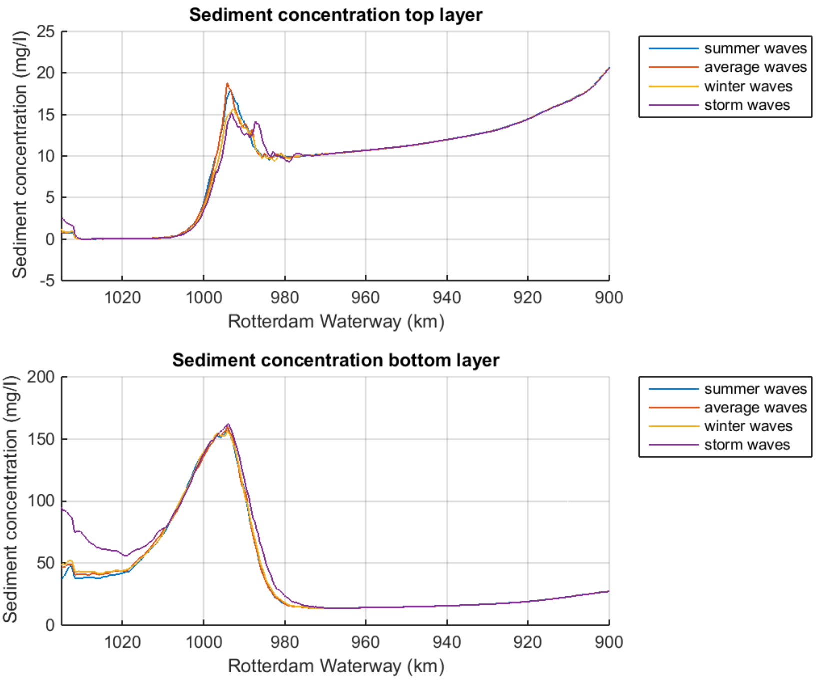

Figure 42 Tide averaged sediment concentration ETM

The initial response of the ETM for the increased wave height is small. So although the sediment from sea is increasing due to the changing waves, this does not (yet) results in higher sediment concentration in the ETM.

6.1.3.2 Change in time

The long term effect of waves with a significant wave height of summer is shown in Figure 43. The left panel shows the change in suspended sediment concentration due to summer waves for the top and bottom layer. The lower summer waves have almost no impact on the ETM, which means due to the slightly lower import of sediment coming from sea, the suspended sediment concentration does not change. For the average situation the sediment import coming from sea is not contributing to the sediment concentration in the ETM.

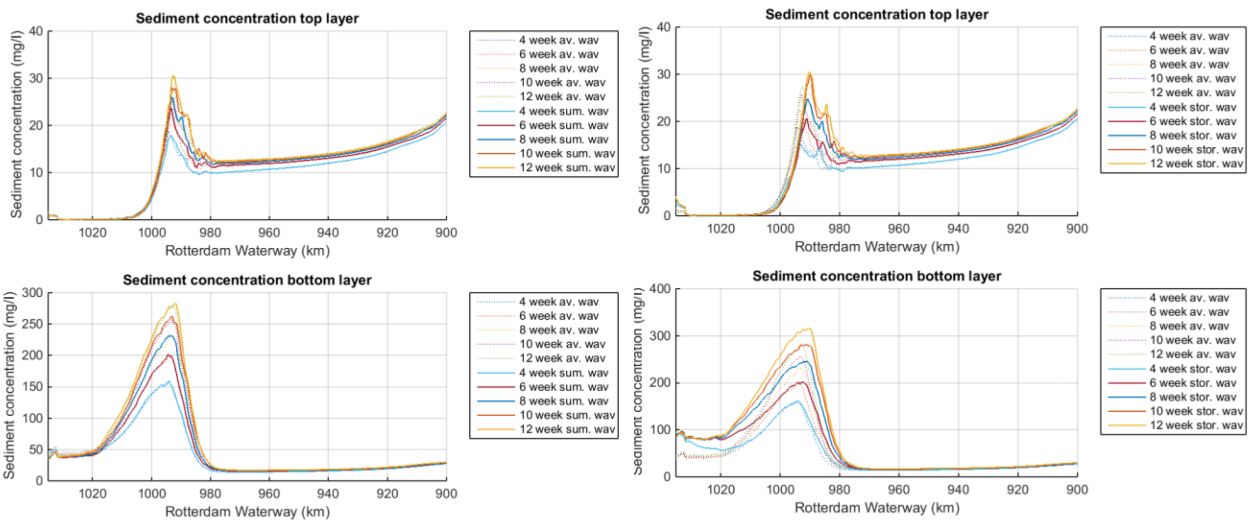

Figure 43 Sediment concentration along the Rotterdam Waterway in the left panel during summer waves; in the right panel for the long term storm waves

The increase in import of sediment from sea has impact for the maximum suspended sediment concentration on the long term, so after one tidal cycle the sediment has not yet reached the ETM. The storm waves increase the sediment coming from the sea and thus increase the suspended sediment concentration in the top and bottom layer of the water column, due to the increase in sediment import coming from sea.

Where the sediment concentration in the top layer slightly decreases during the first tidal cycle. The sediment concentration increases in the following tidal cycles until a maximum after 10 weeks of 30 mg/l which stays constant after the following tidal cycle. The concentration near the bottom layer increases from 280 mg/l towards 310 mg/l.

The available sediment in the active layer of the bottom shows some variation, especially in front of the step where the sediment is blocked which can be seen in the lower panels of Figure 44 for the summer waves and storm waves. During the first spring neap cycle the increase in available sediment is large for the storm waves compared with the average waves. While during the following spring neap cycle the increase compared with the first concentration is small. So there seems to be a maximum in sediment being blocked of about 50 kg/m2. The variation in available sediment for the storm waves is small. The concentration in front of the step also shows only small variation for the following spring neap cycles.

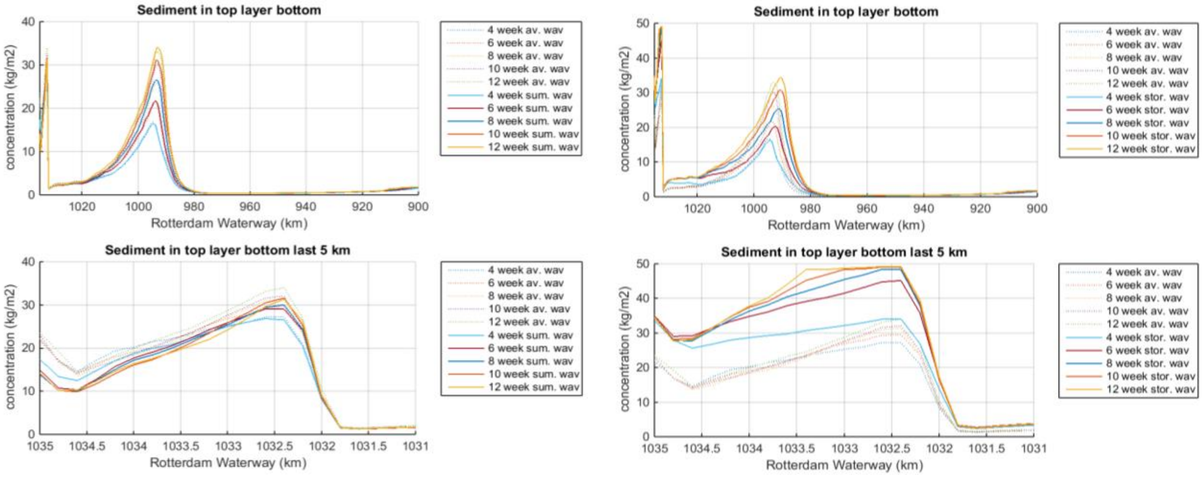

Figure 44 Available sediment in top layer for summer waves (left) and storm waves (right)

The variation of the waves only contributes to the sediment in the ETM for a very small amount within the realistic boundaries, because the decrease in front of the step does not decrease for summer waves and the suspended sediment concentration also shows no change for the summer waves. The concentrations only change for large increases in waves, which results in higher concentration sediment near the seaward boundary, and thus an increase in sediment in front of the step.

6.1.4 Synthesis

6.1.4.1 Salinity

The salinity moves with the tide and the discharge in the estuary. The salinity is moving with the tide in the estuary. Changing discharge leads to a change in location for the null point. The average location of the salinity intrusion is towards 974.2 km for the 5% discharge, 986.8 km for the reference discharge and 994.6 km for the 95% discharge.

The maximal change in salinity is near boundary layers of the salt wedge at the head of the salinity intrusion and at the third and fourth layer of the salinity intrusion. The maximum change in salinity is 10 PSU for both the increasing and decreasing discharge.

Changing the wave conditions leads only to small differences in salinity for the estuary, with maximal change of 3 PSU for storm waves. The increased salinity is more equal over the water column instead of near the boundaries of the salt wedge.

6.1.4.2 Hydrodynamics

The hydrodynamics are determined by the discharge, the tide and the salinity in the estuary. Tidal asymmetry causes tidal pumping in the estuary. The estuary is flood dominant which means higher flood velocities during a shorter period. The average velocity near the bottom decreases towards 0.05 m/s for the 5% discharge and increases for increasing discharge towards 0.1 m/s for the 95% discharge. The increase is mainly due to the increased average flood velocity duration due to the increased barotropic pressure gradient due to increased tidal amplitude during the 95% discharge scenario.

The average velocity near the top is 0.6 m/s estuary outward near the estuary mouth which increases with increasing discharge towards 1.2 m/s estuary outward near the estuary mouth for 95% discharge. The average velocity for the top layers is also mainly due to the increased ebb velocity duration in the top layers.

The turbulence is damped in the top layers of the water column, corresponding with the salinity pattern. The turbulence decreases where the salinity is increasing and the turbulence in the top three layers is eventually damped. Gravitational circulation seems to appear, but the occurrence is very small.

6.1.4.3 Sediment transport

The sediment transport is determined by salinity, tidal asymmetry, discharge, the wave conditions and the availability of sediment in the estuary.

The salinity determines the location of the null point and thus the location of the ETM, because it determines the location where the average velocity is zero. The average location of the null point corresponds with the location where the average velocity is zero near the bottom.

The discharge determines the location of the null point of the salinity and thus determines the location of the null point of the salinity. The discharge also determines the available sediment from the fresh boundary. The increased tidal asymmetry with increasing discharge leads to increased flood duration near the bottom. This means more sediment is trapped in the ETM, because it is driven back into the estuary with the flood velocity.

Long term 5% discharge leads to the same concentration of suspended sediment in the ETM, only moved estuary inward. For the top layer the decreased discharge leads to increased suspended sediment concentration because less turbulence is damped so the sediment is able to remain in suspension in the top layers of the water column. The available sediment in the bottom decreases, so less sediment is settling in the tidal channel. Also less sediment is blocked by the step in the bottom, so less sediment escapes towards the sea because the wave conditions are the same, and sediment erodes from the bottom into the estuary.

Long term 95% discharge does not lead to increased suspended sediment concentrations compared with average in the ETM, although the tidal asymmetry increases and the sediment from the fresh water boundary is also increasing. The sediment in the bottom layer is increased in the tidal channel and in front of the step increased, so more sediment is stored in the bottom.

The wave conditions determine the availability of sediment from sea, but only for a large increase in wave conditions in the sea. During the first spring neap cycle the suspended sediment concentration has not yet increased compared with the reference situation, but during the following spring neap cycles the suspended sediment increase in the ETM. Also the available sediment in the bottom in front of the step increased for the storm waves, so the amount of sediment coming from sea increased.

6.2 Scenario analysis

A scenario analysis is executed to determine the effect of the bathymetry and the effect of deepening for the hydrodynamics and the sediment transport characteristics in the prismatic channel as evaluated in section 6.1. In the first scenario two harbor basins are included in section 6.2.1. The effect of deepening is discussed in section 6.2.2.

6.2.1 Harbor basins

6.2.1.1 Salinity

The effect of the harbor basins for the is the decrease of the salinity intrusion in the study area resulting in the movement of the null point from kilometer 977 towards kilometer 985, see Figure 45. The decrease in salinity intrusion is because part of the tidal prism is flowing into the harbor basin, decreasing the tidal prism increasing in the channel itself.

The salinity in the top layers is not affected by the top layers, because the salinity is already low for the reference scenario.

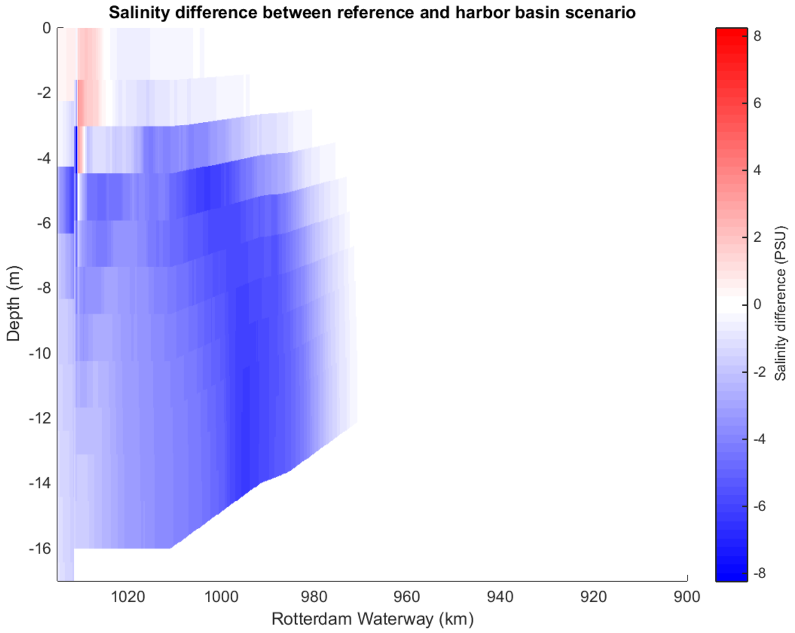

Figure 45 Change is salinity for the harbor basin scenario compared with the reference scenario with average conditions

6.2.1.2 Hydrodynamics

The velocity is influenced by the presence of the harbor basins in the study area, as can be seen in Figure 46. The first change due to the harbor basins is in front of the first step in the bottom line, where the velocity decreases with 0.02 m/s. The decrease in velocity means the increase in ebb velocity at this location. The decrease in velocity is due to the decrease of the flood velocity near the step, as can be seen in the lower left panel of Figure 46. So the tidal asymmetry increases due to the inclusion of the harbor basins.

The changing salinity results in a changing velocity pattern in the area where the null point moves. The flood velocity increases and the length of the area where the null point moves has moved estuary outward with the salinity.

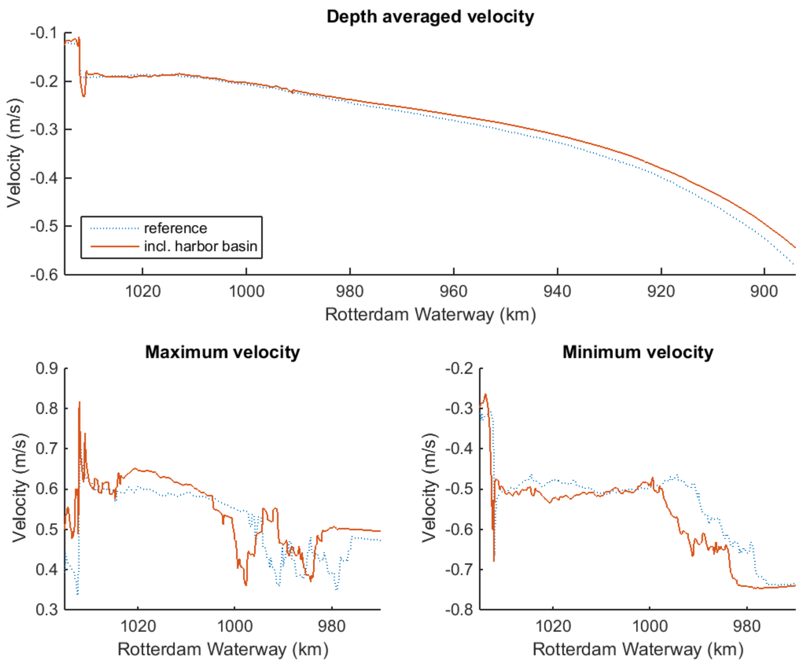

Figure 46 Depth average velocity (upper panel) of the reference scenario and the scenario including the harbor basins. Average flood velocity (lower left panel); Average ebb velocity (lower right panel)

the turbulence does not show much variation between the reference scenario (Figure 47 right panel) and the harbor scenario (Figure 47 in the left panel). So the precense of the harbor basins does not lead to large increased turbulence in the water column.

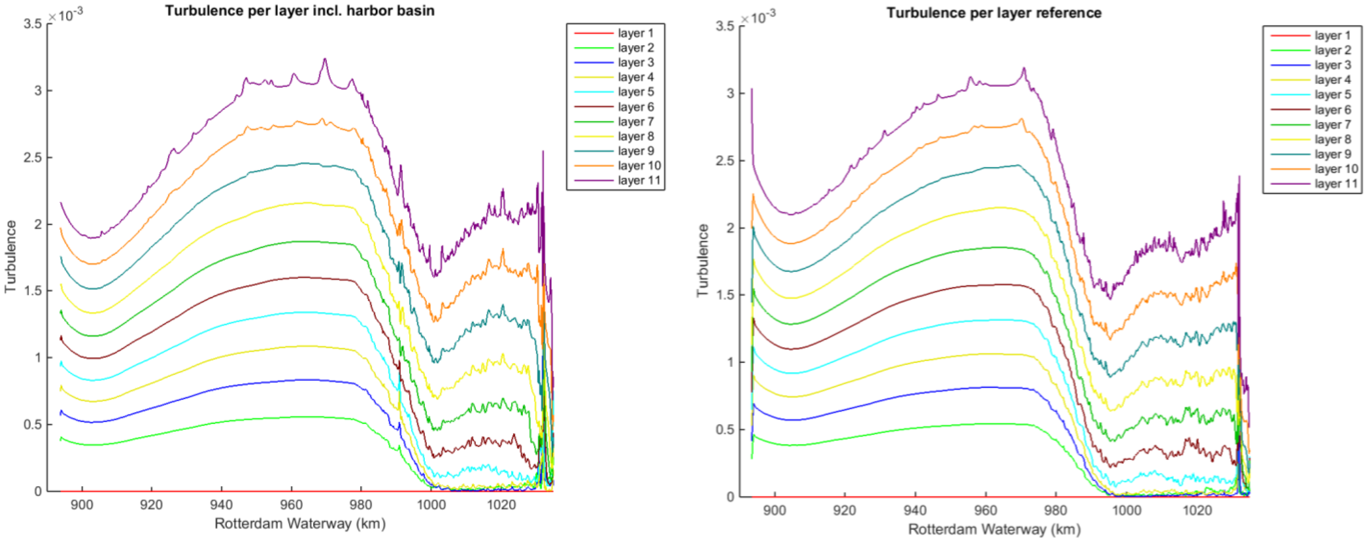

Figure 47 Turbulence for the scenario including harbor basins (left) and without harbor basins (right)

6.2.1.3 Sediment transport

The hydrodynamic changes result in changing sediment transport conditions. Figure 48 shows the evolution of the ETM with the harbor basins compared with the reference data. The changed salinity intrusion also changes the location of the ETM. The harbor basins however also increase the concentration of suspended sediment in the ETM.

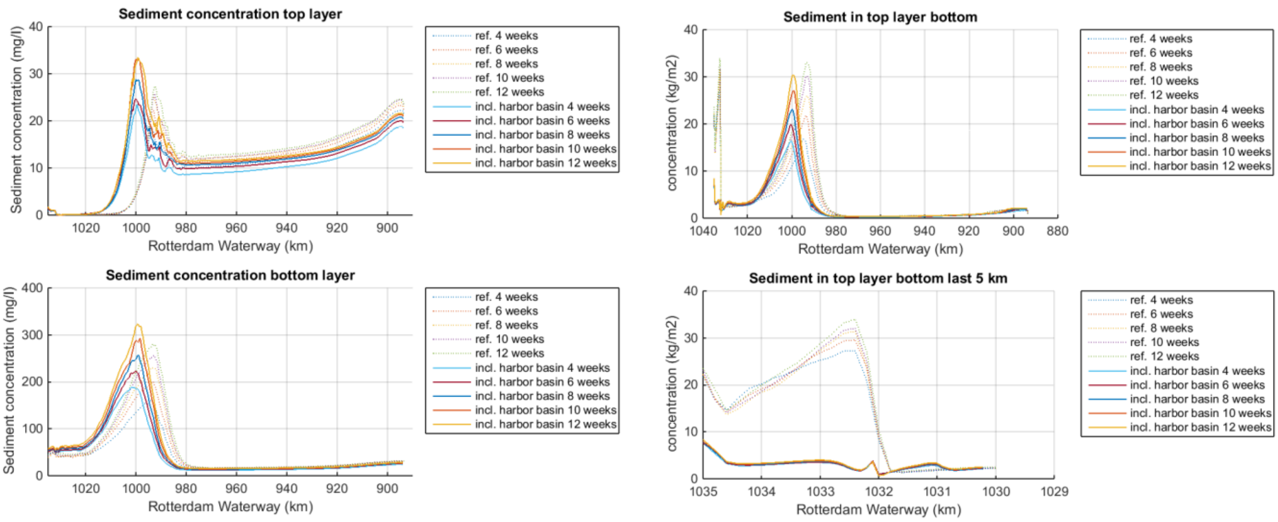

Figure 48 Sediment in the top and near bottom layer for the water column (left); Sediment in top layer bottom (right)

The total concentration of suspended sediment for the maasvlakte is increasing in time, as can be seen in the upper panel of Figure 49. The suspended sediment is the sum of the harbor basin area, which is 20 km^2 for the maasvlakte. The amount of sediment for the bottom layer is also increasing for the maasvlakte in time as can be seen in the lower panel of Figure 49. So the maasvlakte act as sediment trap for the sediment settling at the bottom, for the sediment settling in front of the first step. This is because the entrance of the harbor basin is just in front of the step on the depth of -22.5 meter, so the flow with the sediment is able to flow without being blocked.

The Botlek basin is also a sediment trap, but this is not clearly visible in the suspended sediment concentration (total area of 1.5 km^2) or the available sediment in the active layer of the bottom.

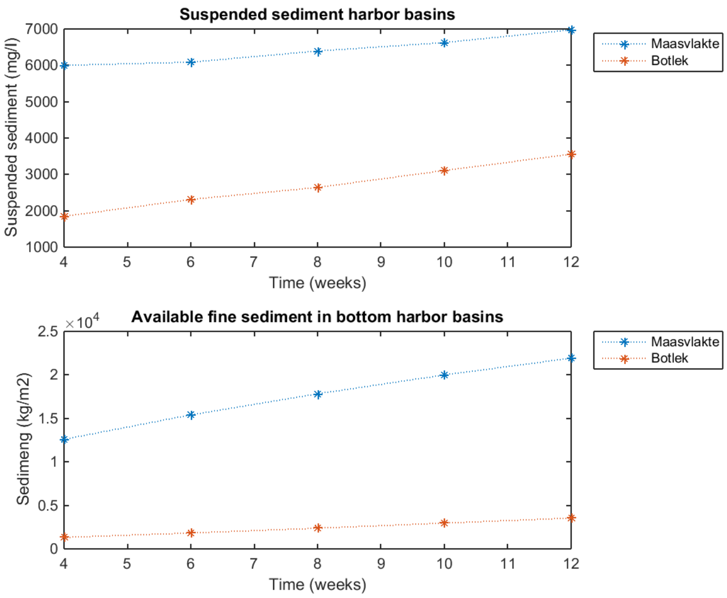

Figure 49 Total suspended sediment (upper panel) in the harbor basins; Total average fine sediment in top layer bottom (lower panel)

6.2.2 The effect of deepening

First the changes in salinity, hydrodynamics and sediment transport are discussed for the average conditions in section 6.2.2.1. Then the sensitivity of the step deepening is discussed in section 6.2.2.2. and the results of the ETM deepening are discussed in section 6.2.2.3.

6.2.2.1 Average conditions

Salinity

The salinity in the reference case is largely blocked the step in the bottom line. Figure 50 shows the difference in salinity compared with the reference situation where increased salinity (red in the figure) indicates increase in salinity for the deepened scenario. The original bottom line is also shown for the lower panels in Figure 50.

The salinity increases and intrudes further into the waterway due to the step deepening . The null point moves from 986 in the reference situation towards kilometer 983.4 in the deepened scenario. The largest increase in salinity is near the new 'step' just in front of the start of the bottom slope in the third and fourth layer (around -3 meter towards -6 meter). The increase is due to the created turbulence at this location, which can be seen in Figure 57. The turbulence mixes the saline and fresh water which results in higher salinity (max 4 PSU) compared with the reference scenario. The upper layers near -2 meter result in realtive longer salt wedge, because the salinity near the bottom increased, but near the top the salinity increases with less than 1 PSU compared with the refference scenario.

The salinity decreases in front of the null point, until the location of the null point for the reference case, near kilometer 990 for the ETM deepening. The salinity intrusion increases where the null point from kilometer 987 towards kilometer 983. So the tidal prism intruding in the estuary has not been increased, but the length of the salinity intrusion increased due to the deepening. This leads to lower salinity in the section towards the original null point and increased salinity from the original null point towards the new null point.

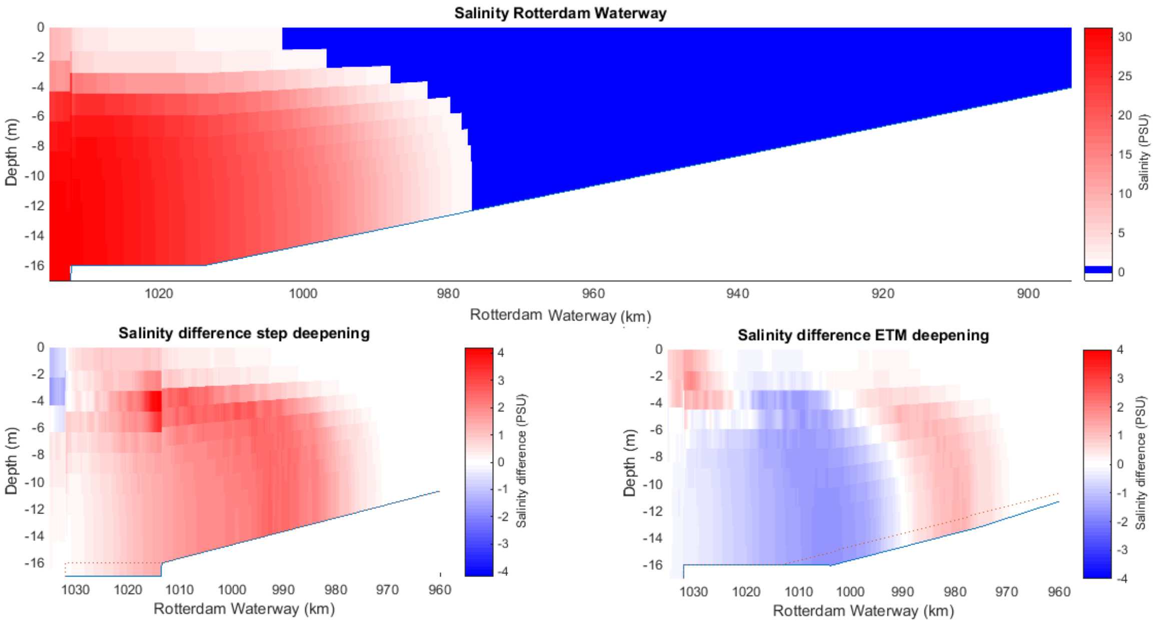

Figure 50 Difference in salinity compared with the reference case

Hydrodynamics

The average velocity foe Hook of Holland, Maassluis and the Botlek can be seen in Figure 51. The step deepening leads to very small variations in the averaged velocity. The setp deepening leads to increased velocity of 0.04 m/s near -7 meter depth for Hook of Holland. The increase is due to the increase in baroclinic pressure gradient. The salinity intrusinion results in the same stratification in the lower water column, but increased stratification in the middle part of the water column. The velocities for the other locations result in the same velocity near the bed, so the increase in baroclinic pressure decreases estuary inward.

The ebb velocity increases from -0.59 m/s towards -0.64 m/s near the top at -3 meter depth near Hook of Holland, while for the Botlek the average velocity decreases from -0.42 m/s to -0.31 m/s for the same depth. This is possibly due to the step in bottom slope just in front of the Botlek, causing a sudden increase in salinity due to increased turbulence near -4 meter depth increasing the baroclinic pressure gradient again. This effect has already been damped out near -6 meter depht. So the decrease in velocity is probably a combination between increased turbulence and increased baroclinic pressure gradient, because for the other cases the increase in baroclinic pressure gradient only results in a small increase or decrease of about 0.04 m/s.

The ETM deepening shows a small decrease in ebb velocity of 0.04 m/s from -1 towards -0.96 m/s for -1 meter depth near the Botlek. The flood velocity shows a very small increase, but this increase is almost neglecible. This means the deepening near the ETM decreases the depth of the average flood velocity.

The average velocity is only sligthly decreasing near the top, while the flood duration is decreasing with 50 minutes per tidal cycle near the top as can be seen in Figure 52. So the velocity is decreasing for the ETM deepening with average conditions near the top. This is due to the small decrease in water level as can be seen in appendix C.4 Figure 96. The decrease in water level leads to a decrease in barotropic pressure gradient leading to decreased tidal velocities. Because the estuary is flood dominant, a decrease in tidal amplitude leads to an increase in flood velocity.

The baroclinic pressure gradient near the bottom however is increasing due to the increasing stratification of salinity leading to the same flood velocity period near the bottom and constant average flood velocity near the bed, even increasing the average flood velocity near the bottom for Hook of Holland with 0.03 m/s.

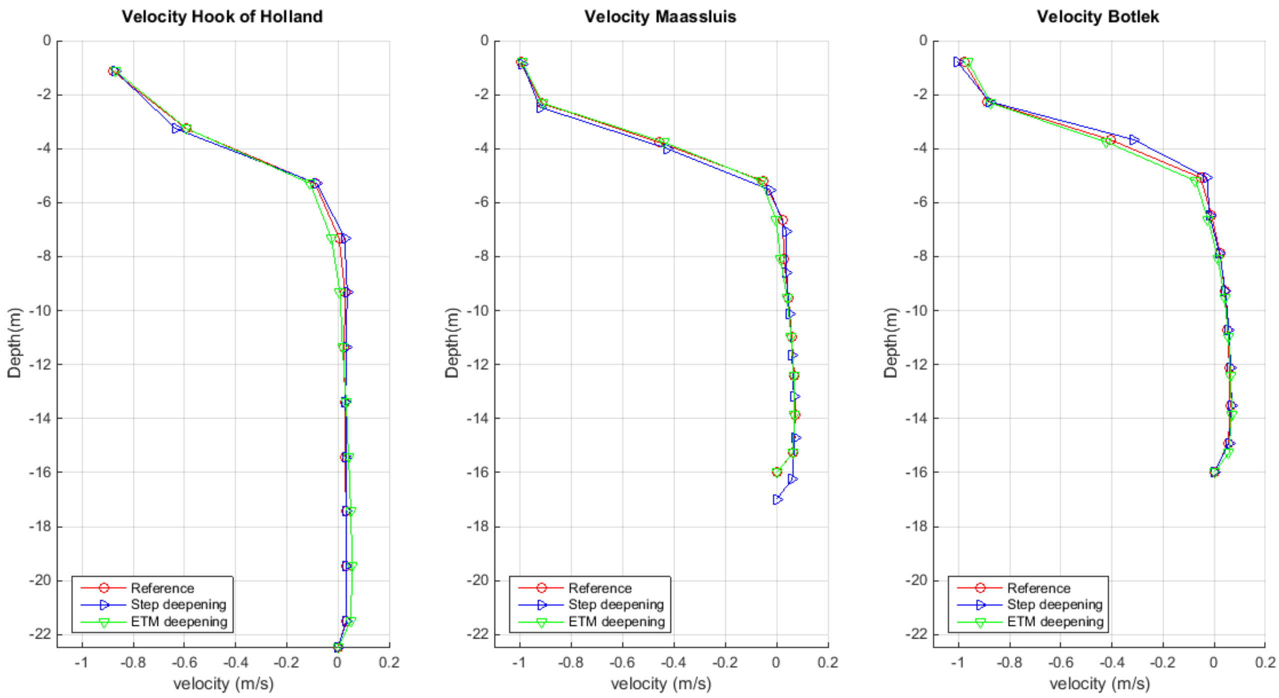

Figure 51 Average velocity for Hook of Holland (km 1034.6), Maassluis (km 1021.8) and the Botlek (km 1009.4) for the reference and deepening scenarios. Negative velocity means ebb velocity, and the positive velocity means flood velocity.

For the step deepening the change in ebb and flood velocity duration are very small near the bottom and at the top as can be seen in Figure 52. The water level shows also no change as can be seen in appendix C.3.

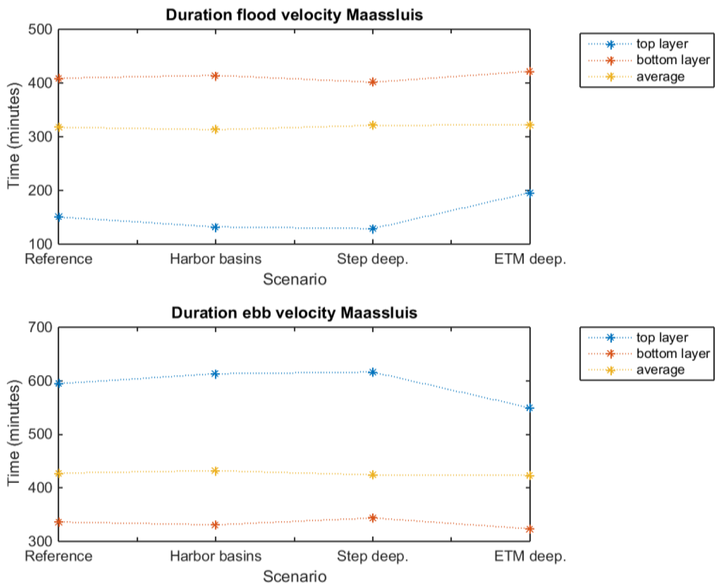

Figure 52 Ebb and flood velocity duration for different scenarios near Maassluis (km 1021.8)

The average velocity for the complete Rotterdam Waterway can be seen in Figure 53 for the step deepening scenario and Figure 54 for the ETM deepening scenario. The increased velocity near the bed also leads to a small increase in average velocity near the bed (-22 m). The average velocity per layer is shown in Figure 53. The average velocity shows a clear decrease near kilometer 1010 where the deepening stops, and the reference depth is reached again which is larges for layer 3 (-6 meter). The decrease is also visible for the top two layers (-4 meter upward), but this decrease is smaller. The increasing salinity shows means also the locations where the upper part of the start to float over the lower part of the water column is moved estuary upward with the same change. The location where the average velocity becomes near the bottom moves from kilometer 990.8 towards kilometer 989.

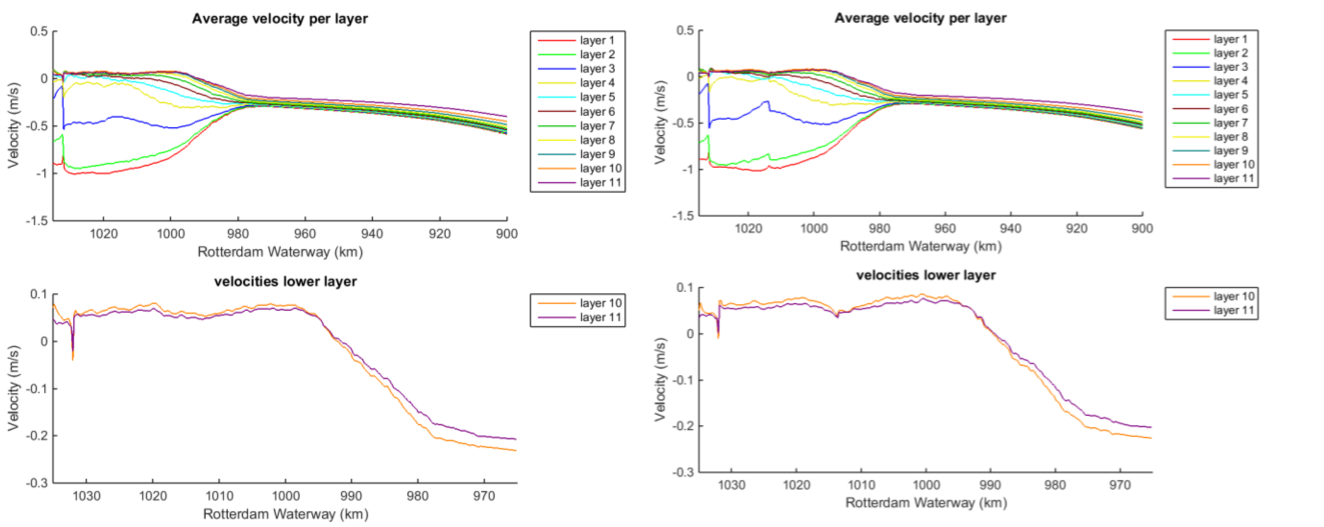

Figure 53 Average velocity for the reference scenario (left) and the step deepening scenario (right)

As is concluded from Figure 51, also Figure 52 shows almost no changes in average velocity for the total length of the Rotterdam Waterway. What is clearly visible is the change of location where the upper part of the water column (top three layers) starts to flow over the lower layers has moved estuary inward towards kilometer 990.

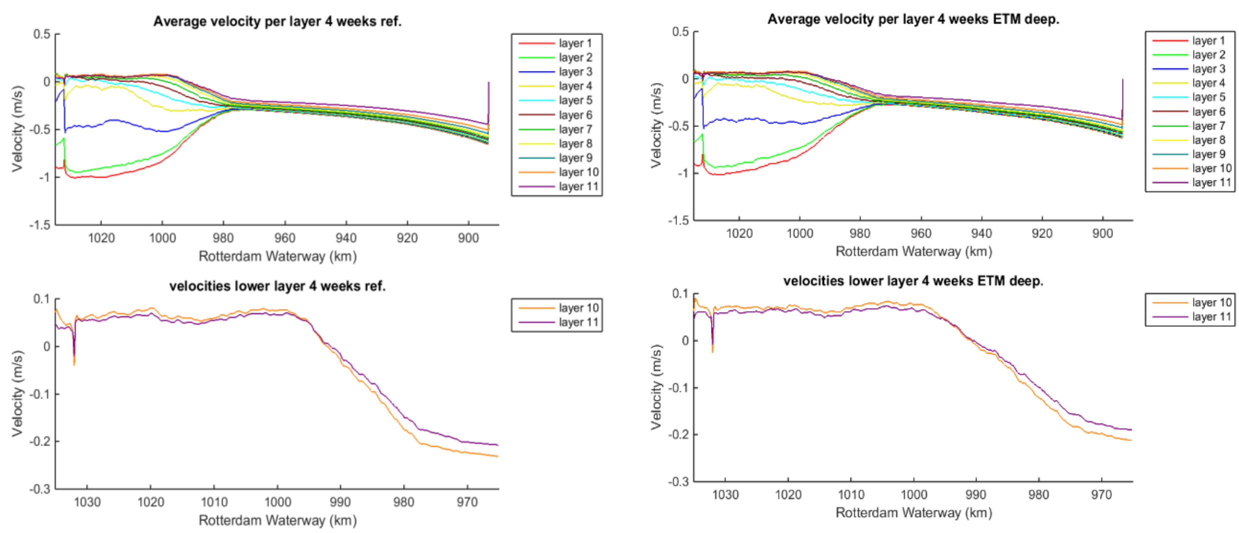

Figure 54 Average velocity per layer for reference scenario (left) and ETM deepening (right)

Figure 55 shows the result of the depth average velocity and the average (maximum) ebb and flood velocity during the spring neap cycle. The depth average velocity in the upper panel shows a decrease of the estuary outward (negative) velocity near the for the step deepening. The depth average velocity for the ETM deepening decrease in with 0,05 m/s near the location of the deepening.

The maximum ebb and flood velocity show an increase in maximum ebb and flood velocity for the step deepening in the lower left panels of Figure 55, especially estuary upward of the deepenening of 0.02 m/s. With the increase of the ebb and flood velocity estuary upward of the deepening the tidal assymetry does not change significant, because the velocities increase equal for both the ebb and flood velocity of 0.03 m/s. The increase between kilometer 990 and 995 is larger, this is due to the increase of salt intrusion. The maximum velocity increases with 0.1 m/s while the minimum velocity decrease with 0.1 m/s. The increase in tidal prism in the same period leads to higher velocities after the deepening, but not for the deepened part due to the deepening.

The velocity asymmetry increases slightly due to stronger increase in flood velocity for the ETM deepening due to the increased baroclinic pressure gradient, but the ebb and flood velocity increase between the step and kilometer 1000. So the ebb and flood velocity do not increase significant near the location of the deepening, but in front of the deepening.

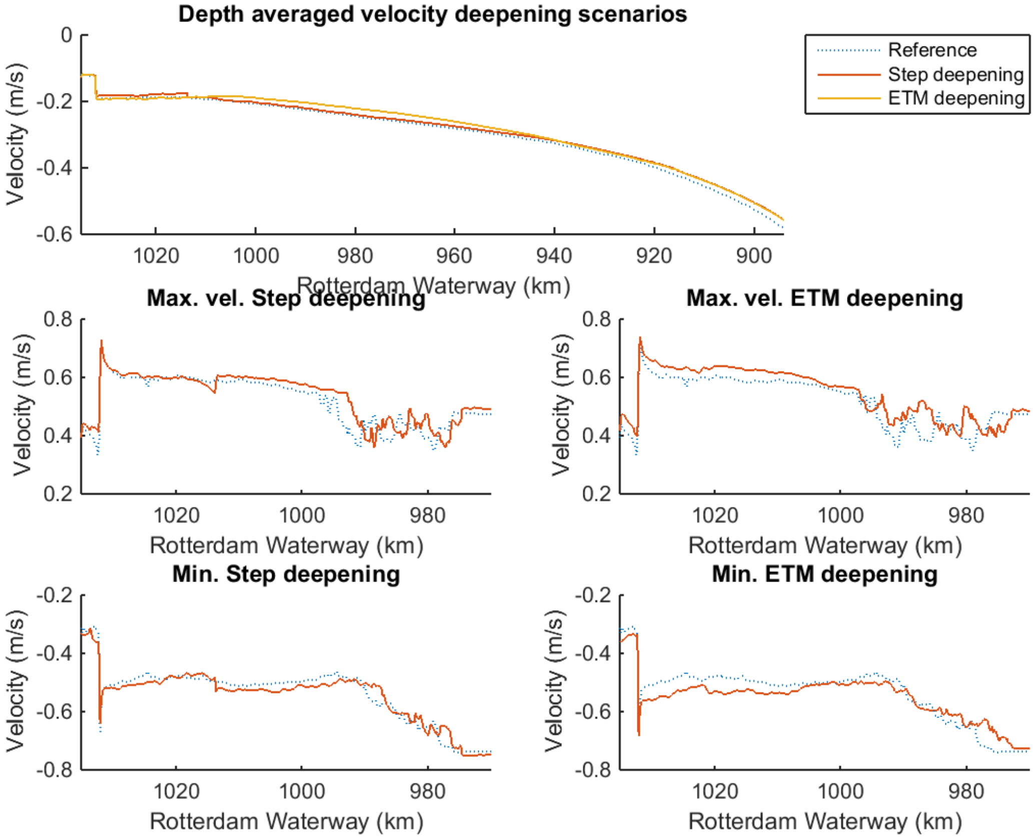

Figure 55 Left: change in minimum and maximum velocity due to deepening

The deepening induces new increase in turbulence near kilometer 1015 due to a sudden increase in both ebb and flood velocity, which causes the increases salinity as indicated in the salinity. The turbulence damping has not increased for the top layers. The fifth layer (-6 meter depth) is still the first layer from top towards bottom with turbulence. The turbulence slightly increases near kilometer 960.

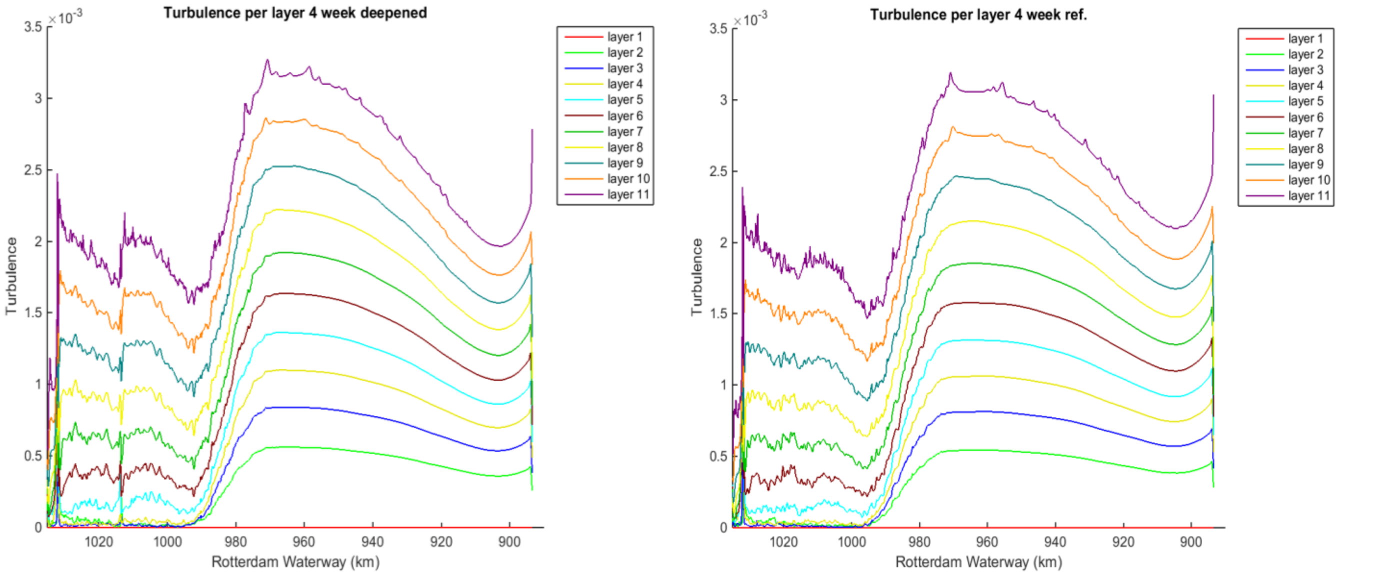

Figure 56 Turbulence for the step deepening scenario (left) and the reference scenario

The ETM deepeing scenario shows the maximum turbulence has shifted a little bit estuary upward, becase the increase in bottom depth is shifted slightly estuary inward. The length of the maximum turbulence has been increased. The increase from the mouth towards kilometer 995 is due to the increased velocity near the bottom.

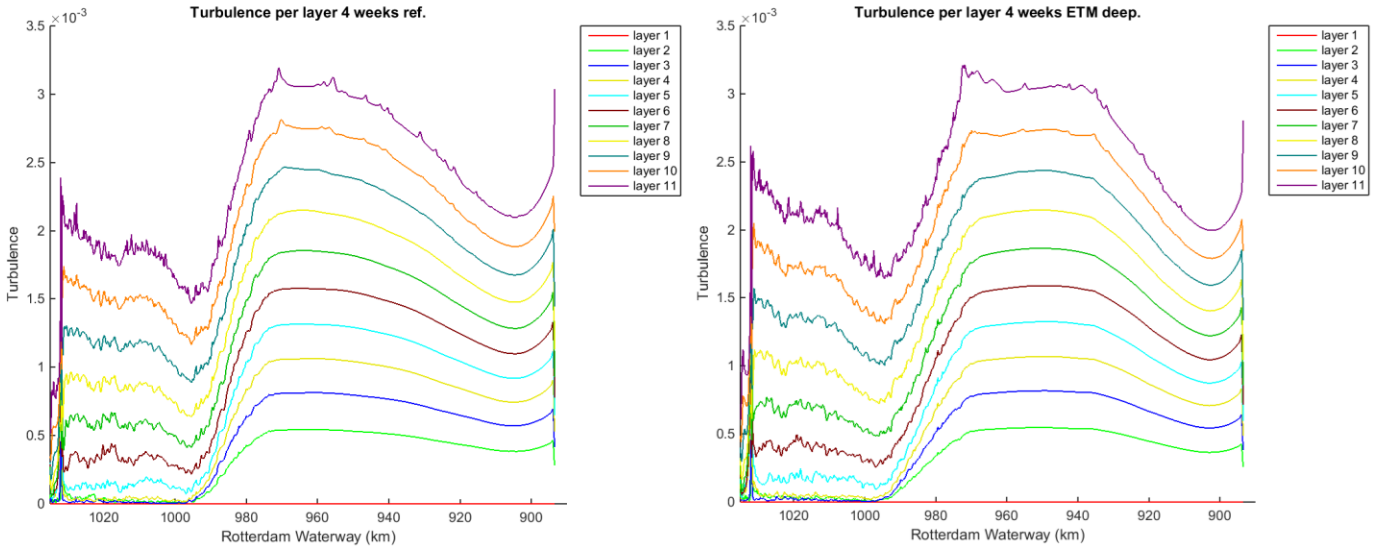

Figure 57 Turbulence for the reference scenario (left panel) and the deepened scenario (right panel)

The gravitational circulation increases for the deepened location, as can be seen in Figure 58 in the right panel. The deepening shows an increase for the vertical velocity near the step, because the flow is forced up and down suddenly. The vertical velocity has increased from the estuary mouth towards the new step for the middle layers (middle part of the water column) due to the increased salinity.

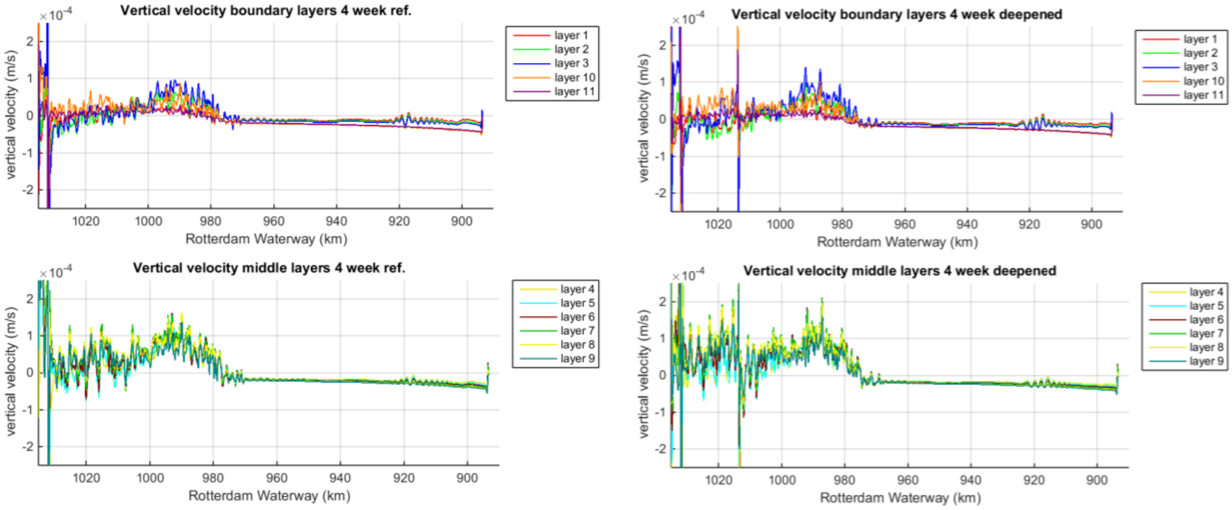

Figure 58 Gravitational circulation for the deepened scenario (left) and for the reference scenario (right)

The gravitational circulation seems to be increased slightly due to the increased salinity from the estuary mouth towards kilometer 1000, although the change is very small as can be seen in Figure 59.

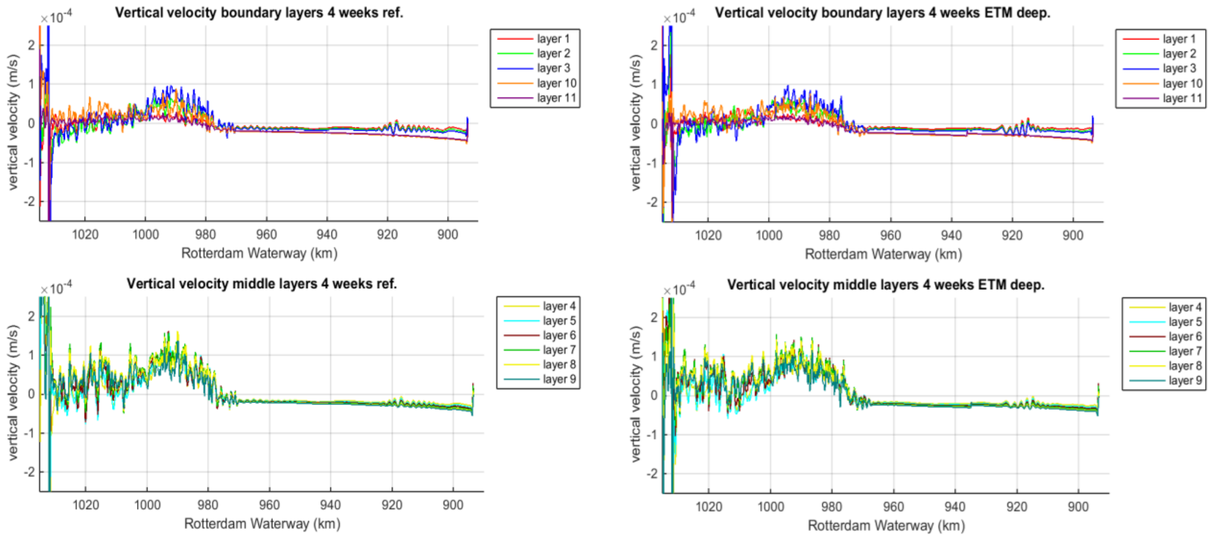

Figure 59 Gravitational circulation for the reference situation (left) and the ETM deepening scenario (right)

Suspended sediment

The change in hydrodynamics result in a small change for both the step- and ETM deepening, as can be seen in Figure 60. The step deepening results in a small movement of the ETM near the bottom and near the top compared with the reference scenario due to the increased salinity intruision. The maximum concentration is equal, the length however has increased. Which could be due to the increased length of the salt wedge, resulting in more sediment trapping near the bottom. Another explanaition could be the increased velocity near the bed between kilometer 990 and 995, leading to increased tidal pumping.

The ETM deepening results in a increased ETM width of 1 kilometer with the maximum suspended sediment located at the same location near the bottom compared with the reference scenario. The increased velocity near the bottom probably moves more sediment estuary upward, but the small decrease in the upper part of the water column leads to a decrease is sediment concentration compared with the reference scenario. The suspended sediment near the top decreased with 4 mg/l due to the decreased velocity in the top layer. The

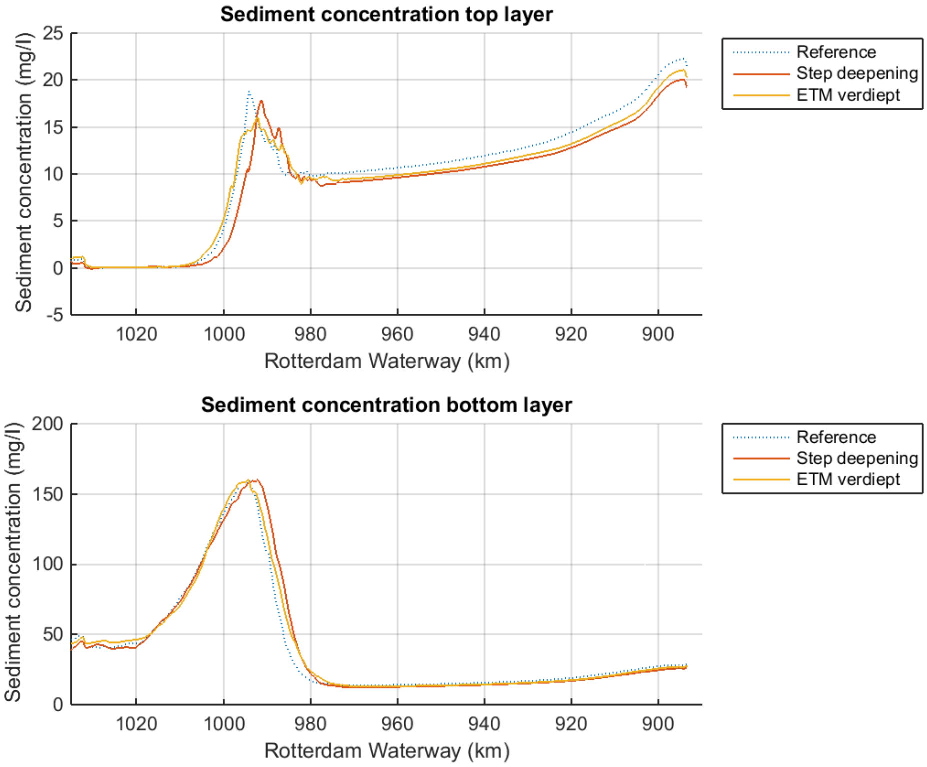

Figure 60 Suspended sediment concentration for the top and bottom layer for the different scenarios

The concentration of sediment in the bottom layer can be seen in Figure 61. The step deepening results in a new location where the sediment is blocked, near kilometer 1012. This increase however is small, about 2 kg/m^2. Combined with the increased sediment concentration, less sediment escapes to the sea meaning the sediment concentration in front of the step decreases.

The concentration in front of the first step due to the ETM deepening result in decreased suspended sediment concentration in front of the first step due to the increased length of the ETM and more sediment is being trapped estuary upward compared with the step deepening. The increase in flood velocity near the bed makes it also more difficult for the sediment to settle. So less sediment is available to settle in front of the step in bottom shape.

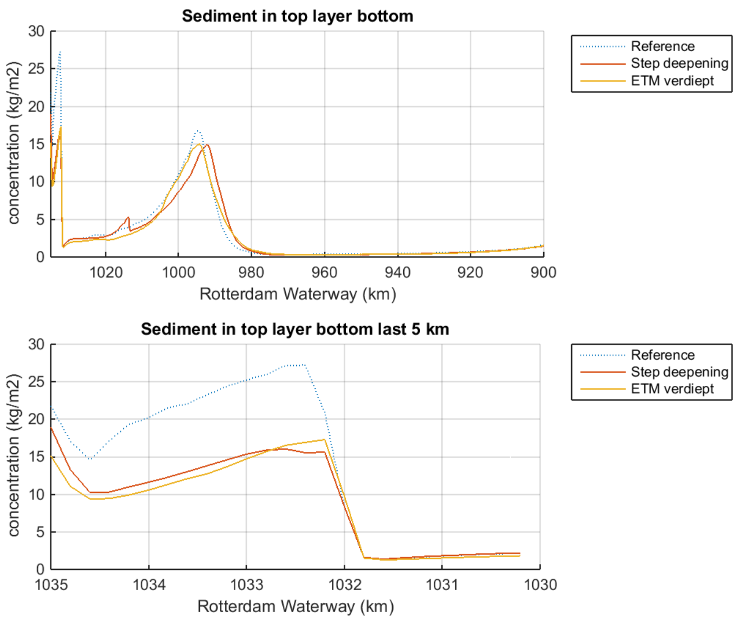

Figure 61 Fine sediment concentration for the different scenarios

Medium term step deepening
Figure 62 shows the evolution of the ETM in time for the deepened grid compared with the original depth for the top layer in the upper panel and the bottom layer in the lower panel.

The increased suspended sediment concentration grows faster in time compared with the reference scenario. The first two spring neap cycles after the run up period show only a small increase in suspended sediment concentration in the ETM. the trapping of sediment is continuing, resulting in increasing suspended sediment concentration during following spring neap cycles which not only increase the length but is also increase the maximum suspended sediment concentration in the ETM. After 12 weeks the maximum concentration has increased from 290 mg/l for the reference scenario near the bottom towards 300 mg/l for the step deepening scenario.

So the increased baroclinic pressure gradient results in more sediment in the estuary. The small increase in velocity near the top leads to movement of sediment estuary upward towards the ETM which results in a small increase of 2 mg/l.

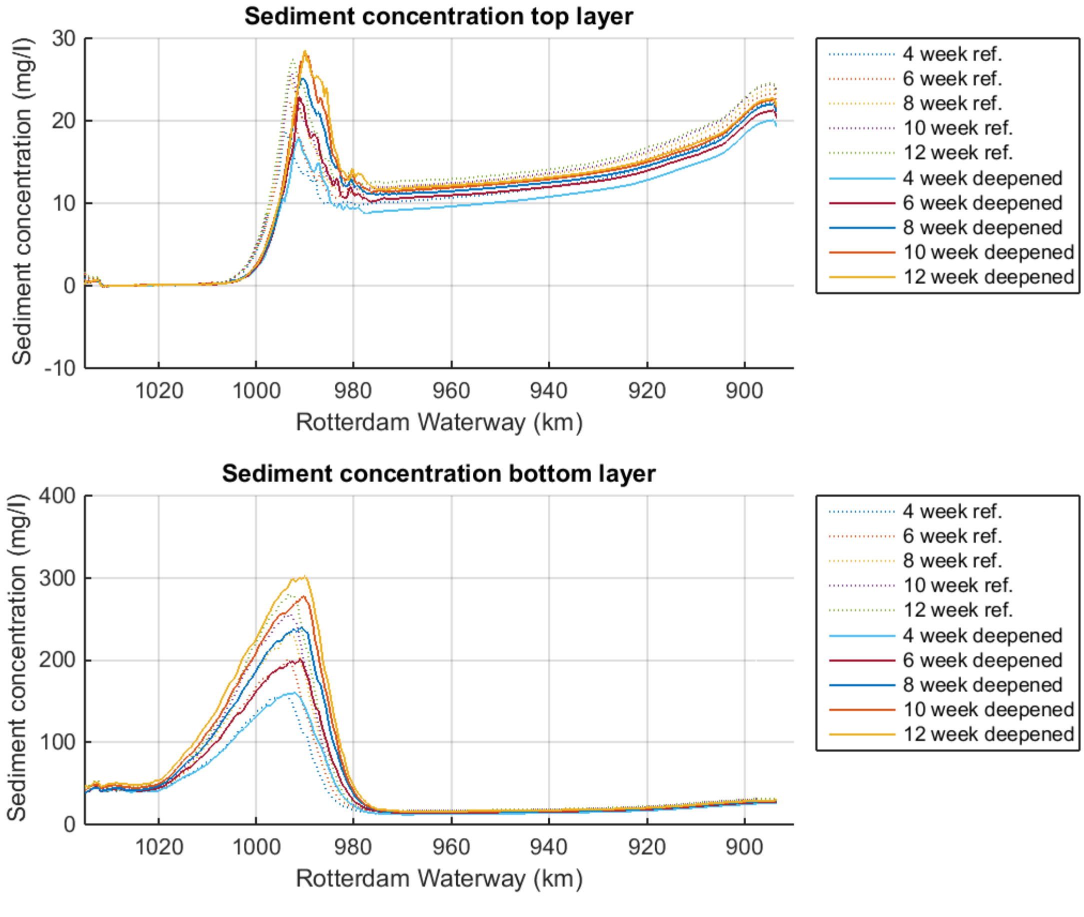

Figure 62 Left: ETM with the deepened grid; Right: available fine sediment in top layer bottom

The fine sediment concentration in the bottom is not growing estuary outward of the step indicating no sediment is not reaching the step because the sediment is trapped in the ETM. A new step (sudden increase of 1 meter near kilometer 1015) also introduces a new location with a decrease in velocity estuary upward, so sediment is able to settle. The increase however is only 5 kg/m^2 which is very small. The maximum concentration of sediment in the bottom of the Rotterdam Waterway near kilometer 990 is growing to the same concentration compared with the reference scenario, only a small increase estuary upward.

Concluding the amount of sediment in the bottom is equal, meaning not enough sediment is being kept in suspension that no sediment will be trapped. It is only not reaching the end of the waterway. The final results is shown in Table 9.

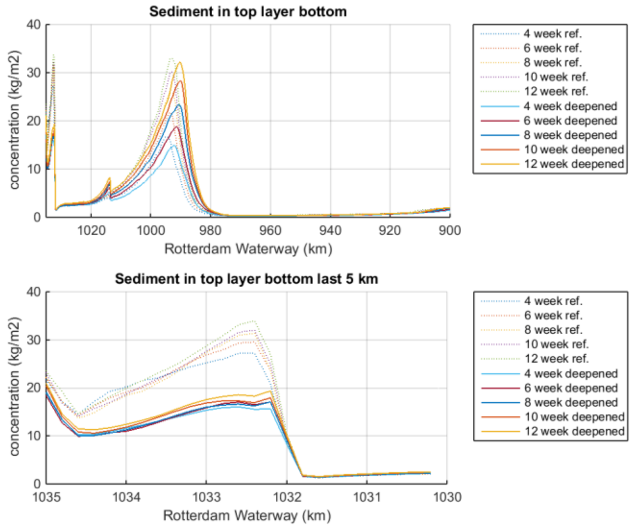

Figure 63 Available sediment in bottom layer for ETM deepening scenario

Table 9 ETM characteristics for the step deepening

	4 weeks	6 weeks	8 weeks	10 weeks	12 weeks
Step deepening					
Loc. max. (km)	994.2	994.6	992.4	991.8	991.8
Length (km)	50.4	50.8	49.4	53.4	50.2
ETM (kg/m³)	1.09	1.36	1.63	1.87	2.09

Medium term ETM deepening

The same analysis holds for the medium term evolution of the ETM in the ETM deepening scenario. The suspended sediment concentration in the ETM is already increasing, but during the first tidal cycles only in length. During the following tidal cycles not only the length increases, also the maximum concentration increases resulting in a suspended sediment concentration after 12 weeks from 290 mg/l for the reference case towards 305 mg/l with the deepening near the bottom. Eventually also the suspended sediment concentration in the top layer increased with 10 mg/l towards 35 mg/l.

So the increasing tidal pumping near the bottom results in increasing suspended sediment concentration near the bottom. For the top layer the increased turbulence keeps the sediment probably more in suspension leading to increased suspended sediment concentrations near the top.

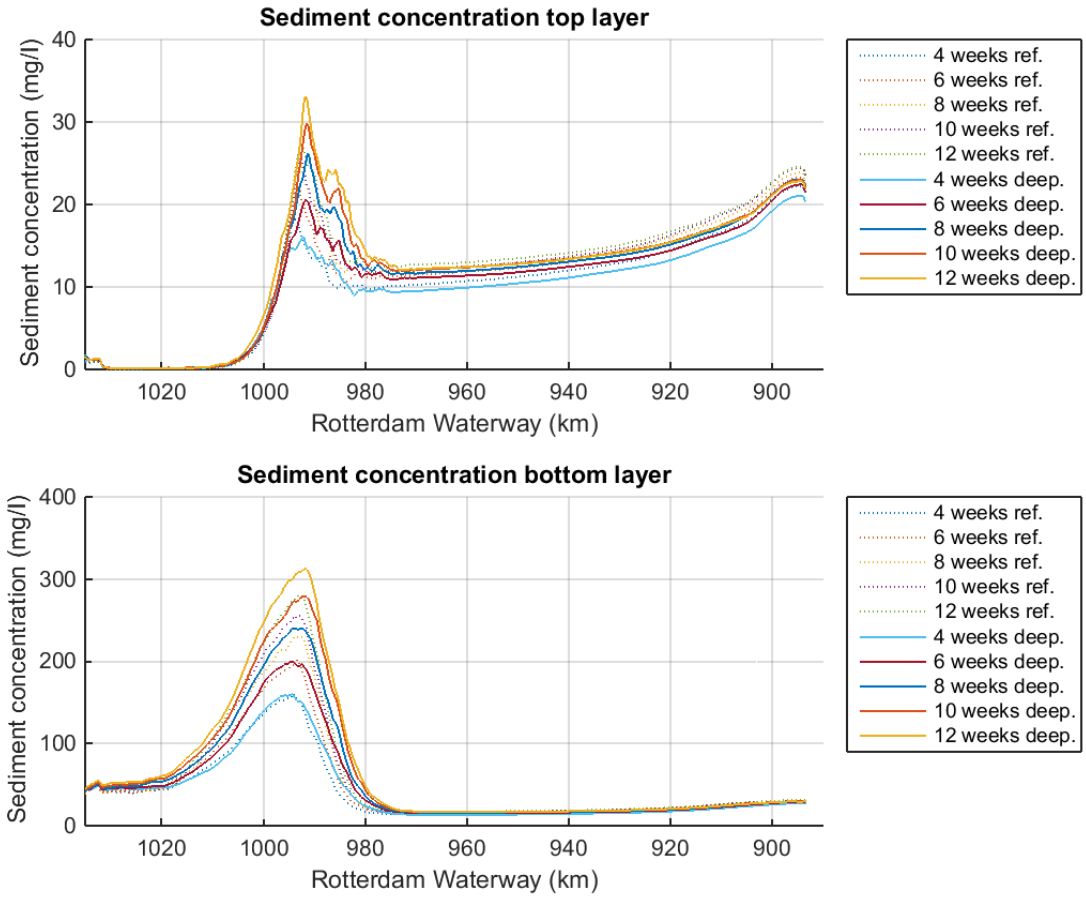

Figure 64 Suspended sediment concentration near the bottom and in the top layer for the deepened scenario compared with the reference scenario

The available sediment in the active bottom layer for the ETM deepening shows the same characteristics compared with the step deepening scenario. So less sediment is trapped in estuary outward the step in the bottom, but the sediment concentration near kilometer 990 is almost equal compared with the reference situation. The results in time for the ETM deepening is shown in Table 10.

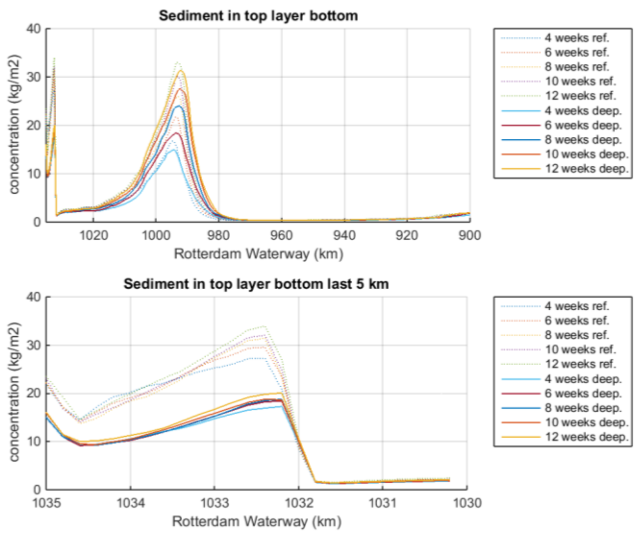

Figure 65 Available sediment in active top layer bottom for step deepening scenario (left) and ETM deepening scenario (right)

Table 10 ETM evolution in time for step deepening and ETM deepening

	4 weeks	6 weeks	8 weeks	10 weeks	12 weeks
ETM Deepening					
Loc. max. (km)	991.6	992.4	990.8	991.8	991
Length (km)	44	47	45.4	47.2	48.2
ETM (kg/m³)	1.09	1.38	1.63	1.89	2.03

6.2.2.2 Sensitivity Step deepening

Sensitivity salinity

The change in salinity for the different scenarios for the step deepening compared with the reference scenario can be seen in Figure 66. There is an overall increase in salinity for all scenarios compared with the reference situation. The increase in salinity decreases for the 5% discharge while the sality increases near the boundary for the 95% discharge. This is because the boundary is decreasing the most for the 95% discharge in the reference situation, and the salinity intrudes further upstream so the increase is also relative large.

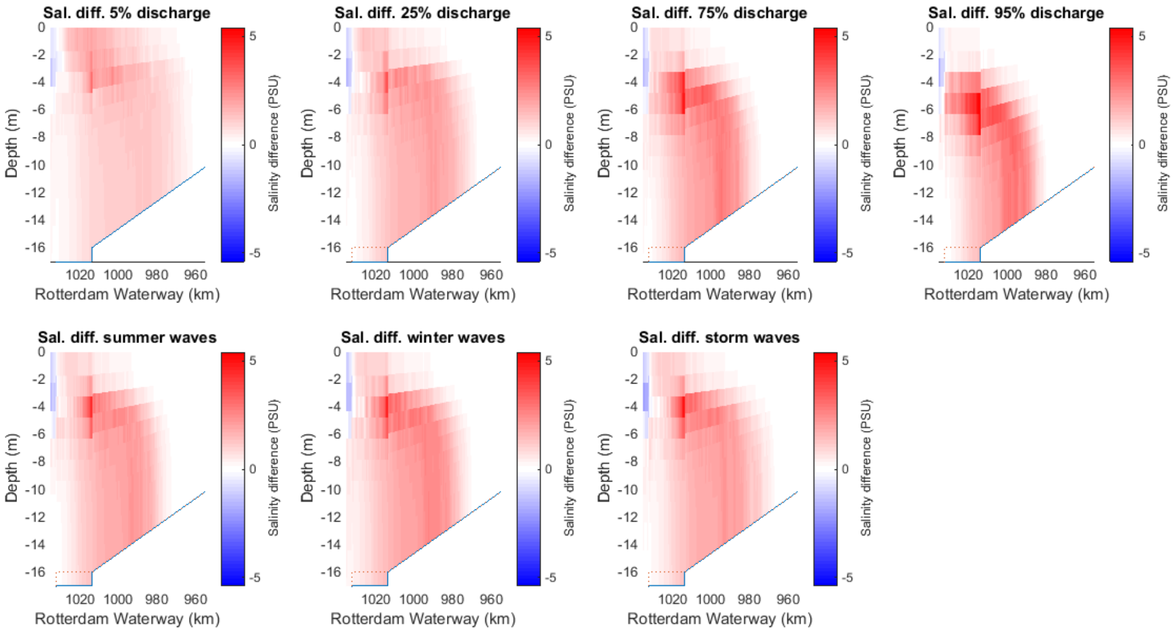

Figure 66 Change salinity sensitivity due to step deepening

The sensitivity due to the movement of the null point is small, as can be seen in Table 11. The movement is the distance of the null point of the changing discharge compared with the average discharge. Only for the 5% discharge the null point is moving less down estuary.

Table 11 Sensitivity salinity for discharge

	5% discharge	25% discharge	Average discharge	75% discharge	95% discharge
Ref. (km)	974.2	982.6	986.8	989.2	994.6
Movement (km)	-12.6	-4.2	0	2.4	7.8
Step Deep. (km)	973.2	980.4	984.6	986.8	992.2
Movement (km)	-11.4	-4.2	0	2.2	7.6

The sensitivity for the null point of the salinity can be seen in Table 12. The movement of the salinity due to waves are neglecible. If the changes differ, like for example for the summer waves, the changes are so small it is uncertain if this really is due to the chaning wave conditions.

Table 12 Sensitivity salinity for waves

	Summer waves	Average waves	Winter waves	Storm waves
Ref. (km)	986.6	986.8	986.2	982.4
Movement (km)	-0.2	0	-0.6	-4.4
Step Deep. (km)	985	984.6	983.6	980.2
Movement (km)	0.4	0	-1	-4.4

Sensitivity discharge

The average velocites for Hook of Holland, Maassluis and the Botlek are shown in Figure 67. The sensitivity due to the changing discharge is similar compared with the reference scenario. The 95% discharge in the top layer shows an increase from -1.18 m/s for the reference scenario towards -1.21 m/s for the step deepening scenario near Maasluis and a increase of 0.06 m/s near the Botlek. Near Hook of Holland however the average velocities are the same near the top. The increase in ebb velocity is due to increase in the middle layers due to the increased baroclinic pressure. The velocity is increasing (flood velocity) in the middle layers meaning more water has to flow over a smaller depth resulting in higher average velocities.

For the 5% discharge the average ebb velocity near the top layer is decreasing from -0.56 m/s towards -0.6 m/s near Maassluis and a decrease of 0.02 m/s near the Botlek. This is because during a low discharge, the stratification due to salinity is less as can be seen in Figure 66. the water column is becoming fresher in depth due to decreasing baroclinic presure and thus the water is flowing through an increased water column. A comparrison with the 5% discharge for the step deepening scenario and the reference scenario is shown in appendix F.1.

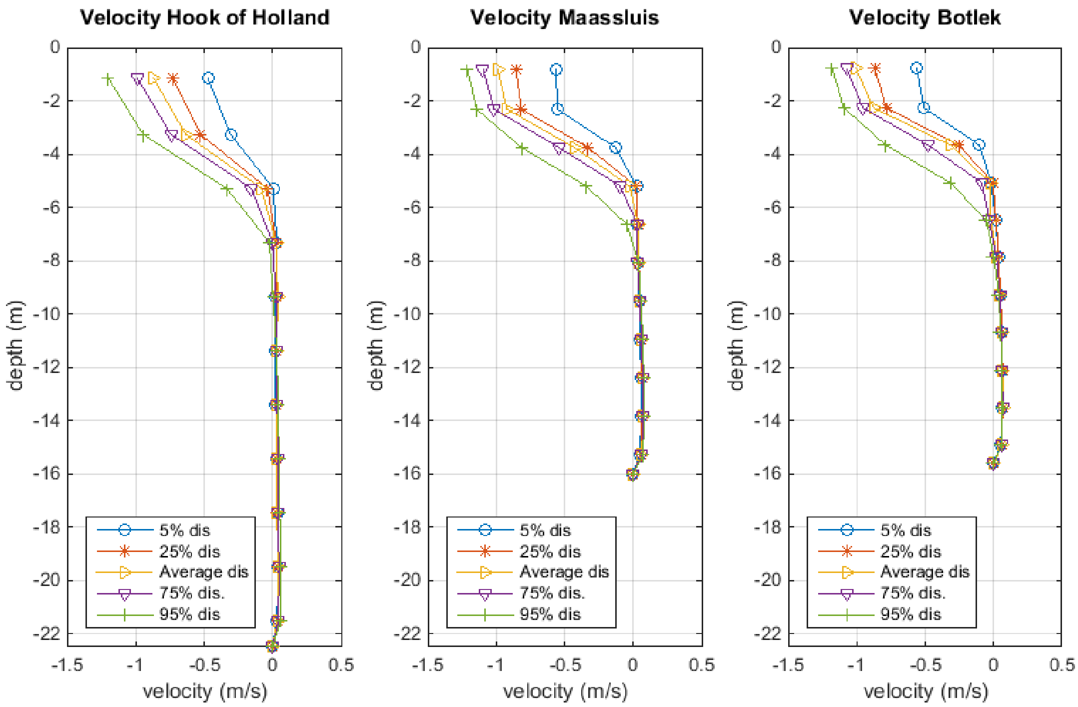

Figure 67 Average velocity for Hook of Holland, Maassluis and the Botlek for the changing discharge

The sensitivity of the ebb and flood velocity near the bed due to the changing discharge can be seen in Figure 68, with the depth average velocity in the upper panel for all discharges.

The increase in ebb and flood velocity for the different discharges is small and almost constant. The ebb velocities show an increase in velocity after the new step, in front of the new step the velocity is approximately constant. For the 95% discharge the change in ebb velocity is almost zero compared with the ebb velocity for the 95% discharge for the reference scenario, while the increase in average ebb velocity for the 5% discharge is 0.02 m/s.

The flood velocity shows a small decrease in velocity at the location of the new step, as can be seen in the lower panels. After the step the velocity slightly increases compared with the reference scenario without deepening. The largest increase in flood velocity is for the 95% discharge with 0.05 m/s, while the change in flood velocity for the 5% is almost zero.

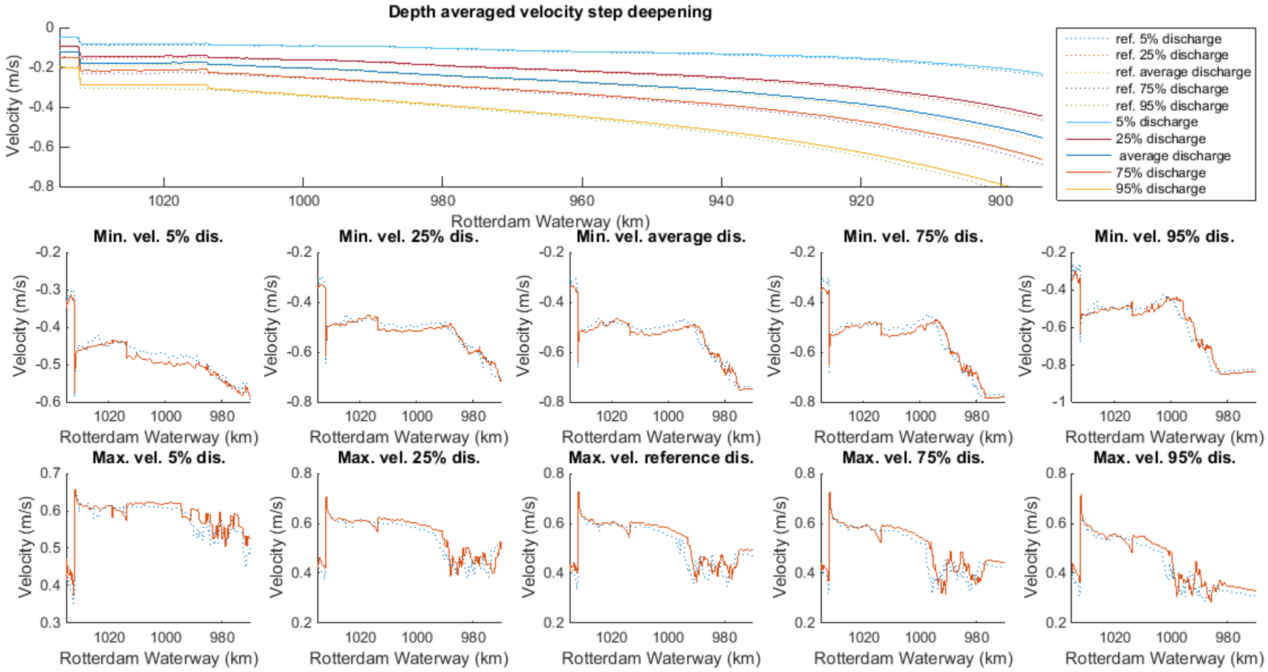

Figure 68 Depth average velocity for discharge sensitivity (upper panel); Flood (maximum) and ebb (minimum) velocity due compared (orange line) with reference depth (dashed line) for discharge sensitivity

Sensitivity waves

The sensitivity due to the changing wave conditions for Hook of Holland, Maassluis and the Botlek can be seen in Figure 69. The changing wave conditions do not result in changing average velocities compared with the average waves.

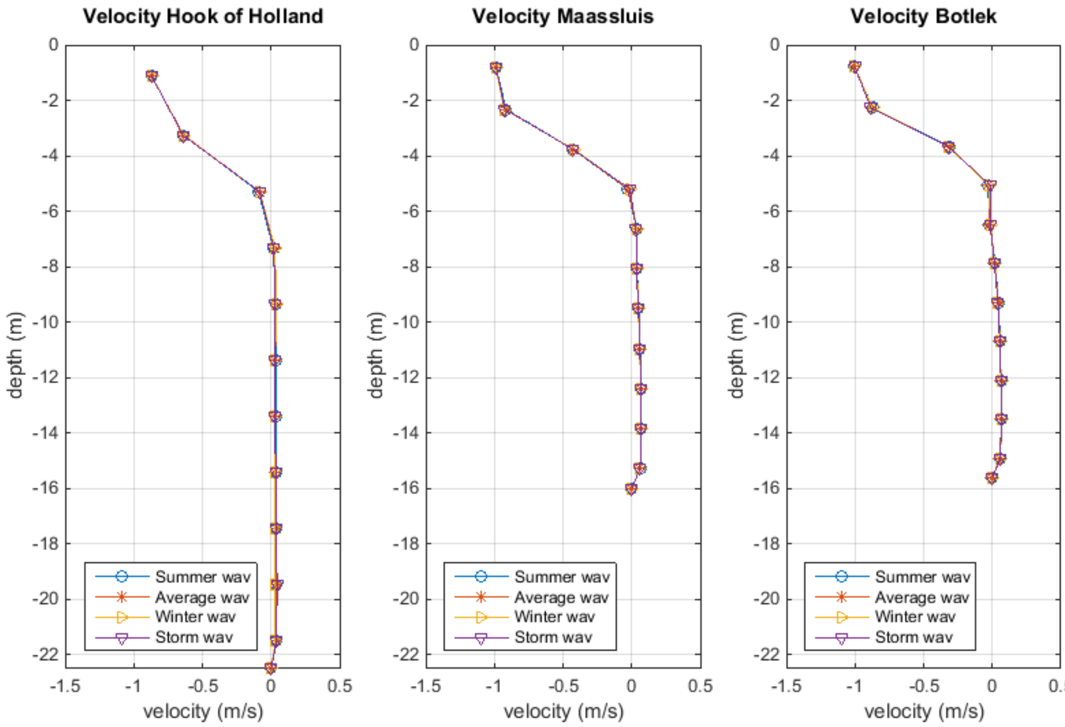

Figure 69 Average velocity for Hook of Holland, Maassluis and the Botlek for the changing wave conditions

The change in ebb and flood velocity near the bed due to the waves is small compared with the reference scenario, as can be seen in Figure 70. The difference for the for the deepening is constant for all wave conditions.

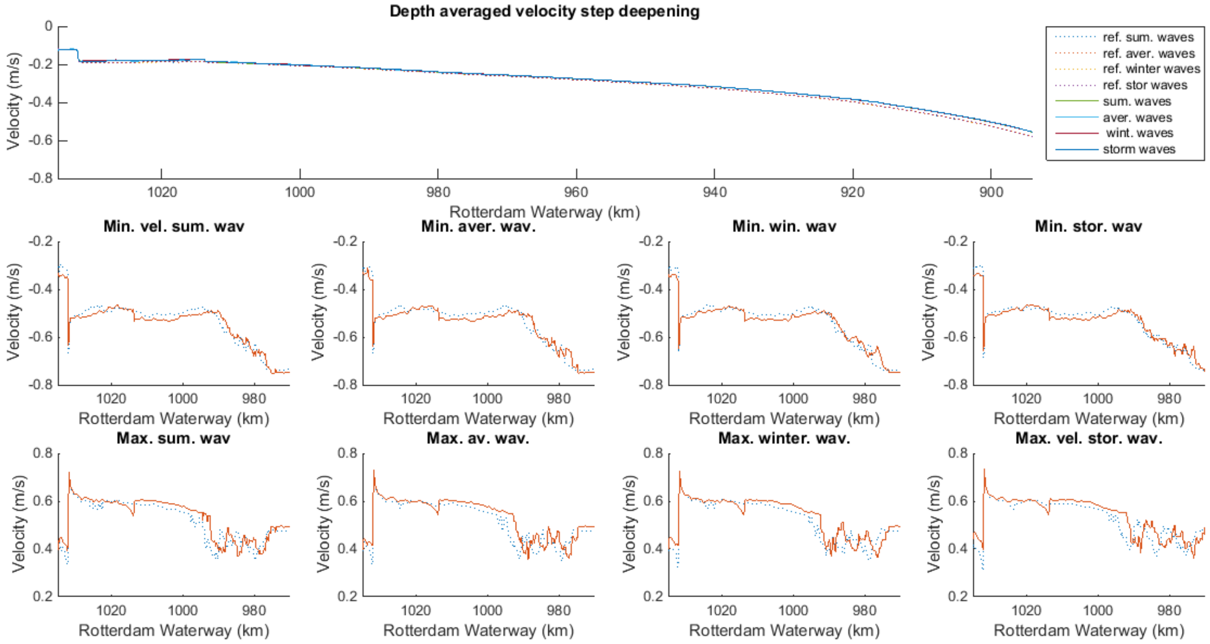

Figure 70 Depth average velocity (upper panel); Average ebb and flood velocities near the bed (lower panels) due to changing waves for the reference scenario (dashed blue) and the step deepening scenario (oragne)

Sensitivity sediment transport

Increasing the discharge over a spring neap cycle increases the suspended sediment concentration in the ETM, comparable with the sensitivity seen for the reference scenario. The maximum suspended sediment concentration increased however and the length also increased. This is because already more sediment is trapped in the ETM due to the runup time, and the decreasing discharge leading to less sediment escaping to sea. The increase in ebb velocity near the top results in decreased sediment concentration estuary upward of the ETM.

The results for the smaller discharge are also comparable with the results for the reference scenario. The 5% discharge shows increase in sediment concentration in the top layer of the water column, while near the bottom the concentration decreases due to the increased flow velocity for the 5% discharge. This is because the concentration velocity is decreasing near the top and more sediment has already been transported to the new location due to the increasing flood velocity near the bottom between kilometer 1015 and 990. The 25% discharge shows no change in the bottom layer compared with the 50% discharge.

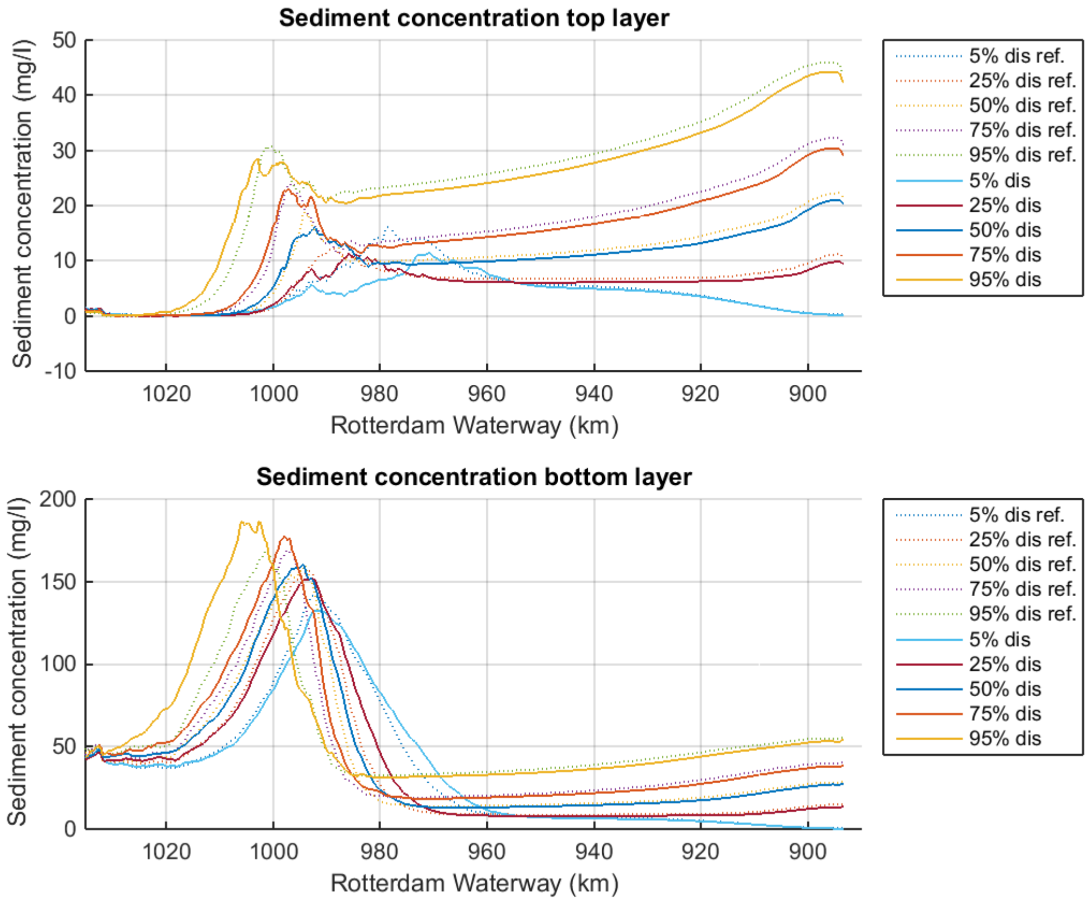

Figure 71 Concentration suspended sediment for the top layer (upper panel) and the bottom layer (lower panel) due to changing discharge for the reference scenario (dashed line) and the step deepening scenario

The change in suspended sediment concentration due to the change in waves can be seen in Figure 72. For the waves the pattern after one spring neap cycle is comparable with the reference scenario, but with the increase due to the increasing baroclinic pressure.

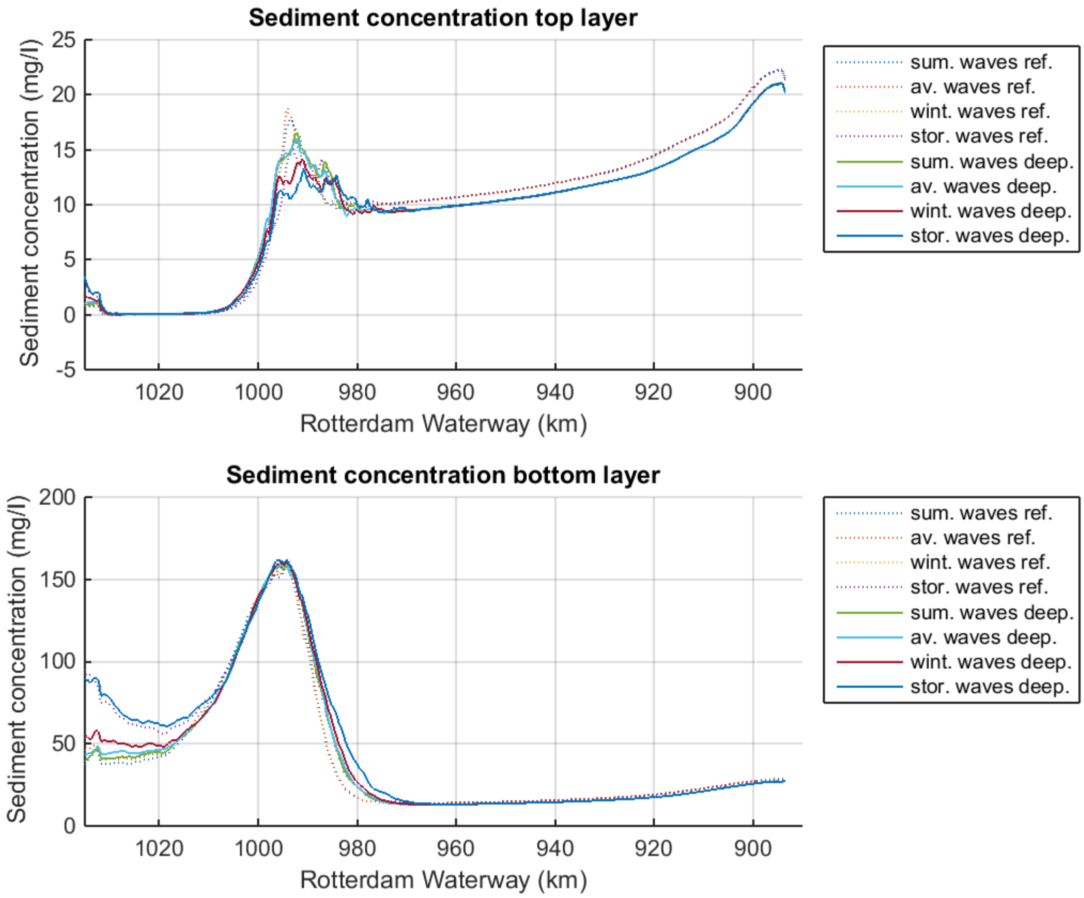

Figure 72 Concentration suspended sediment for the top layer (upper panel) and the bottom layer (lower panel) due to changing discharge for the reference scenario (dashed line) and the step deepening scenario

Medium term

The medium term results for the discharge sensitivity analysis can be seen in Figure 73. For the 5% discharge the ETM decreases in time in both the top layer and the bottom layer. The location of the peak of the ETM moves 2.2 kilometer estuary outward, compared with the 5% discharge of the reference scenario. The maximum suspended sediment concentration is decreasing 27,3 mg/l for the bottom layer and 8 mg/l for the top layer. The decrease in maximum sediment concentration does not lead to a total decrease in sediment concentration in the ETM, because the length of the ETM has increased with 2 kilometers for both the near bottom layer and the top layer. So the small increase in discharge leads to a longer width, but a smaller peak for the ETM. This is due to the decreased velocities for the 5% discharge. The sediment is however still trapped because there is still a flood dominant lower part of the estuary.

For the increased discharge the deepening results in increased suspended sediment concentration in the ETM for the extended period near the bottom with 21 mg/l and is approximately constant for the top layer (decrease of 0.7 mg/l). The location of the ETM is approximately constant for the bottom layer. For the top layer the ETM moved however 3 kilometer estuary upward. This is due to the decreased discharge for the 95% discharge compared with the reference scenario. So the increased stratification leads to a larger flood dominant lower part of the water column trapping more sediment in the lower column. The small increase in velocity for the top layer does not decrease the sediment concentration much.

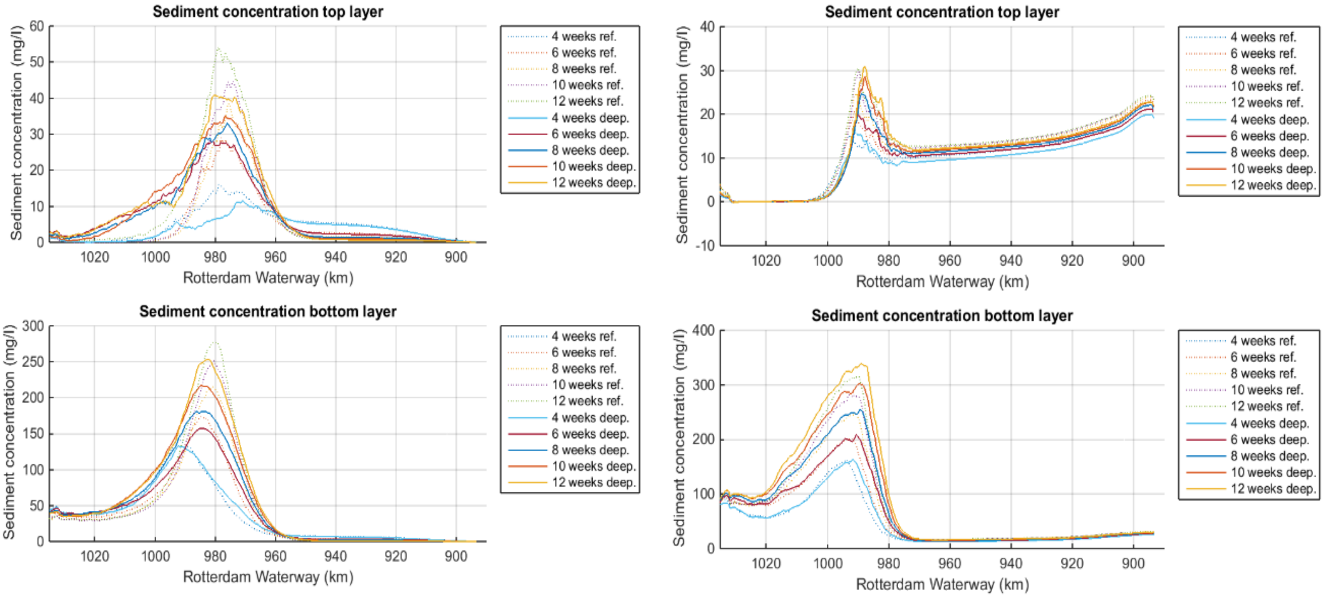

Figure 73 Medium term change due to 5% discharge (left) and 95% discharge (right) for the top layer (upper panels) and the near bed layer (lower panels) for the reference scenario (dashed line) and the step deepening scenario

The change in bottom sediment for the 5% and 95% for the step deepeing scenario can be seen in Figure 74. The decrease in discharge leads also to a decrease in trapped sediment near the bottom, because length of estuary outward of the first step and in the maximum near kilometer 980. The sediment is being trapped in the ETM. The sediment trapped in the bottom for the 95% discharge is decreasing slightly but the location also changed. The introduced new step traps more sediment near kilometer 1015, in stead of near kilometer 1033. The peak in bottom sediment decreased slightly in maximum and width.

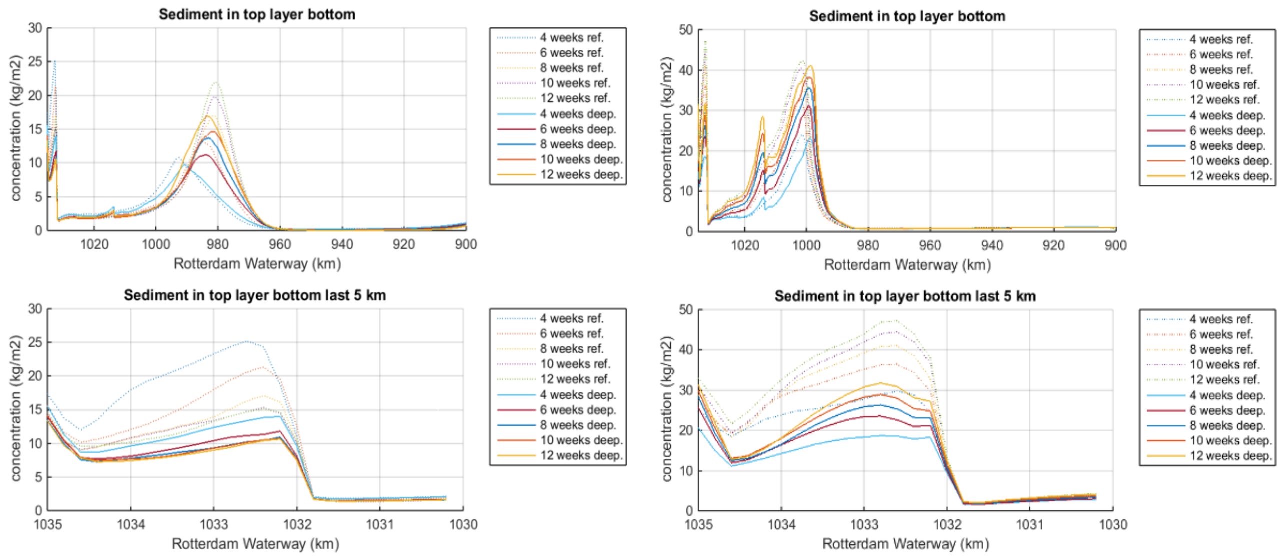

Figure 74 Bottom sediment active top layer for the 5% discharge (left) and 95% discharge (right)

Figure 75 shows the medium term sensitivity of the ETM for changing wave conditions for the step deepening scenario compared with the reference scenario. There is an increase in sediment concentration for both scenarios compared with the reference case with about 25 mg/l. the suspended sediment concentration near the top is constant for both wave conditions.

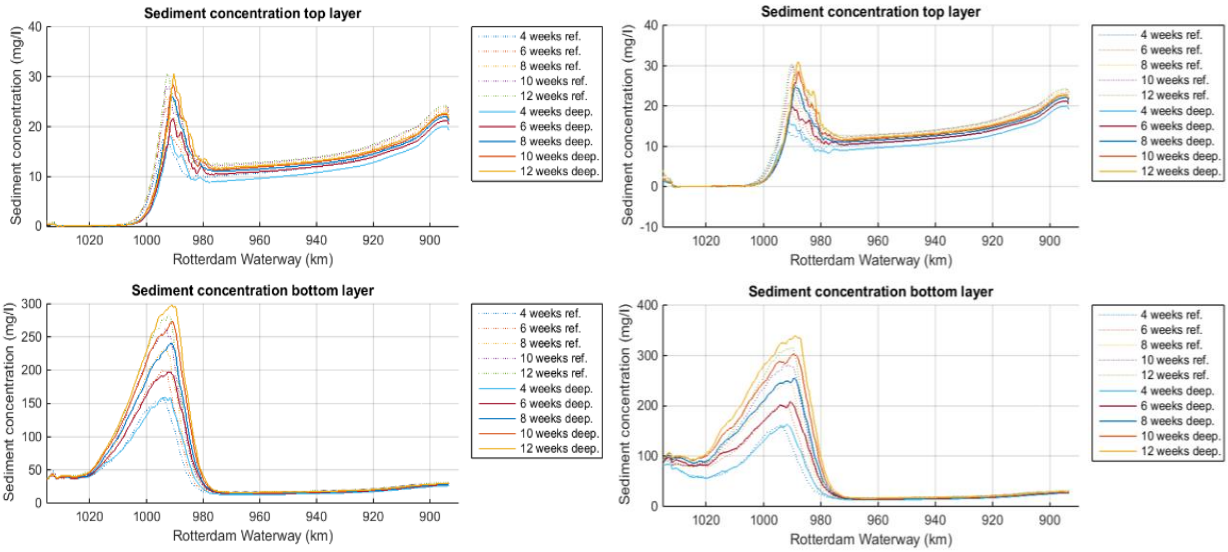

Figure 75 ETM in time for summer waves (left panel) and storm waves (right panel) for the reference depth (dotted line) and the deepened scenario

The available sediment in the bottom for the summer waves show a constant value near the step at kilometer 1033, indicating no new sediment is trapped with the increase in time. The combination of the increased velocity near the step and the decreased velocity due to the discharge leads to decrease in sediment trapping and an increase in concentration in the ETM. The small growth near kilometer 1015 indicates the sediment is not even reaching the new step, because the sediment is already trapped in the ETM. T

he bottom sediment for the storm waves is increasing in front of the step and near the peak at kilometer 990, also after 12 weeks while for the reference scenario the sediment concentration near kilometer 1032.5 is not increasing anymore. The decrease of the step leads to decreased sediment trapping after 4 weeks, but the growth is 20 kg/m2 against a growth of 15 kg/m2 for the reference scenario. So growth increased, but the maximum concentration decreased due to the decrease of the step. The peak near kilometer 1015 is about 15 kg/m2 after 12 weeks, indicating not more sediment is reaching the ETM, and the increase in ETM is due to the sediment which was already available.

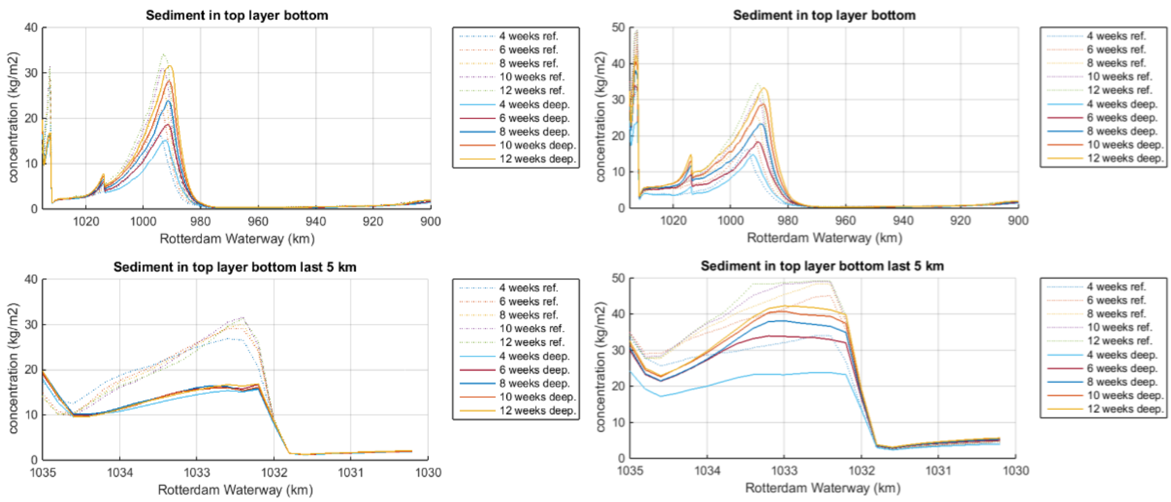

Figure 76 Available sediment bottom layer for summer waves (left) and storm waves (right)

6.2.2.3 Sensitivity ETM Deepening

Sensitivity salinity

The sensitivity due to the ETM deepening scenario can be seen in Figure 77. The overall pattern in changing salinity due to the deepening is the same compared with the reference scenario, the same tidal prism intrudes further into the estuary. For the 5% discharge the change higher in the water column is also changing indicating the total salinity front has moved, while for the 25% and summer waves for example the salinity higher in the water column does not change. For the 25% discharge the salinity is flushed more out of the estuary. This also holds for the 95% discharge. The salinity is decreasing, there is almost no location however where the salinity is increasing.

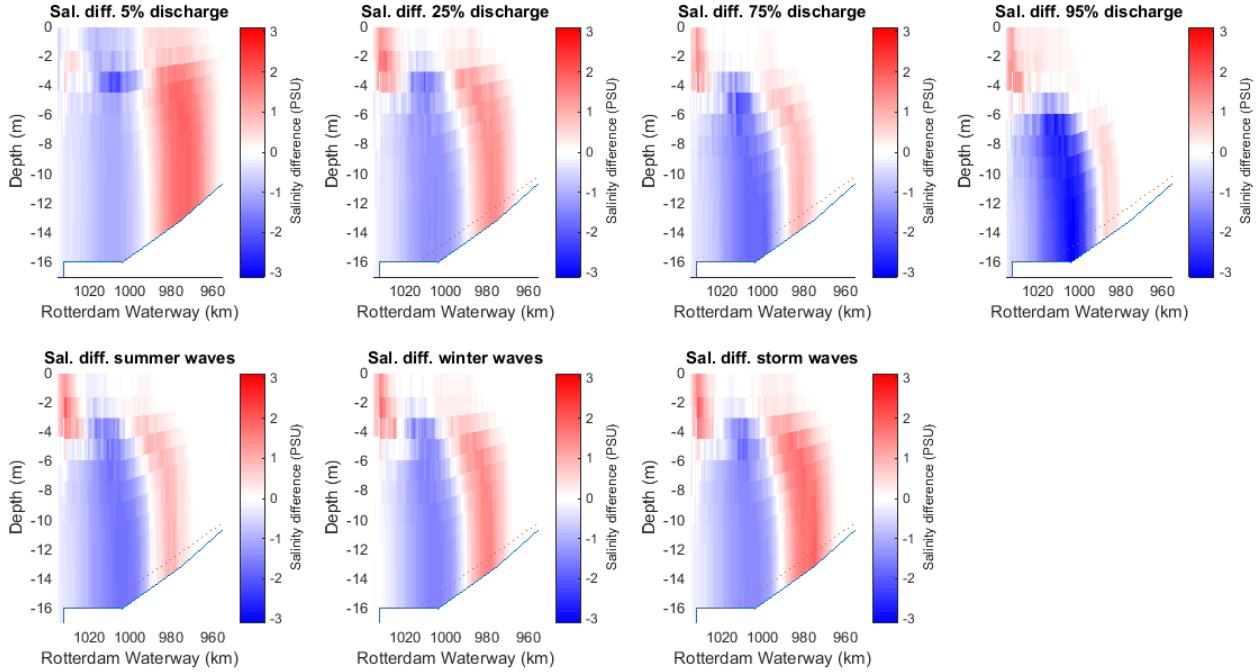

Figure 77 Sensitivity due to ETM deepening scenario

The movement of the null point can be seen in Table 13 for the dischage. The deepening shows increased sensitivity to the discharge for the salinity. The null point moves further up and down estuary compared with the step deepening and the reference case, although the 5% discharge still leads to the largest movement compared with the average conditions.

Table 13 Sensitivity null point due to discharge, including ETM deepening

	5% discharge	25% discharge	Average discharge	75% discharge	95% discharge
Ref. (km)	974.2	982.6	986.8	989.2	994.6
Movement (km)	-12.6	-4.2	0	2.4	7.8
Step Deep. (km)	973.2	980.4	984.6	986.8	992.2
Movement (km)	-11.4	-4.2	0	2.2	7.6
ETM deep. (km)	970.6	979.4	984.2	987	993.2
Movement (km)	-13.6	-4.8	0	2.8	9

The changing wave conditions show very no changes for the null point compared with the sensitivity for the reference case. The storm waves show a decrease in change for salinity near the null point of the salinity.

Table 14 Sensitivity null point due to waves, including ETM deepening

	Summer waves	Average waves	Winter waves	Storm waves
Ref. (km)	986.6	986.8	986.2	982.4
Movement (km)	-0.2	0	-0.6	-4.4
Step Deep. (km)	985	984.6	983.6	980.2
Movement (km)	0.4	0	-1	-4.4
ETM deep. (km)	984.8	984.2	982.8	978.4
Movement (km)	0.4	0	-1	-4.4

Sensitivity discharge

The average velocity for the changing discharge for the ETM deepening scenario can be seen in Figure 78. The average ebb velocity increased near the top of the water column for the 5% discharge near the Botlek, Maassluis and the Hook of Holland with 0.02 m/s, compared with the ebb velocity for the 5% discharge for the reference scenario. The increase in flow velocity due to the decrease in discharge is due to the decrease in barotropic pressure gradient creating less resistance for the flow. Near the bottom the average flood velocity increases for Hook of Holland due to the increased baroclinic pressure gradient.

The average ebb velocity for the 95% discharge decreases compared with the ebb velocity near the top for the 95% discharge for the reference scenario. The strongest decrease is near the Botlek where the ebb velocity decreased from -1.18 towards -1.08 m/s, because of the deepening and the decrease in barotropic pressure, leading to less salinity intrusion for the middle layers of the water column (-10 towards -6 meter depth). This decreases the depth of the flood dominant lower salt layers, increasing the depth over which the fresh layers float. The near bed layers however show and increase in average flood velocity due to the increased baroclinic pressure gradient.

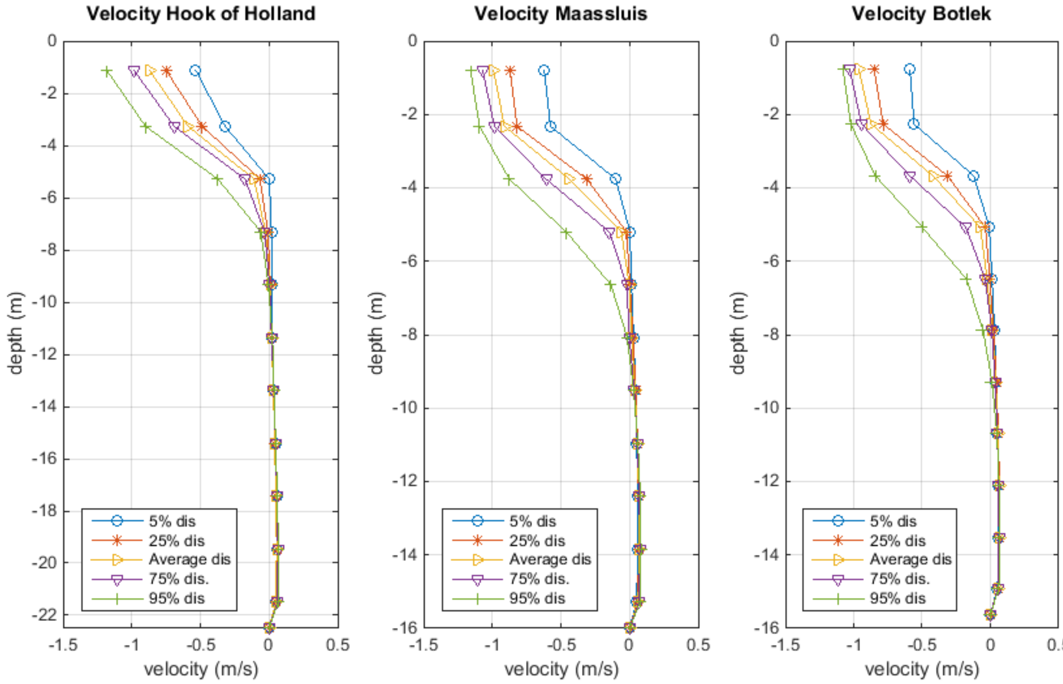

Figure 78 Average velocity for Hook of Holland (km 1034.6), Maassluis (km 1024) and the Botlek (km 1009)

The sensitivity of the ebb and flood velocity due to the discharge can be seen in Figure 79, with the depth average velocity in the upper panel, the ebb (minimum) velocity for the different discharges in the middle panel and the flood (maximum) velocity for the different discharges in the lower panels. The increase in the ebb and flood velocity seems to be the largest for the 5% discharge. The change for the 25%, average conditions and the 75% discharge are constant which is a small increase in ebb and flood velocity. The change for the 95% discharge is also small for the minimum velocity, but constant for the maximum velocity.

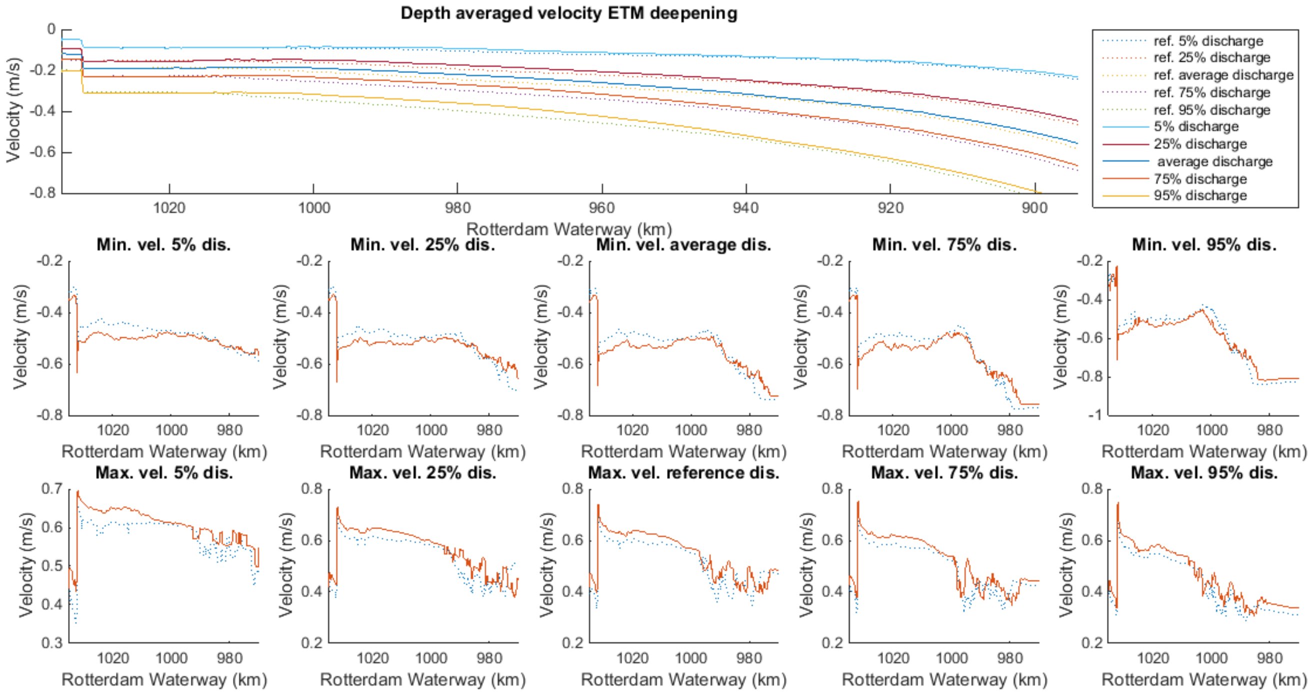

Figure 79 Depth average velocity for discharge sensitivity (upper panel); Flood (maximum) and ebb (minimum) velocity due compared (orange line) with reference depth (dashed line) for discharge sensitivity

Sensitivity waves

The average velocity due to waves for Hook of Holland, Maassluis and the Botlek can be seen in Figure 80. There is no change in average discharge due to changing wave conditions for the ETM deepening scenario.

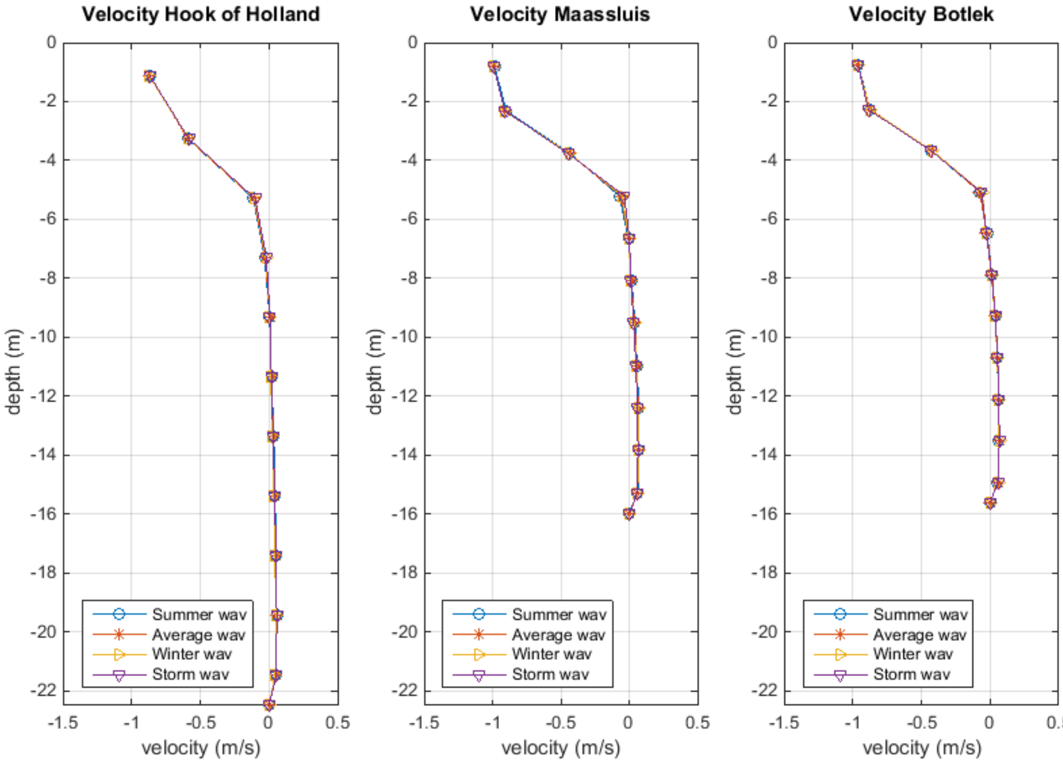

Figure 80 Average velocity for the ETM deepening for Hook of Holland, Maassluis and the Botlek due to changing wave conditions

The ebb and flood velocity for the deepened scenario due to chaning wave conditions are shown in Figure 81. The maximum ebb and flood velocity show no change due to changing wave conditions compared with the average wave conditions.

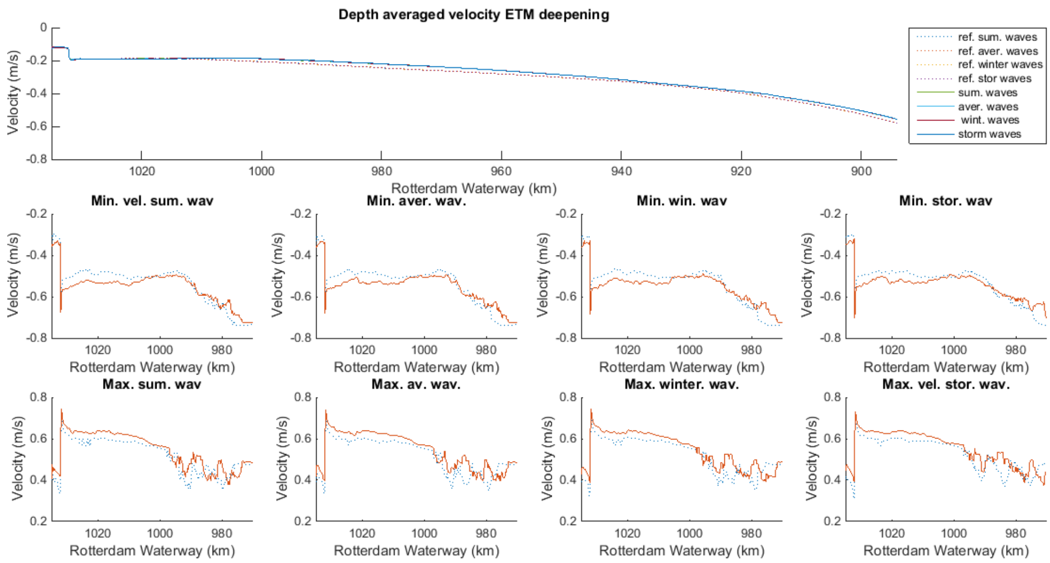

Figure 81 Depth average velocity for changing wave conditions (upper panel); Ebb and flood velocity for different wave conditions (lower panel)

Sensitivity sediment transport

The sensitivity for the different ETM deepened scenario for the discharge can be seen in Figure 82 in the left panel.

The scenario analysis for the changing fresh water boundary shows a change compared with the reference depth. The difference between the 25% and the 50% discharge show no difference in maximum concentration suspended sediment, while the increased depth shows a clearly difference between these discharges. Also the difference between the 5% and 25% increased. Also the difference between the 75% and 95% scenario has increased compared with the reference depth.

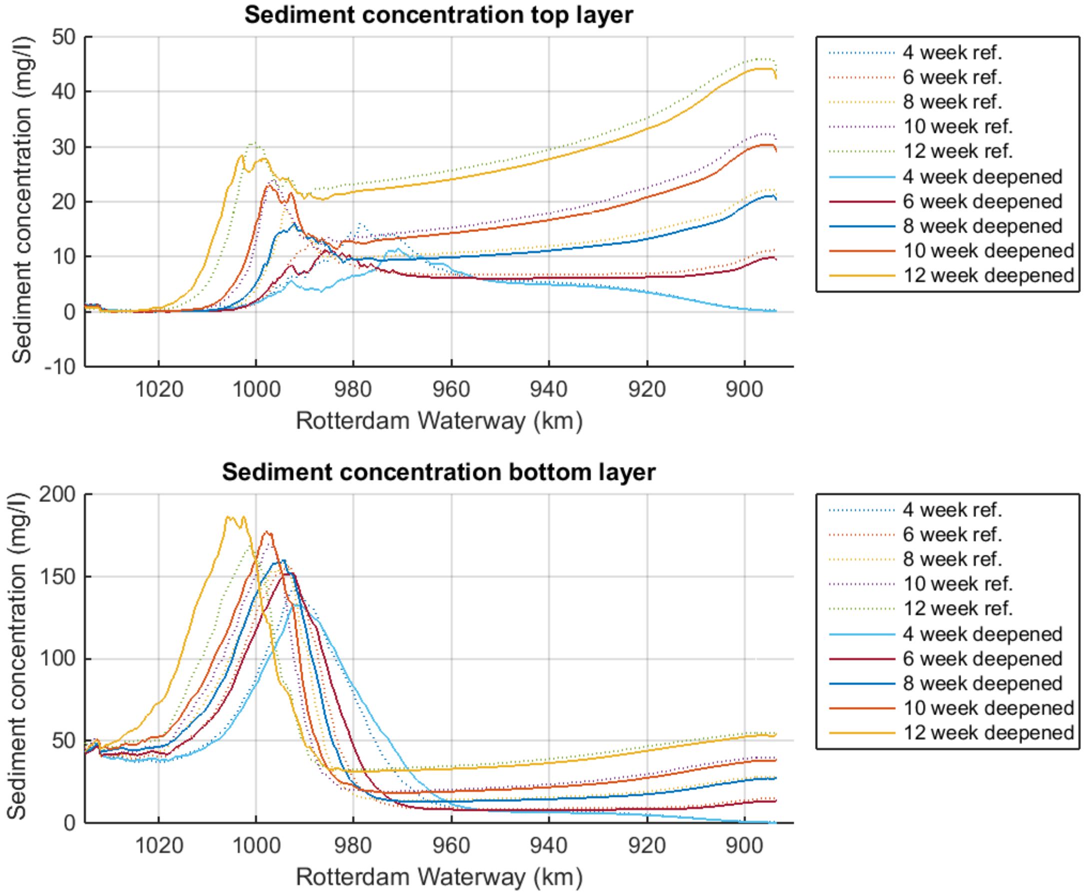

Figure 82 Sensitivity ETM deepening for changing discharge for the ETM deepening scenario, compared with the reference scenario (dashed lines)

The sensitivity analysis for the waves is comparable with the step deepening scenario and the reference scenario, as can be seen in Figure 83. The storm conditions for waves show the an increased import of sediment originated from sea, while the changes for summer and winter waves are negligible. The storm waves also induce a small movement of the ETM estuary upward.

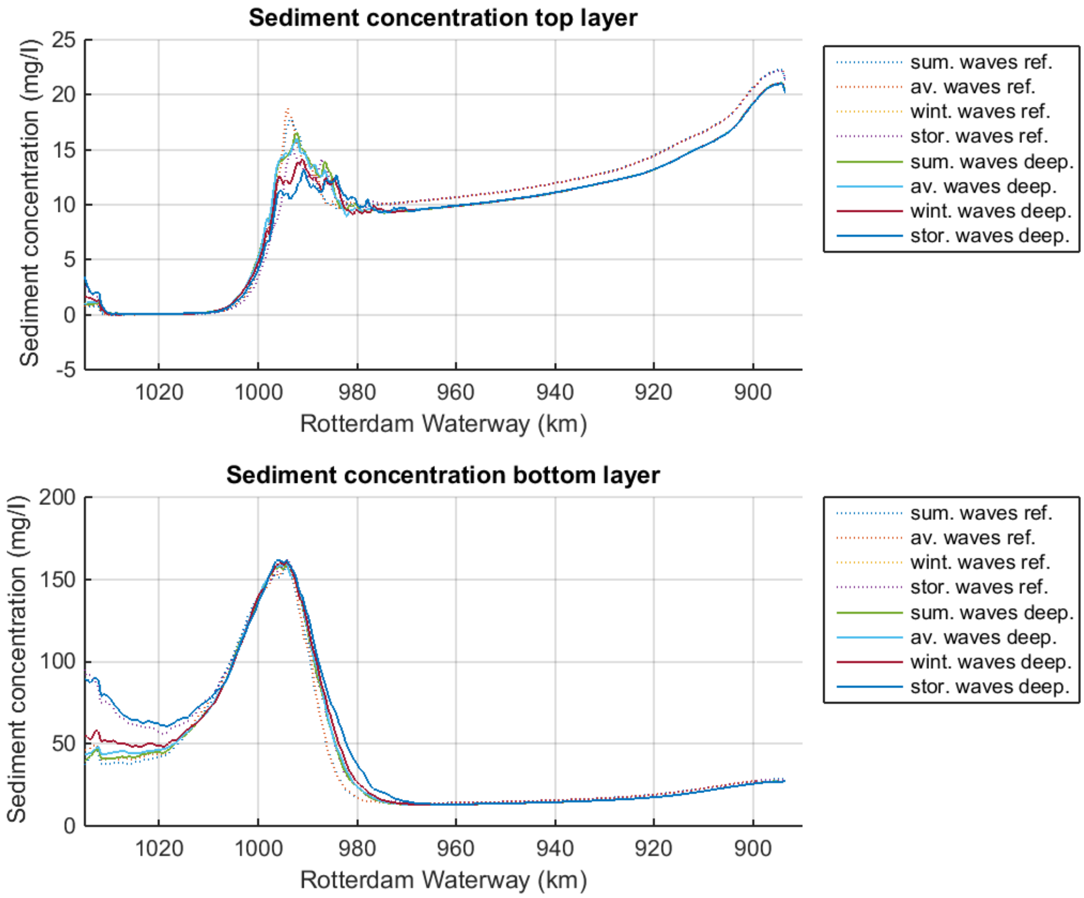

Figure 83 Sensitivity ETM due to changing waves for the ETM deepening, compared with the reference scenario (dashed lines)

Medium term sediment transport

The changes on the medium term response for the discharge can be seen in Figure 84, with the 5% discharge in the left panel and the 95% discharge in the righter panel. The concentration of suspended sediment for the changing discharge in time has decreased in both the near the top and near the bottom for the 5% discharge. The top layer decreases from 280mg/l towards 250 mg/l. For the 95% discharge there is a small increase in suspended sediment, comparable with the 95% discharge ETM for the reference scenario. The increase is towards 270 mg/l, which is less compared with the increase due to the step deepening (283 mg/l).

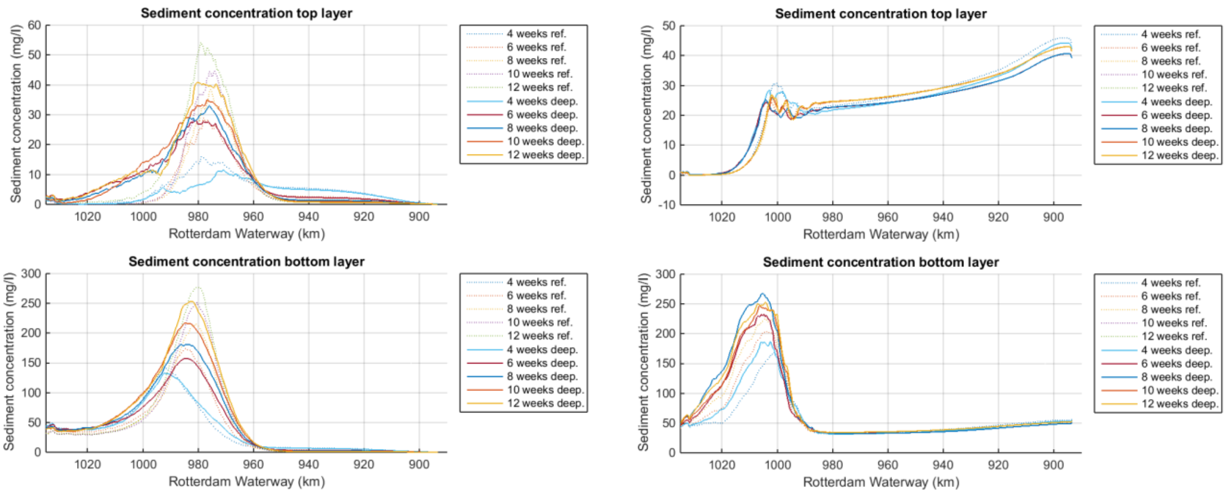

Figure 84 Medium term growth of the ETM for the 5% discharge (left) and for the 95% discharge right

Figure 85 shows the available sediment for the active bottom layer for the 5% and 95% discharge. The sediment concentration in the bottom shows little change, compared with the step deepening scenario. More sediment is trapped in the ETM, so less sediment is trapped in the bottom. The only change is the location where the sediment is trapped, for the 95% discharge. No new step is introduced so the sediment is trapped estuary outward of kilometer 1033 and in the maximum suspended sediment concentration near kilometer 1000.

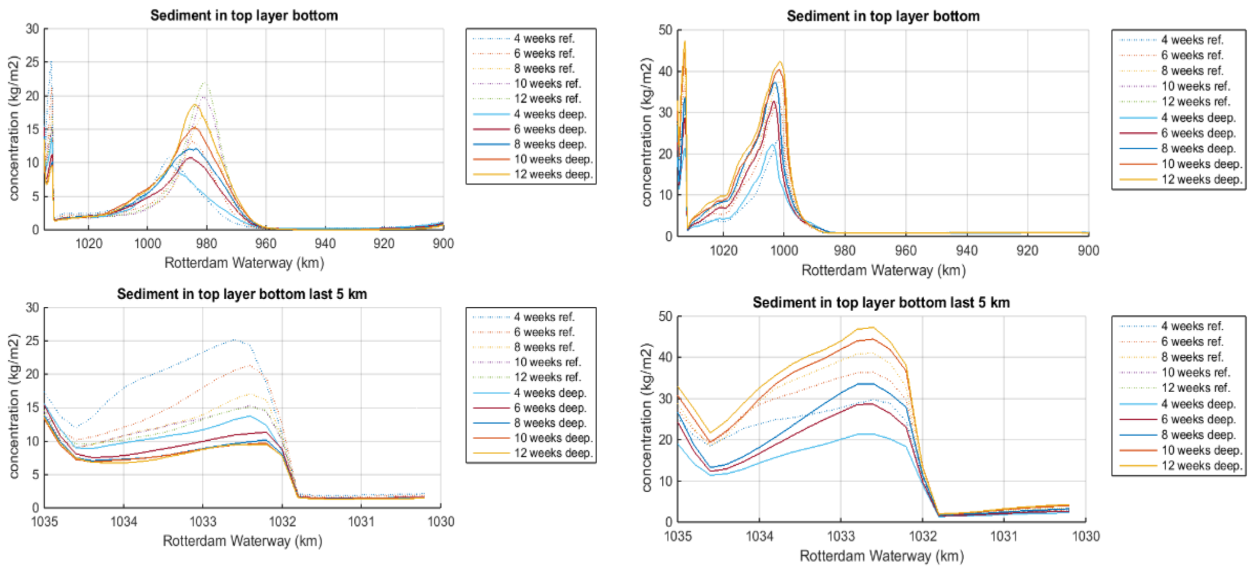

Figure 85 Available sediment in bottom layer for 5% discharge (left) and 95% discharge (right) for the ETM deepening scenario and the reference scenario (dashed lines)

The changes on the long term for the waves can be seen in Figure 86, with the summer waves in the left panel and the storm waves in the righter panel. The changes due to the changing wave conditions have not changed more than the increase due to the deepening for average conditions for the storm wave conditions. The summer waves do not seem to have an increase in concentration at all.

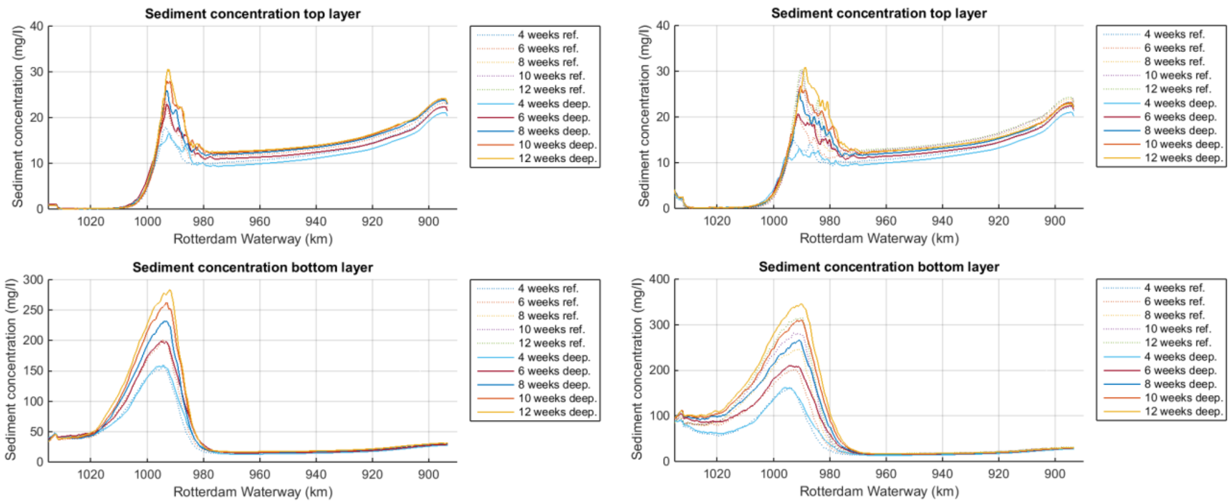

Figure 86 Medium term growth of the ETM for the summer waves (left) and for the storm waves right

The change in bottom sediment for the ETM deepening scenario can be seen in Figure 87. Also for the changing wave conditions the available sediment in the bottom is decreasing in front of the step near kilometer 1033 due to the increased suspended sediment in the ETM. The decrease for the storm waves however is small, indicating a lot of sediment has been settled before it reaches the ETM.

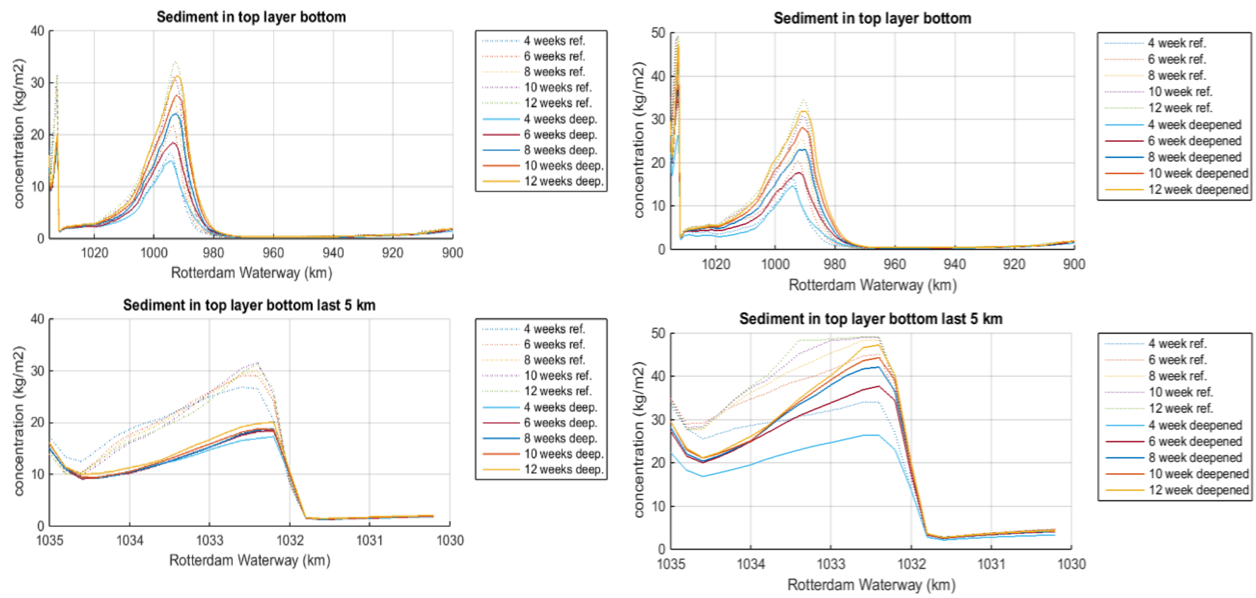

Figure 87 Available sediment in bottom layer for summer waves (left) and storm waves (right) for the ETM deepening scenario, compared with the reference scenario

7 DISCUSSION

First the use of the numerical model is discussed. Second the results are discussed compared with the known knowledge of the Rotterdam Waterway and compared with the funnel shaped estuary Ems-Dollard.

7.1 Numerical model

The use of a numerical model implies assumptions which are necessary to use the model, but do not represent reality. A first important factor is the solution method of the numerical model. The solution method is done by separate calculations for the tide and short waves. The waves are calculated every 60 minutes. This means the interaction between the waves and tides is quite static. Although it is possible to decrease the time after which the waves are calculated, this makes the time of the model calculation much longer.

The grid resolution is relative coarse, compared with the detailed model of De Nijs and used by Arcadis for the MER study. With the larger grid resolution details are lost and stability is decreasing. The calculated flow water level, velocity, sediment concentration and

Hydrostatic pressure model means the vertical acceleration is very small. The term very small is not determined any further. The results of the gravitational circulation were very small. It is unknown if the gravitational circulation increases with the use of non-hydrostatic pressure model, because there is gravitational circulation where it is expected based on theory.

The Sigma layer system has several disadvantages, which are important to know. The constant number of layers means for a sudden increase in bottom depth the depth described by one layer also suddenly decreases. The numerical method of the sigma layer system means the value of the next grid cell is based on the surrounding ones. The sudden decrease in area, but the numerical method mean the sediment transport and the salinity of the next cell can be overestimated compared with reality. To solve this problem the Z layer system can be applied, but this system has the disadvantage of disappearing sediment with the sudden decrease.

7.2 Model use

The validation of the model shows acceptable results, but not perfect. The phase lag especially near the Botlek harbor are quite large and the water level is overestimated during spring tide. The model therefore can be improved. The increased spring tide can cause overestimated ebb velocities and therefore disturb the analysis.

The patterns for the salinity, velocity and suspended sediment show the patterns of De Nijs, but the validation is done based on plots, not on values. Therefore it is still guessing how good the validation really is.

No morphological updating which means the erosion and sedimentation of sediment is not taken into account. It creates for example bottom patterns which increase or decrease the roughness. For the study a constant bottom roughness is assumed.

The schematized study area leaves out all kind of details which can be important to describe the system for the Rotterdam Waterway in detail. The aim of the study is however to find the important processes for prismatic estuaries like the Rotterdam Waterway.

Only one grain size for the fine sediment and one grain size for coarser sediment is used. The use of only one sediment size per sort can lead to higher or lower suspended sediment concentration. If the flow velocities are just enough for the used sediment types, the concentration is possibly higher compared with a sediment spectrum with more grain sizes.

Fixed structures in the waterway cause erosion and sedimentation near locations where it is not expected based on the schematized case. This can also influence the location of the ETM and the stratification, velocity and water level.

Flocculation appears to be an important factor in other estuaries for the trapping of sediment in the ETM. The used model showed no flocculation, even decreased fall velocities with increasing density. Although the results are comparable with the results of De Nijs, who also claims flocculation has already been done in the fresh water it is still unknown and doubtable if this is also to be found for measurements in the Rotterdam Waterway.

8 CONCLUSIONS AND RECOMENDATIONS

This chapter contains the conclusions, which answer the research questions. Furthermore, some recommendations are given based on the results of the research.

8.1 Conclusions

The aim of the research was to determine the sediment transport characteristics for prismatic estuaries and to determine the effect of deepening.

1. Which processes determine the salt intrusion in the Rotterdam Waterway?

The salt intrusion is determined by the bathymetry, the tide and the discharge. The tide causes the salt intrusion to move back and forth in the tidal channel, with the null point located at kilometer 977 of the channel. The average length however is also determined by the discharge. Increasing the discharge to the 95% discharge leads to a replacement of the null point of the salinity estuary outward with 7.8 kilometer. Decreasing the discharge to the 5% discharge leads towards a movement of the salt wedge estuary upward with 12.4 kilometer. Increasing the waves only influences the location of the ETM when the significant wave height of the waves has increased significant with 1 meter of significant wave height. With the large increase in significant wave height the salt intrusion has increased with 4 kilometers.

Although the changing discharge is moving the null point, the upper part of the water column stays relative fresh compared with the lower part of the water column. Also the turbulence is low in the upper layers of the water column. The salinity in the upper layer from 0 until -4 meter is 3 PSU while the salinity in the remaining part of the water column is 30 PSU near the estuary mouth.

The bathymetry is important for the length of the saline intrusion near the bottom. The step in bottom height at the beginning of the channel decreases the salinity of the upper layers of the water column. Including harbor basins decreases the salinity intrusion near the bottom, because the tidal prism entering the channel is constant but part of the tidal prism is entering the harbor basin instead of the channel. The harbor basins decrease the length intrusion with 2 kilometers.

2. Which processes determine the hydrodynamics in the Rotterdam Waterway?

The discharge and the tide determine the hydrodynamics in the Rotterdam Waterway. The waves from the sea have already been broken and do not influence the hydrodynamics in the prismatic channel. Tidal asymmetry causes tidal pumping in the estuary. The estuary is flood dominant which means higher flood velocities during a shorter period. The average velocity near the bottom decreases towards 0.06 m/s for the 5% discharge and increases for increasing discharge towards 0.08 m/s for the 95% discharge. The increase is mainly due to the increased average flood velocity duration near the bed.

The average velocity near the top is 0.9 m/s estuary outward near the estuary mouth for average conditions which increases with increasing discharge towards 1.2 m/s estuary outward near the estuary mouth for 95% discharge. The average velocity for the top layers is also mainly due to the increased ebb velocity duration in the top layers.

The turbulence damping is decreasing towards the top of the water column from 3×10^{-3} m^2/s^2 near the bottom towards 0 m^2/s^2 at the top of the top layer. From the null point estuary outward, the turbulence decreases near the bottom due to the smaller flood velocity. For this area the turbulence is damped in in the top three layers, where also the salinity is less and the ebb velocity is much larger. The turbulence moves with the null point for the changing discharge.

Gravitational circulation seems to exists in the area from the null point estuary outward, with a peak just after the null point. With the increasing discharge, the gravitational circulation also increases. The vertical velocity however is very small with the used model settings.

Increased discharge leads to increased ebb velocity duration with 114 minutes and increased velocity in the upper layers towards 1.2 m/s for 95% discharge. For the saline layers however the increased discharge result in increased flood velocity duration of 38 minutes increased flood velocity towards 0.08 m/s for the 95% discharge.

Decreased discharge leads to decreased ebb velocity duration with 62 minutes and increased velocity in the upper layers towards 0.5 m/s for 5% discharge. For the saline layers however the increased discharge result in decreased flood velocity duration of 24 minutes increased flood velocity towards 0.02 m/s for the 5% discharge.

After a change in discharge the system needs one two spring neap cycles to adapt to the new situation, but the largest change is during the first tidal cycle.

3. *Which processes determine the Estuarine turbidity maximum in the Rotterdam Waterway?*
The use of the hydrostatic pressure model results in an ETM which grows in time. The concentration suspended sediment after a spring neap cycle with four weeks' run-up time is at maximum in the channel 100 mg/l near kilometer 1000, where also the average velocity is 0 m/s near the bottom.

The turbulence damping results in the raining out of sediment from the top layers into the lower layers of the water column. And in general it can be concluded that flocculation does not play a role in the formation of the ETM in the Rotterdam Waterway. The fall velocity changes with the salinity, but the fall velocity does not increase as expected. The fall velocity decreases with increasing salinity.

Both the discharge and the significant wave height influence the concentration of suspended sediment in the ETM in the Rotterdam Waterway. Increasing discharge leads to a movement of the ETM estuary outward with 8 kilometers for the 95% discharge. The flood duration increases near the bed with increased velocity so more sediment is trapped near the bottom. The sediment availability from the fresh water boundary is also increases with the increasing discharge. The initial response of the ETM is to increase. After several spring neap cycles the suspended sediment concentration however is decreased compared with the average conditions.

Decreased discharge leads to a movement of the ETM 2 kilometer estuary inward. Velocities decrease leading to smaller suspended sediment concentrations. After several spring neap cycles the concentration is 80 mg/l, which is almost equal with the suspended sediment concentration for the average conditions.

Long term 5% discharge leads to the same concentration of suspended sediment in the ETM near the bottom, only moved estuary inward. For the top layer the decreased discharge leads to increased suspended sediment concentration because less turbulence is damped so the sediment is able to remain in suspension in the top layers of the water column. The available sediment in the bottom decreases, so less sediment is settling in the tidal channel. Also less sediment is blocked by the step in the bottom, so less sediment escapes towards the sea because the wave conditions are the same.

Long term 95% discharge does not lead to increased suspended sediment concentrations compared with average in the ETM, although the tidal asymmetry increases and the sediment from the fresh water boundary is also increasing. The sediment in the bottom layer is increased in the tidal channel and in front of the step increased, so more sediment is stored in the bottom.

The wave conditions determine the availability of sediment from sea, but only for a large increase in wave conditions in the sea. During the first spring neap cycle the suspended sediment concentration has not yet increased compared with the reference situation, but during the following spring neap cycles the suspended sediment increase in the ETM form 250 mg/l towards 300 mg/l. Also the available sediment in the bottom in front of the step increased, so the amount of sediment coming from sea increased. For decreasing wave conditions there is no change in suspended sediment.

Adding harbor basins to the study area influences the sediment transport of the study area. The locations of the harbor area make it possible to act as sediment trap for sediment which settles near the bottom. Also the suspended sediment concentration increases with the inclusion of the harbor basins.

4. *What is the effect of channel deepening for the described processes for the Rotterdam Waterway?*

4.1. Salinity
The location of the deepening determines the increase in salinity intrusion, although the location of the null point increased for both scenarios. The step deepening results in an increased tidal prism, so the total salinity intruding increases. The ETM deepening results in an increased salt intrusion with the same tidal prism, leading to increased salinity estuary upward, but decreased salinity in the estuary between the estuary mouth and the formal null point.

The step deepening scenario and the ETM deepening scenario decreased the length over which the null point is changing due to changing discharge, increasing discharge leads to increased movement estuary downward. Decreasing the discharge leads also to increased movement of the null point estuary upward. The ETM deepening only changed the length of the salinity intrusion.

4.2. Hydrodynamics
The hydrodynamics change with the changing salinity and water level. The step deepening scenario results in a small increase of 0.04 m/s in the middle part of the water column. This is due to the increased baroclinic pressure gradient due to the increased salinity. Near the bottom this effect has already been damped out and

the velocity is equal to the reference scenario. The tidal pumping near the bottom increases from the new step, because the ebb- and flood velocity increase due to the increasing tidal prism and the decreasing cross section near the step.

The new step in the bottom line introduces a new turbulence peak for the step deepening scenario in the Rotterdam Waterway leading to increased salinity higher in the water column. The turbulence damping does not change for the deepening scenario. The gravitational circulation is increasing near the new step for the step deepening scenario, but is not increasing near the ETM. The gravitational circulation shows no significant change for the ETM deepening scenario.

The step deepening decreases the ebb velocity near the top for the 5% discharge and increases the ebb velocity near the top for the 95% discharge compared with the reference scenario, although the changes are small. The decrease for the 5% discharge is due to the decreased baroclinic pressure gradient. The increased stratification leads to decreased velocities in the middle of the water column forcing the fresh water to flow over an increasing depth. The increase in velocity due to the increasing discharge is due to the increased baroclinic pressure gradient forcing the fresh water over a smaller depth, increasing the flow velocity.

ETM deepening shows a small decrease in ebb velocity in the upper part of the water column with a small increase in average velocity near Hook of Holland, and the same flood velocities estuary upward. The duration of the ebb velocity near the top is decreasing due to decreased tidal amplitude leading to a decreased barotropic pressure. The average velocity near the bottom is not decreasing due to the increasing baroclinic pressure gradient which is caused by the increased stratification. The tidal pumping however increases near the bottom near the estuary mouth due to the deepening. This is due to the salinity increases further into the estuary leading to increased velocities near the bottom.

The ETM deepening increases the ebb velocity near the top for the 5% discharge and decreases the ebb velocity near the top for the 95% discharge. This is due to the decrease in barotropic pressure gradient due to the deepening. Near the bed however the increase in stratification increases the baroclinic pressure gradient.

4.3. Sediment transport
Both the step deepening and ETM deepening result in increased ETM length, because more sediment is trapped due to the increasing velocities near the bed, or in the middle layer. The step deepening results in a small movement of the maximum concentration estuary upward, while the ETM deepening has the maximum concentration near the same location. The increased trapping of sediment leads to lower fine sediment concentrations in the bed for both scenarios. The maximum concentration in the bottom near the ETM is constant however.

For the step deepening the increase in suspended sediment in the ETM is small, the length of the ETM however increases. The increased trapping is due to the increased tidal pumping. The 5% discharge leads to a smaller peak after 12 weeks, but an increased length. The 95% discharge results in an increased suspended sediment peak in the ETM. The waves show increase for both the summer and storm waves with the same magnitude of 25 mg/l. The sediment being trapped in front of the step near kilometer 1033 is decreasing.

The ETM deepening leads to similar changes for suspended sediment characteristics for the ETM. The ebb and flood velocity increase but the suspended sediment concentration in the ETM does not change compared with the step deepening, because the changes due to changing discharge is rather small. The suspended sediment concentration increases the difference between 5% and 25% and between 75% and 95% discharge compared with the scenario without the deepening.

The waves are not influenced by the deepening. Increasing the waves increases the suspended sediment concentration in the ETM, however the increase in concentration has not been increased compared with the increase for the average conditions of the deepened scenario.

8.2 Recommendations

The Harbor Authorities of Rotterdam need to evaluate the effect of deepening for the salinity intrusion and dredging campaign. The salinity intrusion need to be evaluated for the water intake locations near the Rotterdam Waterway, especially when the deepening is like the step deepening because the tidal prism increases for the step deepening leading to increased salinity in the total water column.

Both deepening scenarios lead to increased trapping of suspended sediment. The harbor basins act as sediment trap leading so more sediment will settle in the harbor basin. The effect in the Rotterdam Waterway is increased over an increased length, so if the Rotterdam Waterway needs to be dredged, an increased distance probably needs to be dredged.

The gravitational circulation is evaluated based on the hydrostatic pressure model. To evaluate the contribution of the gravitational circulation for the formation of the ETM, a non-hydrostatic pressure model should be used in continuous research to evaluate the contribution of gravitational circulation for the prismatic estuary.

To distinguish the difference between the funnel-shaped estuary and a prismatic estuary, an extensive comparison of the effects of deepening for funnel-shape and prismatic estuaries should be made. For example, by identifying similar conditions for a schematized estuary, one prismatic and one funnel shaped. The difference between the two could give interesting result in the contribution of the different processes towards the hydrodynamics and the sediment transport processes.

If the study area is evaluated again with a numerical model, it is useful to have more validation data. For this research the plots of De Nijs are used to validate the pattern of the salinity, velocity and suspended sediment. More validation data for the Rotterdam Waterway, specific on velocity and salinity would help increase the skill of the model.

Constant boundary conditions create constant conditions in which the sediment settles at one location, and picks up at another location. To know more real conditions, several discharge events can be picked so see the difference between the steady conditions and the varying conditions.

The contribution of sediment originating from sea and fluvial sediment is still unknown. Although two types of mud were set as boundary condition, the contribution of the sediment was equal for all scenarios and is therefore not included in the report. It is interesting however to see where the sediment is originated and if one type of sediment is being trapped more. Further research could be done for this specific topic to evaluate the contribution of the different sediment towards the ETM in the estuary.

The morphological development of the estuary is an interesting case for further research. During this study the morphological updating was disabled. This makes it possible to determine where the sediment would like to settle, but the morphological change also possibly changes the hydrodynamics, resulting in different sediment transport etc. and to see the really long term (years) change in the prismatic estuary.

Flocculation appears to be an important factor for the settling of sediment in estuaries. For the study however the flocculation decreased with increasing density (salinity). This corresponds with the synthesis of De Nijs, where he states the flocculation probably appeared in the fresh water. This is contra dictionary with other estuaries, where flocculation only appears when the sediment enters the saline water. Therefore, more research should be done to the flocculation in the Rotterdam Waterway.

BIBLIOGRAPHY

Arcadis. (2015). *MER verdieping Nieuwe Waterweg en Botlek Achergrondstudie Morfologie (in dutch).* Zwolle: Arcadis.

Bathymetry. (2016, 6 20). Opgehaald van Emodnet: http://portal.emodnet-bathymetry.eu/mean-depth-full-coverage

Brennon, I., & Le Hir, P. (1999). Moddeling the Trubidity Maximum in the Seine Estuary (France): Identificaiton of Formation Processes. *Estuarine, Coastal and Shelf Science*, 525-544.

Brenon, I., & Le Hir, P. (1999). Moddeling the Turbidity Maximum in the Seine Estuary (France): Identification of Formation Processes. *Estaurine, Coastal and Shelf Science* , 525-544.

Colling, A., & Park, D. (1999). *Waves, Tides and Shallow-water processes.* Oxford: Butterworth-Heinemann.

Colling, A., & Park, D. (1999). *Waves, Tides and Shallow-water processes .* Oxford: Butterworth-Heinemann.

De Nijs, M. A., & Pietrzak, J. (2012). Saltwater intrusion and ETM dynamics in a tidally-energetic stratified estuary. *Ocean Moddeling*, 60-85.

de Nijs, M. A., Pietrzak, J. D., & Winterwerp, J. C. (2011). Advection of the Salt Wedge and Evolution of the Internal Flow Structure in the Rotterdam Waterway. *Journal of Physical Oceanography*, 3-27.

De Nijs, M. A., Winterwerp, J., & Pietrzak, J. D. (2009). On harbour siltation in the fresh-salt water mixing region. *Continental Shelf Research*, 175-193.

Deltares. (2014a). *Delft3D-FLOW, User manual.* Delft: Deltares.

Deltares. (2014b). *Delft3D-WAVE, User Manual.* Delft: Deltares.

Friederichs, C. T., & Aubrey, D. G. (1988). Non-linear Tidal Disortion in Shallow Well-mixed Estuaries: a synthesis. *Estuaries, Coastal and Shelf Science*, 521-544.

Guo, L., van der Wegen, M., Roelvink, J. A., & He, Q. (2014). The role of river flow and tidal assymetry on 1-D estuarine morphodynamics. *Journal of Geophysical Research: Earth Surface*, 2315-2334.

Komar, P. D., & Miller, M. C. (1975). On comparison between the threshold of sediment motion under waves and unidirectional currents with a discussion on the practical evaluation of the threshold. *Journal of Sedimentary Petrology*, 362-367.

O'Brien, M. P. (1969). Equilibrium flow areas of inlets on sandy coasts. *Journal of Waterway, Port, Coast and Ocean Engineering*, 43-52.

Pritchard, D. (1967). What is an estuary: physical viewpoint. *Estuaries: Amercian Association for the Advancement of Science Publication*, 3-5.

Rijkswaterstaat. (2014). *Getijdentafels voor Nederland 2015.* Den Haag: SDU uitgevers.

Rijkswaterstaat. (2016, 06 22). *live.waterbase.* Opgehaald van waterbase: http://live.waterbase.nl/waterbase_wns.cfm?taal=nl

Rijkswaterstaat directie beneden rivieren. (1987). *Waterbeheersing noordelijke deltabekken m.b.v. lozingsprogramma haringvlietsluizen.* Dordrecht: Notanummer AXK/87/45.

Roelvink, J. A. (2006). Coastal morphodynamic evolution techniques. *Coastal Engineering*, 177-187.

S., v. M., van Kessel, T., Cronin, K., & Sittoni, L. (2015). The impact of channel deepening and dredging on estuarine sediment concentration. *Continental Shelf Research*, 1-14.

Savenije, H. H. (2005). *Salinity and Tides in Alluvial Estuaries.* Delft: Delft University of Technology.

Talke, S. A., de Swart, H. E., & Schuttelaars, H. M. (2009). Feedback between residual circulations and sediment distribution in highly turbid estuaries: An analytical model. *Continental Shelf research*, 119-135.

Van de Ven, G. P. (2008). *De Nieuwe Waterweg en het Noordzeekanaal; Een Waagstuk*. Den Haag: Deltacommissie.

Van der Kaarij, T., van den Boogaard, H., Kuijper, C., Sloff, C. J., & van Zetten, J. (2010). *Herstel van de trapjeslijn in de Nieuwe Waterweg en de Nieuwe Maas.* Delft: Deltares.

van Dreumel, P., & Struyk, A. (1988). *Trapjeslijn in de Nieuwe Waterweg en de Nieuwe Maas.* Den Haag: Rijkswaterstaat.

van Maren, D. S., van Kessel, K. T., & Sittoni, L. (2015). The impact of channel deepening and dredging on estuarine sediment concentration. *Continental Shelf Research*, 1-14.

van Rijn, L. (2007a). Unified View of Sediment Transport by Currents and Waves. I: Initation of Motion, Bed Roughness and Bed-Load Transport. *Journal of Hydraulic Engineering*, 649-667.

van Rijn, L. (2007b). Unified View of Sediment Transport by Currents and Waves. II: Suspended Transport. *Journal of Hydraulic Engineering*, 668-689.

Verdieping Nieuwe Waterweg. (2014, November 19). Opgehaald van Staatscourant: https://zoek.officielebekendmakingen.nl/stcrt-2014-32793.html

Verlaan, P. A., & Spandhoff, R. (2000). Massive sedimentation events at the mouth of the Rotterdam Waterway. *Journal of Coastal Research*, 458-469.

Winterwerp, J. C. (2011). Fine sediment transport by tidal assymetry in high-concentrated Ems River: indications for a regime shift in response to channel deepening. *Ocean Dynamics*, 203-215.

Winterwerp, J. C. (2011). Fine sediment transport by tidal assymetry in the high-concentrated Ems River: indications for a regime shift in response to channel deepening. *Ocean Dynamics*, 203-215.

APPENDICES

A. Numerical modeling in estuaries

Analytical models are extensively used to indicate the different processes in estuaries. Two types of analytical models have been used to indicate the processes in estuaries: analytical equations or idealized models. The analytical equations summarize the processes in several dimensionless parameters to describe the estuary and the response of the estuary on changes (Savenije, 2005; Chai *et al.*, 2012). In the idealized models simulate the different processes with the use of analytical equations (Talke *et al.*, 2009; Chernetsky *et al.*, 2010; de Jonge *et al.*, 2014). Idealized models need assumptions for example about the depth and the width need to be made, this ignores the spatial and density differences in the estuary. These differences are included in numerical modeling. Another advantage of numerical modeling is the feedback mechanisms between hydrodynamic and morphologic processers are conveniently updated via a robust morphological updating scheme (Roelvink, 2006).

Numerical models have been used as alternative for analytical modeling in many ways. For the study the process-based numerical model Delft3D is used (Lesser *et al.*, 2004). The Delft3D model is used in this research for several reasons. First Delft3D is a numerical model including tidal waves, short waves (optionally), river discharge, difference in density and the inclusion of morphology (optionally). These features are crucial for the modeling of estuaries. Also the results of previous studies in using Delft3D give sufficient to good results. The scientific research modeling the Rotterdam Waterway by De Nijs *et al.* (2012) concluded the model was sufficient to use for the Rotterdam Waterway. The last reason to choose the Delft3D model is the availability of Delft3D at ARCADIS and the experience with similar case studies at ARCADIS for the Rotterdam Waterway using Delft3D.

Delft3D has been used extensive for the numerical evaluation of estuaries in 1D (Guo *et al.*, 2014), 2D (Hu *et al.*, 2009a) or 3D (Hu *et al.*, 2009a; de Nijs *et al.*, 2012).

The 1D simulation are done based on schematized estuary with converging width and converging cross section for the Yangtze river (Guo *et al.*, 2014). The 1D model was preferred to model the long term (10 years with a morphological factor of 400) morphological development, because it takes less computational time. 1DV point model is used to compute the morphological evolution of the Ems estuary (Winterwerp, 2011). The 1DV point model needs input for velocity and water level to determine the sediment transport in the estuary, which makes it impossible to determine the hydrodynamic and sediment transport changes for the estuary with the same model.

The 2D simulation is also done for the Seine (Brenon & Le Hir, 1999), the Yangtze (Hu *et al.*, 2009a) or the Ems (van Maren *et al.*, 2015). For the studies using the 2D model, most of them used a depth integrated 2DH model. The justification for using the depth integrated model despite the density difference between the fresh water and the sea water is a neglected discharge input from the river (Ems), or the small contribution of gravitational circulation in the estuary compared with other processes like tidal pumping in the Seine estuary (Brenon & Le Hir, 1999).

3D simulations are done more extensive for estuaries, because 3D includes the varying width of converging estuaries and it includes salinity distribution in the depth direction. Examples of 3D modeling are the Yangtze estuary (Hu *et al.*, 2009a), the Seine (Brenon & Le Hir, 1999), the Ems (van Maren *et al.*, 2015) or the Rotterdam Waterway (De Nijs *et al.*, 2012). The reason to prefer 3D modeling differ, based on the aim of the study. A comparison between the 2D and 3D model is common to incorporate the 3D model. The bathymetry of the estuary is also important for the 3D model to prefer. The 3D model incorporates the converging width and includes the dynamics between the fresh and saline water.

The numerical modeling for funnel-shaped estuaries resulted in fairly good results (Brennon & Le Hir, 1999; Hu *et al.*, 2009a; Guo *et al.*, 2014). For prismatic estuaries however, the results were less good (De Nijs *et al.*, 2012). The baroclinic pressure gradient and the pressure damping have been underestimated in the model, due to assumptions in the turbulence model. The barotropic asymmetry however is well reproduced by the model. De Nijs *et al.* (2012) overall concluded that the model is applicable in simulating the dynamics for the Rotterdam Waterway, because it represents the overall processes fairly well.

B. Delft3d model description

Delft3d simulates the unsteady hydrodynamic flow in two or three dimensions resulting from tidal and or metrological forcing. Although the research does not focus on the cross shore differences in the Rotterdam Waterway, the schematization is in 3D. Thus the three dimensional equations are explained in this section.

B. 1 Governing equations tide

B.1.1 The horizontal

$$\frac{\partial u}{\partial t} + u\frac{\partial u}{\partial x} + v\frac{\partial u}{\partial y} + g\frac{\partial \zeta}{\partial x} = fv + v_h\left(\frac{\partial^2 u}{\partial x^2} + \frac{\partial^2 u}{\partial y^2}\right) + \frac{gu\left|\sqrt{u^2+v^2}\right|}{hC^2} + \frac{\rho_{air} C_d W_x \sqrt{{W_x}^2 + {W_y}^2}}{\rho_0 h} \qquad \text{(eq.14)}$$

$$\frac{\partial v}{\partial t} + u\frac{\partial v}{\partial x} + u\frac{\partial v}{\partial y} + g\frac{\partial \zeta}{\partial y} = fu + v_h\left(\frac{\partial^2 v}{\partial x^2} + \frac{\partial^2 v}{\partial y^2}\right) + \frac{gv\left|\sqrt{u^2+v^2}\right|}{hC^2} + \frac{\rho_{air} C_d W_y \sqrt{{W_x}^2 + {W_y}^2}}{\rho_0 h} \qquad \text{(eq.15)}$$

In which the first term is the inertia, the second and third term is the advection, the fourth term is the horizontal pressure gradient, the fifth term is the Coriolis force, the sixth term is the horizontal viscosity, the seventh term is the friction and the eighth term is the wind force. For this study however the wind force is neglected, so the last term is zero.

$$\frac{\partial \zeta}{\partial t} + \frac{\partial \lfloor hU \rfloor}{\partial x} + \frac{\partial \lfloor hV \rfloor}{\partial y} = S \qquad \text{(eq.16)}$$

Where ζ is the water surface elevation (m), h is the water depth (m), U is the flow velocity in the x direction (m/s), V is the flow velocity in the y direction (m/s) and S is the contributions per unit area due to the discharge or withdrawal of water, evapotranspiration, and precipitation.

The vertical velocity is computed from the continuity equation (Lesser *et al.*, 2004):

$$\frac{\partial \omega}{\partial \sigma} = -\frac{\partial \zeta}{\partial t} - \frac{\partial \lfloor hU \rfloor}{\partial x} - \frac{\partial \lfloor hV \rfloor}{\partial y} \qquad \text{(eq.17)}$$

B.2 Governing equations waves

Wind generated short waves are generated with the SWAN module. In SWAN the waves are described with two dimensional wave density spectrum. The wave spectrum is described by:

$$\frac{\partial}{\partial t}N + \frac{\partial}{\partial x}c_x N + \frac{\partial}{\partial y}c_y N + \frac{\partial}{\partial \sigma}c_\sigma N + \frac{\partial}{\partial \theta}c_\theta N = \frac{S}{\sigma} \qquad \text{(eq.18)}$$

In which:
c = celerity (m/s)
N = energy density

In which the first term represents the change wave action (density) in time. The second and third term represent the propagation of the waves in the x-y domain. The fourth term represents the shift in relative frequency of the wave due to currents and changing depth. The fifth term represents the refraction of the waves. The sixth term on the right hand side is the source term. This represents the change in energy density due to generation, dissipation and non-linear wave-wave interactions.

B.3 Salinity

The salinity is included in the model is calculated based on the advection- diffusion equation:

$$\frac{\partial[hc]}{\partial t} + \frac{\partial[hUc]}{\partial x} + \frac{\partial[hVc]}{\partial y} + \frac{\partial[\omega c]}{\partial \sigma} = h\left[\frac{\partial}{\partial x}\left(D_H\frac{\partial c}{\partial x}\right) + \frac{\partial}{\partial y}\left(D_H\frac{\partial c}{\partial y}\right)\right] + \frac{1}{h}\frac{\partial}{\partial \sigma}\left[D_v\frac{\partial c}{\partial \sigma}\right] + hS \qquad \text{(eq.19)}$$

Where D_H and D_V are the diffusivity coefficients in the horizontal and vertical direction, c is the salinity concentration (PSU). The advection and diffusion equation determines the concentration which is already in suspension. The sink or source term introduces new sediment to the domain or takes sediment out of the domain.

B.4. Turbulence

Turbulence is important for the sediment processes, but the scale of the turbulence is often small. It is too time consuming to adjust the grid size and/or the time step to these scales. To simulate the turbulence well, a turbulence model is included. Three options for the inclusion of turbulence exist for Delft3d. First option is to use a constant turbulence determined by the user. The second option is to use an k-L turbulence model. this model solves the turbulence . The last option is to use the k-e turbulence model. This model solves the turbulence based on the energy balance. For this research the k-e turbulence model is included:

$$v = c_{\mu}\frac{k^2}{\varepsilon} \qquad \text{(eq.20)}$$

In which:

c'_{μ} = constant of Kolmogorov-Prandtl [-]
k = turbulent kinetic engery [m^2/s^2]
ε = dissipation of turbulent kinetic energy [m^2/s^3]

B.5 Vertical sigma coordinates

If there is no depth integration of the system, σ coordinate system is often used (Lesser *et al.*, 2004) with several layers as shown in Figure 88.

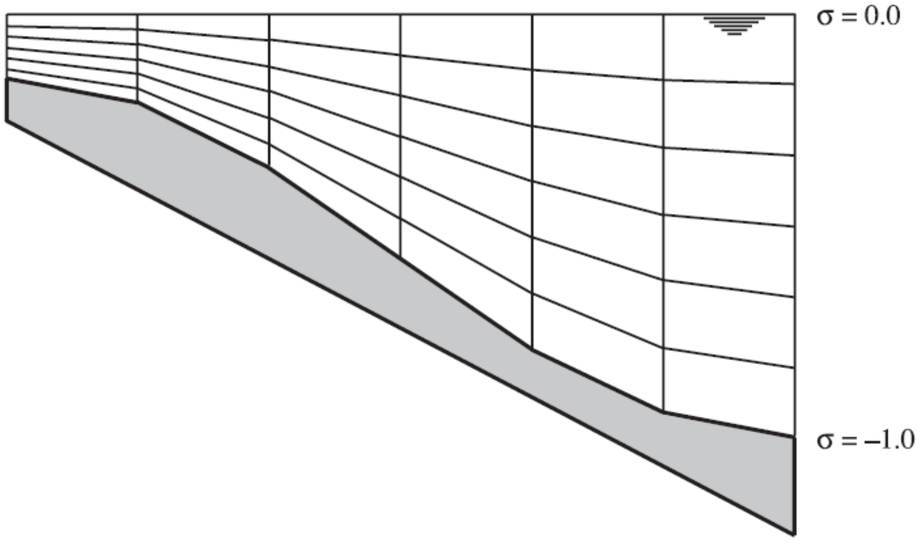

Figure 88 Layer system Delft3d (Lesser et al., 2004)

The number of layers need to be determined and is input for the model. The number of layers is constant in the total study area, only the depth described by one layer is different with changing depths in the channel.

The model can also be uses with the so-called Z layer system. In the Z layer system the layers are vertical stable, so if the depth changes also the number of layer changes. Due to the numerical solution of the grid, it can be less desirable to determine according to the σ coordinate system. If large geographical steps occur in the bottom shape, the layers have a large geographical step also. The solution method for the model is implicit, so based on neighboring grid cells. In reality it is unlikely the cell on top of the step is for such a large extend determined by the layer at the bottom of the geographical step. Therefore the salinity concentration (and sediment concentration) can be overestimated using the numerical model using the σ coordinate system.

B.6 Grid and boundary conditions

The described equations are solved on a staggred grid, see Figure 89. Staggred means the model uses several 'subgrids' to solve the equations of the variables. The water level points are defined in the center of a cell (+ in Figure 89). The velocity component is defined perpendicular on the grid cell.

The grid can be defined using Cartesian notation which results in a grid in meters, or a spherical grid where the grid is determined in decimal degrees. A latitude needs to be specified in order to calculate the Coriolis force if the Cartesian notation is applied.

The model need to be orthogonal. This means the grid lines must intersect (approximately) perpendicular. The maximum angle between two lines allowed is cos = 0.02. The grid is closed by a boundary which is defined in the enclosure file.

Several boundary conditions can be applied in Delft3d. This includes Neumann boundary, Riemann boundary, water level (harmonic or constant), discharge or a velocity boundary.

B.7 Solution procedure

The solution procedure of Delf3d is based on finite differences. The solution method used in this study is the circular method as shown in Figure 89.

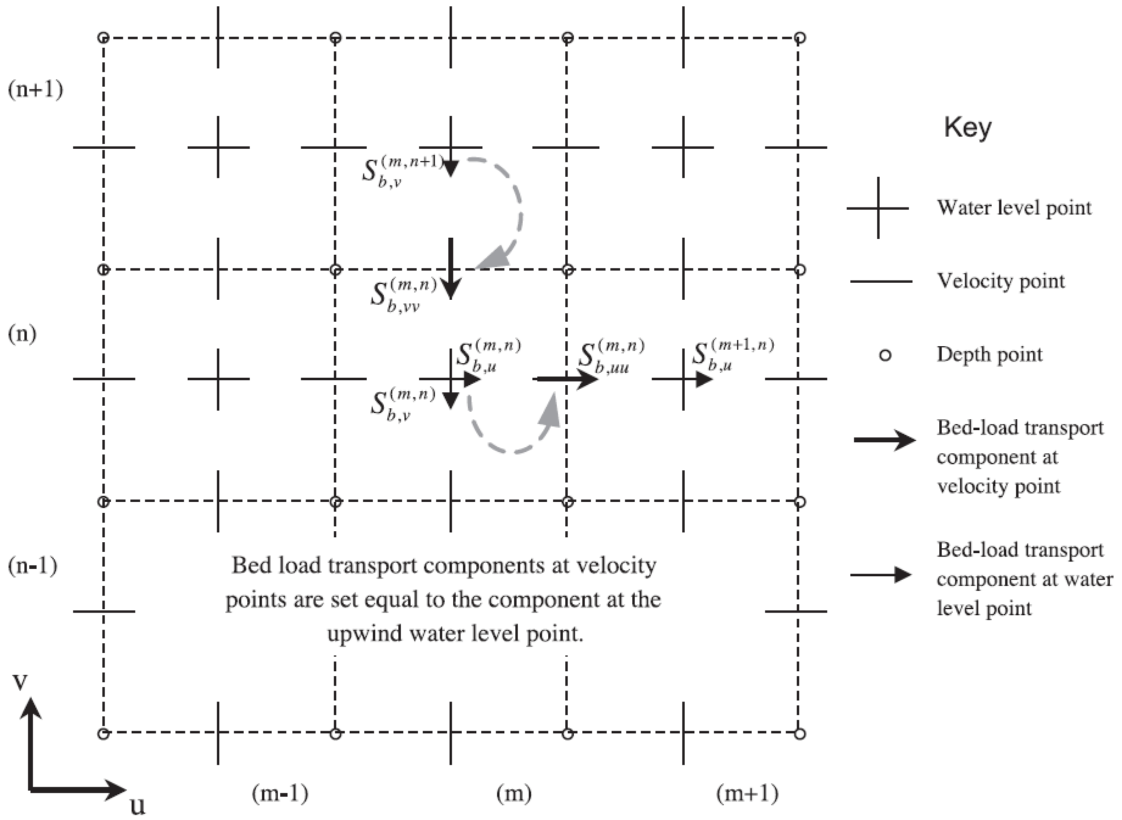

Figure 89 Solution procedure Delft3d (Lesser et al., 2004)

C. Ebb and flood duration

The ebb and flood duration are influenced by the changing boundary conditions, especially for the fresh water boundary. The ebb and flood duration are summarized in in minutes. The plots with the water levels are situated in this appendix.

C.1. Sensitivity analysis reference scenario

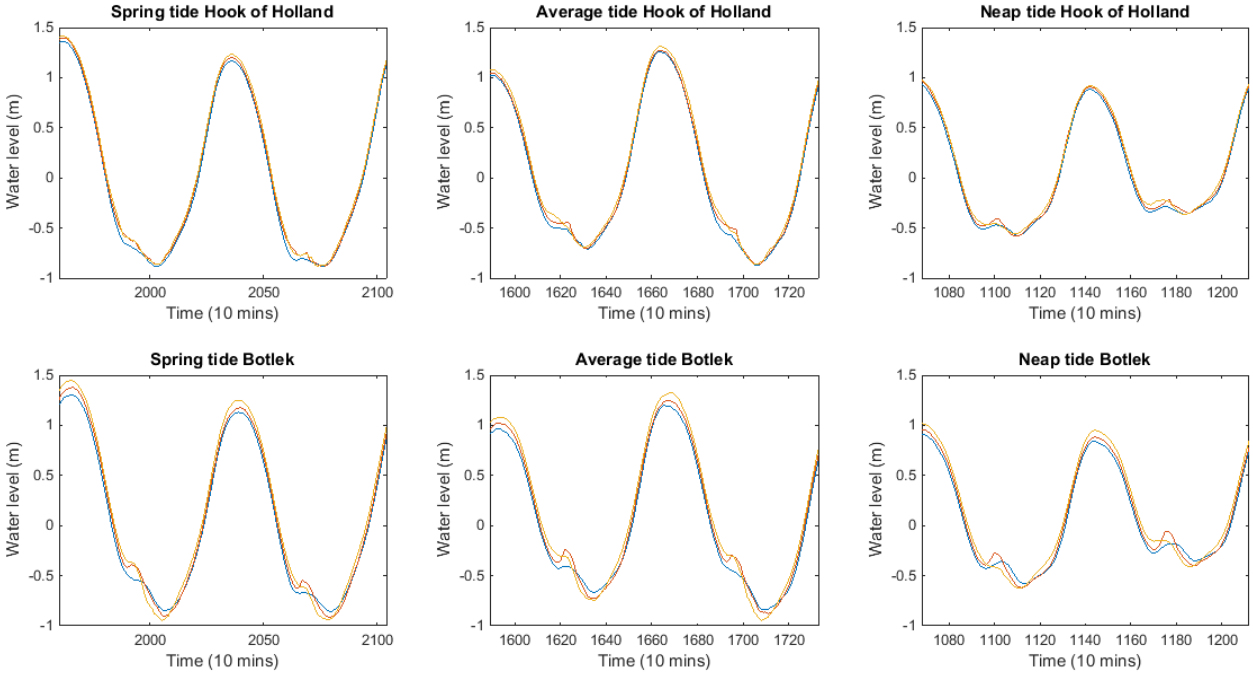

Figure 90 Water levels Hook of Holland and Maassluis discharge sensitivity with 5% discharge in blue, average discharge in orange and 95% discharge in yellow

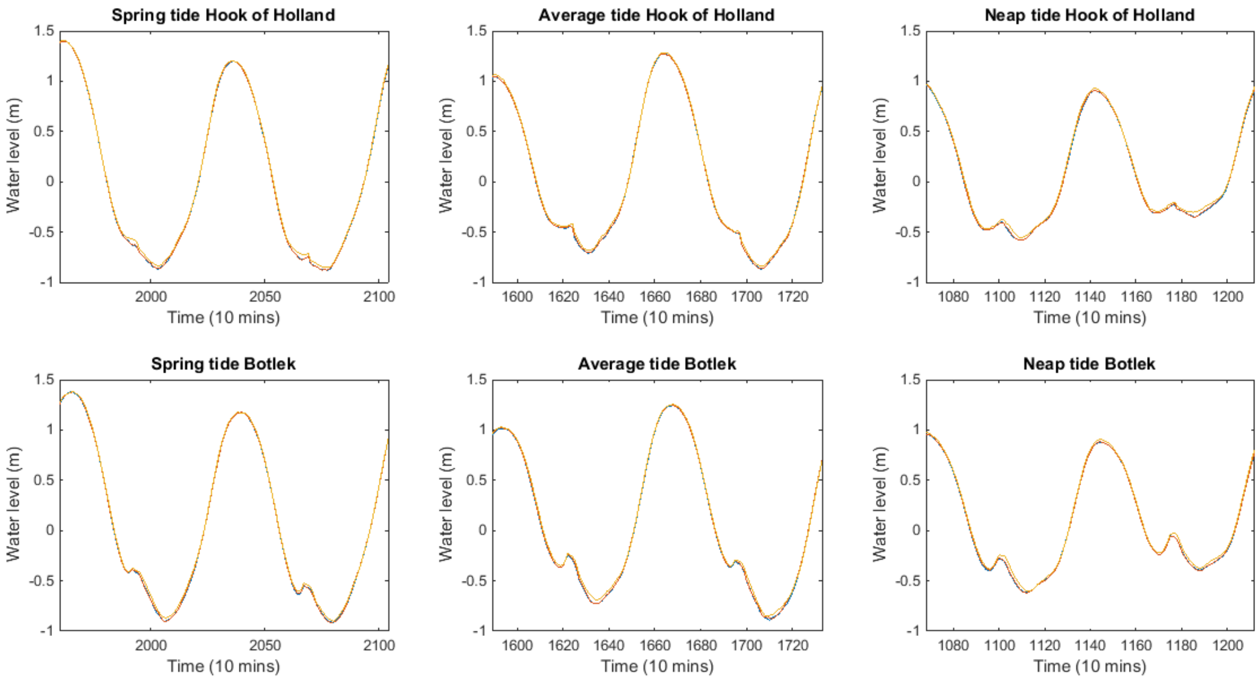

Figure 91 Water levels Hook of Holland and Maassluis discharge sensitivity with summer discharge in blue, average waves in orange and storm waves in yellow

C.2. Harbor Basin

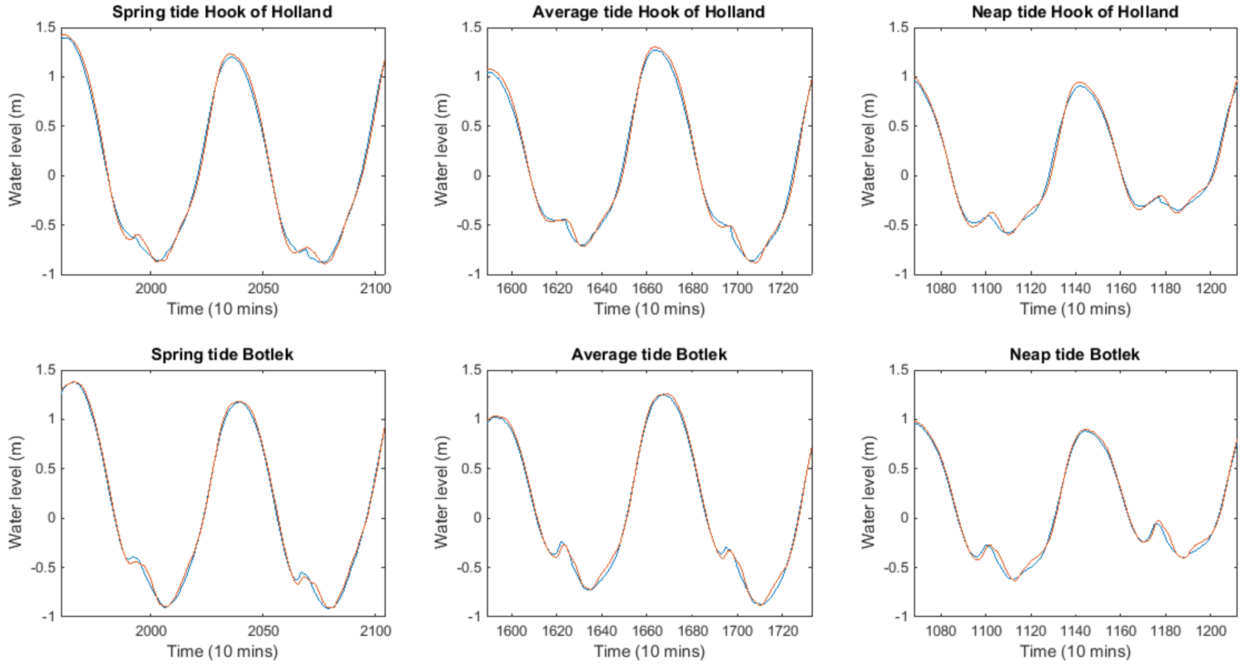

Figure 92 Water level reference scenario average conditions (in blue) and for the scenario including harbor basin (orange)

C.3. Step deepening

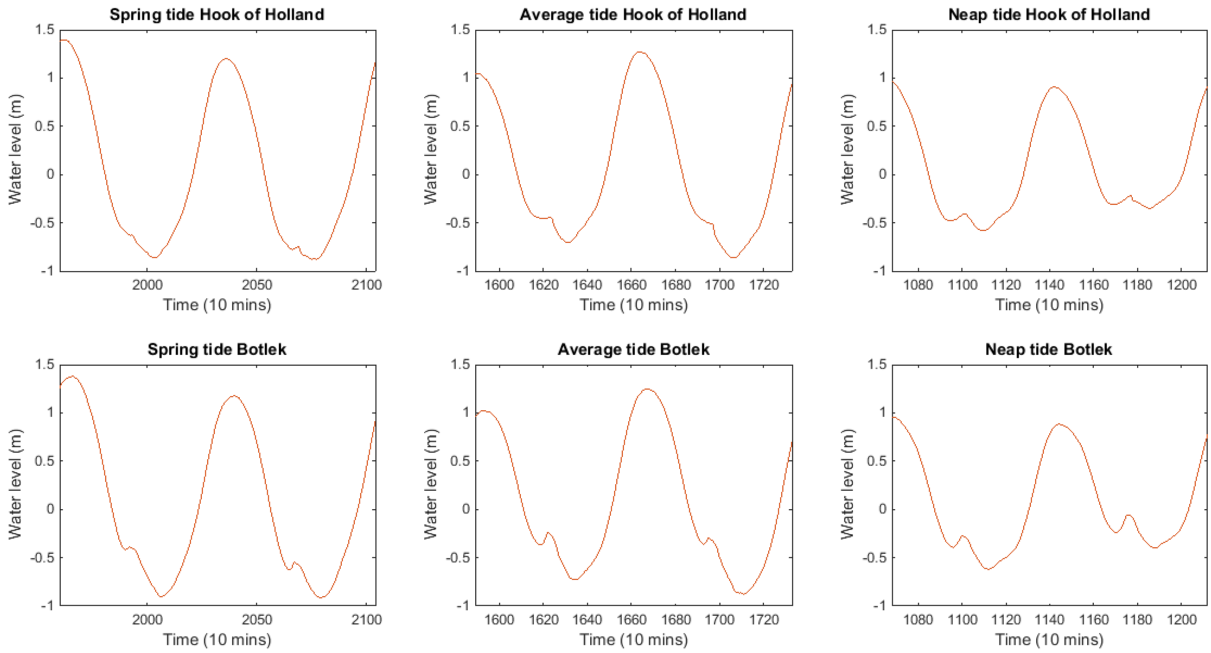

Figure 93 Water level average conditions for reference scenario (in blue) and step deepening scenario (in orange). The plot shows no blue line, meaning the water levels are exactly the same

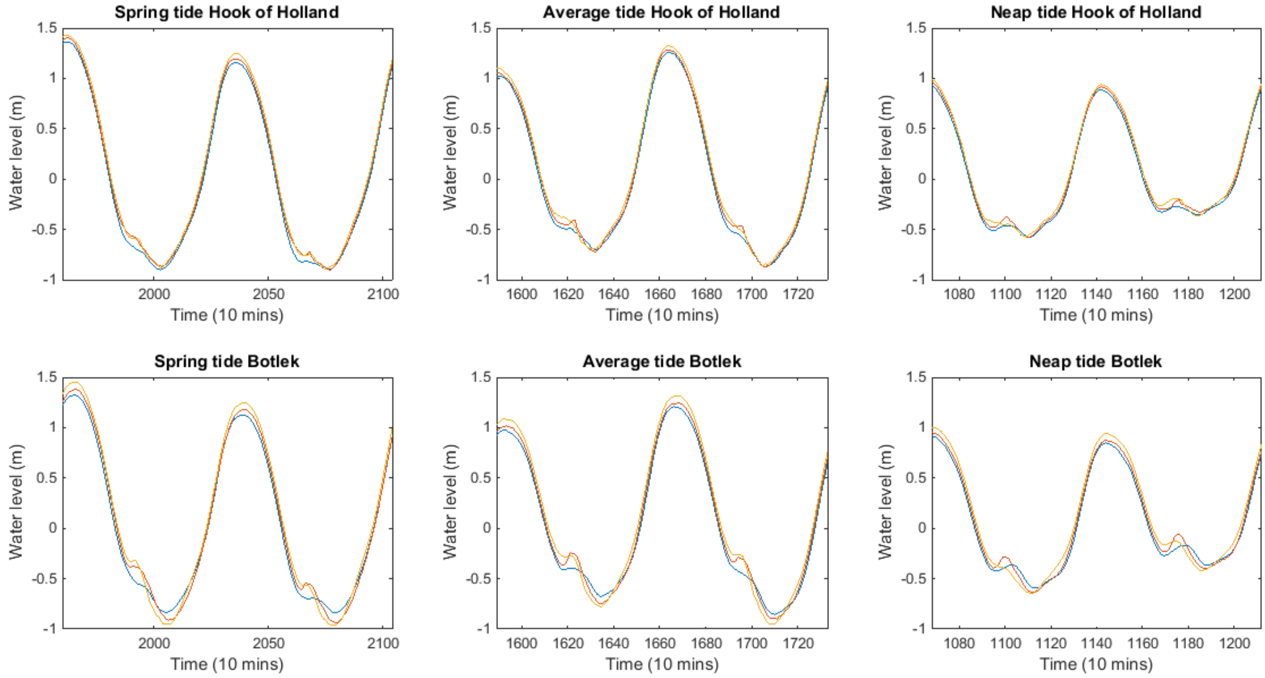

Figure 94 Water levels Hook of Holland and Maassluis for discharge sensitivity with 5% discharge in blue, average discharge in orange and 95% discharge in yellow for the step deepening scenario

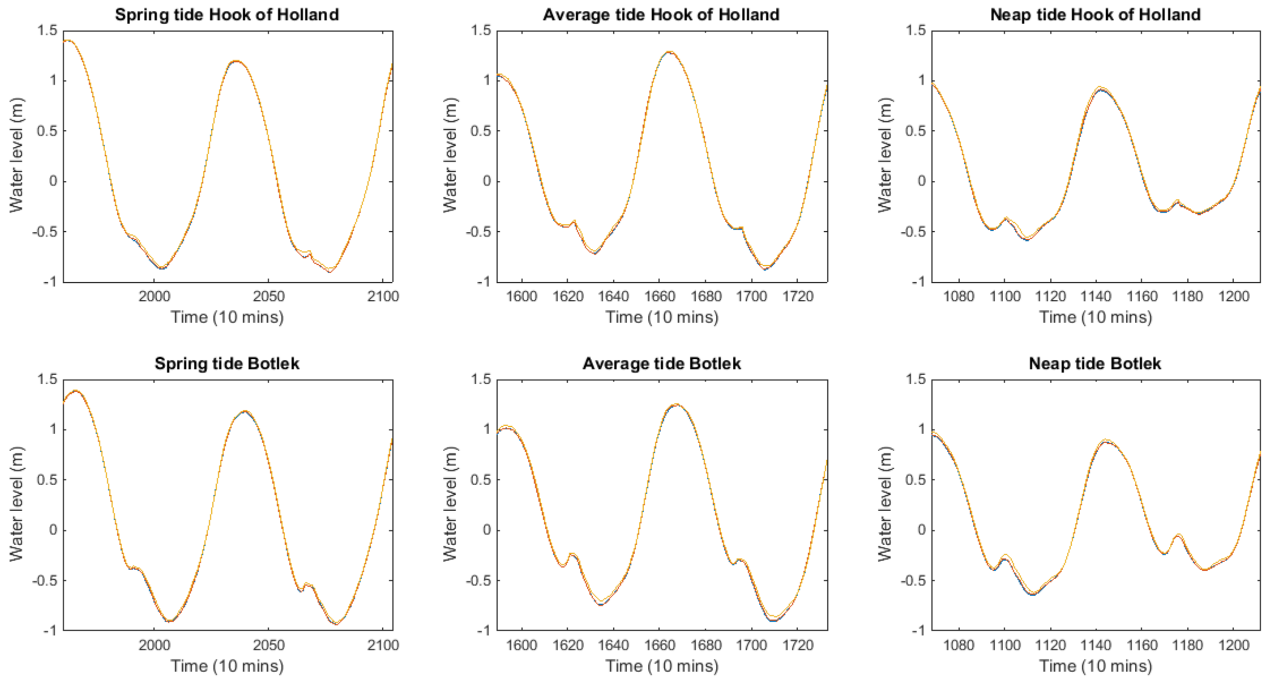

Figure 95 Water levels Hook of Holland and Maassluis discharge sensitivity with summer discharge in blue, average waves in orange and storm waves in yellow for the step deepening scenario

C.4. ETM deepening

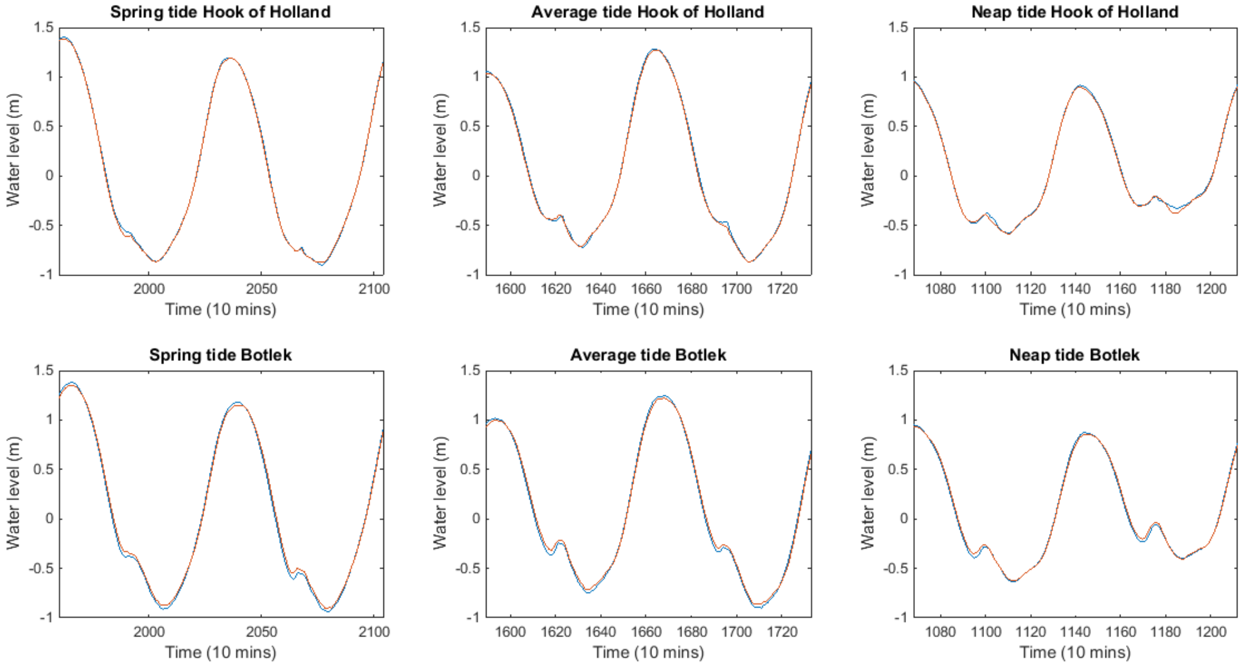

Figure 96 Water level average conditions for reference scenario (in blue) and step deepening scenario (in orange)

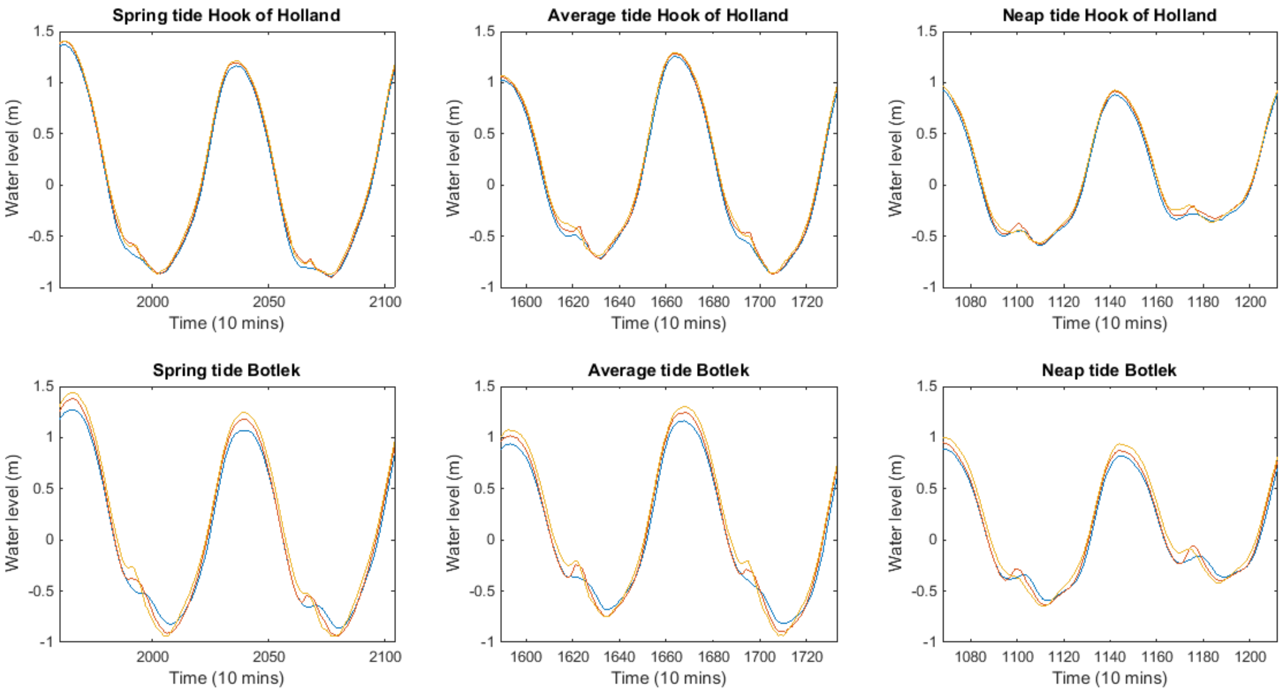

Figure 97 Water levels Hook of Holland and Maassluis discharge sensitivity with 5% discharge in blue, average discharge in orange and 95% discharge in yellow for the ETM deepened scenario

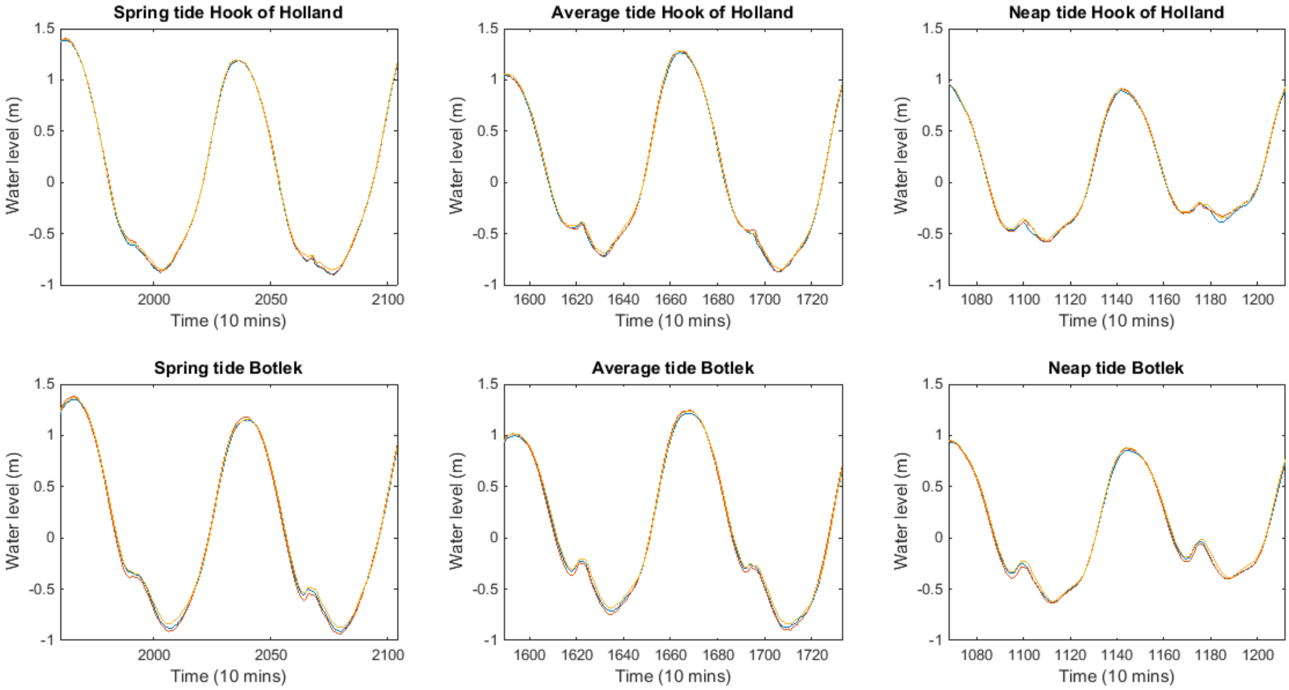

Figure 98 Water levels Hook of Holland and Maassluis discharge sensitivity with summer discharge in blue, average waves in orange and storm waves in yellow for the ETM deepenend scenario

D. Results reference boundary conditions

All plots of the results can of the reference boundary conditions can be found in this appendix. The reference scenario has a fresh water discharge boundary condition of 1350 m^3/s and an incoming wave height of 1.3 meters with a wave period of 4.48 seconds and an incoming wave angle of 205 degrees.

D.1 Summarized results

The results for the evolution of the ETM in time are summarized in Table 6. More details can be found in the plots for the different layers. The plots can be seen in chapter 11.2.2.

D.2 Plots of results ETM in time

Results after 4 weeks

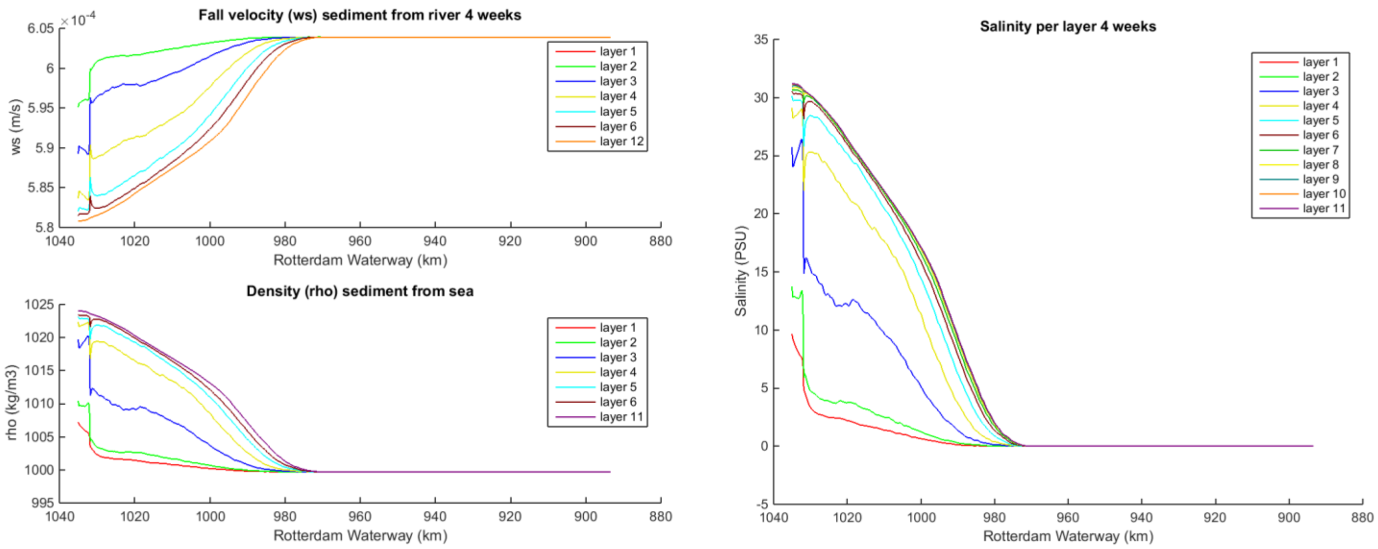

Figure 99 Fall velocity, density and salinity per layer

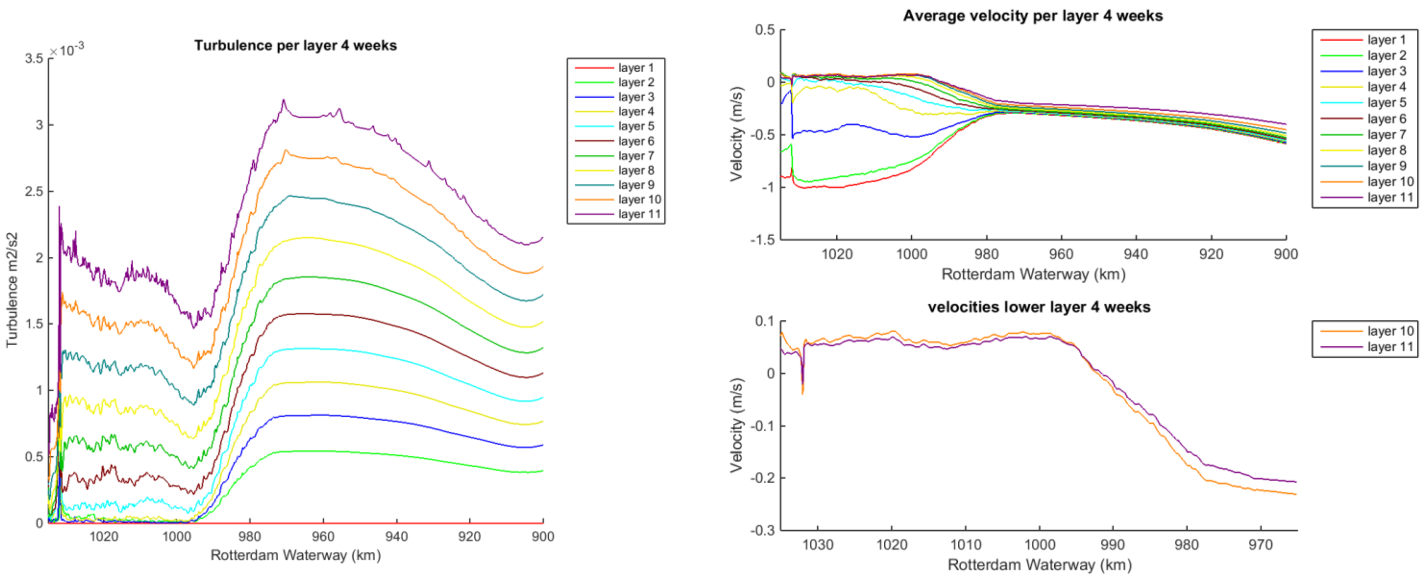

Figure 100 Turbulence, average velocity and velocity for lowest layers

Results after 6 weeks

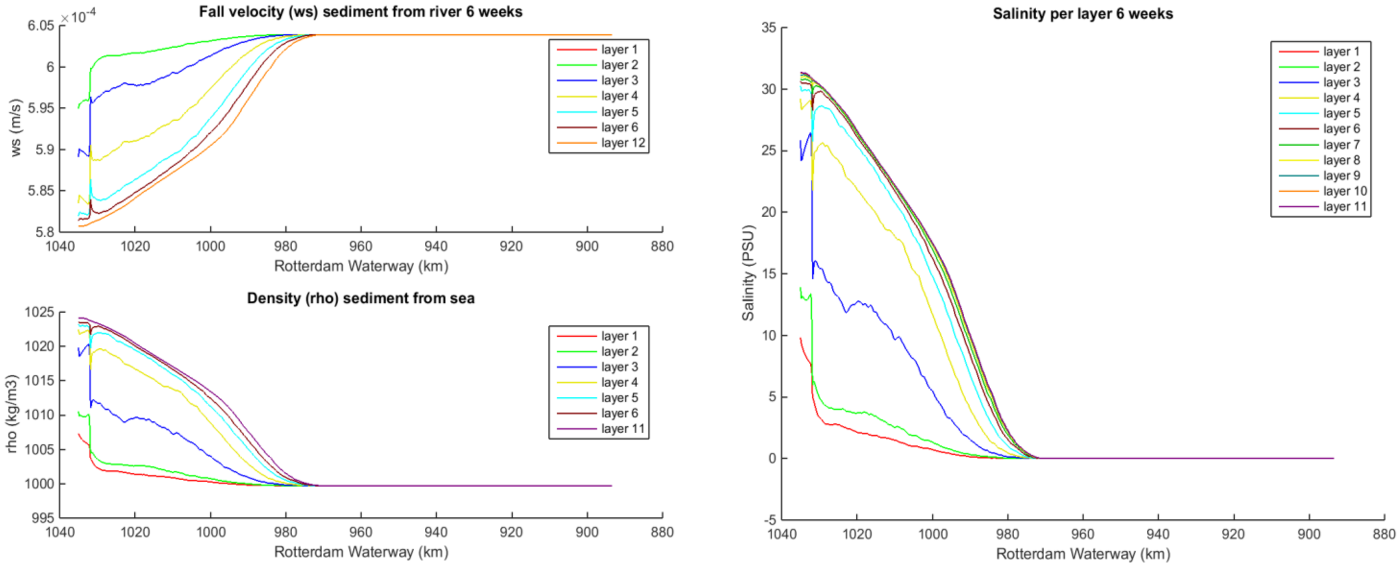

Figure 101 Fall velocity, density and salinity per layer for average discharge

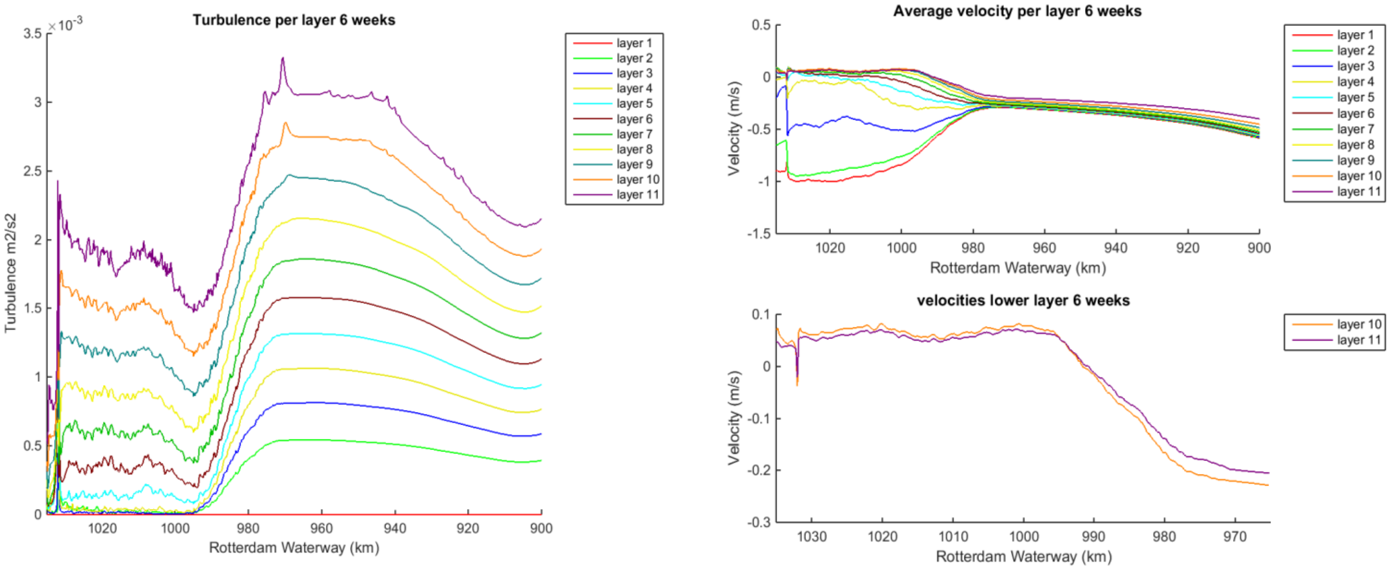

Figure 102 Turbulence in the Rotterdam Waterway on the left; Velocity per layer in the upper right figure; velocity profile of the nearbed layers in the lower right panel. Positive velocity indicates flood, a negative velocity indicates ebb

Results after 8 weeks

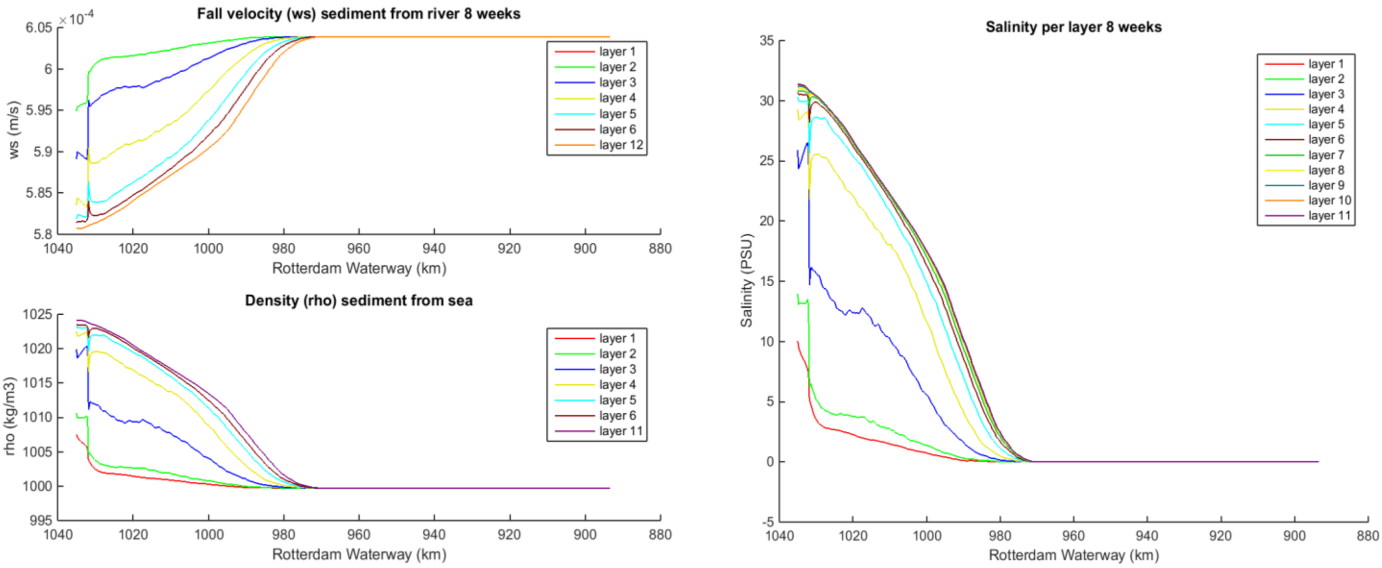

Figure 103 Fall velocity, density and salinity per layer for average discharge

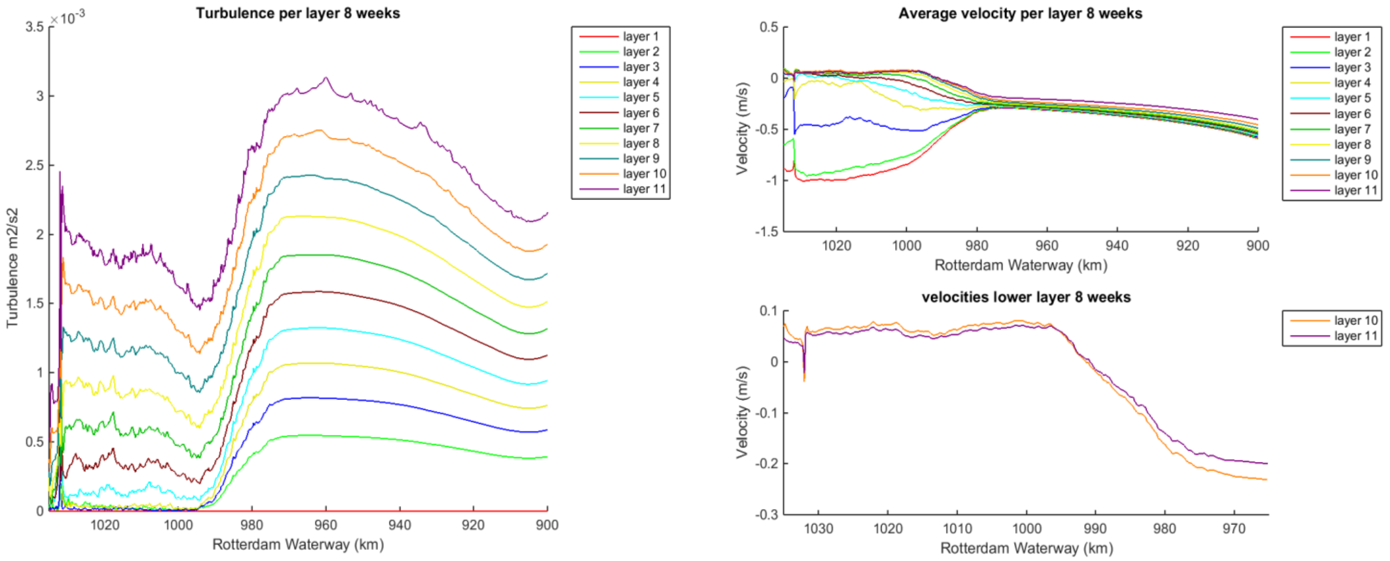

Figure 104 Turbulence in the Rotterdam Waterway on the left; Velocity per layer in the upper right figure; velocity profile of the nearb ed layers in the lower right panel. Positive velocity indicates flood, a negative velocity indicates ebb

Results after 10 weeks

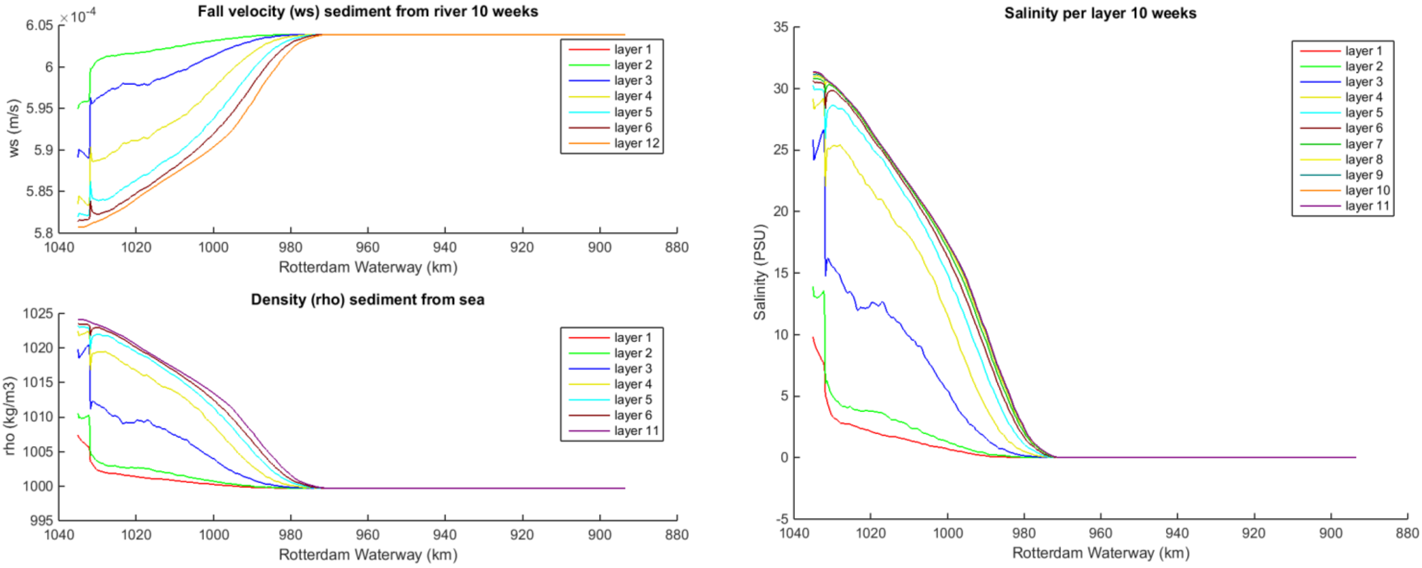

Figure 105 Fall velocity, density and salinity per layer for average discharge

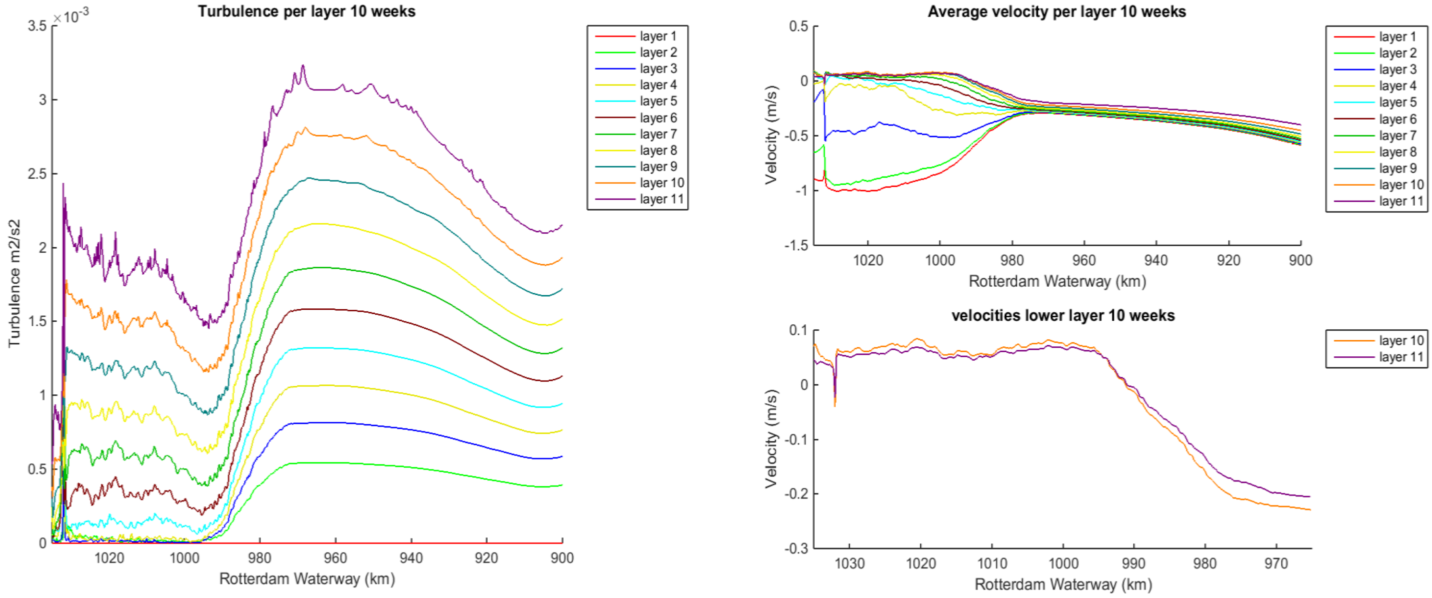

Figure 106 Turbulence in the Rotterdam Waterway on the left; Velocity per layer in the upper right figure; velocity profile of the nearb ed layers in the lower right panel. Positive velocity indicates flood, a negative velocity indicates ebb

Results after 12 weeks

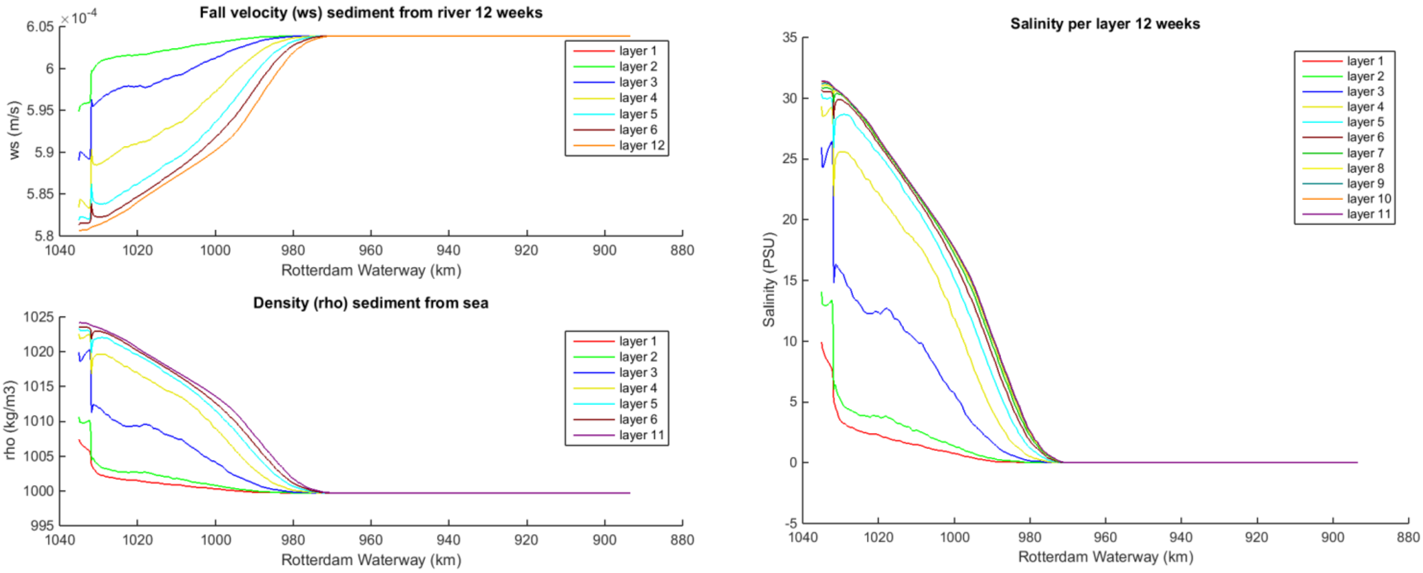

Figure 107 Fall velocity, density and salinity per layer for average discharge

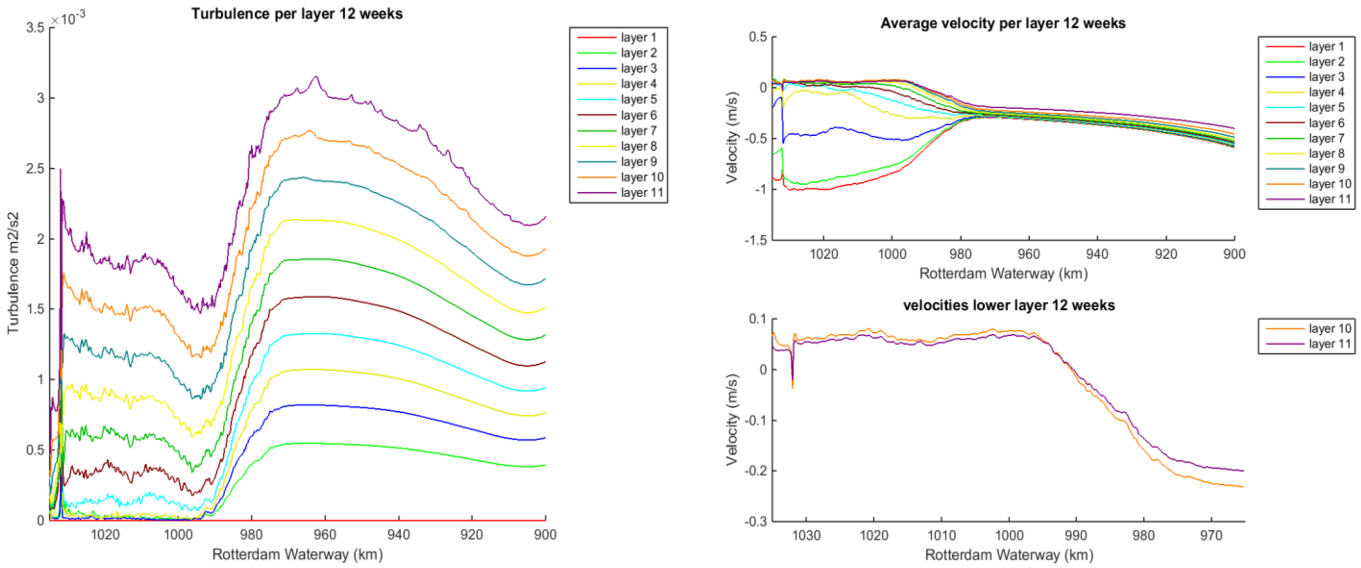

Figure 108 Turbulence in the Rotterdam Waterway on the left; Velocity per layer in the upper right figure; velocity profile of the nearbed layers in the lower right panel. Positive velocity indicates flood, a negative velocity indicates ebb

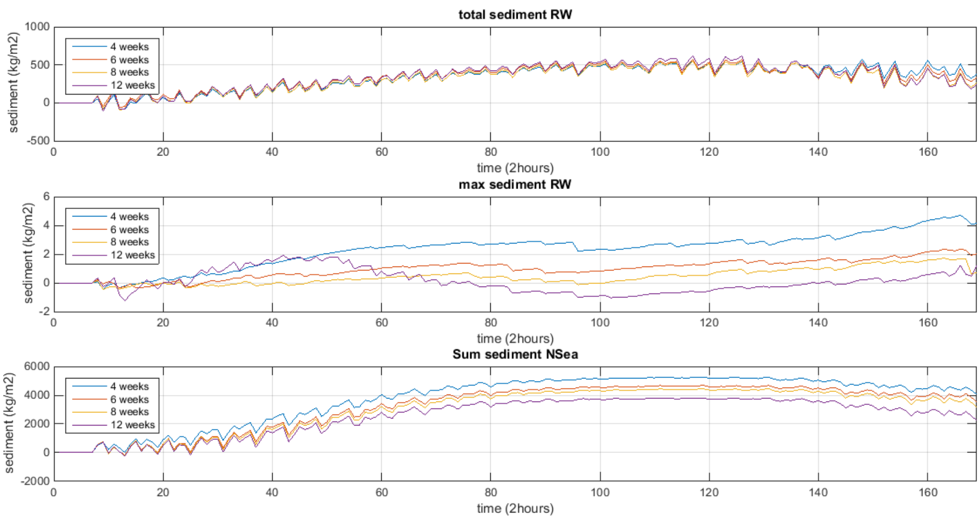

Figure 109 Growth of the sediment in bottom layer (upper panel); The growth of the peak of the ETM (middle panel); Growth of sediment at North Sea (bottom panel)

D.3 Plots of results changing discharge boundary

The plots for the different fresh water boundary discharges in this appendix are from the initial change (with a run up of 4 weeks) and the long term change (with a run up of 12 weeks).

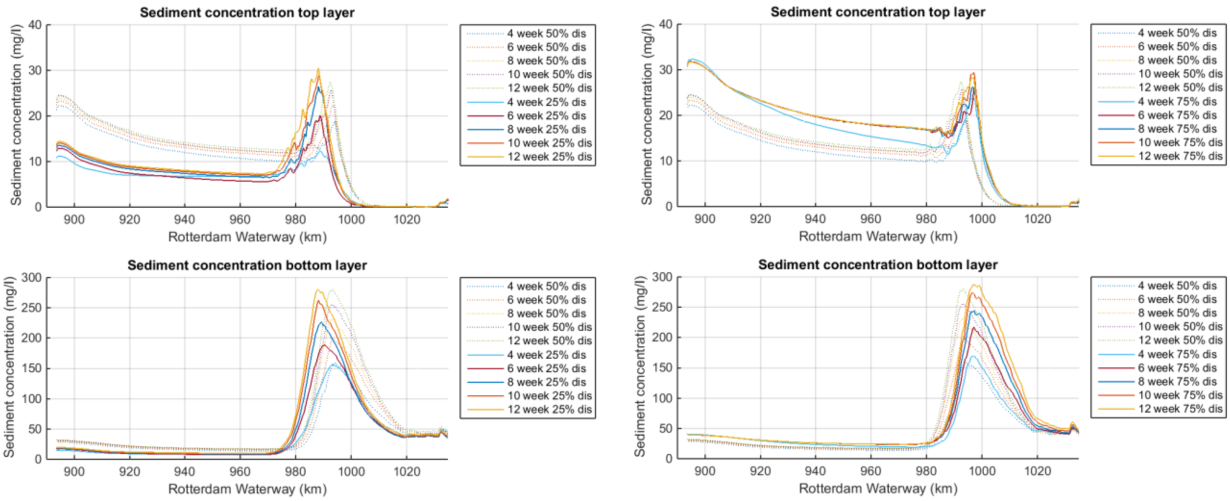

Figure 110 Bottom sediment in time for 25% discharge left and 75% discharge right

D.3.1 5% discharge

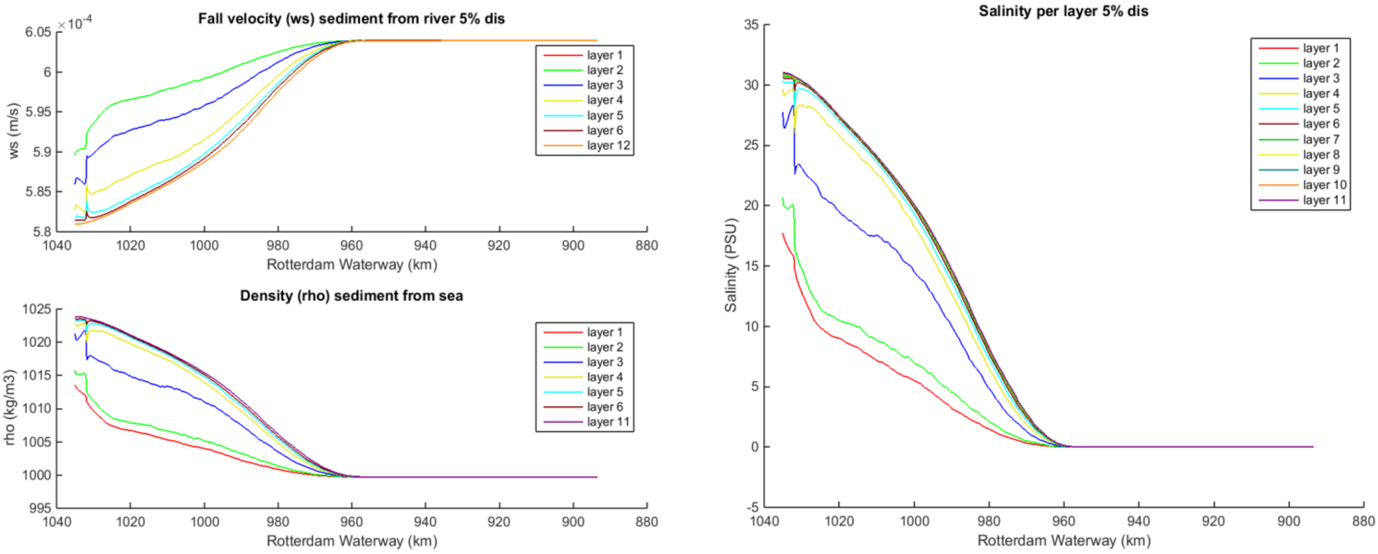

Figure 111 Fall velocity and density (left panels) and salinity for 5% discharge (right)

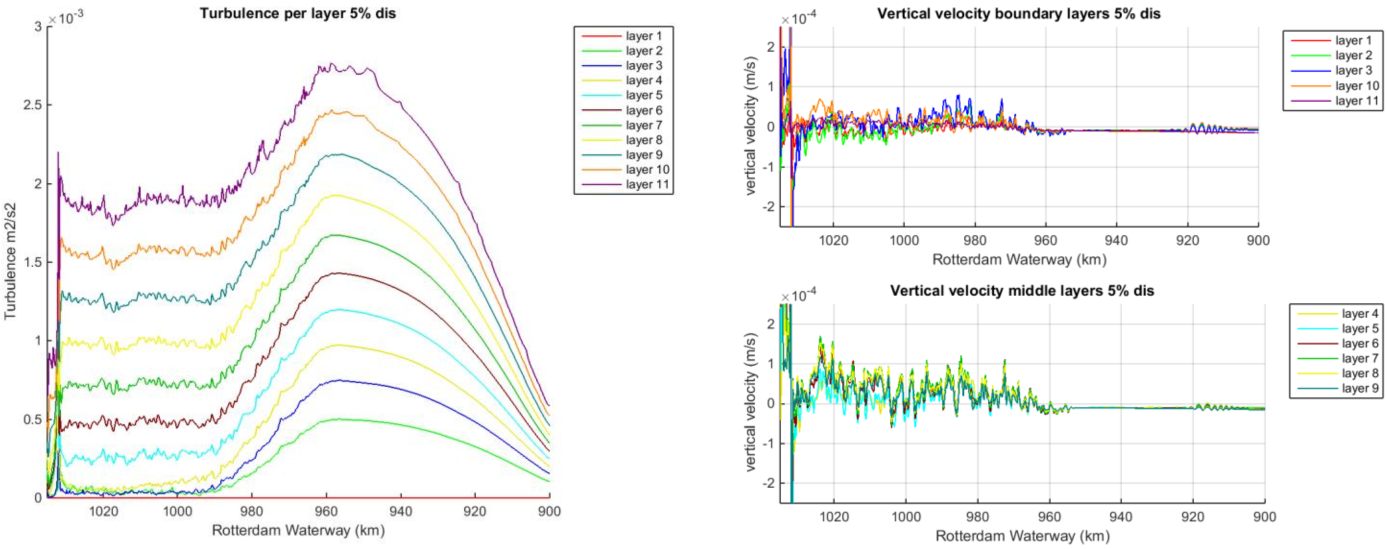

Figure 112 Turbulence (left) and vertical velocity for boundary layers and middle layers for 5% discharge

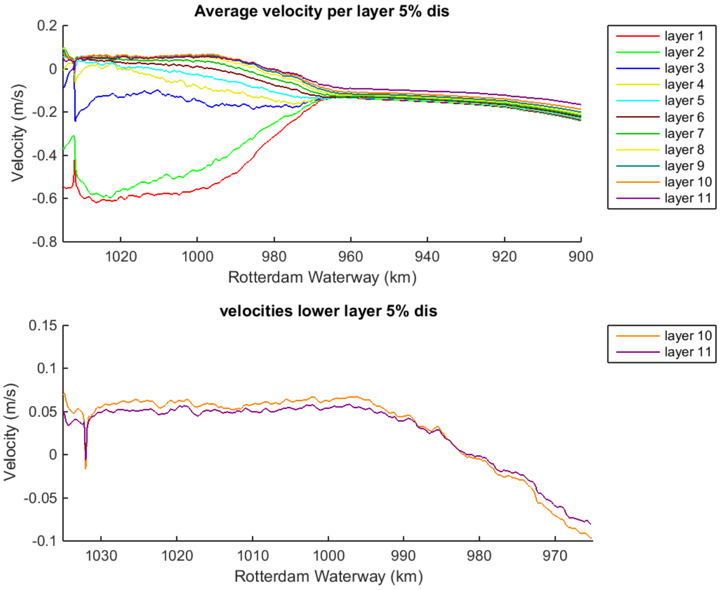

Figure 113 Average velocity per layer for 5% discharge (upper panel) and lowest two layers (lower panel)

D.3.2 25% discharge

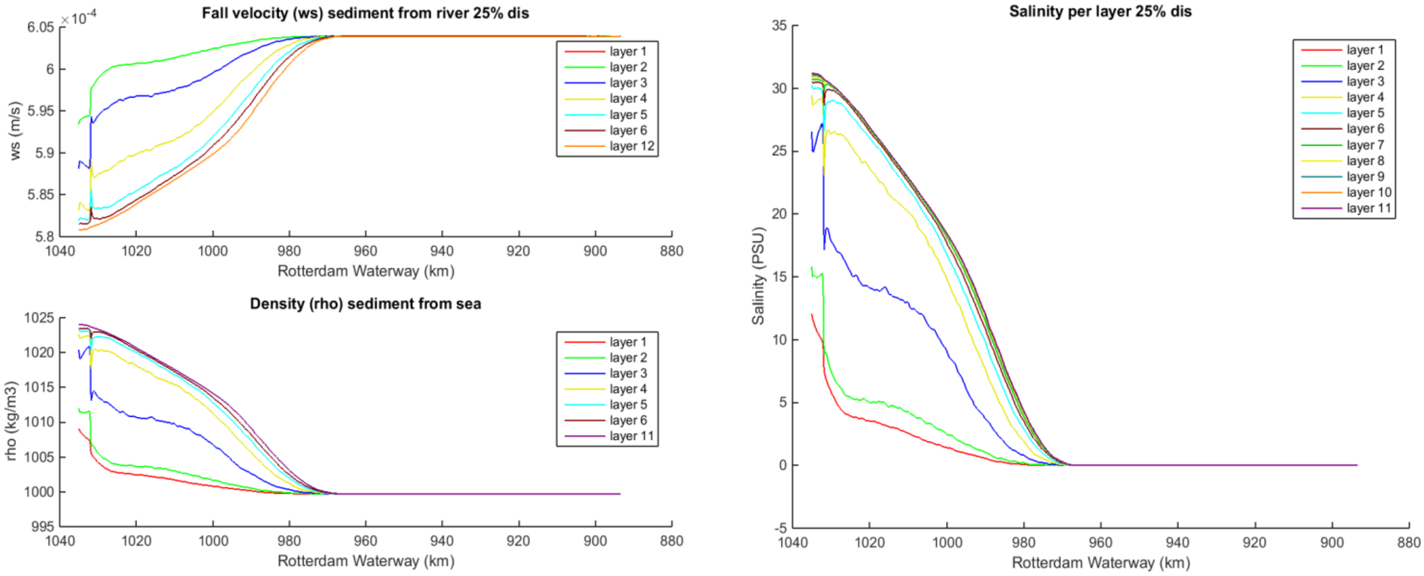

Figure 114 Fall velocity and density (left panels) and salinity for 25% discharge (right)

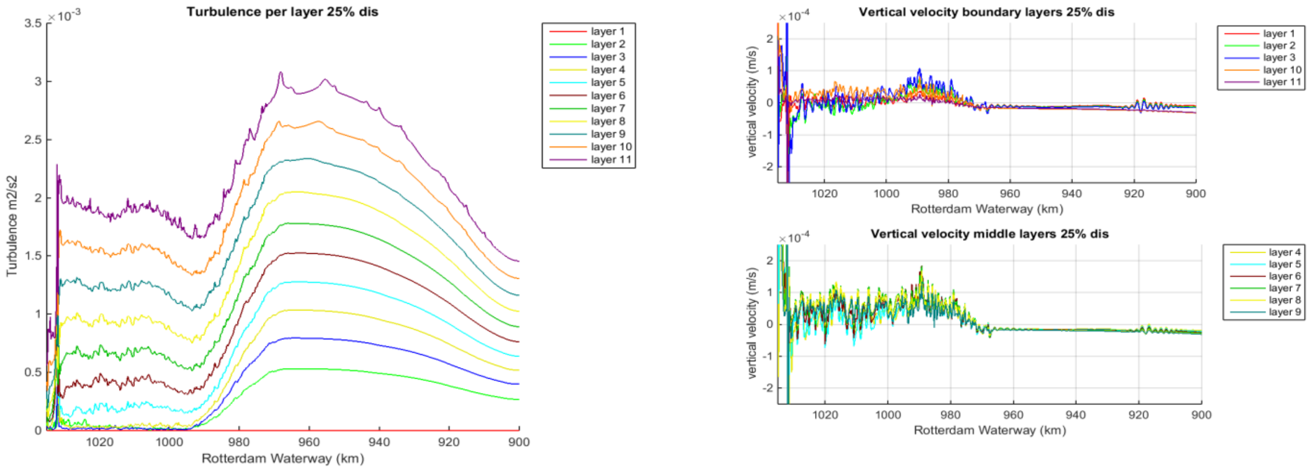

Figure 115 Turbulence (left) and vertical velocity for boundary layers and middle layers for 25% discharge

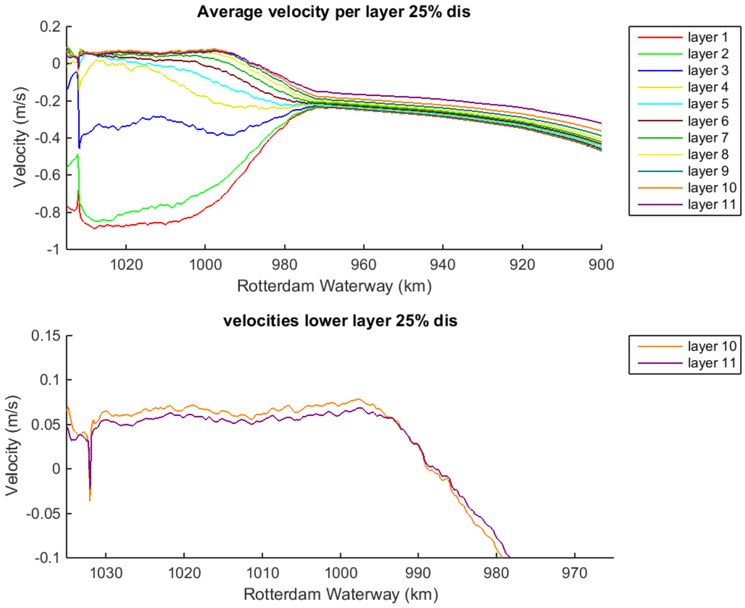

Figure 116 Average velocity per layer for 25% discharge (upper panel) and lowest two layers (lower panel)

D.3.3 75% discharge

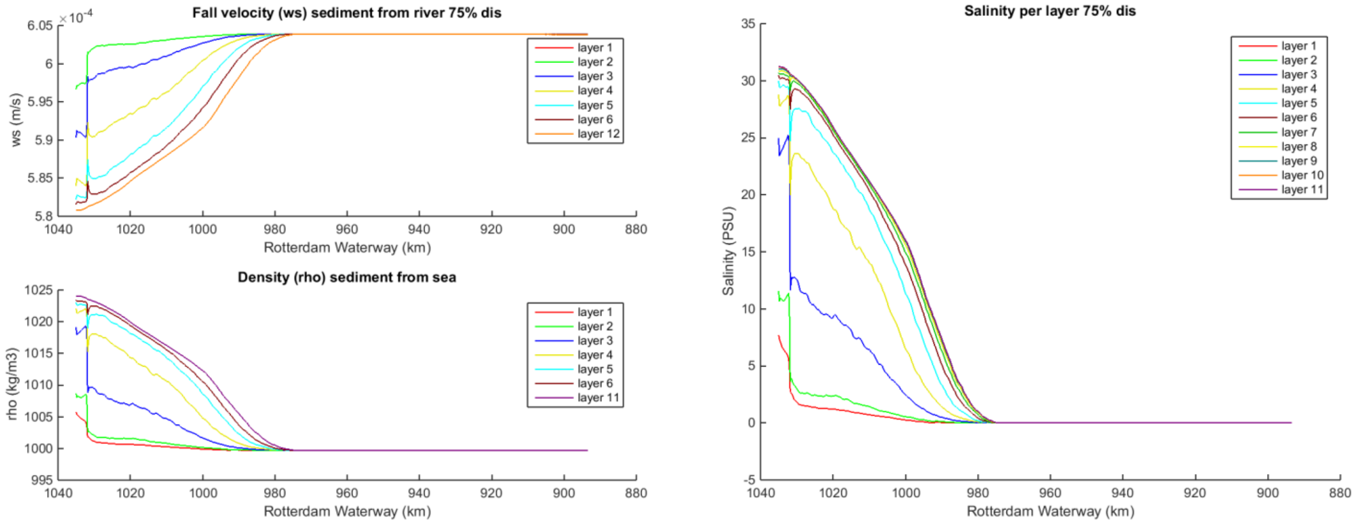

Figure 117 Fall velocity and density (left panels) and salinity for 75% discharge (right)

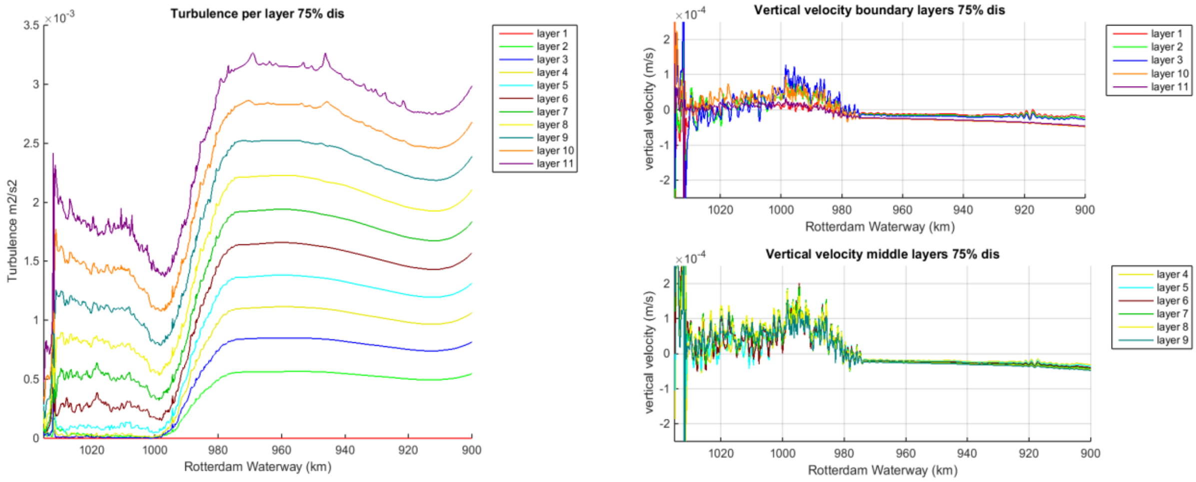

Figure 118 Turbulence (left) and vertical velocity for boundary layers and middle layers for 75% discharge

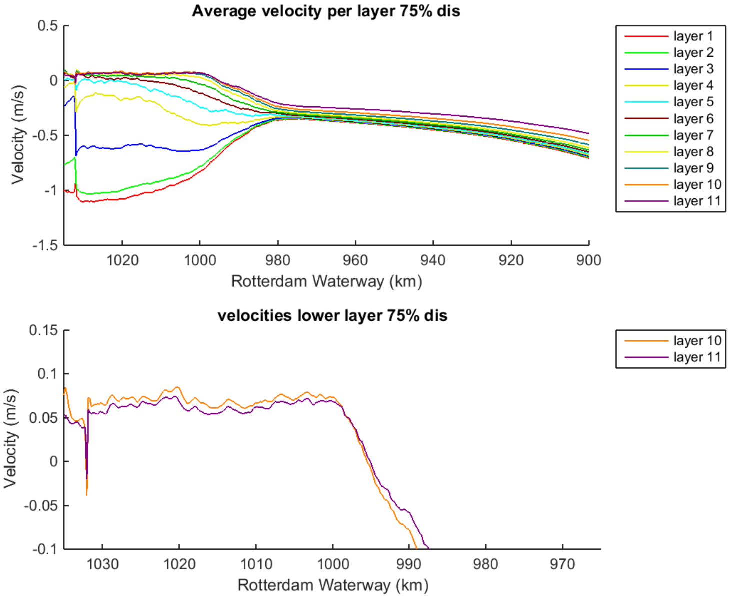

Figure 119 Average velocity per layer for 75% discharge (upper panel) and lowest two layers (lower panel)

D.3.4 95% discharge

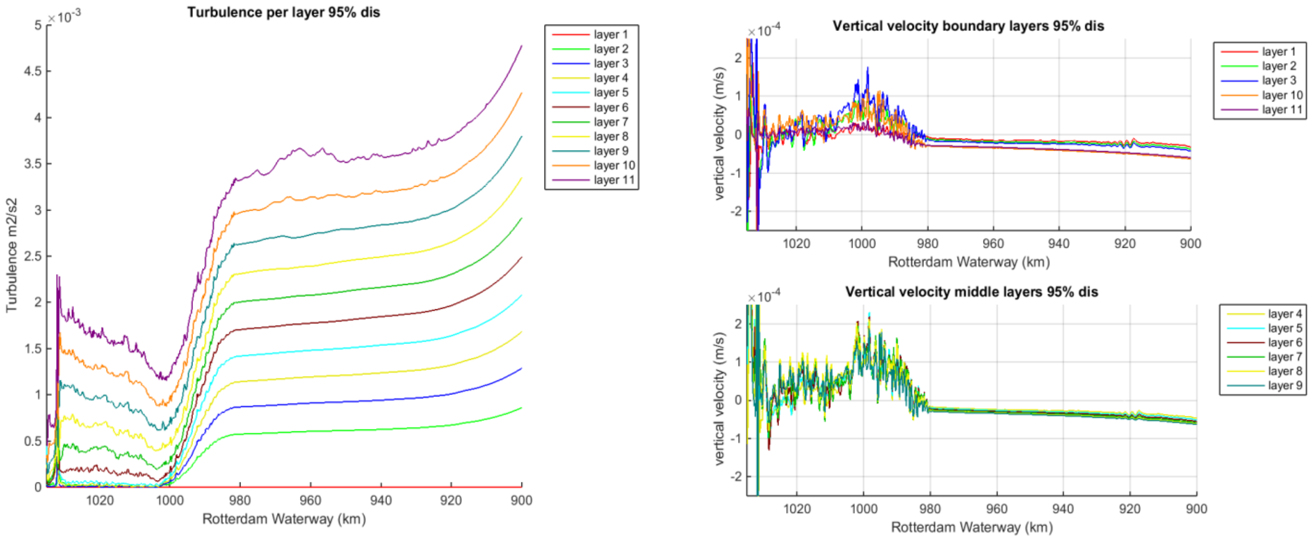

Figure 120 Turbulence (left) and vertical velocity for boundary layers and middle layers for 95% discharge

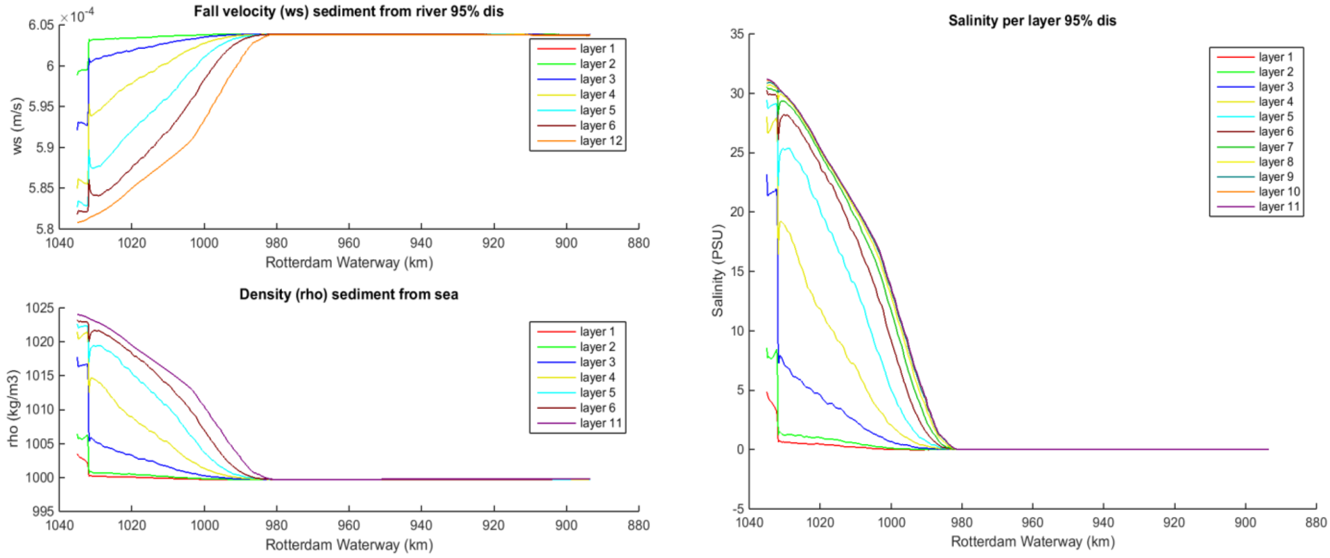

Figure 121 Fall velocity and density (left panels) and salinity for 95% discharge (right)

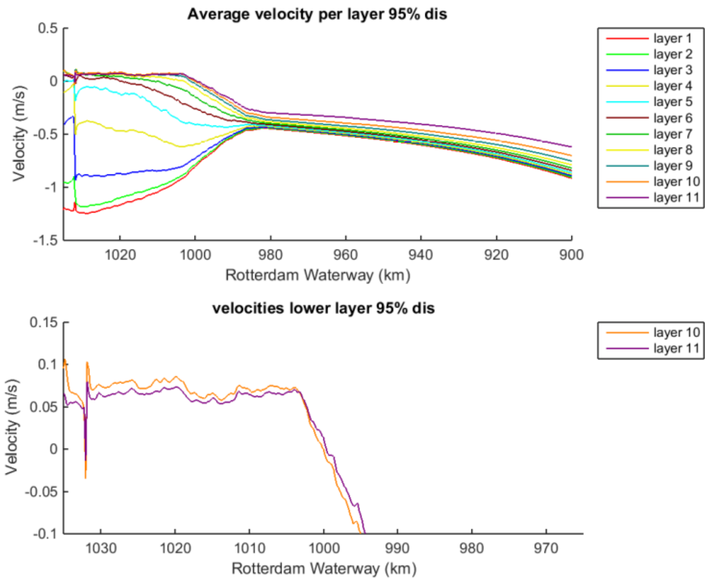

Figure 122 Average velocity per layer for 95% discharge (upper panel) and lowest two layers (lower panel)

D.4 Plots of results changing wave boundary

The plots for the different fresh water boundary discharges in this appendix are from the initial change (with a run up of 4 weeks).

D.4.1 Summer waves

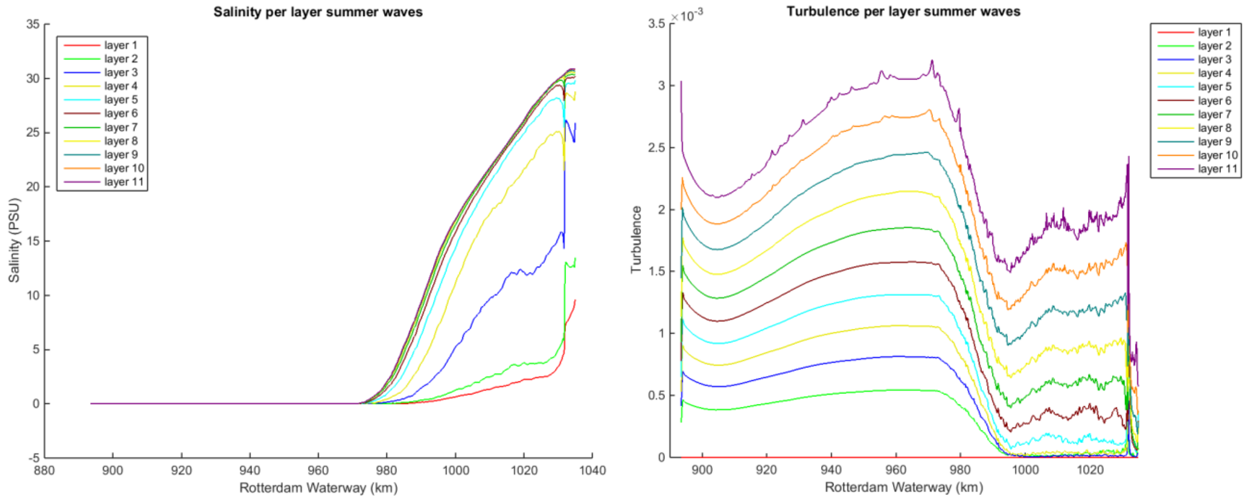

Figure 123 Salinity (left) and turbulence (right) for summer waves

D.4.2 Winter waves

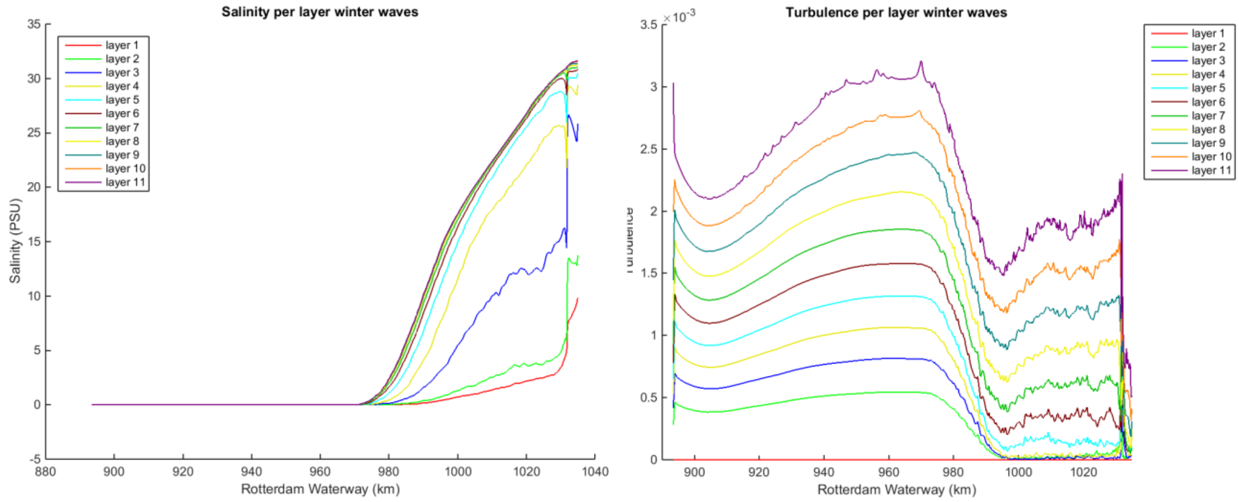

Figure 124 Salinity (left) and turbulence (right) for winter waves

D.4.3 Storm waves

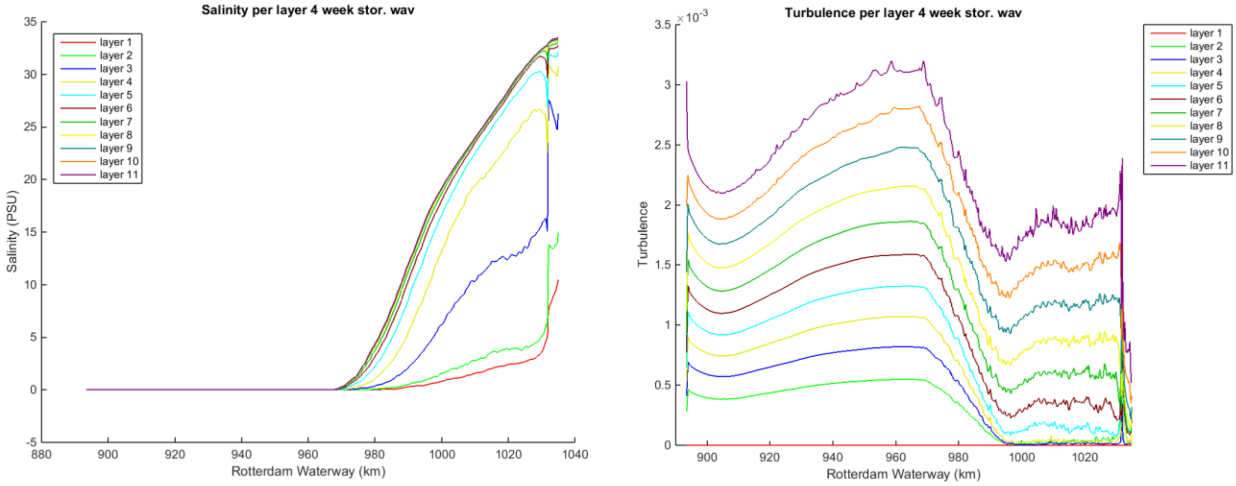

Figure 125 Salinity (left) and turbulence (right) for storm

D.5 Sediment in bottom

Figure 126 shows the available sediment of the sum of MUD and MUD2 in the active top layer in the Rotterdam Waterway. Large availability means a lot of sediment is available for the ETM. A large availability indirect indicates a large concentration of suspended sediment in the water column on top, especially if the peak in sediment concentration in the bottom layer is narrow and high.

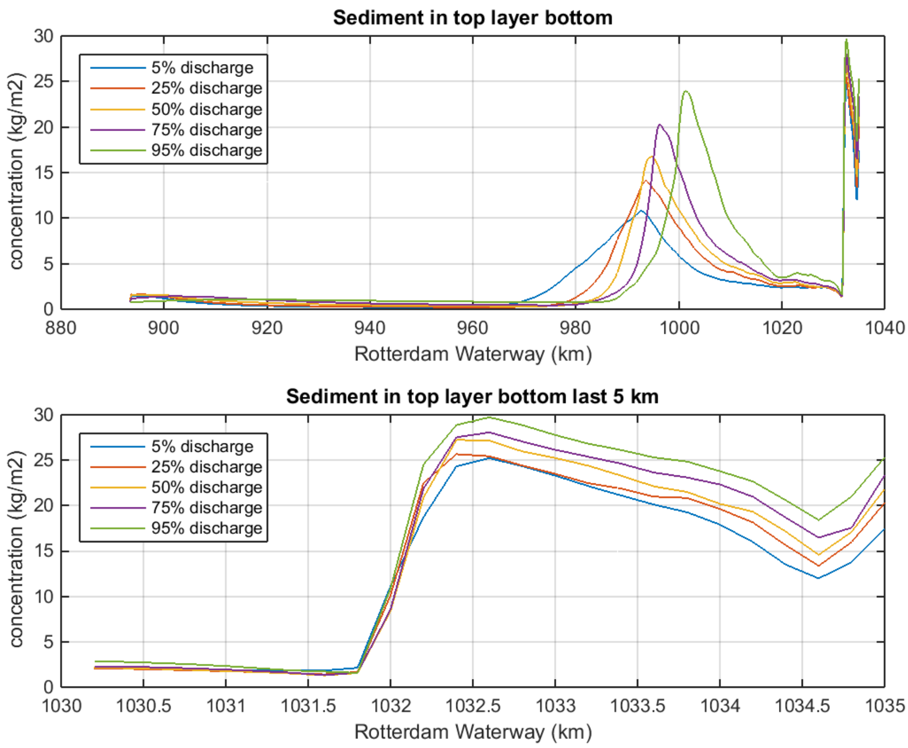

Figure 126 Available sediment in top layer of the bottom after 4 weeks

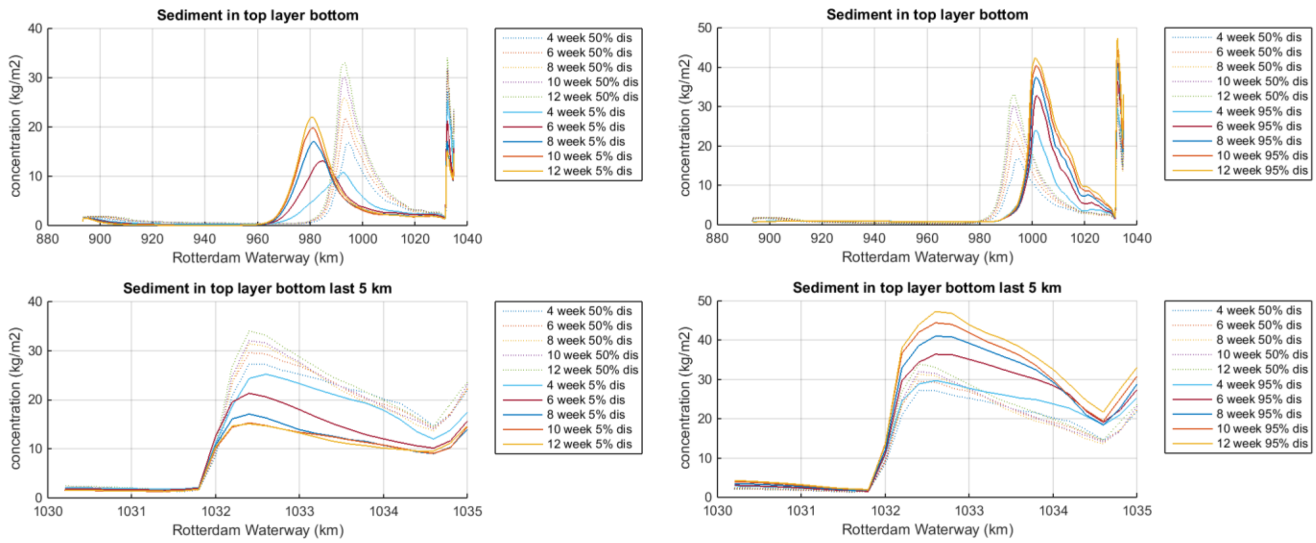

Figure 127 Fine sediment concentration in top layer bottom for 5% discharge (left panel) and 95% discharge (right panel)

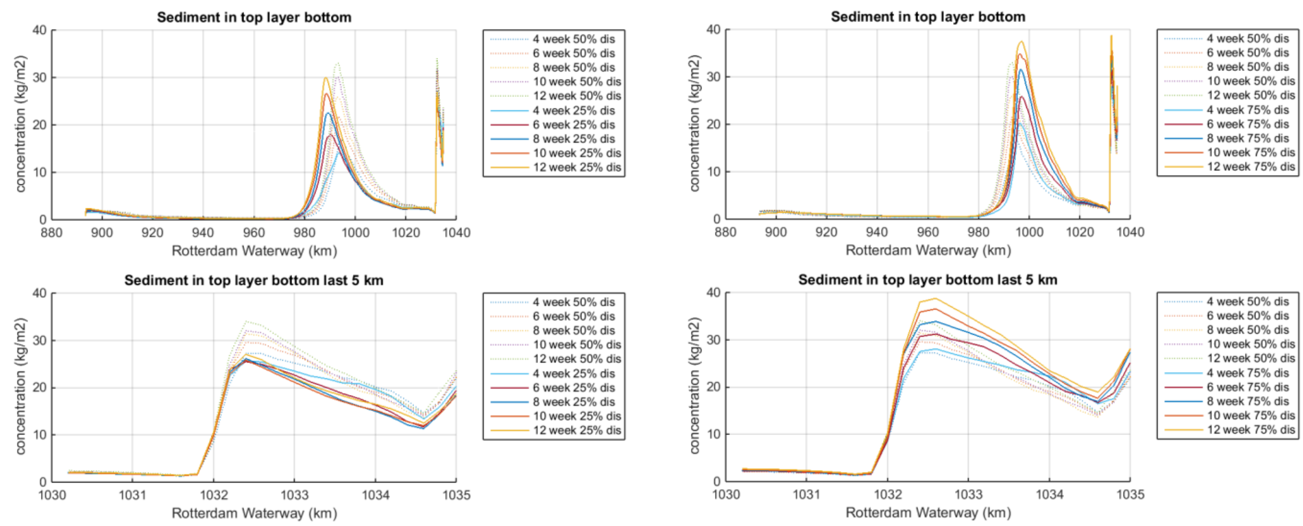

Figure 128 Fine sediment concentration in top layer bottom for 25% discharge (left panel) and 75% discharge (right panel)

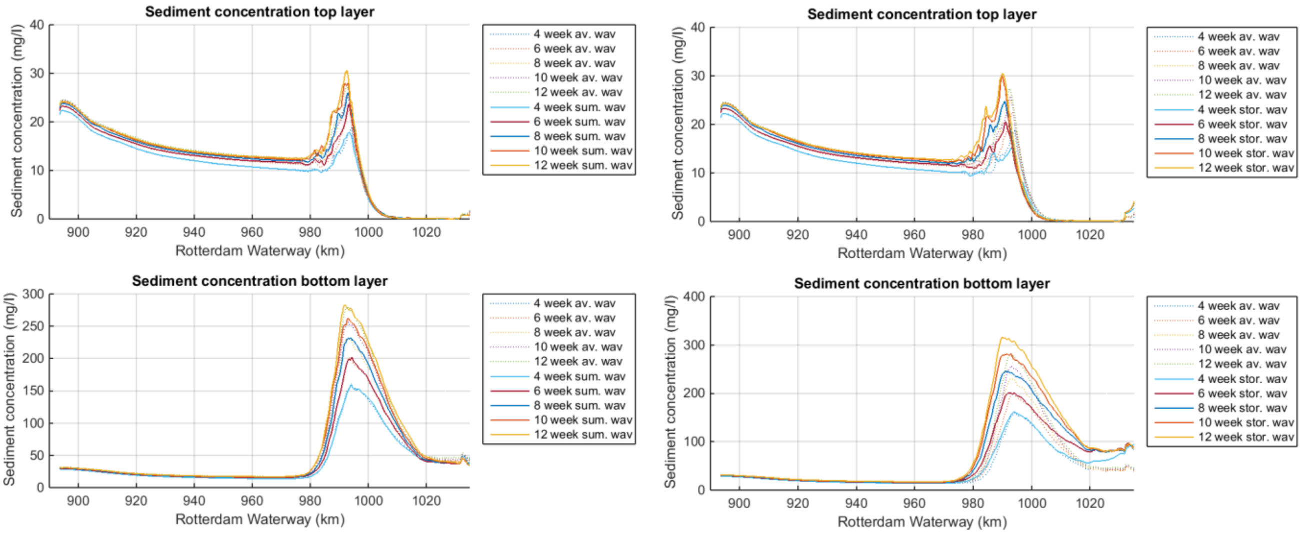

Figure 129 Fine sediment concentration for summer waves (left panel) and storm waves (right panel)

E. Results harbor basins

Plots of the hydrodynamic conditions of the simulations including harbor basins are shown in this appendix.

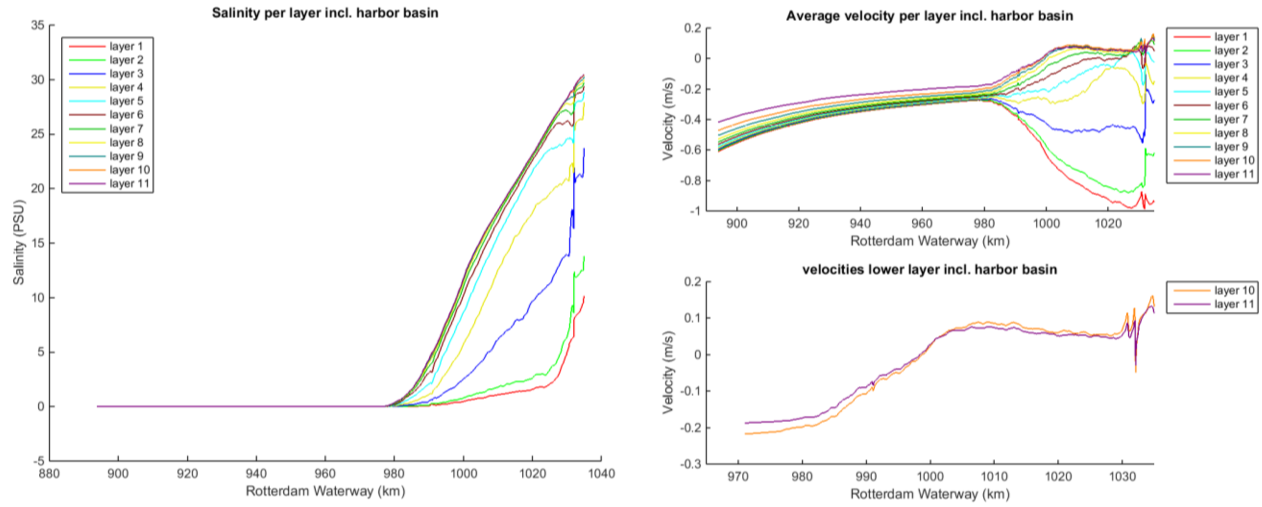

Figure 130 Salinity of the Rotterdam Waterway (left); averaged velocity (right)

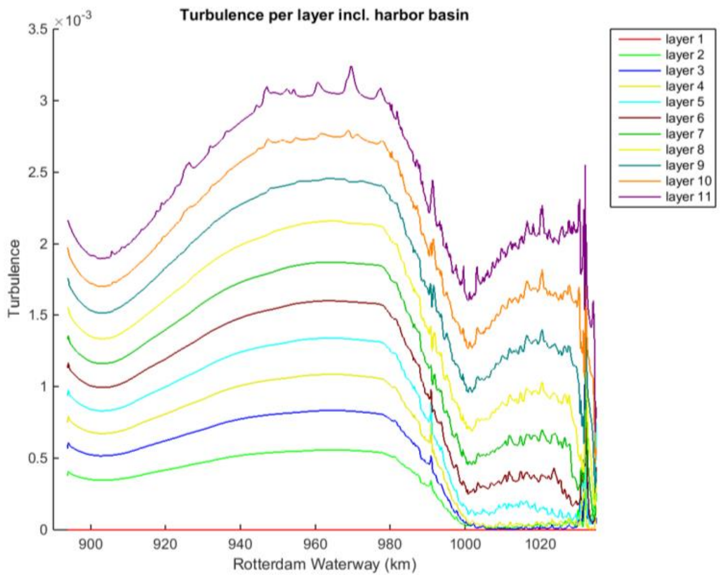

Figure 131 Turbulence per layer for study area including harbor basins

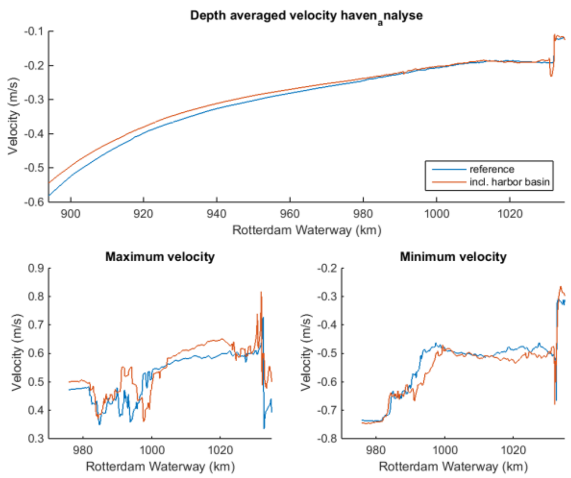

Figure 132 Depth averaged velocity (upper panel); average flood and ebb velocity (lower panel)

F. Results deepening

F.1 Deepening of the step

F.1.1 Hydrodynamics

The change between the average velocity and the step deepening scenario can be seen in Figure 133, Figure 134 and Figure 135.

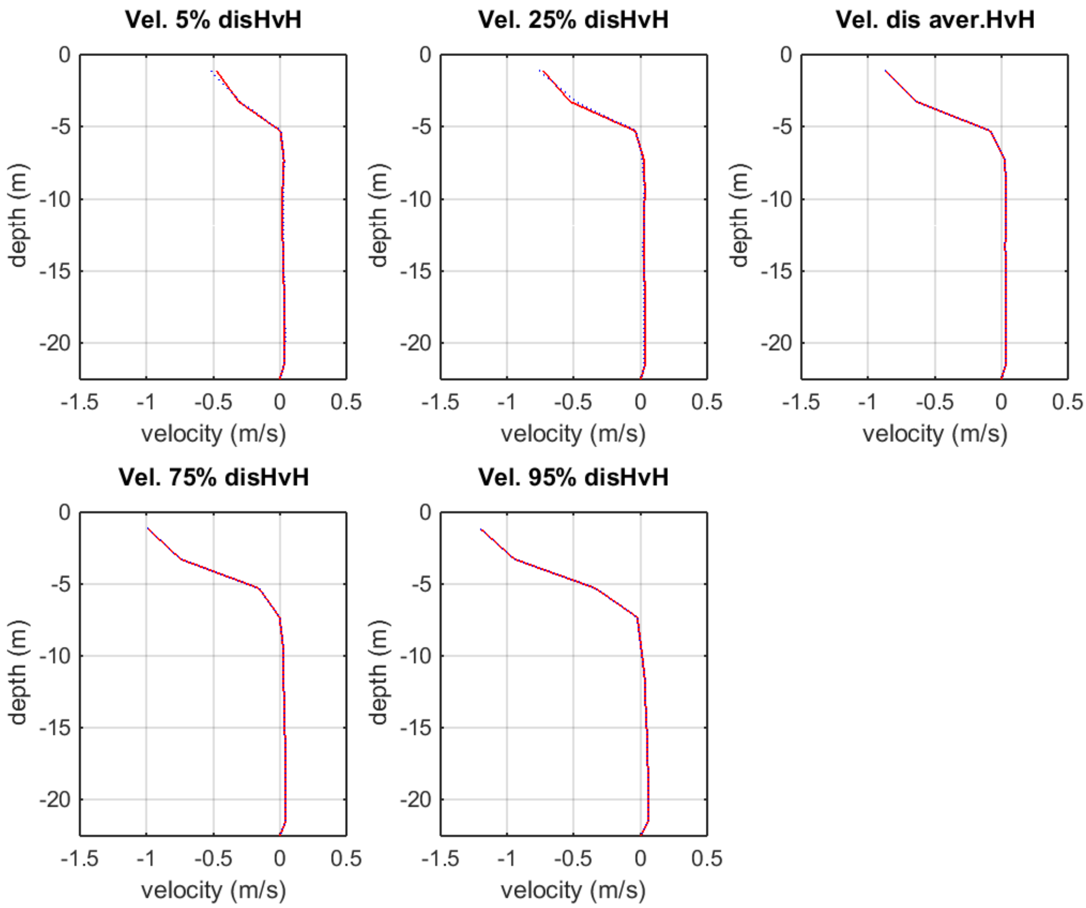

Figure 133 Change in velocity due to changing discharge for the reference scenario (dashed blue line) with the step deepening scenario (in red)

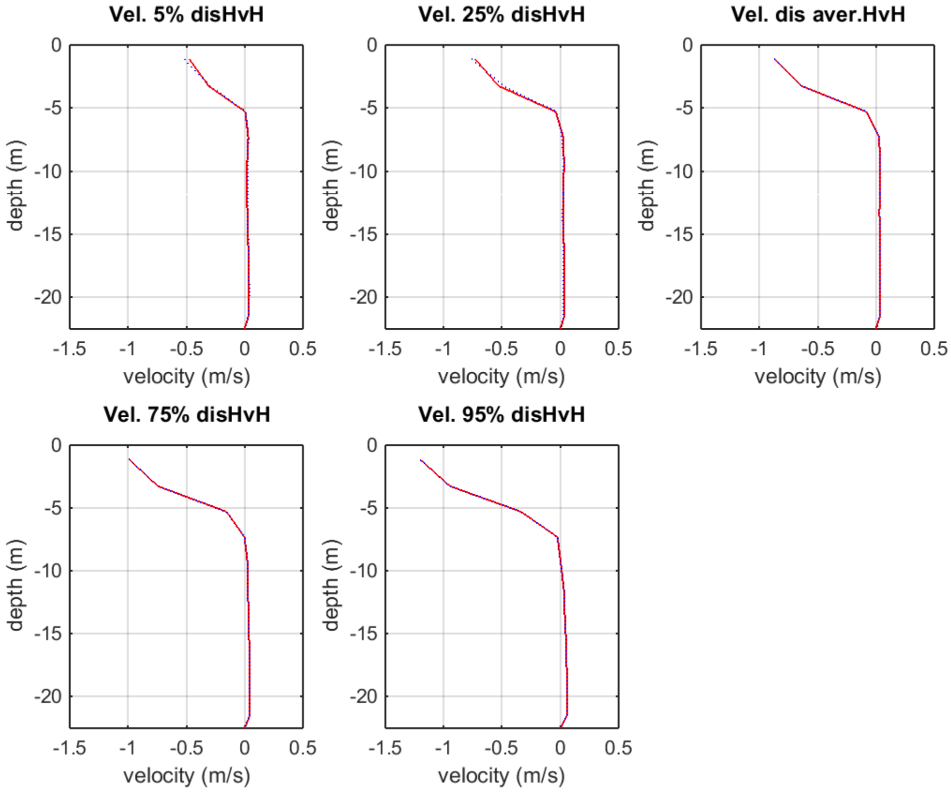

Figure 134 Change in velocity due to changing discharge for the reference scenario (dashed blue line) with the step deepening scenario (in red)

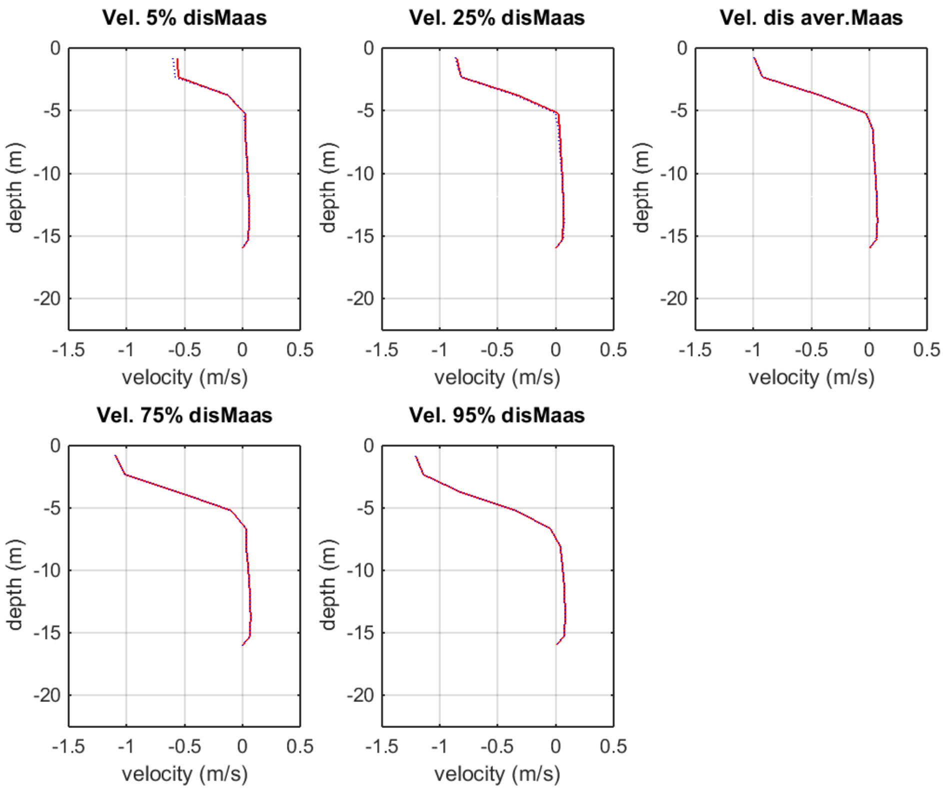

Figure 135 Change in velocity due to changing discharge for the reference scenario (dashed blue line) with the step deepening scenario (in red)

F.1.1.1. 5% discharge

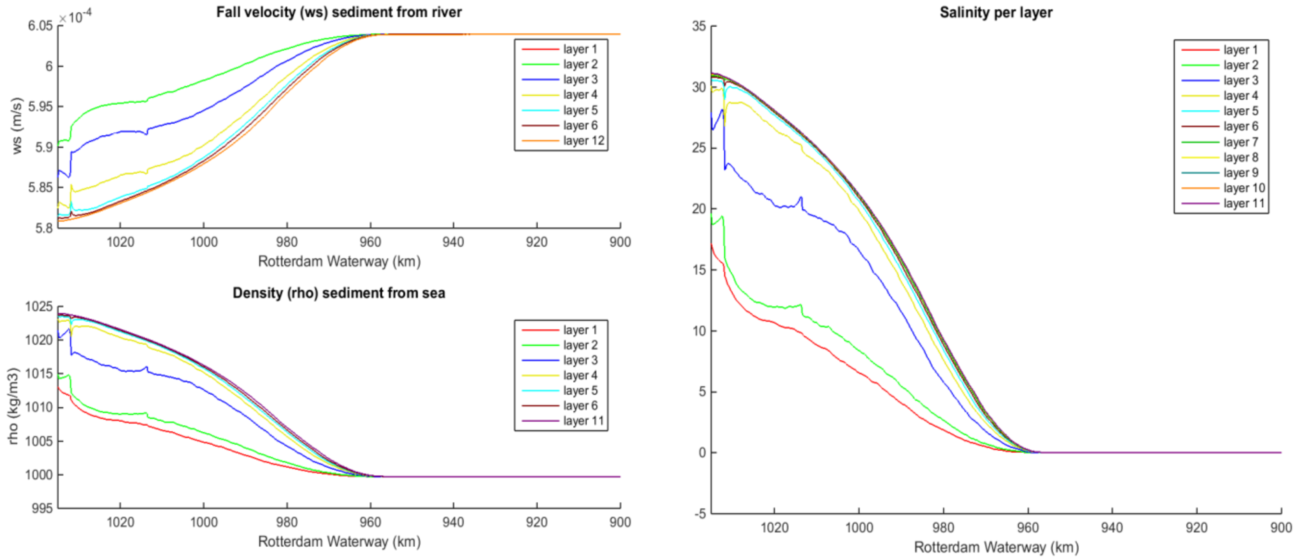

Figure 136 Fall velocity, density and salinity per layer for the deepened scenario

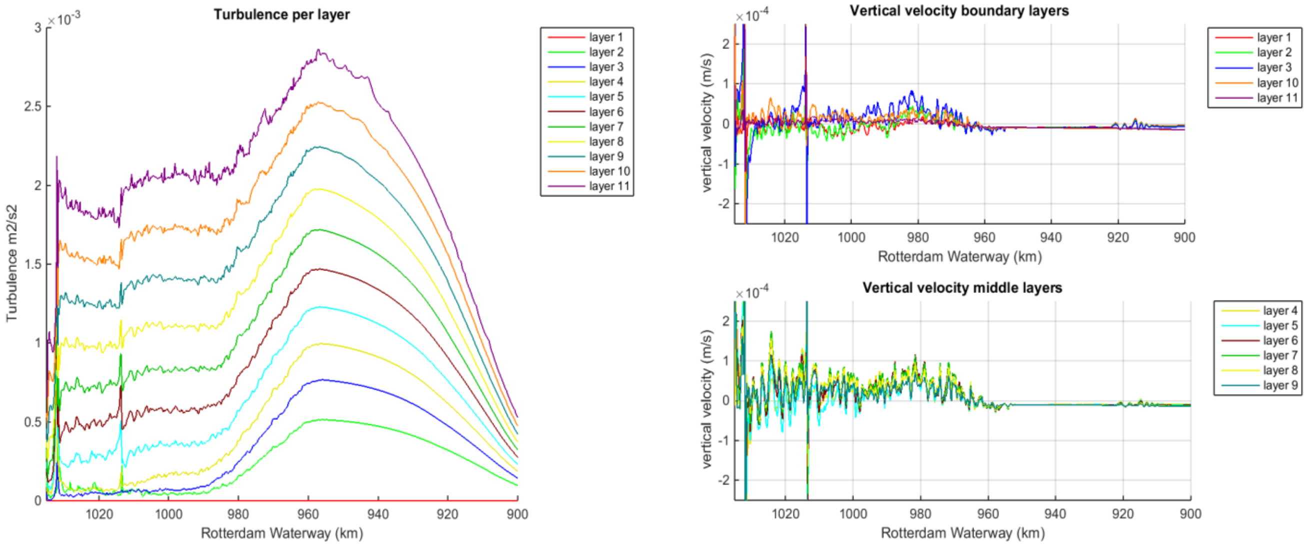

Figure 137 Turbulence, average velocity for all layers and specific for the two lowest layers

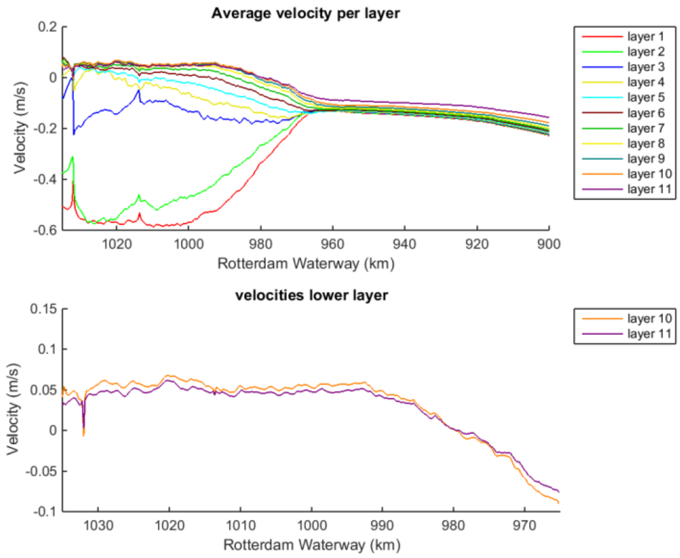

Figure 138 Average velocity 5% discahrge

F.1.1.2. 25% discharge

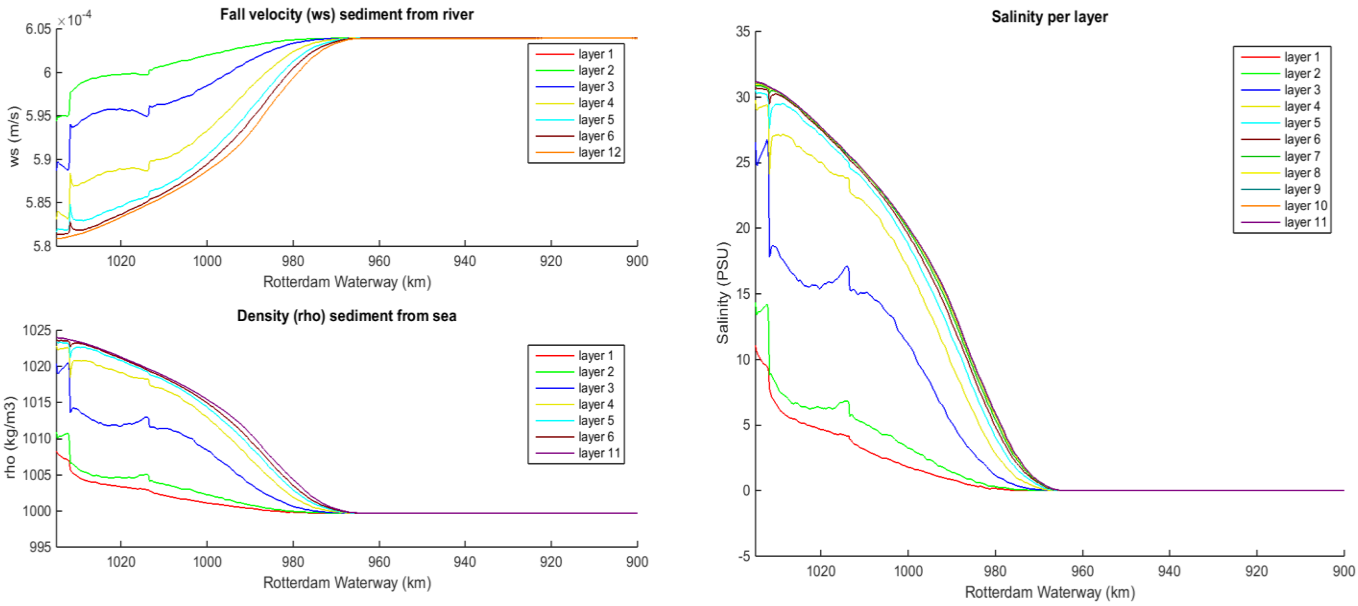

Figure 139 Fall velocity, density and salinity per layer for the deepened scenario

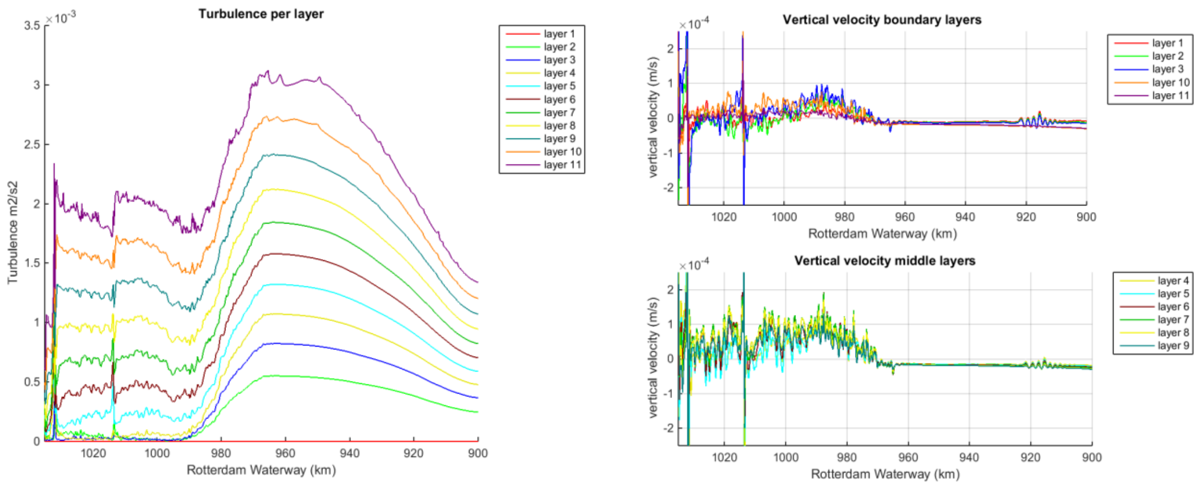

Figure 140 Turbulence, vertical velocity for boundary layers and middle layers

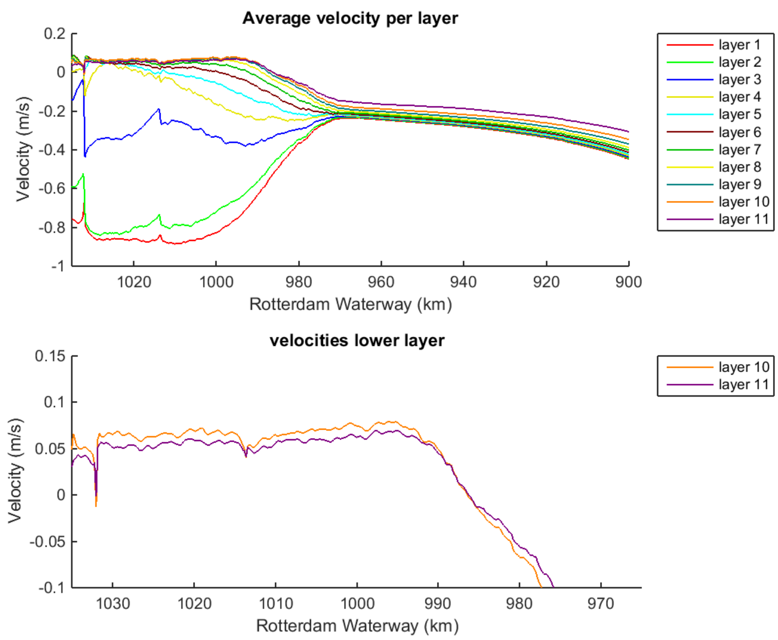

Figure 141 Average velocity for all layers and specific for the two lowest layers

F.1.1.3. 75% discharge

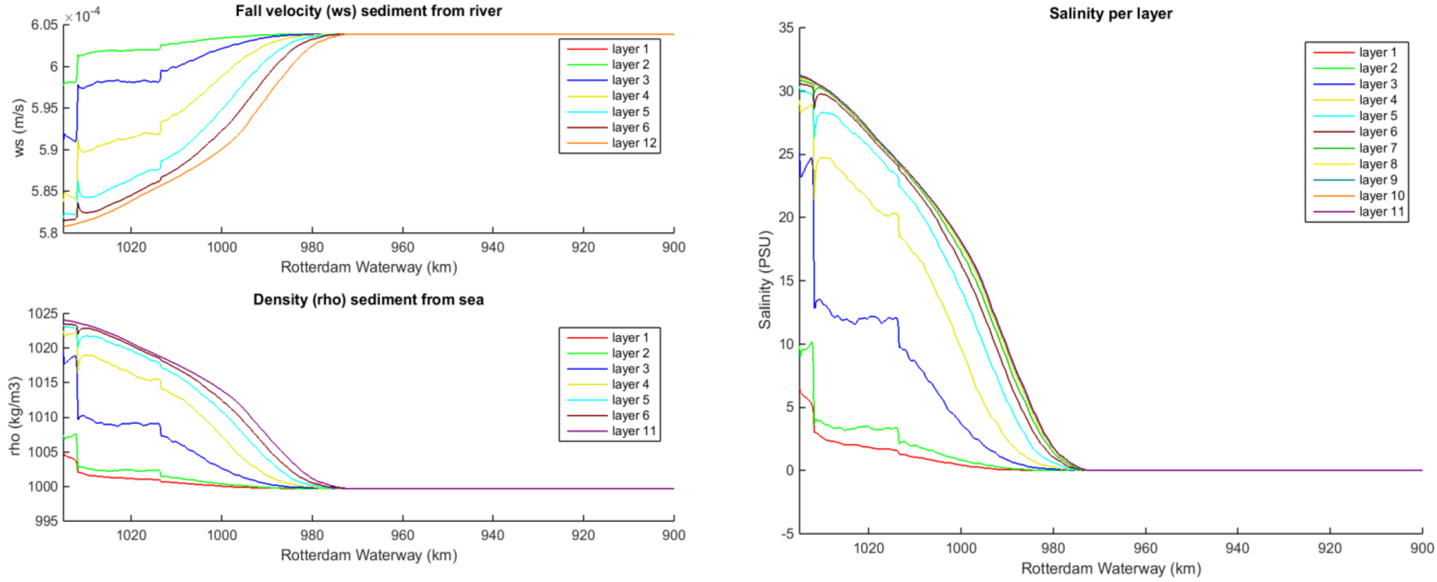

Figure 143Fall velocity, density and salinity per layer for the deepened scenario

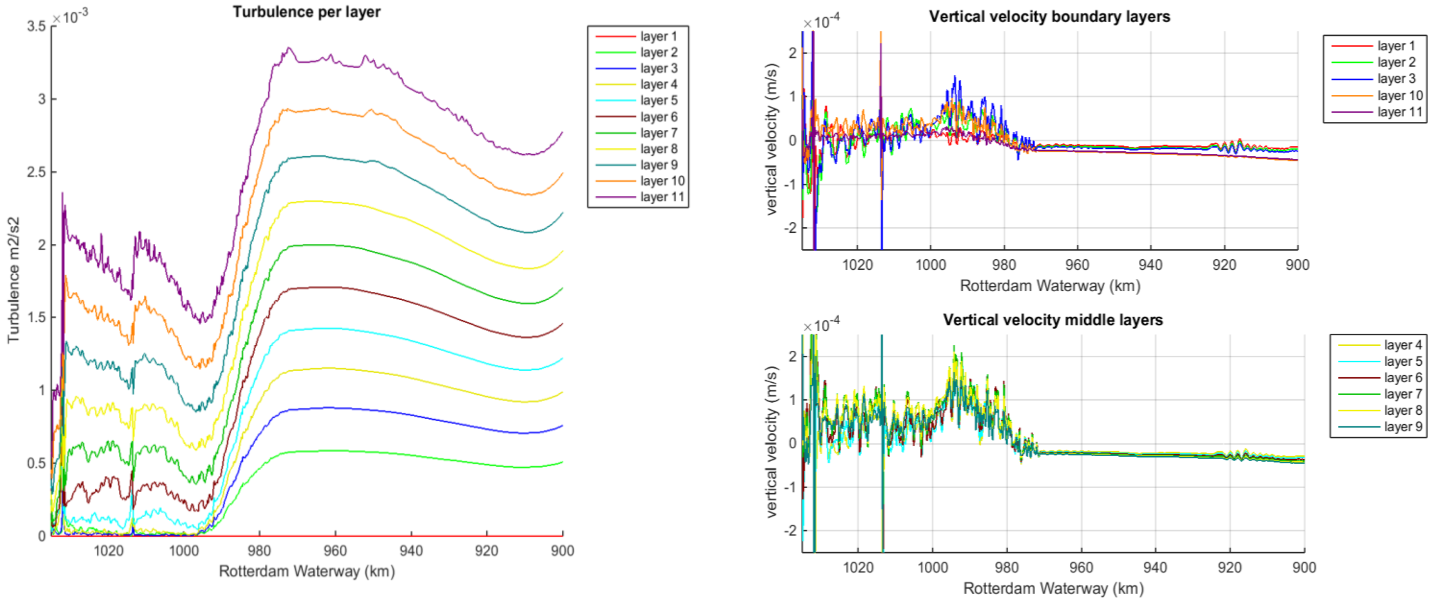

Figure 142 Turbulence, average velocity for all layers and specific for the two lowest layers

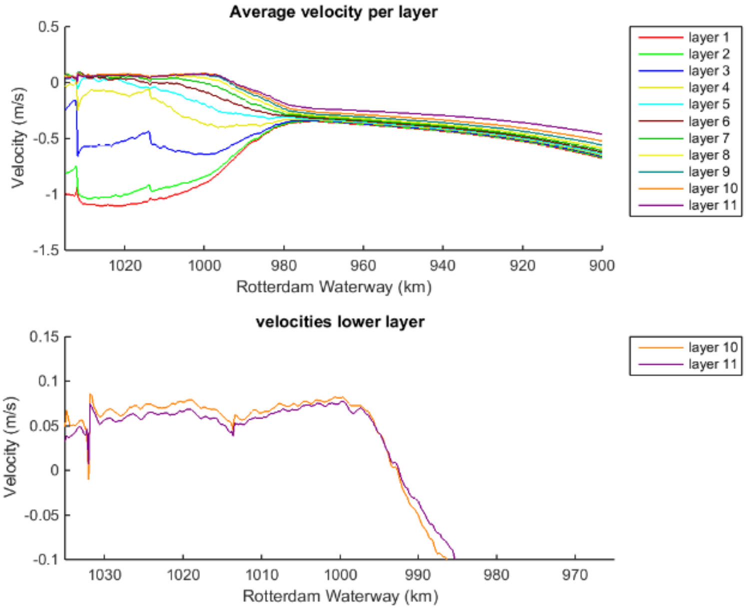

Figure 144 Average velocity 75% discharge

F.1.1.4. 95% discharge

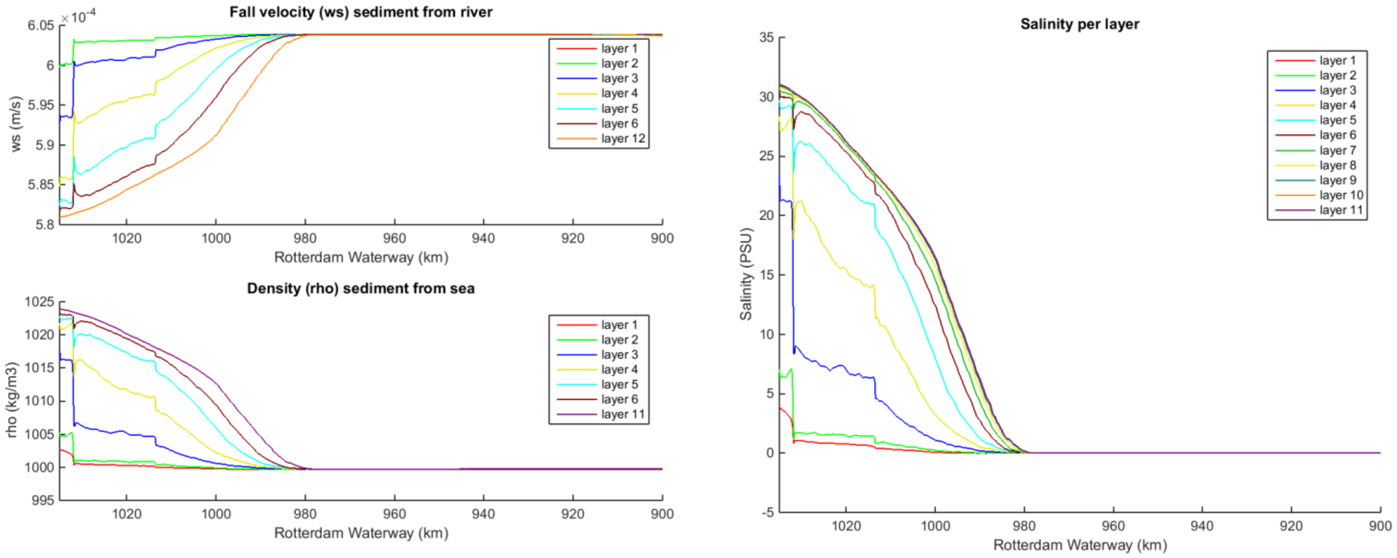

Figure 146 Fall velocity, density and salinity per layer for the deepened scenario

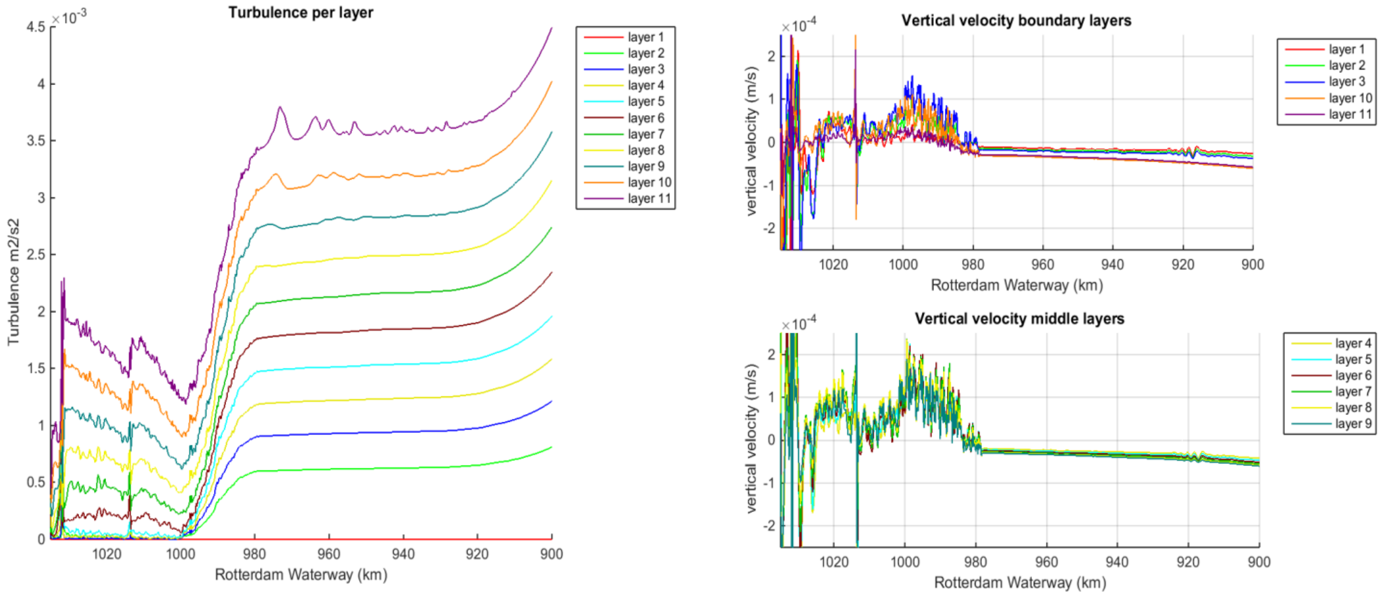

Figure 145 Turbulence, average velocity for all layers and specific for the two lowest layers

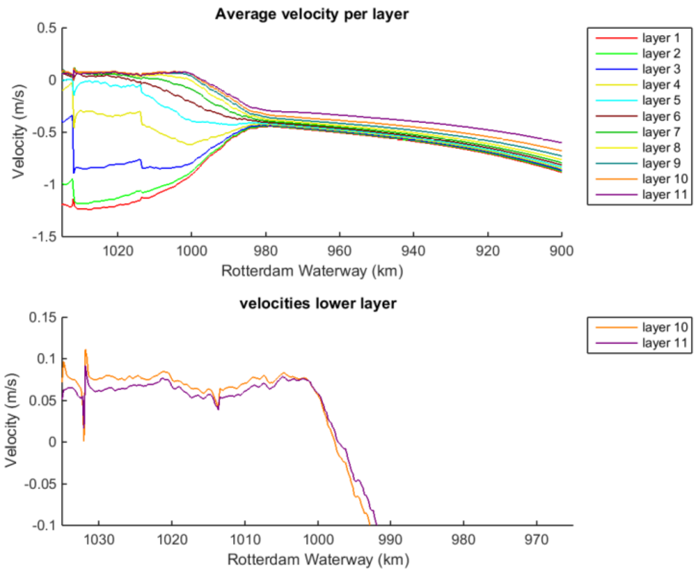

Figure 147 Average velocity for all layers (top) and bottom layers

F.2 ETM deepening

F.2.1. Hydrodynamics

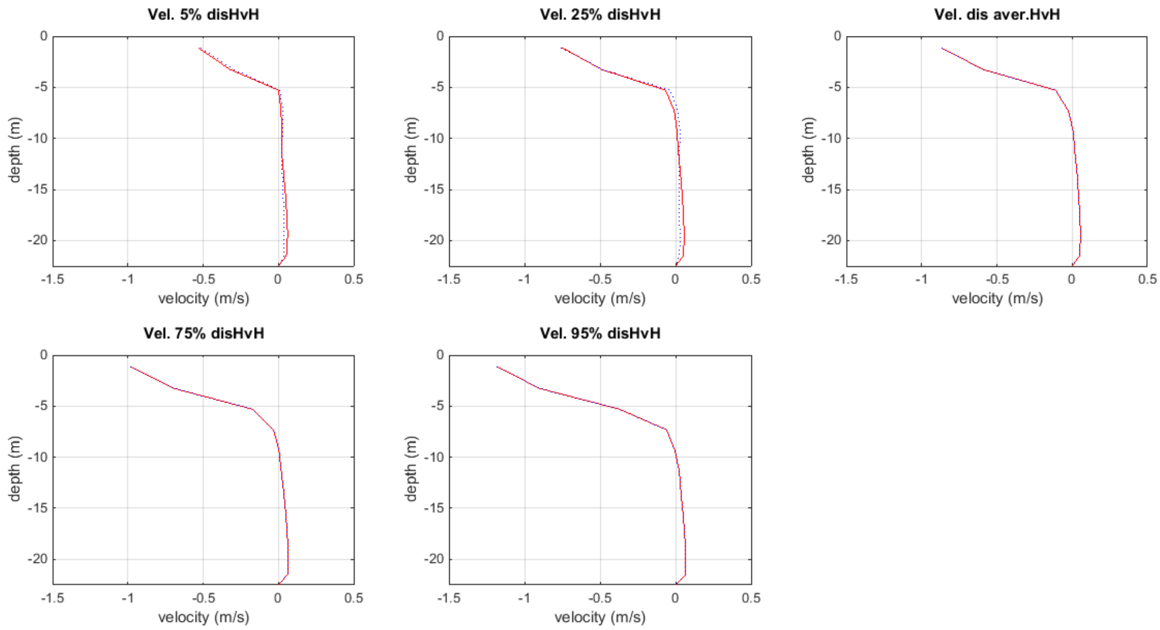

Figure 148 Changing average discharge for changing discharge near Hook of Holland due to ETM deepening

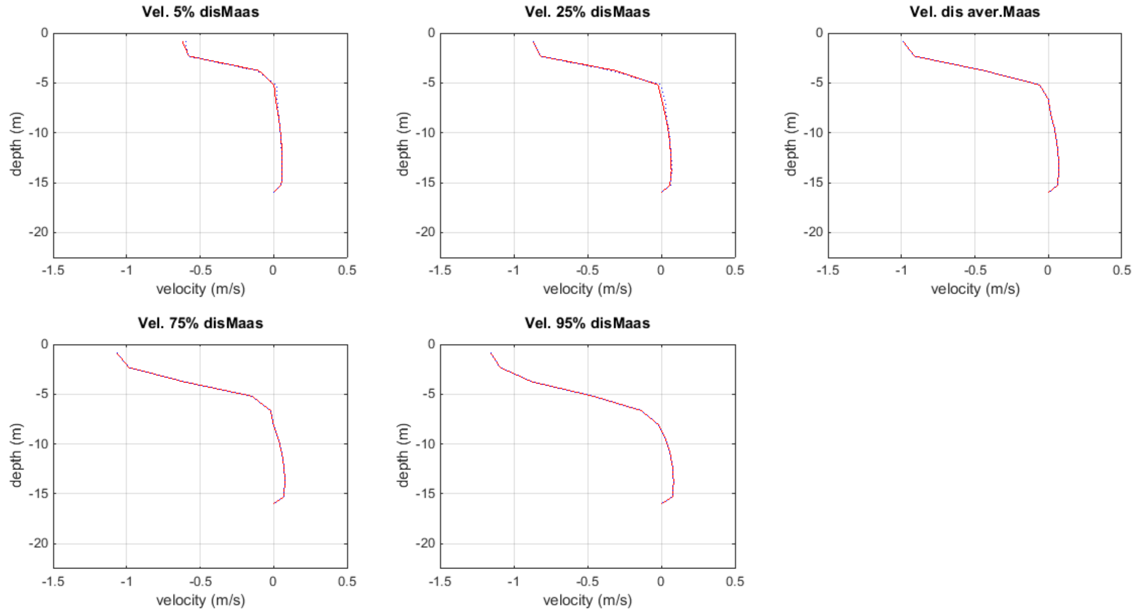

Figure 149 Changing average discharge for changing discharge near Maassluis due to ETM deepening

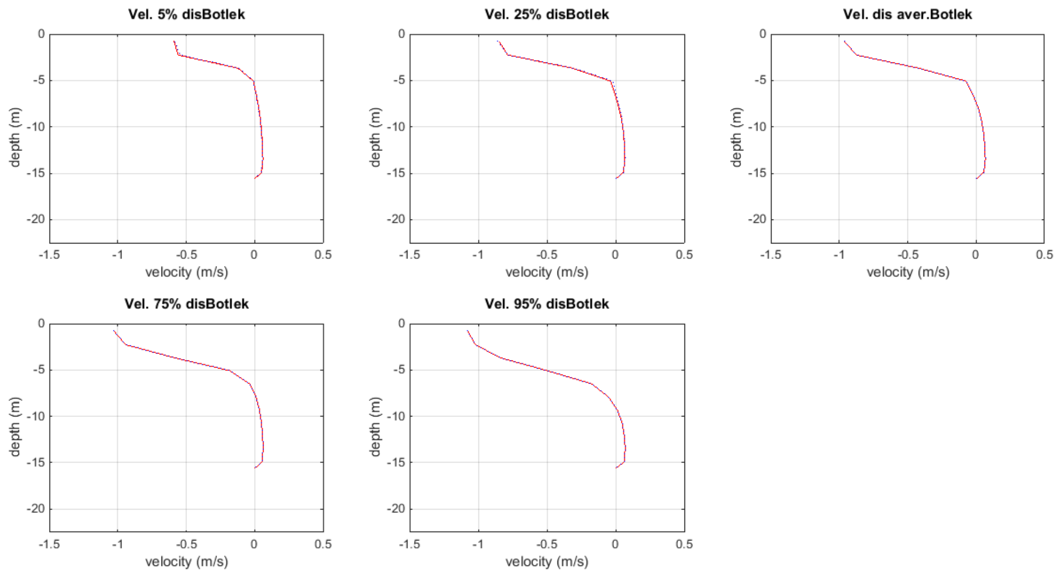

Figure 150 Changing average discharge for changing discharge near Botlek due to ETM deepening

F.2.1.1. 5% discharge

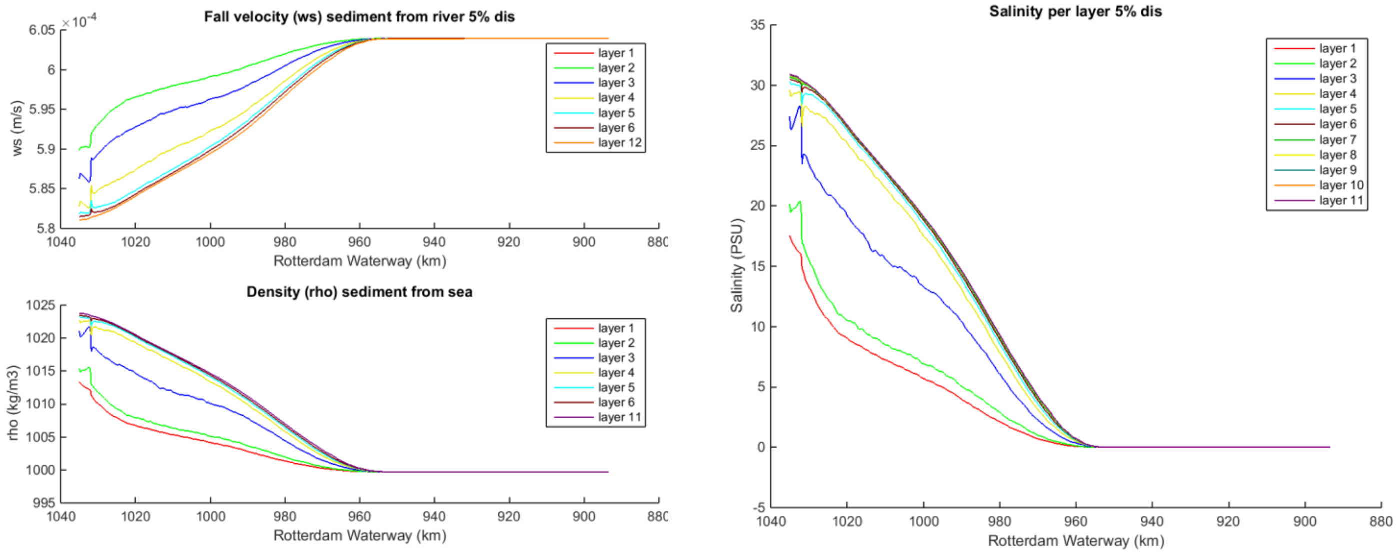

Figure 151 Fall velocity and density (left) and salinity (right) for the ETM deepening scnenario 5% discharge

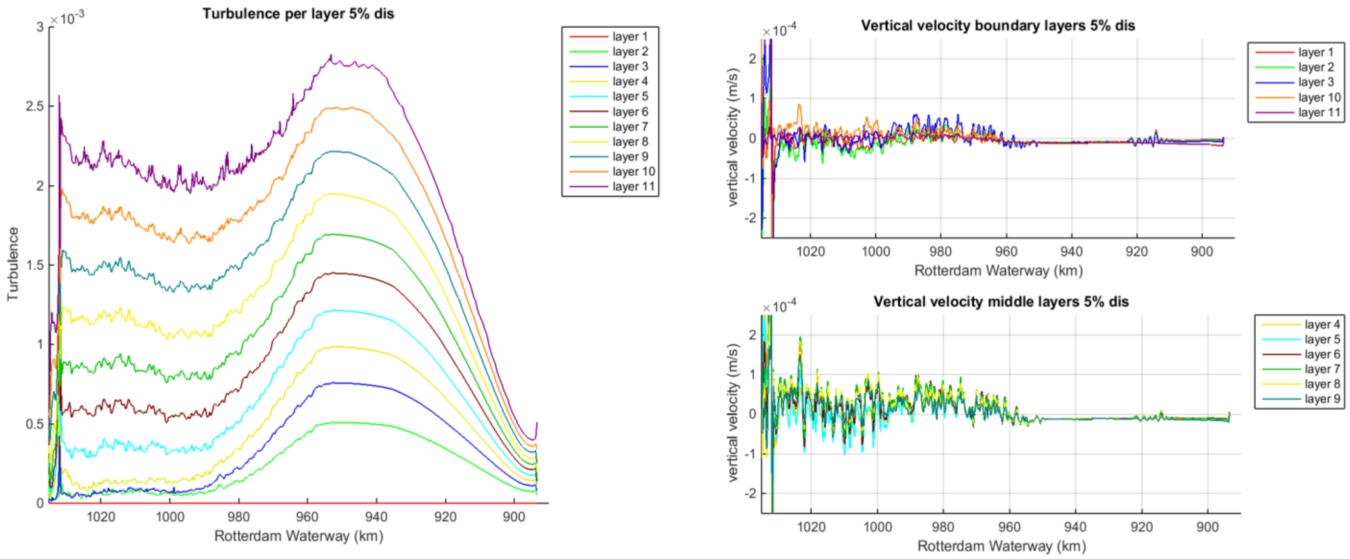

Figure 152 Turbulence (left) and vertical velocity for boundary layers and middle layers for 5% discharge

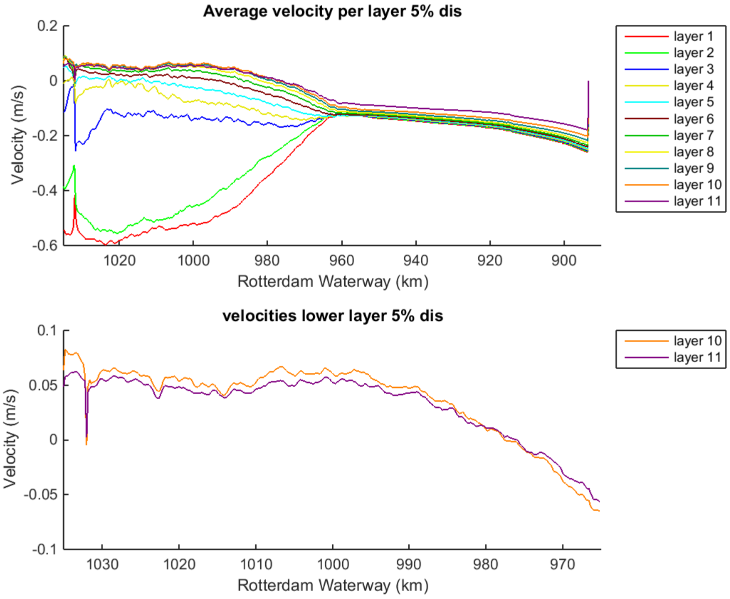

Figure 153 Average velocity for all layers (upper panel) and for the lowest two layers for the 5% discharge

F.2.1.2. 25% discharge

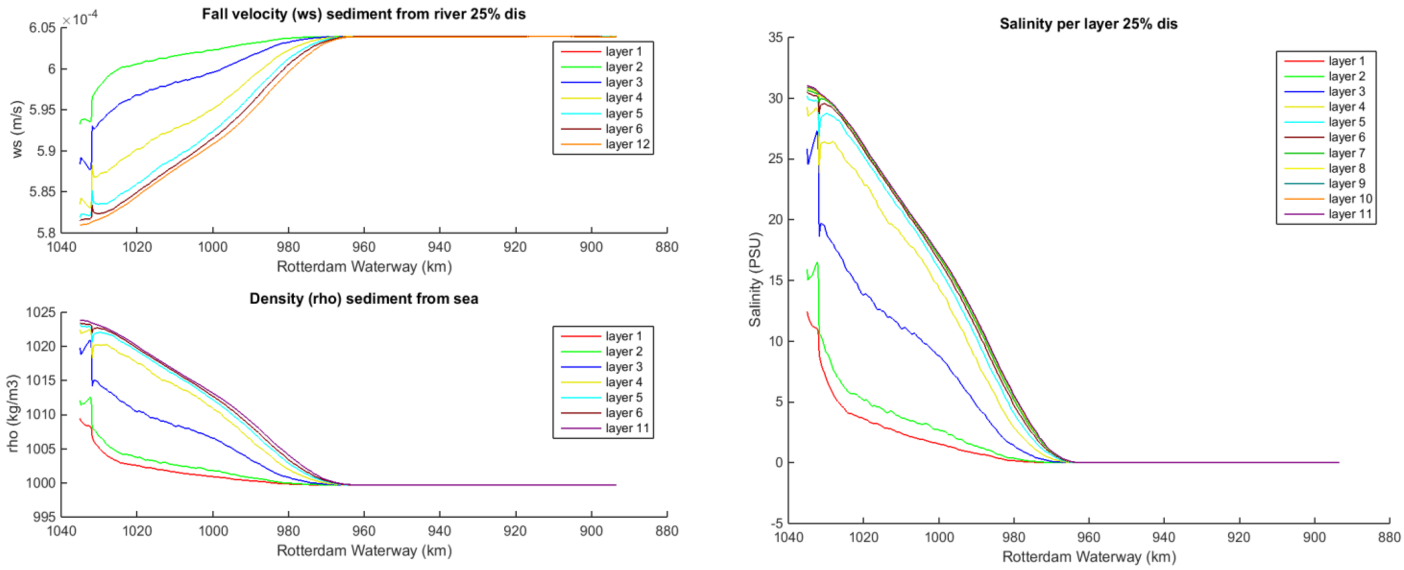

Figure 154 Fall velocity and density (left) and salinity (right) for the ETM deepening scenario 25% discharge

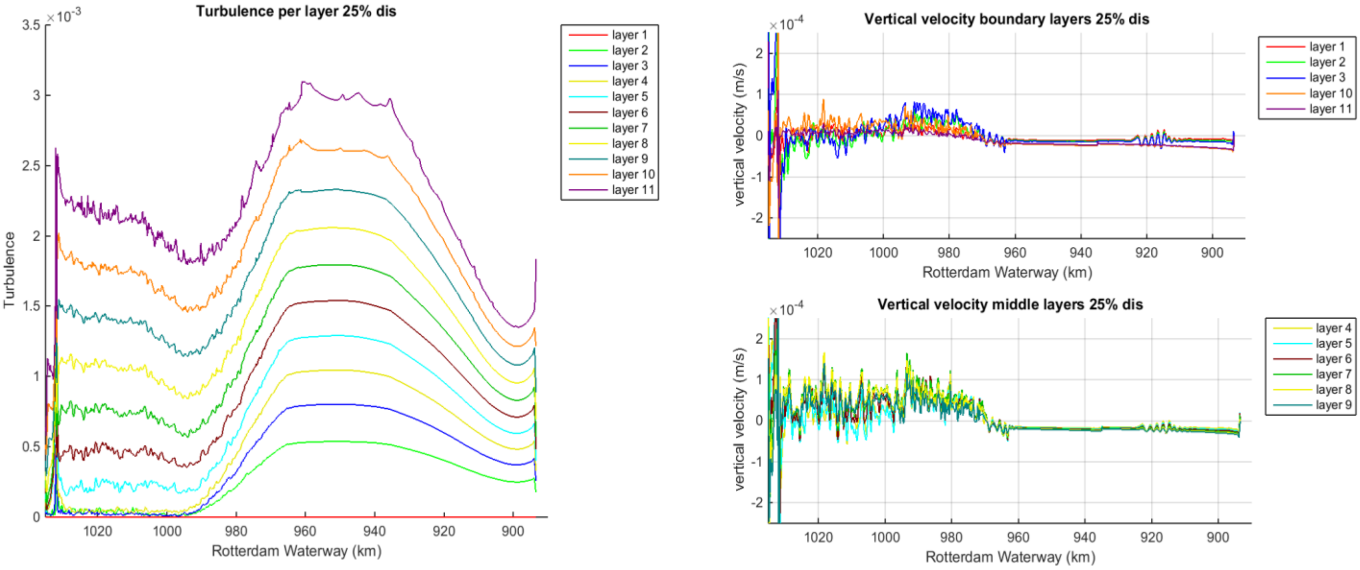

Figure 155 Turbulence (left) and vertical velocity for boundary layers and middle layers for 25% discharge

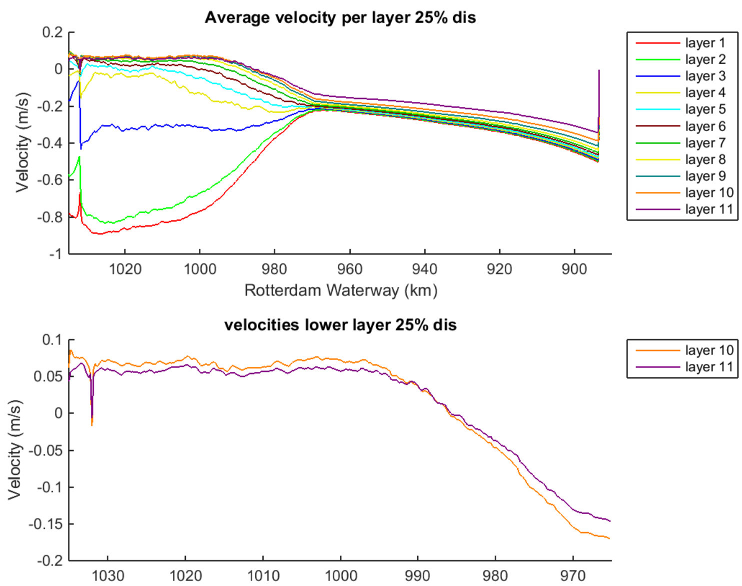

Figure 156 Average velocity for all layers (upper panel) and for the lowest two layers for the 25% discharge

F.2.1.3. 75% discharge

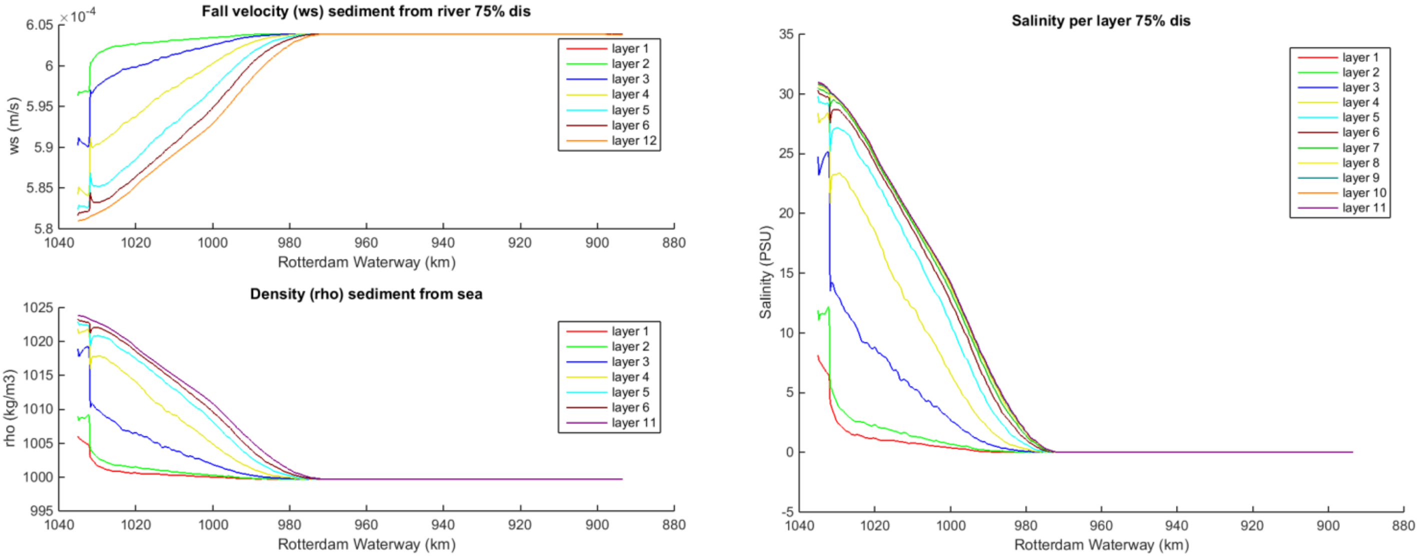

Figure 157 Fall velocity and density (left) and salinity (right) for the ETM deepening scnenario 75% discharge

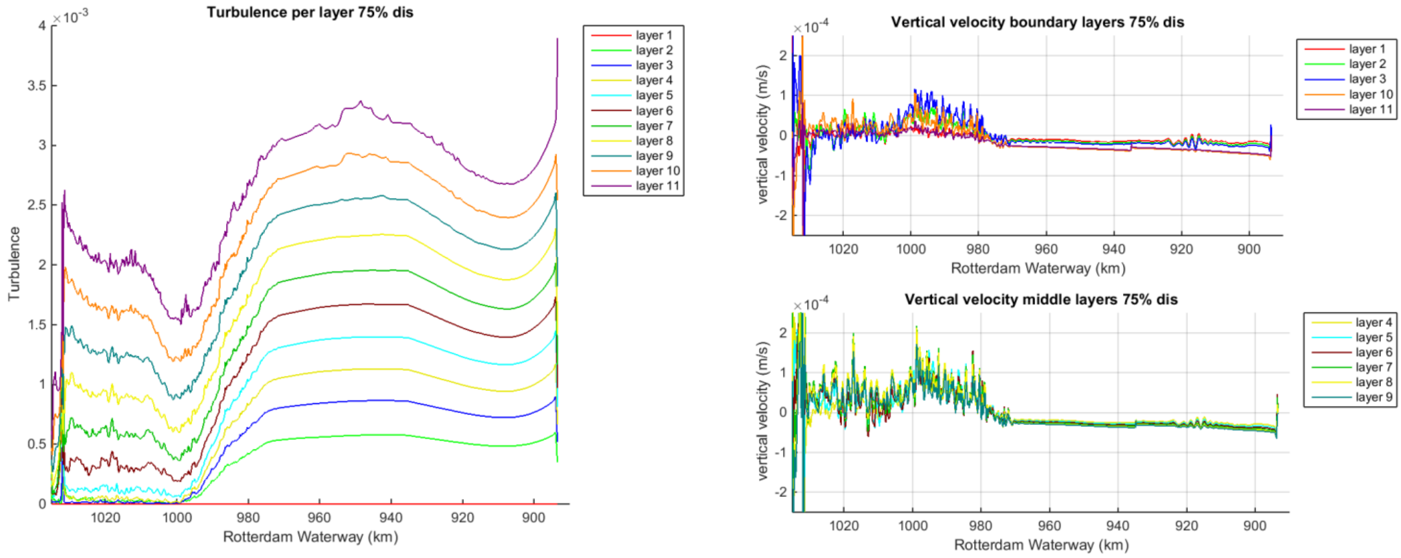

Figure 158 Turbulence (left) and vertical velocity for boundary layers and middle layers for 75% discharge

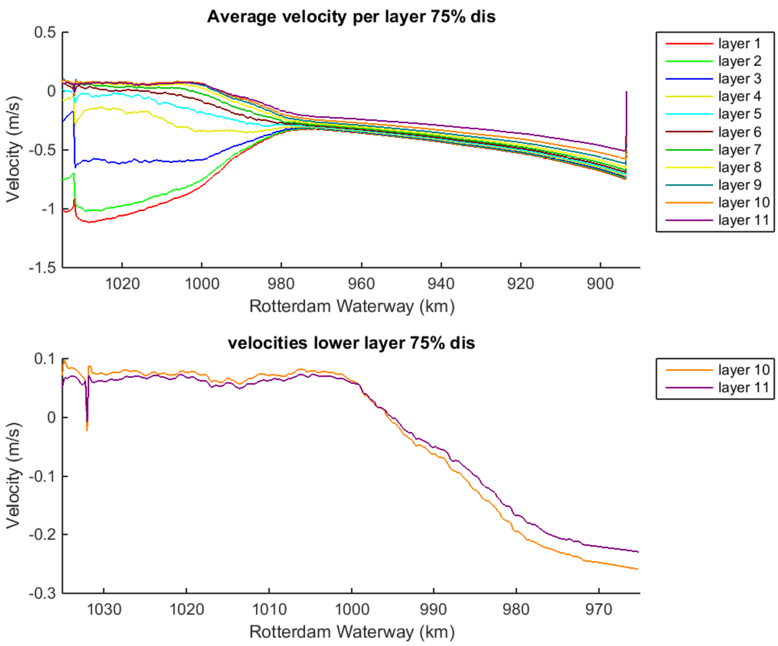

Figure 159 Average velocity for all layers (upper panel) and for the lowest two layers for the 75% discharge

F.2.1.4. 95% discharge

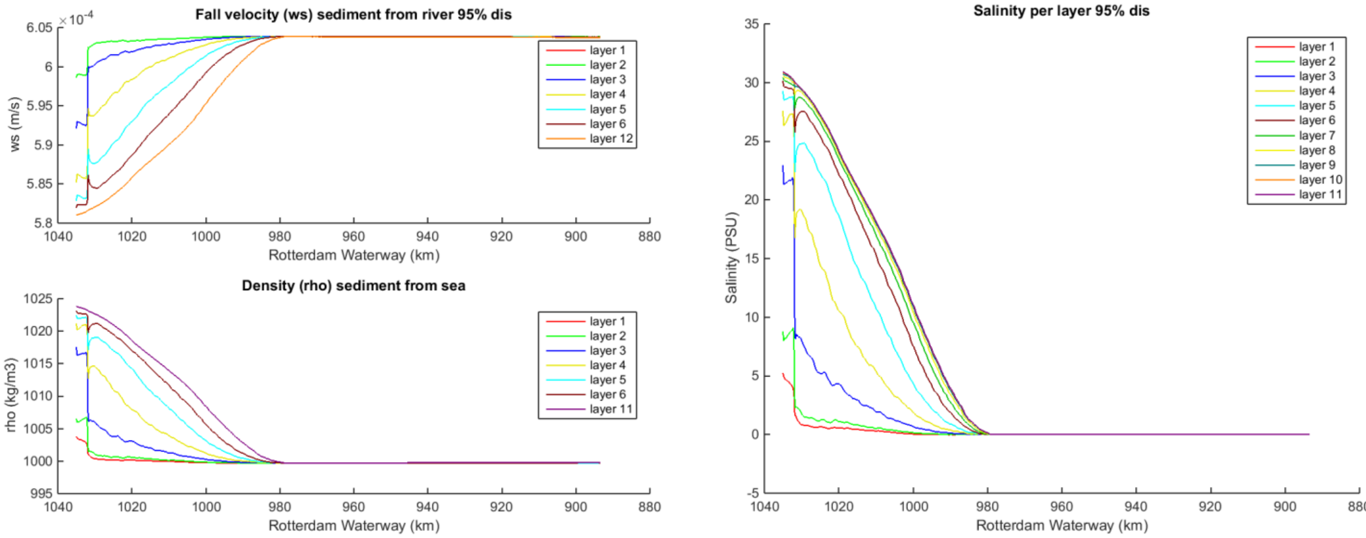

Figure 160 Fall velocity and density (left) and salinity (right) for the ETM deepening scnenario 95% discharge

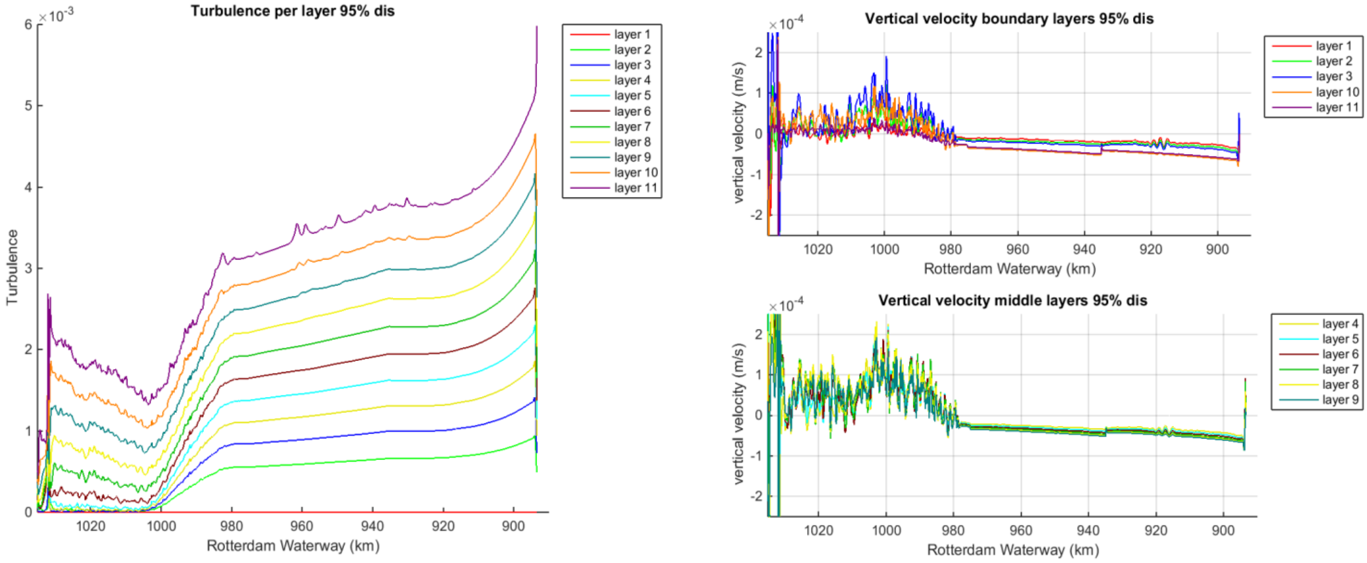

Figure 161 Turbulence (left) and vertical velocity for boundary layers and middle layers for 95% discharge

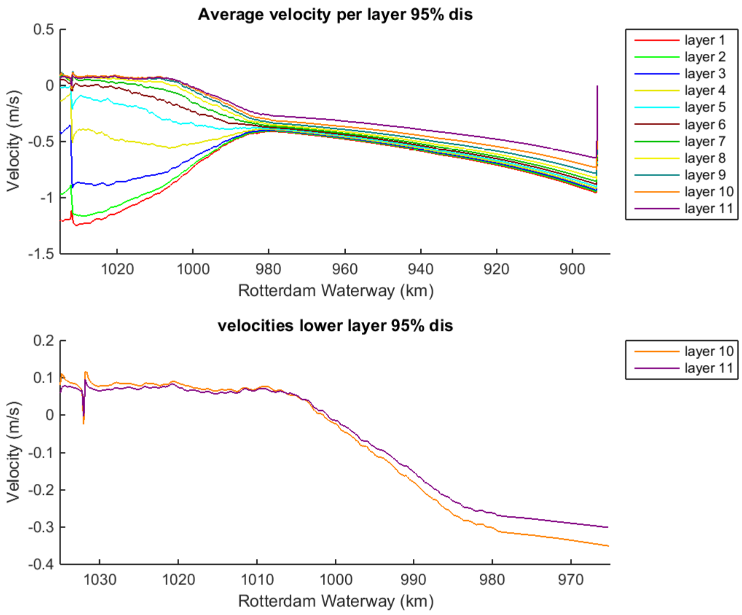

Figure 162 Average velocity for all layers (upper panel) and for the lowest two layers for the 95% discharge

G. Internal asymmetry

The internal asymmetry is important for the deformation of the tide. As can be seen in Table 15 the contribution of the M4 over the M2 tide is constant for the reference scenario for average conditions. The estuary is also flood dominant for the whole estuary as expected.

The deepening decreases the importance of the M4 tide, but the asymmetry is still small for the estuary. The estuary is increasing in flood dominance.

Table 15 Results internal asymmetry for the amplitude and phase between Hook of Holland and the Botlek

	Ampl. HvH	Ampl. Botlek	Phase HvH	Phase Botlek
Reference				
Average conditions	0.207	0.204	7.231	15.177
Step deepening				
Average conditions	0.210	0.207	9.256	17.682
ETM deepening				
Average conditions	0.201	0.197	11.031	19.988